REGULATING STEM CELL FATE WITHIN MICROENVIRONMENTAL NICHES

Thesis submitted for the degree of Doctor of Philosophy at the University of Oxford

Suranahi K. Buglass BSc (Hons)

Keble College

Supervisor Prof. Suzanne Watt

Nuffield Division of Clinical Laboratory Sciences
Radcliffe Department of Medicine
University of Oxford
& NHS Blood and Transplant

Hilary Term 2014

ABSTRACT

REGULATING STEM CELL FATE WITHIN MICROENVIRONMENTAL NICHES. SURANAHI K BUGLASS, KEBLE COLLEGE, DEGREE OF DOCTOR OF PHILOSOPHY, HILARY TERM 2014.

Improving the repopulation potential of human umbilical cord blood (UCB) haemopoietic stem cells (HSCs) remains a paramount goal in HSC transplantation (HSCT) therapy. This implies enhancing the homing and engraftment potential of UCB-$CD34^+CD133^+$ cells to the bone marrow (BM). Although an array of molecules continues to be identified as 'key' homing molecules, the molecular mechanisms controlling HSC homing are still not fully understood. The regulatory implications of hypoxia in the BM, with the concomitant stabilisation of hypoxia inducible transcription factor-1α (HIF-1α), are becoming more apparent, yet at the commencement of this thesis no study had explored whether hypoxia induced signalling can be adopted to regulate the homing and engraftment of transplanted HSCs.

The aim of this DPhil project was thus to investigate whether hypoxic conditions as detected in the BM influence the adhesion of UBC-$CD133^+$ cells to osteoblasts, BM stromal cells and BM endothelial cells-60 (BMEC-60), as well as their transmigration towards chemokine SDF-1α across BMEC-60. Increasing the exposure of UCB-$CD133^+$ cells to 1.5% O_2 doubled the percentage of transmigrating cells ($p<0.05$), and while hypoxia stimulated UCB-$CD133^+$ cells preferentially adhered to IL-1β stimulated BMEC-60, their adhesion to non-stimulated (BMEC-60) was significantly improved ($p<0.001$). To help unravel the underlying molecular mechanisms, we attempted to examine the potential involvement of hypoxia regulated scaffolding protein HEF-1/NEDD9/Cas-L (HEF-1) in the increased percentage of migrating UCB-$CD133^+$ cells after hypoxia pre-conditioning. The role of HEF-1 in HSCs is unexplored, and its multifunctional contribution in a variety of processes including cell migration, attachment and invasion make HEF-1 a prime candidate as a contributing homing molecule. After identifying a suitable short-hairpin RNA (shRNA) sequence to knockdown HEF-1, generating lentiviral (LV)-particles in house and optimising transduction protocols, HEF-1 knockdown was achieved in haemopoietic model cell lines KG-1 and KG-1A (KG-1/KG-$1A^{-HEF1}$). Significantly decreased KG-$1A^{-HEF1}$ cell adhesion to non-stimulated BMEC-60 was detected. Together, these studies provide a promising platform to further explore the role of HEF-1 in hypoxia induced UCB-$CD133^+$ cell transmigration towards the key homing molecule SDF-1α.

I dedicate this thesis to working parents.

Little did I know how precious every minute of a 24 hour day could be.

I cannot go without also dedicating this work to Emeritus Professor Derek Lamport who inspired me to pursue this doctoral training (after working together on the evolution of land plants at the University of Sussex), and continues to provide intellectually stimulating discussions that spark my eureka moments.

ACKNOWLEDGMENTS

I would like to sincerely thank my supervisor Professor Suzanne Watt for giving the opportunity to carry out my DPhil studies in her laboratory and introducing me to the fascinating world of BM biology and HSCT therapy. I continue to pursue my career in this field, making all that I have learned during this journey an invaluable foundation. I also sincerely thank Professor Watt and NHS Blood and Transplant for funding my studies. I thank the University of Oxford for creating such a splendid learning environment, attracting so many interesting and life-enriching people, and most of all for making Oxford such a wonderful home, where I met my loving husband and had my first child. I thank Keble College for their pastoral care and providing excellent study facilities. They have a truly exceptional administration staff and such approachable and helpful porters.

I would also like to greatly thank my dyslexia tutor Jane Clarke for her invaluable study support and helping me appreciate the trials and tribulations that come with this learning difficulty. The university's Disability Advisory Service was also very helpful and supportive throughout my studies.

I give thanks to my laboratory colleagues for creating a friendly work environment and always keen on having special occasion celebrations. It was wonderful to work with Chao-Hui (now Dr. Chao-Hui), enjoying scientific discussions and exchanging research ideas over lunch breaks. I thank the senior researchers of the laboratory, Dr. Sarah Hale, Dr. Enca Martin-Rendon and Dr. Lee Carpenter, for their scientific advice and mentoring. Many thanks to Sandy Britt and Jan Walton for obtaining consent from mothers to donate placenta and cord, and for collecting most of the cord blood. I also thank them for taking the time to show me how to collect human umbilical cord blood. My work the in laboratory could not have been done without the help of Sindu and Pat, who kept the labs fully stocked and were so patient with the ordering of reagents.

Thank you David and Leida for always being there for me. I owe my achievements to such loving and supportive parents. Thank you dear Tom and Anahí for all your patience, great cooking and housekeeping during the writing of my thesis.

DECLARATION

I was unable to donate my blood, however I gave it all the "…toil, tears, and sweat" that Churchill would have offered (Winstson Churchill, Houses of Parliament 1940)

I certify that I carried out 100% of the research for this thesis.

TABLE OF CONTENTS

TABLE OF FIGURES

TABLE OF TABLES

COMMON ABBREVIATIONS

BM	Bone marrow
BMEC-60	Bone marrow endothelial cells-60 (immortalised)
BMECs	Bone marrow endothelial cells
BMSCs	Bone marrow stromal cells
CB	Cord blood
CFU	Colony forming units
FACS	Fluorescence activated cell sorting
GFP	Green fluorescent protein
HEF-1	Human enhancer of filamentation-1 (also NEDD9/CAS-L)
HEK293T	Human embryonic kidney 293T
HIF-1α	Hypoxia inducible transcription factor-1α
Ho	Hoechst 33342 dye
HRE	Hypoxia response element
HSCs	Haemopoietic stem cells
HSCT	Haempoietic stem cell transplant
HSPCs	Haemopoietic stem progenitor cells
iPS	Induced pluripotent stem cells
ITR/IT	Intermediate repopulating
Lin^-	Lineage negative
LTR-	Long-term repopulating
LV	Lentiviral
MACS	Magnetic activated cell sorter
MFI	Median fluorescence intesity
mirRNA	MicroRNA
MOI	Multiplicity of infection
mPB	Mobilised peripheral blood

MPPs	Multi-potent progenitors
MSCs	Mesenchymal stem cells
PIM	Pimonidazole
pri-miRNA	Primary transcripts
shRNA	short hairpin RNA
shRNAmir	shRNAs expressed mimic human microRNA-30 (mirRNA-30) pri-miRNAs
siRNA	Small interfering RNA
STR-	Short-term repopulating
$Thy1^{-}$	Thymocyte differentiation antigen 1 (CD90)
TU	Transducing units
UCB	Umbilical cord blood

Chapter I General Introduction

I.1. Brief history

The history of stem cells begins in the 19th century with Ernst Haeckel, who first used the term “Stammzelle” to describe the fertilized egg that gives rise to all cells of the embryo. This is not too far removed from the definition of an embryonic stem cell today. In the 1960s, James Till, Ernest McCulloch and others widened the definition by demonstrating that haemopoietic ‘stem cells’ were those with the potential to self-renew and the ability to generate particular types of offspring for the tissue in question (Ramalho-Santos and Willenbring, 2007). They hypothesised that there was a common stem cell for all blood cell types. That precursor was identified in the 1980s, and subsequently now known as the haemopoietic stem cell (HSC) (Doulatov et al., 2012, Laurenti et al., 2013, Sanjuan-Pla et al., 2013, Smith et al., 1991, Weissman, 2002, Weissman et al., 1989).

I.2. Definitions

Today the term stem cell is even more broadly used and divides stem cells into two distinct types: embryonic and tissue specific. Embryonic stem (ES) cells can generate all tissues and organs and are hence termed totipotent/pluripotent. The tissue specific stem cells (e.g. HSCs) have a more limited capacity than ES cells and are referred to as multipotent. Generally they only propagate cells of the same lineage from their derived tissue. In addition, only small numbers of tissue specific cells may be harvested, which often limits advances in basic research and particularly for medical applications.

Opportunities for stem cell therapy seemed promising when researchers unravelled methods to culture ES cells *in vitro*. However, similar to the sceptical views and ethical controversies over GM crops, exploring such possibilities in the United Kingdom has restrained using embryonic derived stem cells for clinical therapies. Instead, the ingenious emergence of induced pluripotent stem (iPS) offers an alternative avenue for stem cell therapy. They are produced by re-programming tissue specific cells to generate ES-like cells and hence are a combination of both stem cell types (Takahashi and Yamanaka, 2006). Such surrogates are still in early stages of development and will probably not be a therapeutic option within the next few years. Technical hurdles to establish cell banks with a diverse set of high quality iPS cell lines are needed to enable clinical application. Nonetheless, their use is not a pipe dream. “Egg Engineers” (Cyranoski, 2013) have emerged in Japan able to produce fertile murine gametes from primordial germ cell-like cells that were generated from reprogrammed iPS cells (Hayashi et al., 2012). Such study provides a promising platform to investigate and better understand the biology and regulation of female germ cell development.

There have also been remarkable iPS studies involving the haematological system of murine models. Hanna et al. were able to correct sickle cell anaemia in mice using fibroblast derived iPS cells of a humanised sickle-cell anaemia mouse. The β-sickle mutation was corrected in these generated iPS cells, which were subsequently differentiated into embryoid bodies to generate haemopoietic progenitors for transplantation therapy. The haemopoietic progenitors rescued the sickle cell anaemia phenotype in these mice (Hanna et al., 2007). Raya et al. generated human-specific iPS cell to treat

Fanconi anaemia. These iPS cells could also give rise to haemopoietic progenitors of the myeloid and erythroid lineages (Raya et al., 2009). While differentiating iPS into transplantable HSCs remains a future goal, the scope of iPS cell engineering is clearly immense. These studies may lead the way to generating iPS cell without transduction with reprogramming genes.

I.3. Haemopoietic stem cells

Multipotent HSCs are of great interest because of their utilitarian properties in combating various haematological disorders. Human HSCs are most commonly sourced from bone marrow (BM), mobilised peripheral blood (mPB) and umbilical cord blood (UCB) (Sirinoglu Demiriz et al., 2012). They comprise a heterogenous population of cells that have 'stem cell' attributes and are generally classified into subsets based on their clonal life span and repopulation capacity (Doulatov et al., 2012). In mice, HSCs with the ability to permanently repopulate recipients with all blood-cell lineages represent the stable pool, and are termed long-term repopulating (LTR)-HSCs. Those which have a more limited self-renewal capacity (low clonal lifespan and fail to engraft long-term) are known as short-term repopulating (STR)-HSCs. Finally, murine HSCs that have lost the ability to self-renew are termed multi-potent progenitors (MPPs) **[Figure I.1]**. In humans, the model for human haemopoiesis continues to change as new observations emerge **[Figure I.3]**. Currently, human HSCs are divided into LTRs and MPPs—in this thesis, these cells and their progeny are referred to as HSCs and haemopoietic stem and progenitor cells (HSPCs) respectively.

Historically, possessing LTR-capacity was defined by the ability to repopulate the haemopoietic system of immune-deficient mice beyond 12 weeks (Doulatov et al., 2012). However, longer periods (>30 weeks) are now being tested (Benveniste et al., 2010, Notta et al., 2011) as “intermediate” repopulating-HSCs (ITR-HSCs) showed longer repopulating activity than STR-HSCs, yet shorter than LTR-HSCs—between 3-6 months rather than permanent repopulating activity (Benveniste et al., 2010). Engraftment of MMPs peaks by 4 weeks (Görgens et al., 2013b, Notta et al., 2011).

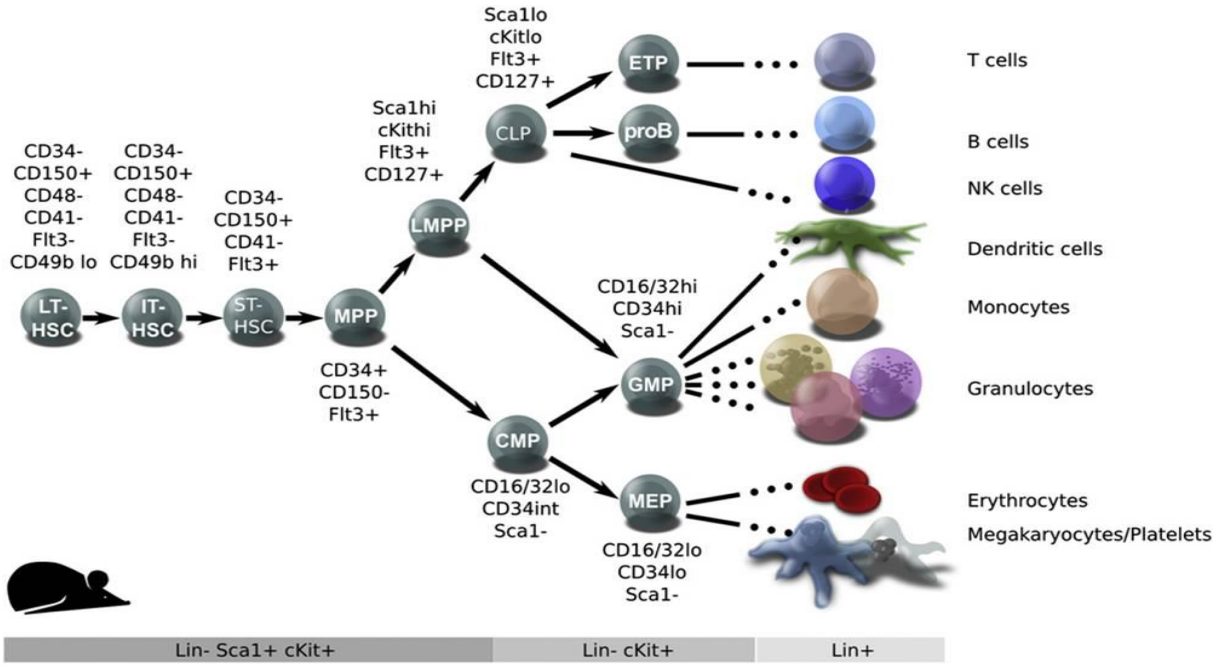

Figure I.1. The haemopoietic stem cell gives rise to all blood cells.

Haemopoesis has been studied extensively in mice. The formation of blood starts in the embryonic yolk sac during the first weeks of fetal development. Primitive nucleated erythrocytes carry the haemoglobin required by the growing fetus. Appearance of 'definitive' haemopoietic cells has been attributed to the aorta-gonad-mesonephros (AGM) region around E10.5 of fetal development. Circulating HSCs colonise the fetal liver, thymus, gastrointestinal tract, and eventually the bone marrow (BM). Whether haemopoietic cells produced in the yolk sack and the AGM share a common precursor is a controversial area amongst experts in this field. However, certain is that in adult mice and humans the major site for haemopoesis is in the BM, where over ten different blood cell types are generated (Medvinsky et al., 2011). The flow chart presented here provides the current model of lineage determination in the adult mouse. Terminally differentiated cells are pictured on the right hand side. LT-: long-term, IT-: intermediate-term, ST-: short-term, HSC: haemopoietic stem cell, MPP: multi-potent progenitor, LMPP: immature lymphoid-biased progentiors, CMP: common myeloid progenitor. Picture credit: Reprinted from Cell Stem Cell 10, Review, Doulatov S., Notta F., Laurenti E., Dick J.E., Hematopoiesis: A Human Perspective, pp.120-136, Copyright 2014, with permission from Elsevier.

The regenerative potential of HSCs was first studied in clonal *in vivo* repopulating assays, where a cell suspension of adult mouse marrow, spleen or fetal liver was transplanted into irradiated mice. Haemopoietic colonies that formed in the spleen (CFU-S) could be divided into two types: CFU-S with the ability to self-renew and CFU-S that gave rise to terminally differentiated daughter colonies, i.e. unable to produce "progeny like itself" (Till et al., 1964). This ground breaking observation gave way to study haemopoiesis at a

functional level and consolidated the idea of a hierarchical structure in the haemopoietic system. Subsequent *in vitro* studies identified precursors of CFU-S, referred to as long-term initiating cells (LTC-ICs) (Sutherland et al., 1990). While colony forming cell and LTC-IC assays are still being used to evaluate haemopoietic activity, they were soon supported by xenotransplantation studies (Weissman, 2002, Weissman et al., 1989), which greatly fuelled advances in studying haemopoiesis of the human blood. Today, numerous murine models are helping to unravel the phenotypic identity of a functional and 'true' LTR-HSC, as well as serving to predict the hierarchical organisation and relationship between individual cell lineages (Görgens et al., 2013a) **[Figure I.2].**

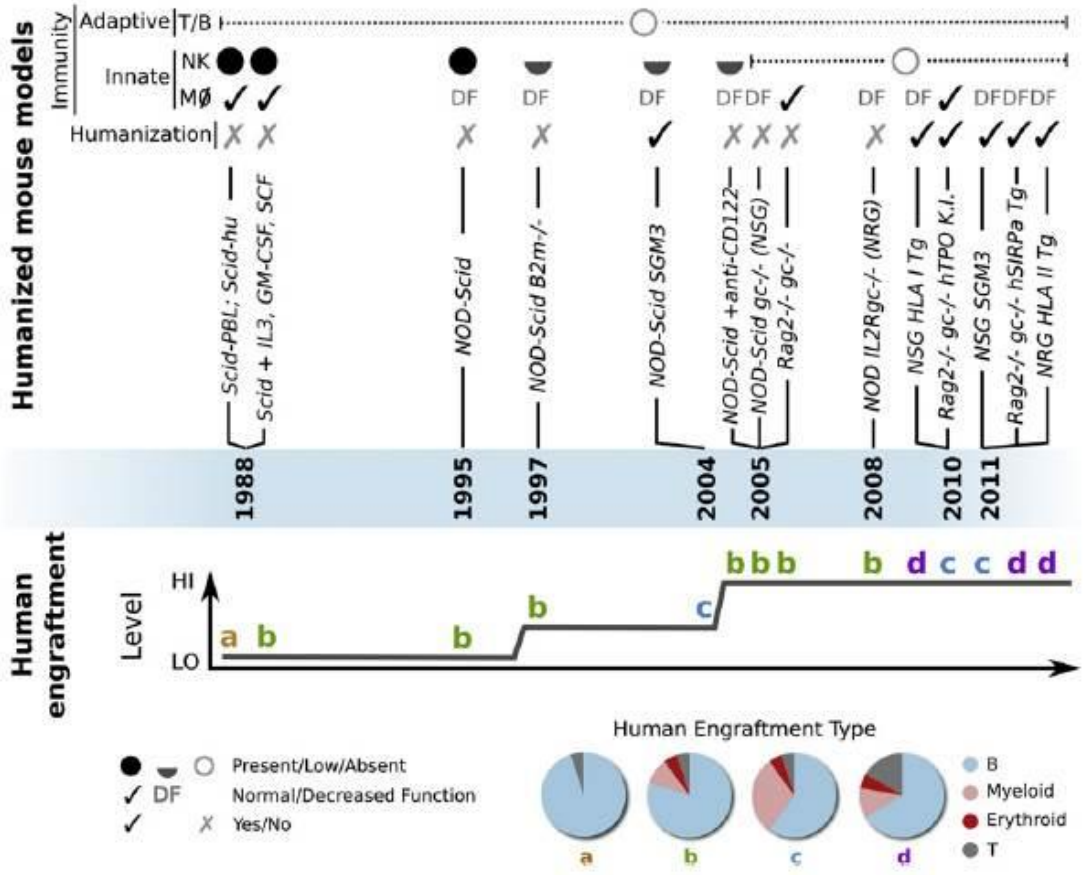

Figure I.2. Two decades of studying human haemopoiesis in immune-deficient mice.

Optimising xenograft models has facilitated better characterisation of human HSCs over the last 20 years. The first model (Dick, 1996, Lapidot et al., 1992), with a severe combined immune-deficient (SCID) system (lacking B and T cells) has been genetically 'tweaked' to create murine models that express human proteins such as human stem cell factor (SCF), Granulocyte-macrophage colony-stimulating factor (GM-CSF), and interleukin-3 (IL-3) (SGM3 mice), or had locus replaced with human genes such as thrombopoietin (TPO). This "humanisation" of murine models has improved engraftment outcomes (illustrated by the plotted line underneath the various murine models) of human HSCs, consequently enabled isolating and better characterising human HSCs and HSPCs. For example, Notta et al. showed that a subpopulation of Thy1^{-} (Thy1^{-}CD49f^{+}) could indeed self-renewal and provide LTR activity, making its lack of expression not a defining marker between LTRs and MPPs as previously thought (Baum et al., 1992). "Less sensitive xenografts" might thus affect engraftment of certain LTR-subsets (Notta et al., 2011). Picture credit: Reprinted from Cell Stem Cell 10, Review, Doulatov S., Notta F., Laurenti E., Dick J.E., Hematopoiesis: A Human Perspective, pp.120-136, Copyright 2014, with permission from Elsevier.

With fluorescence-activated cell sorting (FACS), combinations of cell surface antigens (panel) and metabolic properties are used to isolate and distinguish "HSCs" with LTR-capacity **[Table I.1]**. In mice, the first LTR-defining panel was presented in the mid 90's, where Osawa et al. obtained life-long

blood production (myeloid and lymphoid cells) after transplanting a single mouse $CD34^{lo/-}$, c-kit^+, Sca-1^+, lineage negative (Lin^-) cell (Osawa et al., 1996). A few years later, this profile was further defined by the $CD150^+CD48^-$ SLAM phenotype (Kiel et al., 2005). Kiel et al. confirmed that one out of every 2.1 (47%) $Lin^-CD34^{lo/-}Sca\text{-}1^+c\text{-}kit^+$ (LSK) $CD150^+CD48^-$ cells engrafted and displayed LTR-activity (Kiel et al., 2005). In contrast, a panel defining human LTR-HSCs continues to be fine-tuned. For example, Notta et al.'s engraftment study using UCB-derived HSC/HSPCs not only demonstrated that a sub-population of $Thy1^-$ population have LTR activity, but also elucidated CD49f expression as a defining marker of LTR-capacity. Furthermore, they were able to engraft, 28% in their first experiment and 14% in their second experiment, female NOD-*scid*-IL2*Rgc*$^{-/-}$ (NSG) mice with a single $Lin^-CD34^+CD38^-CD45RA^-Thy1^+Rho^{lo}CD49f^+$ cell (Notta et al., 2011). Thus an updated panel has become available to isolate human HSCs/HSPCs with LTR-capacity. This has been extended further by more recent studies, which seek to finely divide the immature HSPC subsets (Görgens et al., 2013a, Laurenti et al., 2013, Sanjuan-Pla et al., 2013)

Table I.1. Panel of cell surface markers defining mouse and human LTR-HSCs.

Phenotypes Described for LTR-Haemopoietic Stem Cells	
FUNCTIONAL MARKERS	CELL SURFACE MARKERS
$Rh123^{low}$	$CD34^{lo}$c-kit^{+} $Thy1.1(CD90)^{lo}$ $Lin^{-}Sca^{hi}$ (KTLS) [mouse] (Osawa et al.1996)
$Ho33342^{low}$	$CD150^{+}CD48^{-}$ (SLAM) [mouse & human] (Kiel et al. 2005)
$ADLH^{high}$	$Lin^{-}CD34^{+}Thy1^{+}$ [human] (Baum et al.1992; Murray et al. 1995)
PY^{low}	$Lin^{-}CD34^{+}CD38^{-}Thy1^{+}CD45RA^{-}$ [human] (Bhatia et al. 1997; Coneally et al. 1997; Lansdorp et al. 1990)
	$Lin^{-}CD133^{+}CD34^{-}CD38^{-}$ [human] (Gallacher et al. 2000)
	$Lin^{-}CD34^{+}CD38^{-}CD45RA^{-}Thy1^{+}CD49f^{+}$ [human] (Notta et al. 2011)

$Rh123^{low}$, rhodamine 123—vital dye that accumulates preferentially in mitochondria, thus reflecting the active and/or number of mitochondria. Consequently, efflux of Rh123 is most rapid in more primitive and/or quiescent HSC subsets (Uchida N. et al. 1996, Blood); **$Ho33342^{low}$**, Hoechst 33342—fluorescent DNA-binding dye in live cells. As DNA content is highest at the S/G_2-M phase of the cell cycle, low Ho is indicative of quiescent cell populations. The rapid efflux of Ho in quiescent cells enabled identifying this "side population" (SP) and demonstrate their LTR-activity (Goodell M. et al. 1996, J. Exp. Med.). **$ADLH^{high}$**, aldehyde dehydrogenase—$ADLH^{high}$ HSCs were found to be highly enriched for $Lin^{-}CD34^{+}CD133^{+}$ expressing cells. Agents such as cyclophosphamide conjugated to a fluorochrome are metabolised by endogenous ADLH resulting in fluorescing cells, thus levels of ADHL activity can used to select for the most primitive HSCs (Hess D. et al. 2004, Blood); **PY^{low}**, pyronin—dye that intercalates and stains RNA. In conjuction with Ho33342, G_0 HSCs can be differentiated from HSCs in G_1. In G_0 no or very low levels of PY are detected vs Ho^{low} + Py^{high} in cells in G_1 (Roy S. et a. 2012, PlosOne).

For clinical treatment, HSCs/HSPCs enriched samples are harvested by screening for cell surface CD34 antigen expression. In research studies, a wider selection of markers is used to isolate or identify HSC/HSPC enriched populations. Phenotypes listed above showed LTR-activity *in vivo*. Functional markers have also helped elucidate the influential role specialised locations in the BM have on their LTR capacity.

In the haemopoietic stem cell transplantation (HSCT) setting, protocols use a less refined "stem cell" defining profile to infuse HSC/HSPCs into patients for treatment. Antigen CD34, belonging to a family of proteins (CD34-family) which functional role remains unclear, is used as an indicator of the "HSC" dose. CD34 expression has been associated with cell proliferation, enhanced trafficking and migration of haemopoietic cells, cell morphology, as well as blocking differentiation of progenitor cells (Nielsen and Mcnagny, 2008).

Although this cell surface marker is not specific for human HSCs/HSPCs, there are logistical benefits in the clinic to equate quantified $CD34^+$ expression to "HSC" dose. Firstly, screening for a single marker is certainly easier and less costly, and secondly, the number of $CD34^+$ cells/Kg of patient weight can be correlated to the rapidity of haemopoietic reconstitution (Ivanovic, 2010). Interestingly, a recent study proposes using mathematical modelling to carry out a more personalised assessment for determining $CD34^+$ cell dose requirements (Stiehl et al., 2014). Currently, the impact of $CD34^+$ cell dose on HSCT outcome, i.e. speed of neutrophil and platelet reconstitution, is based on retrospective and randomised clinical trials, which give "an idea of the average impact" different treatment alterations have rather than patient specific scenarios (Stiehl et al., 2014). A small cohort of individuals' HSCT therapy is thus put at risk of failing.

Antigen CD133 is a surface glycoprotein (also known as prominin-1) that is increasingly being proposed as alternative or additional cell surface marker for large-scale clinical isolations of HSCs/HSPCs (Handgretinger and Kuçi, 2013). $CD133^+$ HSCs/HSPCs were identified as a subset of $CD34^+CD38^-Lin^-$ and $CD34^-CD38^-Lin^-$ cells able to repopulate NOD/SCID mice (SRC), with $CD133^+CD34^-CD38^-Lin^-$ being precursors of $CD34^+$ progenitors (Gallacher et al., 2000). The purification level of $CD133^+CD34^-CD38^-$Lin is very low (~0.2% within the $CD34^-CD38^-$Lin population) (Bhatia et al., 1998, Gallacher et al., 2000, Takahashi et al., 2013), indicative of a rare HSC/HSPC population. Recently, Görgens et al. used CD133 expression in conjunction with CD34 antigen to distinguish different human HSPC subsets and proposed a new model for human haemopoiesis **[Figure I.3].** Part of their study showed that $CD133^{low}CD34^+CD38^+CD45RA^-$ HSCPs lacked STR-engraftment potential—

they assessed reconstitution activity 8 weeks post-tranplantation—compared to their $CD133^{+}CD34^{+}CD38^{+}CD45RA^{-}$ counterparts, providing corroborating evidence that antigen CD133 is a marker of a more primitive HSCs/HSPCs population than cell surface marker CD34. Numerous other studies have also demonstrated the stem progenitor cell attributes of CD133 on HSC/HSPCs (Calloni et al., 2013, Hess et al., 2006, Pasino et al., 2000, Summers et al., 2004), thus making CD133 an interesting contestant for large-scale clinical "HSC" screening and improving HSC/HSPC engraftment. It will be of interest to screen $Lin^{-}CD34^{+}CD38^{-}CD45RA^{-}Thy1^{+}Rho^{lo}CD49f^{+}$ HSCs/HSPCs for CD133 expression and confirm that this $CD133^{+}CD34^{+}CD38^{+}CD45RA^{-}$ population has LTR-capacity.

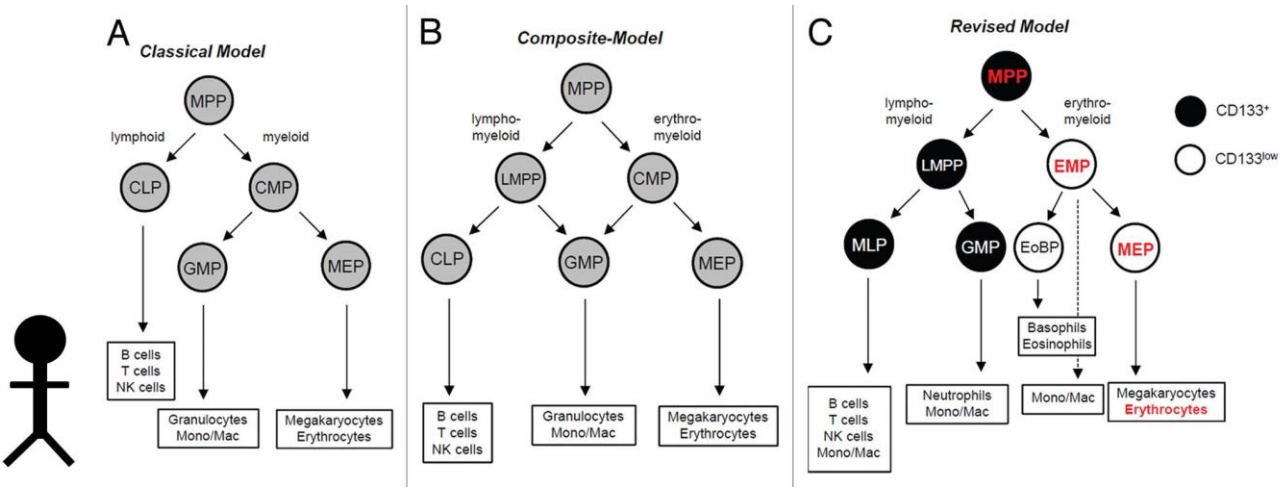

Figure I.3. Models of human haemopoiesis.

[A] In the classical model, haemopoiesis progresses from a multi-potent haemopoietic progenitor (MPP) that was generated from an asymmetric HSC division (Ho and Wagner, 2007) into two lineage committed progenitors: the common lymphoid progenitor (CLP) and the common myeloid progenitor (CMP). These two branches would in turn give rise to successive blood cells of the haemopoietic system. [B] The classical model was challenged when a set of progenitors (GMPs) were shown to possess the ability to differentiate into some of the blood cells (granulocytes and macrophages) of the myeloid lineage but not all. This juxtaposition was translated into the "composite-model", where MPPs give rise to lymphoid-primed multi-potent progenitors (LMPP) and CMPs, both precursors of GMPs (Görgens et al., 2013a). [C] Screening for antigen CD133 enabled demonstrating for the first time asymmetric division in primitive human haemopoietic cells (Beckmann et al., 2007) as well as defining more clearly the cell surface profile of GMPs. MPPs that retain high CD133 expression after differentiation become precursors of GMPs or multi-lymphoid progenitors (MLPs), whereas $CD133^{low}$ expressing cells have been named erythromyeloid progenitors (EMPs) (Görgens et al., 2013b). CD133 antigen has elucidated significant phenotypes of the human haemopoietic tree. Picture credit: Reprinted from Cell Cycle 12:22, Görgens A., Radtke S., Horn P.A., and Giebel B., New relationships of human hematopoietic lineages facilitate detection of multipotent heatopoietic stem and progenitor cells, 2013, pp.3478-3482, under the Content Terms of Usage of Landes Bioscience Terms and Agreement, https://www.landesbioscience.com/user_agreement/.

I.4. The haemopoietic stem cell niche

The home of post-natal HSCs is the BM (Morrison and Scadden, 2014). Here HSCs and HSPCs reside, self-renew, propagate, and get ready to join the main circulatory system. To support such a rich nest of cells, the BM benefits from a number of diverse cell types. Together, these cells form distinct microenvironments, most often referred to as stem cell niches. In fact, the 'HSC niche' was one of the first examples defining the role of a unique microenvironment to support 'stemness' (Schofield 1978). Significant BM niche

cells so far identified and commonly examined include osteoblasts, BM endothelial cells (BMECs), BM stromal cells (BMSCs) more recently referred to as perivascular stromal cells (Ding and Morrison, 2013), mesenchymal stem cells (MSCs), chemokine CXCL12 (also SDF-1)-abundant reticular cells (CAR), sinusoidal endothelial cells (SECs), arteriolar endothelial cells (AECs), and nerve cells (Ehninger and Trumpp, 2011, Morrison and Scadden, 2014). Osteoblasts appeared to play a key role in the retention of HSCs at the endosteum and together with osteoclasts (Miyamoto, 2013) were thought to create a unique osteoblastic or endosteal niche (Calvi et al., 2003, Zhang et al., 2003b). However, BM sections show HSC/HSPC clusters also localise in bone-distal regions, in direct contact with SECs, BMECs (Butler et al., 2010, Ding et al., 2012, Kiel et al., 2005, Rafii et al., 1997), perivascular mesenchymal stem cell populations (Méndez-Ferrer et al., 2010), and even AECs (Kunisaki et al., 2013, Silberstein and Lin, 2013), thus also providing specialised microenvironments that are often referred to as the vascular/perivascular stromal niche **[Figure I.4]**. More interestingly, Lo Celso et al. showed that the osteoblastic niche is in fact well vascularised; BM endothelium to which infused murine LTR-HSCs attached preferentially (Lo Celso et al., 2009) **[Figure I.5A]**. In fact, there are at least two distinct vascular niches: a sinusoidal niche and an arteriolar niche found closer to the endosteal region of the bone, both harbouring LTR-HSCs however the latter maintaining HSCs in a quiescent state (Nombela-Arrieta et al., 2013, Silberstein and Lin, 2013). A three dimensional imaging and antibody staining experiment also showed that osteoblasts are surrounded by SECs, which regeneration ability after myelosuppression directly correlated with levels of haemopoietic recovery (Hooper et al., 2009). Other

vascular zones may also exist in the BM. Lin et al. identified small BM regions containing mesenchymal stromal cells, haemopoietic cells and perivascular HSPCs encapsulated within the trabeculae of murine femoral bones near the growth plate, and have termed these structures haemospheres (Lin et al., 2012).

In contrast to the endosteal/osteoblastic niche, the vascular/perivascular stromal niche was portrayed as a major site for ready-to-migrate HSPCs (Kiel and Morrison, 2006). However, various studies have since provided evidence that both microenvironments are vital for haemopoiesis and HSC/HSPC maintenance. E*x vivo* real-time imaging technology and immunoassaying, which traced the homing of purified green-fluorescent-protein-expressing (GFP^+) HSCs/HSPCs, demonstrated that retaining LTR- and quiescent HSCs are not unique traits of the osteoblastic niche (Xie et al., 2009). Although Xie et al. found that transplanted murine enriched LTR-HSC tended to home to the endosteum in irradiated mice, they localised randomly in non-irradiated mice (Xie et al., 2009). Furthermore, some of the homed LTR-HSCs were actively dividing in the irradiated mice, highlighting a dynamic shift in the role niche cells can play under different physiological conditions **[Figure I.5B]**. Recent studies by Ding et al. investigated the impact of chemokine SDF-1 secretion and stem cell factor (SCF) expression by BM niche cells—perivascular stromal cells, BMECs and osteoblasts—on murine HSC fate, and demonstrated that only perivascular stromal cells were required to retain HSCs and colony-forming progenitors in the BM (Ding and Morrison, 2013, Ding et al., 2012). SDF-1 secretion by osteoblasts specifically maintained early lymphoid progenitors, while not affecting myeloerythroid protenitor maintenance or retention. Oguro et al. also showed that most LTR-HSCs and quiescent subpopulations

disappeared in mice with endothelial and perivascular stromal cells conditionally depleted of SCF (Oguro et al., 2013). On the other hand, while LTR-HSCs can be harvested from the central BM region, more primitive subsets were found to be highly enriched in endosteal zones (Nombela-Arrieta et al., 2013). Supporting evidence was shown by Grassinger et al. in competitive transplantation assays. Murine HSCs derived from the endosteum had "superior proliferation capacity and homing efficiency" compared to their counterparts isolated from the central BM despite being phenotypically identical (Grassinger et al., 2010). Most interestingly, they observed that HSPCs previously defined as B-lymphoid primed haemopoietic cells were also capable of multilineage reconstitution provided they were isolated from the endosteal region. The same year, Winkler et al. also reported that murine $CD41^{-}CD48^{-}CD150^{+}$LSK isolated from the low blood perfused endosteum, measured by Hoechst 33342 (Ho) staining, were more quiescent (Ho^{neg}) and capable of serial transplantation compared to their Ho^{med} counterparts (Winkler et al., 2010) **[Figure I.6B]**. Using micro-computed tomography, histomorphometry, homing and spatial distribution assays, Ellis et al. also observed that $Lin^{-}Sca^{+}Kit^{+}$ homed preferentially to the endosteal niche in the trabecular-rich metaphysis of long bones, and also showed that vasculature was anatomically an integral part of this niche (Ellis et al., 2011). Together, these *in situ* tissue analyses with advanced laboratory techniques revealed that the endosteal area is perivascular and the localisation of LTR-HSCs is not restricted to the "osteoblastic niche". However, evidently, LTR-HSCs regardless of their phenotype preferentially reside close to the perivascular networks at the endosteum.

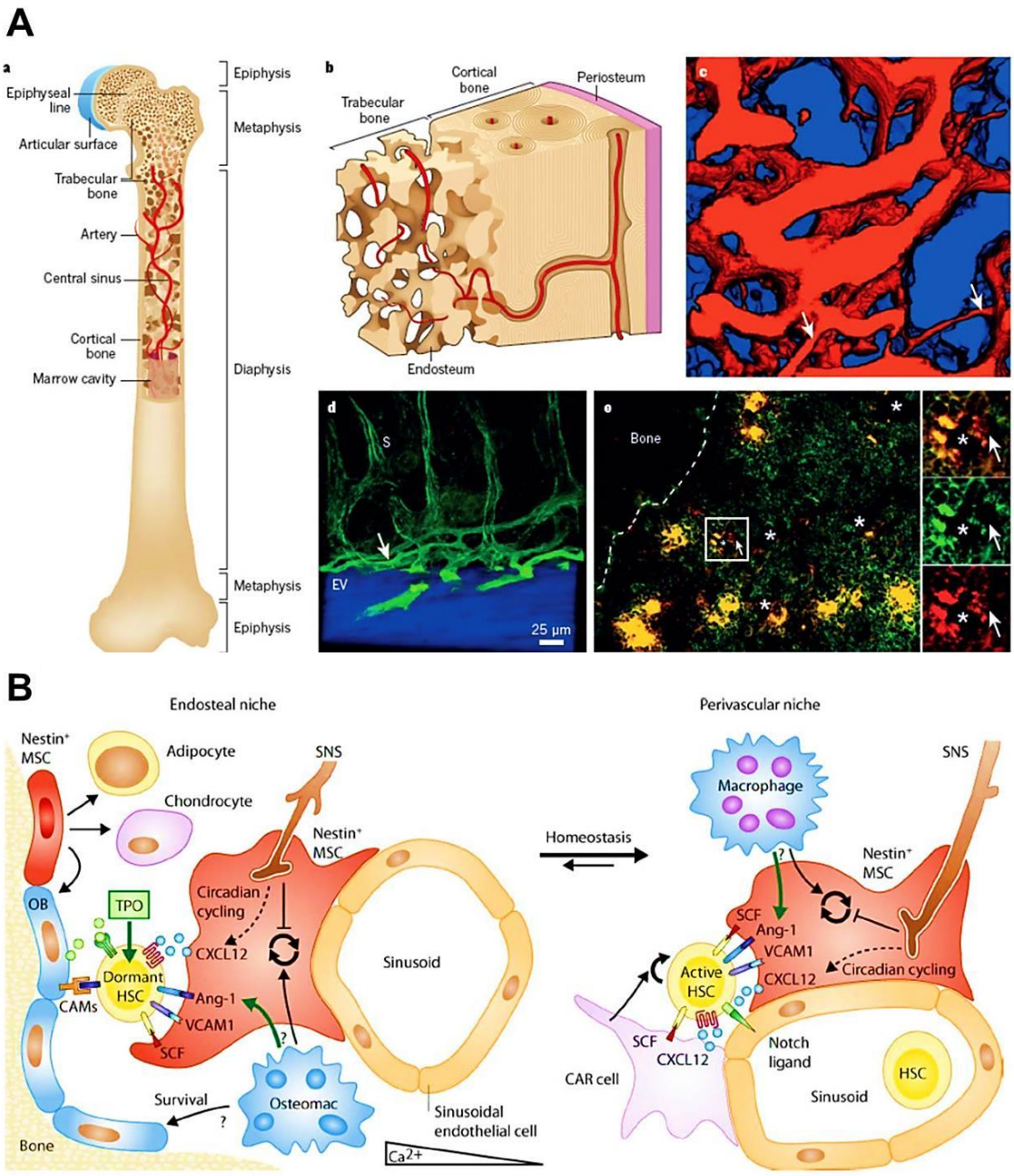
A
a
Epiphyseal line
Articular surface
Trabecular bone
Artery
Central sinus
Cortical bone
Marrow cavity
Epiphysis
Metaphysis
Diaphysis
Metaphysis
Epiphysis
b
Trabecular bone
Cortical bone
Periosteum
Endosteum
c
d
S
EV
25 μm
e
Bone
B
Endosteal niche
Perivascular niche
Nestin+ MSC
Adipocyte
Chondrocyte
SNS
Nestin+ MSC
OB
TPO
Circadian cycling
CXCL12
Dormant HSC
CAMs
Ang-1
VCAM1
SCF
Sinusoid
Survival
?
Osteomac
Sinusoidal endothelial cell
Bone
Ca2+
Homeostasis
Macrophage
SNS
Nestin+ MSC
SCF
Ang-1
VCAM1
CXCL12
Circadian cycling
Active HSC
SCF
CXCL12
Notch ligand
HSC
CAR cell
Sinusoid

Figure I.4. The home of HSCs and progenitor cells.

[A] (a-b) A central sinus feeds oxygenated blood, nutrients and growth factors into the bone marrow (BM) cavity, where arteries branch out towards the trabecular bone to form (c) highly vascularised networks; white arrows point at smaller arteriolar vessels. (d) Cross-sectional images of blood vessels at the endosteum reveal sinusoidal endothelium (white arrow) connected to the central sinus (Nombela-Arrieta et al., 2013). (e) LTR-HSCs/ITR-HSCs were found in close contact with vascular cells, perivascular cells, megakaryocytes (fluorescing yellow) and other haemopoietic cells (Kiel and Morrison, 2008). [B] Cartoon interpretation of the HSC/HSPC microenvironments. Chemokine CXCL12 (also SDF-1)-abundant reticular cells (CAR) cells and nestin^{+} MSCs support the specialised niches found in the BM. HSCs/HSPCs preferentially localised next to CAR cells (Sugiyama T. et al 2006, Immunity). CAR cells surround sinusoidal endothelial cells as well as the endosteum, illustrating their important role in both HSC niches. HSCs and their progeny respond to microenvironmental cues released by the BM niche cells surrounding them. The sympathetic nervous system (SNS) regulates SDF-1 secretion, influencing HSC retention and mobilisation (Katayama et al., 2006, Méndez-Ferrer et al., 2008). Sympathetic nerve fibres are thought to synapse on perivascular cells, close to BMEC and sinusoids for easy an exit into blood circulation. A number of adhesion molecules and receptors on HSCs/HSPCs, such as KIT and Tie2 (tyrosine kinase receptors), thrombopoietin receptor (TPO), very late antigen-4 (VLA-4) and CXCR4 respond to their respective ligands secreted locally—membrane bound stem cell factor (SCF), angipoietin 1 (Ang-1), TPO and SDF-1, respectively—and maintain HSCs in a quiescent state until the need to self-renew and/or differentiate into other blood cell types (Ehninger and Trumpp, 2011, Trumpp et al., 2010). Picture credit: [A] Reprinted from Nature, Review Insight, Vol. 505, Morrison S.J. & Scadden D.T., The bone marrow niche for haemopoietic stem cells, , pp.327-333, Copyright 2014, with permission from Nature Publishing Group, http://dx.doi.org/10.1038/nature12984 . [B] Reprinted from Journal of Experimental Medicine, Ehninger A. & Trumpp A., The bone marrow stem cell niche grows up: mesenchymal stem cells and macrophages move in., 2011, pp.421-428, under the Creative Commons Public License, http://creativecommons.org/licenses/by-nc-sa/3.0/legalcode .

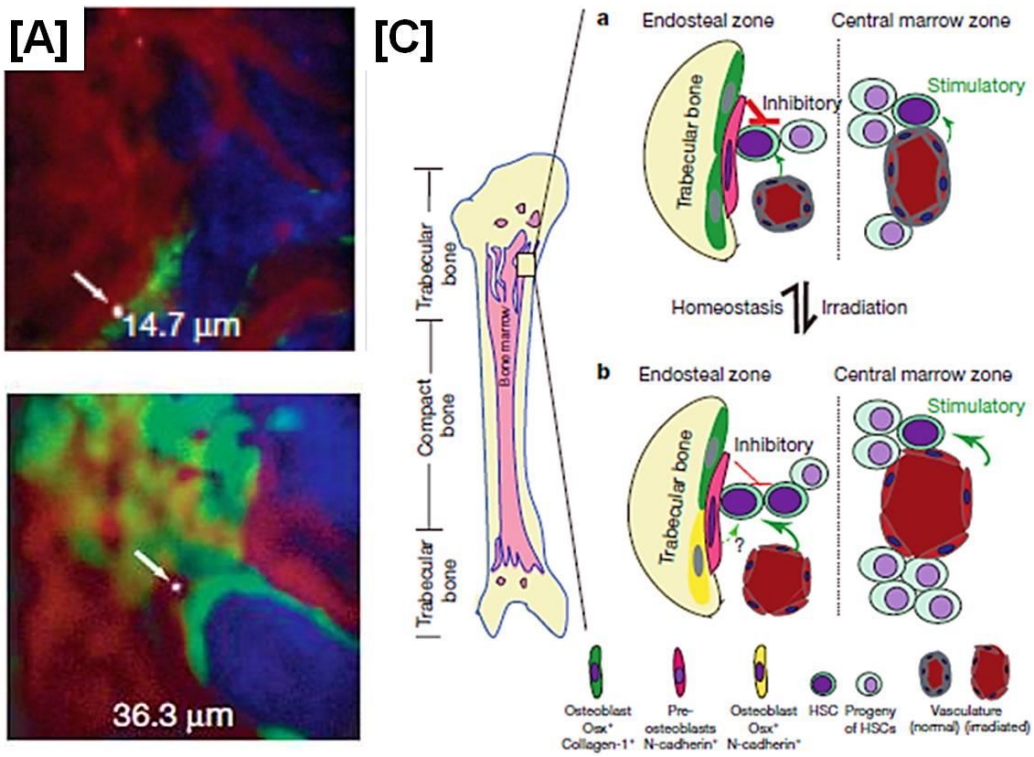

Figure I.5. Real time imaging in the bone marrow elucidates HSC localisation.

[A] GFP+ve osteoblasts (green) and vascular cells stained with Qdots (red dye). HSCs localised between 15-40 µM (>30 µM in non-irradiated mice) from the endosteum, with much closer proximity to vasculature, suggesting that HSCs maintenance in the osteoblastic niche could be coupled with signals from the surrounding vascular cells (Lo Celso et al., 2009). [B] Under healthy conditions, the endosteal region keeps lodged HSCs in a non-cycling state but will support their expansion in response to BM damage (Xie et al., 2009). Picture credit: [A] Reprinted from Nature, Vol. 457, Lo Celso C., Fleming H.E., Wu J.W., Zhao C.X., Miake-Lye S., Fujisaki J., Cote D., Rowe D.W., Lin C.P., and Scadden D.T., Live-animal tracking of individual haematopoietic stem/progenitor cells in their niche, pp. 92-97, Copyright 2014, with permission from Nature Publishing Group, http://www.nature.com/nature/journal/v457/n7225/full/nature07434.html. [B] Reprinted from Nature, Vol. 457, Detection of functional haematopoietic stem cell niche using real-time imaging, Xie Y., Yin T., Wiegraebe W., He X.C., Miller D., Stark D., Perko K., Alexander R., Schwartz J., Grindley J.C., Park J., Haug J.S., Wunderlich J.P., Li H., Zhang S., Johnson T., Feldman R.A. & Li L., pp. 97-102, Copyright 2014, with permission from Nature Publishing Group, http://www.nature.com/nature/journal/v457/n7225/full/nature07639.html.

The idea of two defined and spatially distinct microenvironments has clearly been challenged by a number of recent studies. New data continue to elucidate the complexity of this organ and continues to raise interesting questions. For example, how well blood-perfused are these vascular networks, particularly those identified at the endosteum? Poor blood-perfusion suggests lower oxygen levels and nutrients (Lévesque and Winkler 2011), implicating downstream effects on HSC fate decisions. Oxygen levels as low as 1.3% (Levesque et al., 2007, Parmar et al., 2007) would surely affect intracellular dynamics and interactions between HSCs and their niche cells?

I.5. Hypoxic areas in the bone marrow

Hypoxic oxygen levels are a distinctive feature of the healthy BM environment. In contrast to most mammalian tissue that range between 5% and 13% oxygen (40 mmHg to 100 mmHg) and an atmospheric oxygen tension around 21% (150 mmHg), a mathematical model of (Chow et al., 2001b) predicted that HSCs reside in regions that are almost anoxic. This prediction was supported by improved *ex-vivo* haemopoiesis in 1% and 3% oxygen (Danet et al., 2003). Parmar et al. evaluated the distribution of HSC subsets along a Hoechst dye (Ho) perfusion gradient, where the lowest oxygen tension was correlated with the lowest blood supply and therefore with the lowest uptake of the dye (Parmar et al., 2007). Interestingly, tirapazamine a drug that is only toxic under hypoxic conditions was lethal to LTR-HSCs, strongly supporting earlier observations that HSC preferentially localise in the endosteum. In a corroborative study, Levesque et al. perfused murine BM with pimonidazole (PIM), which only binds to protein thiol groups below 1.3% oxygen **[Figure I.6A]**.

The endosteum showed the highest PIM staining under steady state conditions compared to tissue in the central BM as well as expression of hypoxia inducible transcription factor-1 (HIF-1) (Levesque et al., 2007). Further work by Levesque's group examined the levels of blood perfusion by measuring fluorescence intensity of Ho in harvested BM HSCs/HSPCs, BMECs, MSCs and osteoblasts of mice. They observed an increasing Ho^{neg} population in HSCs expressing a more primitive stem cell phenotype, as well as 80-85% Ho^{neg} osteoblasts. MSCs and endothelial cells were largely Ho^{bright}, however, a very small proportion (but larger than that of MSCs) of endothelial cells were Ho^{neg} (Winkler et al., 2010). Could these be BMEC or SECs found at the endosteum? Levesque et al. propose that the % of Ho^{neg} endothelial cells would increase under shorter *in vivo* Ho incubation times, e.g. <1-2 minutes, as the perfusion time would also be shorter. Consequently only endothelial cells in larger vessels would be stained with Ho (unpublished comments). Conversely, Nombela-Arrieta et al., particularly interested in examining the hypoxic status of BM microenvironments, determined extremely low oxygen supply by the uptake of PIM (termed Pimo) and by the expression of hypoxia inducible transcription factor (HIF-1α) in mice. Remarkably, they frequently observed "$Pimo^{hi}$ perivascular c-kit^{+} progenitors" (HSPCs) directly adjacent to $Pimo^{low/neg}$ $B220^{+}$ cells sharing the same extracellular environment. Furthermore, HSPCs that had localised throughout the different regions of the BM expressed HIF-1α at comparable levels (Nombela-Arrieta et al., 2013). Nombela-Arrieta et al. propose revisiting the accepted notion of a "super hypoxic HSPC niche in the BM". However, despite BM oxygen levels not being physically measured in the human, for example with oxygen probes, previous studies do provide

convincing evidence that oxygen levels at the endosteum are hypoxic, with hypoxic pockets also apparent close to vasculature (Kubota et al., 2008). Notably, the recent review by Morrison and Scadden reveals that a study specifically measuring hypoxic conditions in murine BM using a nanoprobe is *in press* (Morrison and Scadden, 2014). This will provide interesting new insights on hypoxia in the BM.

Local concentrations of oxygen will depend largely on the speed of local blood perfusion (Chow et al., 2001b). The fenestrated composition of sinusoids, for example, causes blood to flow particularly slowly (Takubo and Suda, 2012)—blood refills and empties mechanically at irregular intervals; a dilation phase of 1-2 minutes in rabbits (Branemark, 1961a, Branemark, 1961b). Furthermore, a large proportion of oxygen is taken up by cells consuming it in the central region of the BM, consequently decreasing the rate at which oxygen and nutrients diffuse from blood vessels into adjacent tissue at the endosteum (Dyke et al., 1965). The heterogeneous composition of blood will also influence flow through microscopic vessels (Fung and Zweifach, 1971). Highly vascularised networks even at the endosteum are not indicative of a surplus supply of oxygenated blood. In fact, hypoxia induces angiogenesis via hypoxia up-regulated vascular endothelial growth factor (VEGF) (Shweiki et al., 1992), thus perhaps driving the formation of highly vascularised networks. This could trigger an increase in blood supply in some areas, and provide adequate oxygenation. However, other areas may become compromised, with decreased or irregular blood flow, creating hypoxic microenvironments. These phenomena have been proposed in kidney allografts during chronic rejection (Bruneau et al., 2012).

To adapt to hypoxic conditions, cells benefit from HIFs that regulate gene expression. HIF-1α was found at elevated levels in HSCs/HSPCs (Simsek et al., 2010), which becomes stabilised by prolyl hydroxylase (PHD) under hypoxic conditions. Evolutionary analysis of the HIF system propose HIFα/PHD genes duplicated twice at the base of the vertebrate subphylum creating four genes, with HIF-1 to HIF-3 remaining in humans today (Loenarz et al., 2011). The potential role of isoform HIF-2α was recently investigated in HIF-2α deficient mice, and was found "dispensable" for HSC self-renewal and post-transplantation engraftment; having no impact on murine HSC survival and their long-term capacity (Guitart et al., 2013). However, knowckdown of HIF-2α in UCB-$CD34^{+}CD38^{+}$ cells (late MPPs) impaired their LTR-ability, suggesting HIF-2α may play a key role in the less primitive HSC subsets (Rouault-Pierre et al., 2013). Little has been reported on human HIF-3.

Stabilised HIF-1α translocates to the nucleus and forms a heterodimer dimer with oxygen-independent subunit HIF-1β, to bind to upstream consensus sequences known as 'hypoxia response elements' (HREs) (Brahimi-Horn and Pouyssegur 2009; Wenger et al. 2005). At higher levels of oxygen (>5% O_2) the proline residues on HIF become hydroxylated by PHD (Berra et al. 2003), triggering the degradation of HIF by an E3 ubiquitin ligase protein, Von Hippel-Lindau (VHL). The major consumption of oxygen by aerobic organisms is via the mitochondrial cytochrome system (Chandel et al., 2000). Thus, one could suggest the cytochrome system would function as an oxygen sensor. However, cytochrome oxidase has a very high affinity for oxygen (Km = 1 μM), even under hypoxic conditions where oxygen levels are approximately 100 μM. Clearly, cytochrome oxidase is not limited at hypoxic oxygen levels. On the

other hand, PHD has a Km for oxygen of ca. 200 µM (Ratcliffe, 2013), catalysing the hydroxylation of proline at 50% of the maximal rate. Thus, in hypoxic areas of the BM at 100 µM oxygen, PHD will struggle to hydroxylate proline residues on HIF. This makes PHD an ideal oxygen sensor and explains its use in the HIF-1α system (Berra et al., 2003, Myllyharju, 2013, Myllyharju and Koivunen, 2013). Noteworthy is that stabilisation of HIF-1α in HSCs/HSPCs appears not to be solely regulated by physiological oxygen tension. Other niche factors, interestingly cytokines (thrombopoietin) TPO and SCF, have also been shown to stabilise HIF-1α under normoxic conditions (Kirito et al., 2005, Pedersen et al., 2008). Nonetheless, Levesque et al. showed in their study that hypoxia induced HIF-1α to a much higher extent than the presence of recombinant human granulocyte colony-stimulating factor (G-CSF), human SCF or TPO in BM cells under normoxic conditions. Furthermore, adding these cytokines under hypoxic conditions had marginal effects on HIF-1α protein expression (Levesque et al., 2007).

The role hypoxia signalling may exert on HSCs/HSPCs has already been associated with cell metabolism as well as quiescence and expansion, with HIF-1α at the heart of these tightly regulated processes (D'aprile et al., 2014, Gezer et al., 2014, Pollard and Kranc, 2010, Takubo and Suda, 2012). Most recently, Takubo et al. confirmed LTR-HSCs utilise anaerobic metabolism, and that this is mediated via HIF-1α regulated pyruvate dehydrogenase kinase (Pdk2 and Pdk4) activation. Most importantly, the loss of HIF-1α with subsequent decreased expression of Pdks disrupted cell cycle quiescence and the LTR capacity of these murine HSCs (Takubo et al., 2013), demonstrating the impact HIF-1α expression has on these cellular processes in HSCs. Singh et al.

showed in mice that particularly loss of PHD2 resulted in HIF-1α driven proliferation (self-renewal) specifically of LSK-HSC subsets (early MPPs) under steady-state conditions, having no effect on downstream progenitors (CMPs and LMPs), and enhanced the self-renewal capacity of transplanted PHD2-deficient HSCs (Singh et al., 2013). Similar effects were observed in UCB-$CD34^{+}CD38^{-}$ cells (early MPPs), where knocking down HIF-1α affected their self-renewal and LTR-capacity (Rouault-Pierre et al., 2013).

Further research surrounding the impact hypoxia may have on the HSC niche cells and HSC/HSPC fate is thus of considerable interest. For example, the role HIF-1α stabilisation might play during homing and engraftment of UCB-HSCs to the BM had not been examined at the commencement of this thesis. Rouault-Pierre et al. tested whether knockdown of both HIF-1α and HIF-2α might affect the homing of transduced UCB-$CD34^{+}$ cells and found no significant difference compared to the control group (Rouault-Pierre et al., 2013). However, other unanswered questions remain. Does hypoxia enhance migration towards the endosteum? Does it increase or decrease the ability of UCB-HSCs to attach and lodge in the BM? Answers to these questions would contribute vastly to advances in HSC transplantation (HSCT).

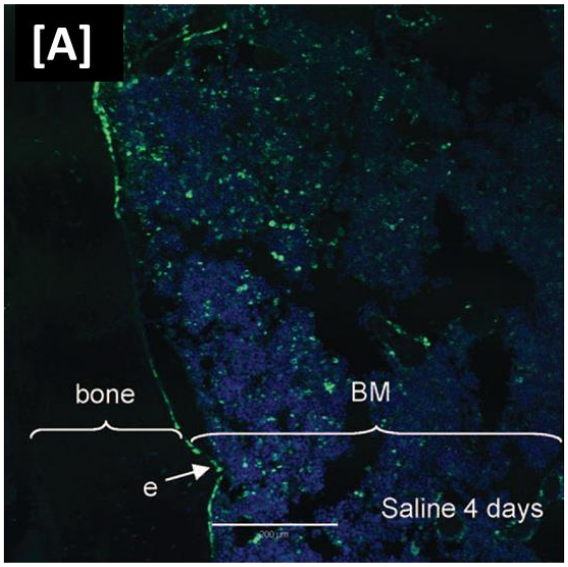

Figure I.6. Hypoxia at the endosteum.

[A] Hypoxic cells show positive PIM staining predominantly at the endosteum (Levesque et al., 2007).Picture credit: [A] Reprinted from Stem Cells, Vol. 25, Lévesque J.P, Winkler I.G., Hendy J., Williams B., Helwani F., Barbier V., Nowlan B., Nilsson S.K.,Hematopoietic Progenitor Cell Mobilization Results in Hypoxia with Increased Hypoxia-Inducible Transcription Factor-1α and Vascular Endothelial Growth Factor A in Bone Marrow, pp. 1954-1965, Copyright 2014, with permission from John Wiley and Sons.

I.6. Molecules regulated by hypoxia in HSCs/HPCs

Intrinsic and extrinsic molecules, including naturally occurring elements such as oxygen and calcium, profoundly influence HSC fate decisions, regulating daily blood cell production (haemapoiesis) to maintain steady state levels in the peripheral circulation. Calcium sensing receptors (CaR) have been identified on HSCs/HSCPs and guide migrating cells towards the Ca^{2+} rich microenvironment in the BM and are required for successful lodging at the endosteal niche (Adams et al., 2006, Lam et al., 2011). The SDF-1/CXCR4 signalling axis is particularly crucial to retain HSCs/HSPCs in the BM (Sugiyama et al., 2006) but also during HSC/HSPC homing and engraftment (Lapidot et al., 2005, Peled et al., 1999a). A number of molecules common to the BM are hypoxia regulated. Not surprisingly, this includes chemokine SDF-1 and its receptor CXCR4. Ceradini et al. were the first to show a direct correlation between elevated levels of SDF-1α with decreasing oxygen levels, both *in vivo* and in endothelial cells *in vitro,* and demonstrated regulation by HIF-1α (Ceradini et al., 2004). HIF-1α regulated expression of Gαi-protein-coupled transmembrane receptor CXCR4 had been reported just a year before (Schioppa et al., 2003) also in haemopoietic cells. The SDF-1/CXCR4 axis activates downstream events that lead to activation of integrins, phosphorylation of focal adhesion kinases and the recruitment of adaptor molecules. For example, phosphatidyl-inositol-3-kinase (PI3K) and phospholipase C (PLC) are activated upon SDF-1α stimulation and mediate the phosphorylation of focal adhesion kinase (FAK). FAK is a major signalling component regulating focal adhesion activity during cell motility (Deramaudt et al., 2011). Another prominent blood associated molecule known to be upregulated by hypoxia is

the vascular endothelial growth factor (VEGF). Already known for being a key regulator in vasodilatation, vascular permeability and angiogenesis, most recent data confirm its strong cooperation in stem cell mobilisation and haemopoiesis. Disruption of HIF-1α VEGF regulation increased the pool of more differentiated HSC progenitor cells, highlighting the vital role hypoxia plays on HSC fate in the BM via HIF regulation (Rehn et al., 2011). A final example of another hypoxia regulated gene is the recently detected soluble as well as a GPI membrane-anchored protein Cripto. Highly expressed on HSCs, researchers demonstrated that hypoxia induced Cripto signalling through its receptor GRP78 and maintained HSCs in a quiescent state at the endosteum, whilst inhibition of this pathway caused $GRP78^{+}$HSCs to mobilise into the central BM area (Miharada et al., 2011, Miharada et al., 2012). Hypoxia clearly plays a role in maintaining the HSC pool in the BM and regulating their 'fate'.

I.7. Intracellular scaffolding protein HEF-1

Our laboratory has also examined the effects of hypoxia on gene regulation in HSPCs. Transcriptional profiling of UCB-$CD133^{+}$ cells in response to 1.5% O_2 identified 183 genes that responded to hypoxia (Martin-Rendon et al., 2007). The vast majority were upregulated, including homing molecules CXCR4, SDF-1α, and VLA-4. HEF-1/Cas-L/NEDD9 (HEF-1) was another of the upregulated protein that captured our attention. HEF-1 is a member of the Crk-associated substrate (CAS) family known to act as scaffold-adaptor molecules to regulate protein complexes involved in migration, apoptosis and cell cycle in other cell systems. Most interestingly, HEF-1 has already been identified as a signal transducer during "inside-out" T cell adhesion and migration, cooperating

with Chat-H—forming the Chat-H-HEF-1 signalling complex—to activate Rap1 upon SDF-1 stimulation (Regelmann et al., 2006) (Regelmann et al., 2006). These attributes and its apparent regulation by hypoxia in UCB-CD133^{+} cells made HEF-1 a particularly interesting molecule to investigate. Indeed, Kim et al. confirmed the binding of transcription factor HIF-1α to a hypoxia-responsive element of the HEF-1 promoter in colorectal carcinoma cells, with consequent upregulation of HEF-1 more than doubling the number of cells migrating through collagen type I (Kim et al., 2010a). They also observed that silencing of HEF-1 significantly disrupts the interaction between HIF-1α and co-transcriptional factor p300, proposing a HIF-1α/HEF-1 positive feedback loop where HIF-1α induction of HEF-1 in turn enhances HIF-1α transcriptional activity. A better understanding of the role and function of this putative signalling molecule is thus not only useful to fight the spread of cancer; it may also be another crucial HSCs homing and engraftment molecule with therapeutic potential.

Today HEF-1 is often described as an oncogene, playing a key role in melanoma metastasis (Kim et al., 2006) and promoting oncogenic development and invasion in lung (Chang et al., 2012), mammary (Izumchenko et al., 2009, Tikhmyanova and Golemis, 2011), colorectal (Li et al., 2011) and brain (Natarajan et al., 2006) tumours. However, HEF-1 was first associated with cell polarization, localising to focal adhesion sites and interacting with integrin effector proteins **[Figure I.7]**. It was discovered in early embryonic brain and named NEDD9 (Neural precursor cell Expressed, Developmentally Down-regulated) (Kumar et al., 1992), but acquired the name of Human Enhancer of Filamentation 1 (HEF-1) for inducing filamentous budding in yeast *Saccharomyces cerevisiae* when screening for genes that coordinate cellular

signalling and morphology (Law et al., 1996). In the same year, HEF-1 was also identified by a different group and named Cas-L (Crk-associated substrate related protein, Lymphocyte type) for binding to the integrin effector proteins Crk, Nck, and SHPTP2 following β1-integrin ligation (Minegishi et al., 1996). The formation of the CasL-Crk-C3G complex activates GTPase Rap1 of the Ras GTPase superfamily, driving integrin-mediated adhesion (Ohashi et al., 1998). HEF-1 can also form a complex with Crk-Dock180 to signal upstream of a second GTPase called Rac (Bouton et al., 2001), enabling HSC migration and engraftment (Cancelas et al., 2005). Other studies support its role in cell motility (Fashena et al., 2002), adhesion (O'neill and Golemis, 2001, Zheng and Mckeown-Longo, 2006), and demonstrate its role in cell proliferation and survival (Dadke et al., 2006, Law et al., 2000, Pugacheva and Golemis, 2005).

The predicted molecular weight of HEF-1 is ~93 kDa. However it is most commonly visualised from SDS-PAGE gels in its phosphorylated forms of 105 and 115 kDa. In the simple model for HEF-1 activation, FAK tyrosine phosphorylates HEF-1 (p105) in response to “outside-in” signalling. During outside-in signalling ligation of β1-integrins occurs (Minegishi et al., 1996) during cell attachment and activates FAK. Phosphorylated 105[HEF-1] triggers binding site for non–receptor tyrosine kinases c-Src (Src) that hyper-phosphorylates p105-HEF-1 to the 115 kDa form (p115) (Singh et al., 2007). It is thus the action of cell contact (adhesion) that regulates the conversion of p105 to p115 HEF-1 (Liu et al., 2000b, Zheng and Mckeown-Longo, 2006, Zheng and Mckeown-Longo, 2002). Hence, the p115 is not detected in protein extractions from cells in suspension.

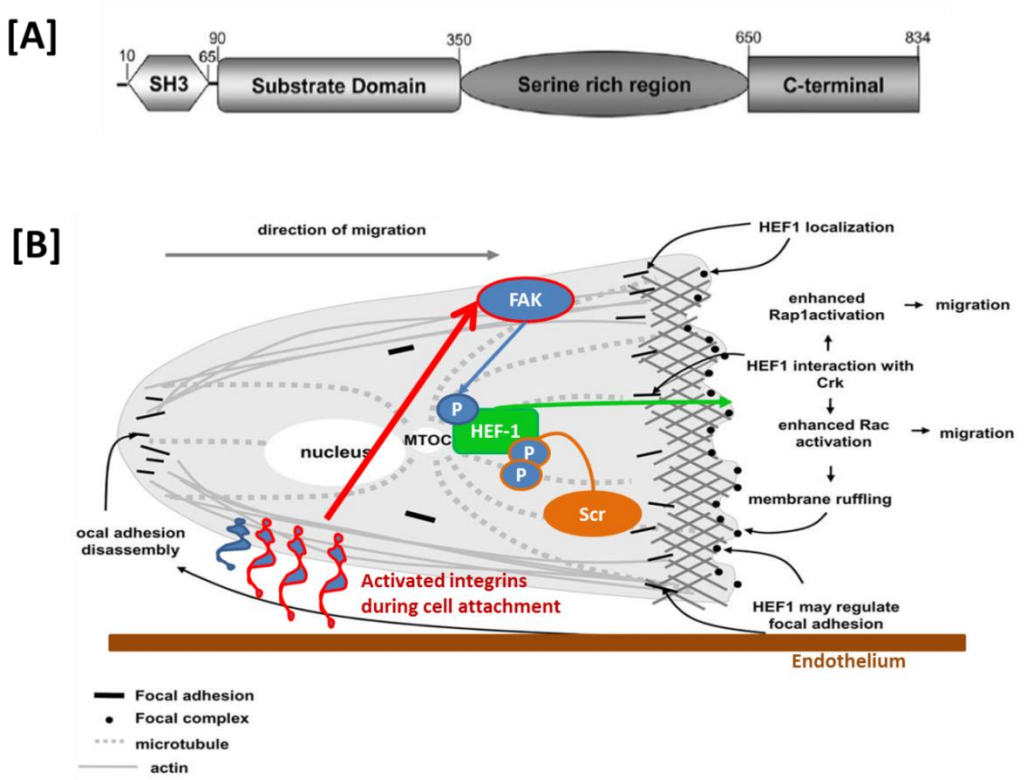

Figure I.7. HEF-1 activation and consequent signalling to induce cell migration.

[A] HEF-1 is a scaffolding adaptor protein with its full length comprised of 824 amino acids divided into four main binding sites: i) the N-terminal SH3 domain, which enables binding of proteins containing a poly-proline motif; ii) the substrate domain largely comprised of SH2 binding sites with tyrosine-containing motifs when phosphorylated allow binding to molecules also presenting SH2 domains; iii) a serine rich region that is conserved amongst focal-adhesion associated proteins; and finally iv) the carboxyl (C)-terminal domain, which is highly conserved in the Cas protein family (Singh et al., 2007). Both the SH3- and C-terminal domain can be targeted to disrupt focal adhesions (O'neill and Golemis, 2001, Stefan et al., 2002). [B] HEF-1 has no catalytic activity but instead localises to focal adhesion sites where it recruits and assembles with other focal adhesion molecules to regulate cell attachment or drive cellular movement (Fashena et al., 2002, Kim et al., 2006, Tikhmyanova et al., 2010).Picture credit: Reprinted from Cell Biochemistry and Biophysics, Singh M.K., Cowell L., Seo S., O'Neill G.M., Golemis E.A., Molecular basis for HEF1/NEDD9/Cas-L action as a multifunctional co-ordinator of invasion, apoptosis and cell cycle, p. 54-72, Copyright 2014, with the permission from Springer.

The multifunctional ability of HEF-1 is evident, exerting its role at the centre of various signalling cascades that drive migration, adhesion and proliferation in various cell types, including haemopoietic cells. We thus hypothesise that HEF-1 plays a direct role in enhancing the transmigration of UCB-CD133^{+} cells towards chemokine SDF-1α, and its upregulation by hypoxia facilitates lodgement of HSCs at the endosteum.

I.8. Practical applications to transplantation therapy

Patients with leukaemia, aplastic anaemia, and some immune deficiency diseases may receive a BM transplant to help cure the disease. However, human leucocyte antigen (HLA)-mismatching limits BM transplantation from unrelated adult donor and may carry a high risk of graft-versus-host disease (GvHD)(Fürst et al., 2013). The promise of stem cells in transplantation therapies has fuelled a fast growing and pioneering research area, which offers treatments for degenerative diseases, replacement of tissue and organs, and drug discovery. HSCs can be harvested from BM, mPB or UCB and transplanted into the recipients' myeloablated BM. If non-diseased stem cells cannot be obtained from the patient (autologous transplantation), a healthy related or unrelated donor needs to be found (allogeneic transplantation). UCB have become an accepted source of HSC therapy. Thanks to the more naïve nature of HSCs/HSPCs enriched isolations from UCB, less stringent HLA-matching is required prior to transplant (Cheuk, 2013, Harris et al., 1992, Kita et al., 2011, Wagner et al., 1996). Although, new studies suggest using more advanced HLA-typing methods even for UCB, i.e. high resolution HLA typing, as increasing mismatches of the HLA-loci were associated with increased transplant-related mortality (TRM) (Van Besien, 2013).

The ability to cryopreserve UCB-HSCs for future use greatly benefits ethnic minorities who cannot readily find a donor on BM registries. Over 600,000 cryopreserved UCB units have been stored worldwide for clinical use . However, a major drawback associated with UCB is the limited cell number obtained from each donation (Ballen et al., 2013, Rocha et al., 2009). The

recommended threshold for transplantation is currently 2-3 x10^6 total nucleated cells (TNC)/Kg (Marquez-Curtis et al., 2011, Van Besien, 2013), with higher numbers required for treating non-malignant disorders. For cord blood derived HSCs/HSPCs, as high as 5x10^7 TNC/Kg are infused (Ballen et al., 2013). The total number of HSCs/HSPCs transplanted is important because "cord-blood cell dose is a crucial determinant of engraftment and transplant-related mortality, particularly in adolescent and adult recipients of HLA-mismatched cord blood" (Eapen et al., 2007). For efficacy, HSCs/HSPCs infused into the bloodstream need to home to the BM and engraft in the specialised microenvironmental niches that support the maintenance and regulate the function of these progenitor cells. Current protocols may use double cord blood units to inoculate higher cell numbers into recipients, whilst additional strategies such as *ex vivo* UCB- HSCs/HSPCs expansion, co-transplanting cord blood with haploidentical HSCs/HSPCs from BM or co-infusion of cord blood with MSCs are being evaluated in clinical studies (Scaradavou et al., 2013, Stanevsky et al., 2010). Thus, it is of paramount interest to improve the homing and engraftment ability of UCB- HSCs/HSPCs.

One of the long term goals of our laboratory is to improve HSCT therapy by enhancing the potential of $CD133^+CD34^+$ cord blood stem cells for transplantation therapy. As with most complex biological systems, the molecular mechanisms governing haemapoiesis, including homing and engraftment are many, with overlapping interactions and some redundancies. The challenge is to elucidate molecules, such as the SDF-1/CXCR4 interaction, that are key players in directing the 'fate' of HSC, i.e. their localisation in the BM and ability to generate progenitor cells. Improving our understanding of the *milieu intérieur*

of the BM should facilitate manipulating molecular mechanisms that enhance homing and engraftment, hence increase the number of successful HSCTs. A number of recent studies have already explored the potential hypoxia conditioning may have on inducing HSC expansion, as well as maintaining HSC in a quiescent state until stimulated to proliferate (Csaszar et al., 2012, Danet et al., 2003, Hofmeister et al., 2007). Furthermore, to optimise the clinical outcome of HSCT, many laboratories routinely "manipulate" the graft before and after transplantation (Austin et al., 2008). Thus, investigating how naturally occurring conditions in the BM such as hypoxia might influence HSC fate by inducing the stabilisation of HIF-1α and/or hypoxia regulated genes should be considered as potential non-invasive interventions to enhance HSCT.

I.9. Specific aims & objectives

The main aim of this DPhil was to investigate mechanisms that govern the fate of HSCs in the BM and enhance the homing and engraftment potential of UCB-CD133$^+$ cells for HSCT. To achieve this aim, specific research objectives included examining the effects of hypoxia on adhesion and transmigration of HSCs with special reference to the possible role of HEF-1. The research described here falls into three main phases:

1. Optimising functional assays, which included:

    a. Isolating CD133$^+$ cells from human umbilical cord blood.

    b. Defining model cell lines KG-1 and KG-1A.

    c. Cell surface profiling BM niche cells osteoblasts, BMSCs and BMEC-60.

d. Determining the optimal concentration of cells for the adhesion assay.

e. Determining the optimal dose response to chemokine SDF-1α for UCB-CD133^{+} cell migration across BMEC-60.

f. Validating hypoxic conditions in all participating cell types.

2. Effects of hypoxia on adhesion and transmigration by:

a. Testing 3 different hypoxic treatments on adhesion of UCB-CD133^{+} and KG-1 cells.

b. Determining an effective time-course for hypoxia pre-conditioning on UCB-CD133^{+} cell transmigration towards chemokine SDF-1α.

c. Determining the effects of hypoxia on HEF-1 protein expression in KG-1 and UCB-CD133^{+} cells.

3. Achieving long-term HEF-1 knockdown in UCB-CD133^{+} cells. This involved identifying a suitable lentiviral-based vector system to knockdown HEF-1 by:

a. Testing 3 transfer vectors and 6 shRNAs

b. Developing a suitable transduction protocol for UCB-CD133^{+} cells.

c. Testing 3 different high titre lentiviral stocks

Chapter II Materials and Methods

II.1. Reagents

Reagents	Manufacturer
Accutase	PAA Laboratories GmbH, Pasching, Austria
Anti-human Actin	BD Transduction Laboratories™, UK
Anti-human GAPDH	Abcam®, Cambridge, UK
Anti-human HEF-1, mouse monoclonal [2G9]	Abcam®, Cambridge, UK
Anti-human HIF-1α	BD Transduction Laboratories™, UK
Anti-human α-tubulin	Abcam®, Cambridge, UK
BCECF-AM (2',7'-bis-(2-carboxyl)-5(and -6)-carboxyfluoresce)	Invitrogen™ Ltd., Life Technologies, Paisley, UK
Blood and Hank's balanced salt solution (HBSS)	PAA Laboratories GmbH, Pasching, Austria
Bovine Serum Albumin (BSA)	Sigma Aldrich Co. LLC., Gillingham, UK
CD133 Microbeads	Miltenyi Biotec Ltd., GmbH, Bergisch, Gladbach, Germany
Collagenase from *Clostridium histolyticum*	Sigma Aldrich Co. LLC., Gillingham, UK
Dimethylsulphoxide (DMSO)	Sigma Aldrich Co. LLC., Gillingham, UK
Dulbecco's Modified Eagle Medium (DMEM)	Lonza Ltd., Wokingham, Berkshire, UK (Lonza)
Dulbecco's Phosphate Buffer Saline (DPBS)	PAA Laboratories GmbH, Pasching, Austria
ECL anti-mouse IgG horseradish peroxidise linked	AmershamTM, GE Healthcare UK Ltd.
ECL Western Blot Detection Reagents	Amersham™, GE Healthcare UK Ltd., Buckinghamshire, UK
Endotheliumm Cell Basal Medium-2 with EGM-2® SingleQuot® Kit Suppl. & Growth Factors = EGM-2	Lonza Ltd., Wokingham, Berkshire, UK (Lonza)
Ethanol	VWR International Ltd., Lutterworth, UK

Fetal bovine serum (FBS)	PAA Laboratories GmbH, Pasching, Austria
Geneticin (GIBCO)	Invitrogen™ Ltd., Life Technologies, Paisley, UK
Hydrocortisone	Sigma Aldrich Co. LLC., Gillingham, UK
Interleukin-1β (IL-1β)	BioSource International, Inc., USA
Isopropanol	VWR International Ltd., Lutterworth, UK
Lipofectamine 2000	Invitrogen Ltd., Life Technologies, Paisley, UK
LSM 1077 lymphocyte Separation Medium (LSM 1077)	PAA Laboratories GmbH, Pasching, Austria
Luria Broth	Sigma Aldrich Co. LLC., Gillingham, UK
MEM Non-Essential Amino Acids Solution 100x (GIBCO)	Invitrogen™ Ltd., Life Technologies, Paisley, UK
Myelocult medium	STEMCELL Technologies™, Grenoble, France
OptiMem medium (GIBCO)	Invitrogen™ Ltd., Life Technologies, Paisley, UK
Osteoblast Basal Medium with OGM™Single™Quotes® = OGM	Lonza Ltd., Wokingham, Berkshire, UK (Lonza)
Penicilin-Streptomycin (P/S) 100x	PAA Laboratories GmbH, Pasching, Austria
Puromycin from *Streptomyces alboniger*	InvivoGen, BioScience, Life Sciences, Nottingham, UK
Recombinant human Fms-like tyrosine kinase 3 ligand (Flt-3)	R&D systems, Minneapolis, MN, USA
Recombinant human Interleukin-6 (IL-6)	R&D systems, Minneapolis, MN, USA
Recombinant human Stem Cell Factor (SCF)	R&D systems, Minneapolis, MN, USA
Recombinant human thrombopoietin (TPO)	R&D systems, Minneapolis, MN, USA
Retronectin	Clontech Laboratories Inc., Takara Bio Company ©, Saint-Germain-en-Laye, France
Roswell Park Memorial Institute (RPMI) 1640	PAA Laboratories GmbH, Pasching, Austria

Sodium pyruvate	Invitrogen™ Ltd., Life Technologies, Paisley, UK
StemSpan serum-free expansion medium (StemSpan SFEM)	Stem Cell Technologies, Grenoble, France
Stromal derived factor-α (SDF-1α)	PeproTECH, Rocky Hill, NJ, USA
SuperSignal West Dura Extended Duration Chemiluminescent Substrate	Thermo Fisher Scientific Inc., Rockford, IL USA
To-pro3 Iodide	Invitrogen™ Ltd., Life Technologies, Paisley, UK
Trisodium Citrate	VWR International Ltd., Lutterworth, UK
Trypan Blue stain 0.4% (w/v)	Invitrogen™ Ltd., Life Technologies, Paisley, UK
Trypsin-EDTA x1	PAA Laboratories GmbH, Pasching, Austria

II.2. Cell lines

KG-1 and KG-1a cells were maintained in a suspension culture of RPMI-1640 medium (PAA Laboratories GmbH) containing 1% (v/v) penicillin and streptomycin (P/S) (PAA Laboratories GmbH), 20% (v/v) fetal bovine serum (FBS, PAA Laboratories GmbH) at an initial density of 5.0 x10^5/mL. Jurkat cells were also maintained in a suspended cultured in RPMI-1640 medium, 1% (v/v) P/S and 10% (v/v) FBS, at an initial density of 5.0 x10^5/mL. Human embryonic kidney cells (HEK293FT) were purchased from Lonza Ltd. (Lonza) and cultured in Dulbecco's Modified Eagle Medium with L-glutamine (DMEM; PAA Laboratories GmbH) with 10% (v/v) FBS (PAA Laboratories GmbH), 1% (v/v) P/S, 500 µg/L Geneticin (Invitrogen™ Ltd., Life Technologies), 0.1 mM (Invitrogen™ Ltd., Life Technologies) and 1 mM sodium pyruvate (Invitrogen™ Ltd., Life Technologies). HEK293T cells were cultured up to 90% confluency. Adherent cells, human primary osteoblasts (osteoblasts) and bone marrow

stromal cells (BMSCs) were purchased from Lonza. Osteoblasts, catalogue number CC-2538, batch number 5F0335, were maintained in OGM (Lonza). OGM was made up of Osteoblast Basal Medium (OGB™) and OGM™Single™Quotes® (Lonza) containing growth supplements: FBS, 50 mL; ascorbic acid, 0.5 mL; GA-1000, 0.5 mL. BMSCs**,** catalogue number 2M-302, batch number 090391B, were cultured in Myelocult H5100 medium (StemCell Technologies) and 1µM hydrocortisone (Sigma Aldrich Co. LLC.). Adherent bone marrow endothelial cells (BMECs) were kindly provided by Professor CE van der Schoot. These immortalised BMEC (BMEC-60) were generated specifically to study the adhesion of HSCs to human BMECs (Rood et al., 2000a) and cultured in EGM-2® (Lonza). This medium was made up of Endothelial Cell Basal Medium enhanced (Lonza) with EGM-2® SingleQuot® Kit Suppl. & Growth Factors (Lonza): 2% (v/v) FBS, 0.5 mL epidermal growth factor, 0.5 mL heparin, 0.2 mL hydrocortisone, 0.5 mL VEGF, 0.5 mL recombinant long R insulin-like growth factor, 0.5 mL ascorbic acid, 2 mL human fibroblast growth factor, and GA-1000. Once confluent, adherent cells were detached using trypsin-EDTA x1 and reseeded at 3.5-5.0x10^5 cells/75 cm^2 flask. All cultures were maintained at 37^{o}C, 5% CO_2, 20% O_2, in air and 100% humidity.

II.3. Flow cytometry analysis

Analysis of cell surface markers**,** green fluorescence protein (GFP) or BCECF-AM dye were determined by flow cytometry (FACS). Flow cytometry enables detection of these fluorescent molecules (fluorochromes) through immunofluorescence detection at different wavelengths; fluorochromes accept

light energy at a given wavelength (excitation) and re-emit light energy at a lower wavelength (emission) **[Table II.1]**. Cell size and granularity are also detected by light scatter characteristics, side scatter (SSC) and forward scatter (FSC) respectively **[Figure II.1]**. The SSC and FSC are unique to every cell. These features allow to selectively visualise cells of interest. Flow cytometer BD Biosciences LSR II (filter configuration 660/20) was used to carry out flow cytometry analysis.

Table II.1. Fluorochrome emission and excitation

Fluorochrome (channel)	Excitation wavelength (nm)	Emission wavelength (nm)	Filter in BD LSII
APC	633	660	660/20
FITC	488	520	530/30
PE	488	578	575/26
PerCP	488	678	670/14
Pe-Cy5	488	667	660/20
Pe-Cy7	488	785	780/60
BCECF-AM	488	535	530/30
GFP	488	509	530/30
To-pro3	633	661	660/20

To detach adherent BMSCs, a 90% confluent monolayer of BMSCs was first incubated with 8 mL/75cm^2 flask of reconstituted collagenase from *Clostridium histolyticum* (Cat# C1639-50MG, Sigma Aldrich Co. LLC.) Collagenase treated BMSCs and adherent cells osteoblasts and BMEC-60 cells were washed twice with 10 mL Dulbecco's Phosphate Buffer Saline (DPBS; PAA Laboratories GmbH) before treating cells with 2.5 mL accutase (PAA Laboratories GmbH) to detach cells. Cells were then suspended in 100 uL

HBSS and 0.5% (w/v) BSA (FACS buffer) and incubated at 4^{o}C for 30 minutes with the relevant test antibodies at 1-10 µg/mL. After incubation, cells were washed with FACS buffer and centrifuged at 300 x g for 5 minutes and resuspended in 400 µL FACS buffer for FACS analysis. Cells in suspension were centrifuged at 300 x g for 5 min to remove culture medium and then resuspended in 100 uL FACS buffer for antibody staining. Where possible, a separate cell sample was stained with Topro-3 at 1:1000 dilution (Invitrogen™ Ltd., Life Technologies) to verify viability of cell population used in an experiment. Dead cells take up Topro-3 and can be detected at 642/661 nm (APC channel). This enabled gating on viable cells. An isotype control was used to determine non-specific antibody binding, thus the isotype control provided a baseline level of non-specific binding **[Figure II.1].** Data interpretation and analysis was conducted using BD Diva 5.0 software (BD Biosciences, Becton, Dickinson and Company). A list of antibodies is presented in **Table II.2.**

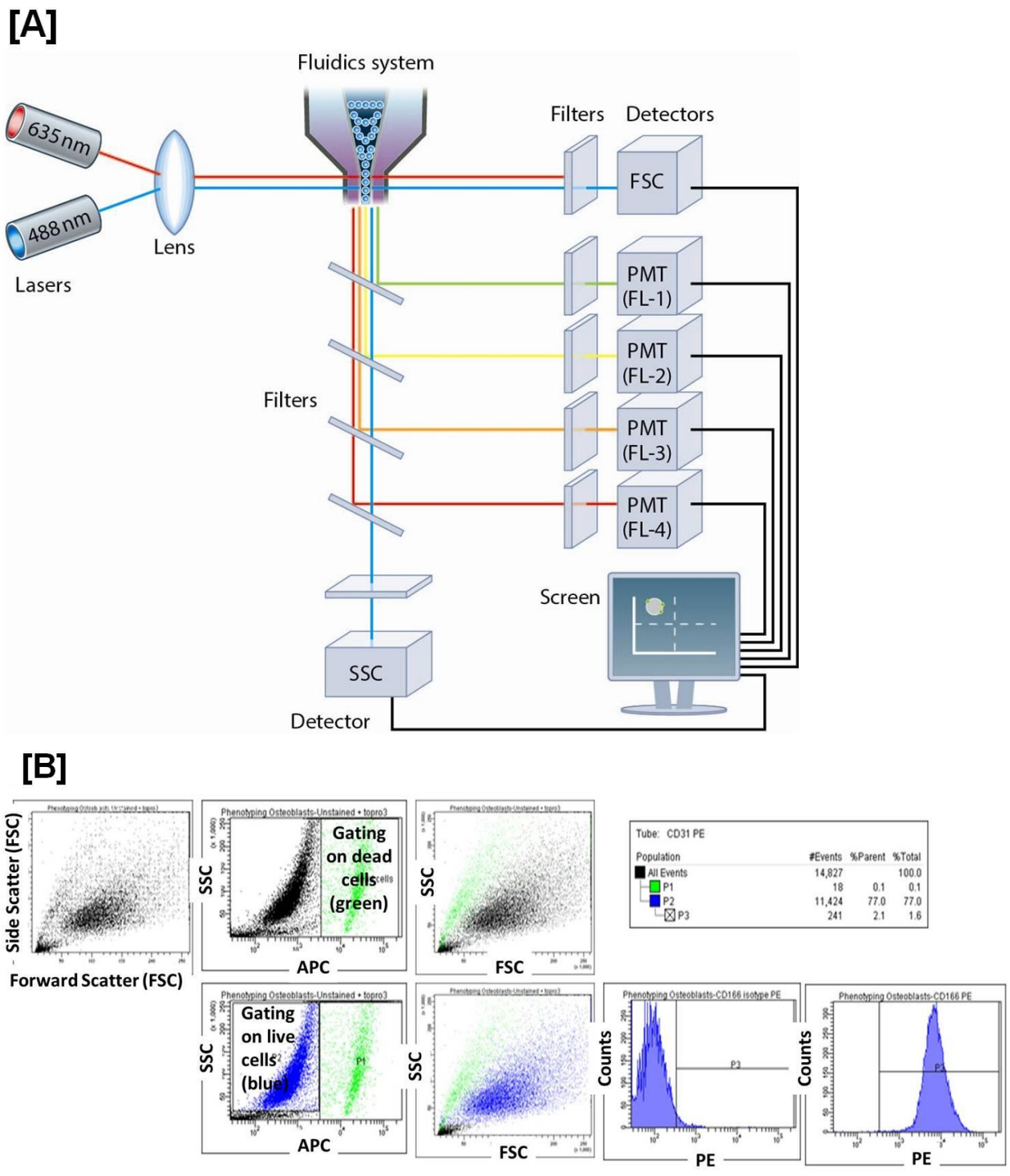

Figure II.1. Schematic diagram of typical flow cytometer setup.

[A] The BD LSR II flow cytometer contains lasers covering the following wavelengths: 355nm (UV), 488nm (blue) and 630nm (red). Filters in front the fluorescent detectors allow measurement of the particular wavelength of light. Detected signals are transmitted to the connected computer and displayed on the screen for data analysis and interpretation. Based on the granularity, measured at approximately a 90^{o} angle to the excitation line (side scatter [SSC]), and size, measured at approximately 20^{o} from the laser beam's axis (forward scatter [FSC]). Cells are taken up in solution into the flow cytometer through a fine probe, which injects the sample into a central channel (core) enclosed by an outer sheath that contains faster flowing fluid. The cells pass through a vibrating nozzle and this allows cells to flow in a single file past the laser beam. Analytical software packages such as BD Diva 5.0 display the SSC, FSC and fluorescence parameters detected and enable data analysis and interpretation (Rahman et al., 2006). [B] Example of the displayed results showing FSC and SSC of detected cells, as well as relative fluorescence intensity to cell count (number of events). Using a viability dye (Tropo-3), which is detected at 642/661 nm (APC channel; green cells), enabled 'gating' on the viable population (blue cells). Antibody staining with a fluorochrome detected at 488/578 nm (PE), enable detecting cell surface marker CD166-PE. Picture credit: [A] Reprinted from AbD Serotec Ltd. 2006, Rahman M., Lane A., Swindell A., Bartram S., Introduction to Flow Cytometry, p.1-33, Copyright 2014, with the permission from AbD Serotec.

Table II.2. List of antibodies used for flow cytometry analysis.

Cell surface marker	Antibody	Isotype	Fluorophore	Supplier	Clone
Endothelial and haemopoietic cells	CD 31	IgG1	PE	BD	WM59
BMSCs and endothelial cells	CD 73	IgG1	PE	BD	AD2
Activated lymphocyte, endothelial or fibroblastic cells (adhesion molecule)	CD 166	IgG1	PE	R &D	105902
Progenitor cell subsets, fibroblast, BMSCs	CD 90	IgG1	FITC	BD	5E10
BMSCs and endothelial cells (endoglin: part of TGF-β receptor complex)	CD 105	IgG1	FITC	R &D	166707
Activated endothelial cells (VCAM-1)	CD 106	IgG1	FITC	BD	51-10C9
Haemopoietic and endothelial progenitor cells	CD 34	IgG2a	APC	Miltenyi	AC136
Haemopoietic stem and progenitor cells	CD133	IgG2b	PE	Miltenyi	AC133
Leukocytes	CD 45	IgG1	PerCP	BD	345809
Monocytes	CD 14	IgG2a	Pe-Cy7	BD	557742
β1 integrin (adhesion molecule)	CD 29	IgG1	PE	BD	MAR4
Adhesion receptor/addressin	CD 44	IgG1	PE	BD	515
Homing molecule/sialomucin	CD164	IgG2a	PE	BD	N6B6
Homing molecule	CD184 (CXCR4)	IgG2a	APC	BD	12G5
Adhesion molecule/integrin	CD49d (VLA-4)	IgG1	PE	BD	9F10
Adhesion molecule/integrin	CD49e (VLA-5)	IgG1	PE	BD	IIA1
Adhesion receptor	F11 (JAM-A)	IgG1	PE	BD	M.Ab.F11
Adhesion molecule/integrin	CD54 (ICAM1)	IgG1	APC	BD	HA58
Adhesion molecule/integrin	CD11a (LFA-1)	IgG2a	FITC	BD	G43-25B
Adhesion molecule/selectin	CD62E (E-selectin)	IgG1	PE	BD	68-5H11
Adhesion molecule/integrin	CD51/61	IgG1	FITC	BD	23C6

II.4. CD133$^+$ cell isolations

CD133$^+$ cells were isolated from mononuclear cells (MNCs) derived from human umbilical cord blood that was collected from normal births of consenting donors at the John Radcliffe Hospital, Women's Centre (Oxford, UK) with ethical approval and informed written consent. Cells were used as anonymised linked donations either under a Human Tissue Authority (HTA) licence or with ethical permission from the Berkshire Research Ethics Committee (10/H0505/34). UCB units were either processed fresh or kept at 4°C overnight. A total of 208 cord blood units were processed during this DPhil project to obtain CD133$^+$ cells for experiments. Standard operating procedure SCR.SOP.036v2 (SOP), NHSBT Oxford, was followed to isolate these cells as follows. MNCs were isolated using ACCUSPIN^{TM} System-HISTOPAQUE®-1077 tubes (Sigma Aldrich Co. LLC.) or LSM 1077 (PAA Laboratories GmbH). Blood and HBSS (PAA Laboratories GmbH) without phenol red were equilibrated to room temperature before use. Each unit of cord blood was diluted with 500 mL HBSS without phenol red (PAA Laboratories GmbH), without calcium and magnesium, 0.5% (w/v) BSA, and 3g/L trisodium citrate, final pH 7.4 (MACS buffer). Cord blood units with a white blood cell count (WBC) greater than or equal to 7 x 10^6 cell/mL were diluted in equal amounts of MACS buffer. The WBC was provided by the nurses who collected the cord blood, using an automated haematology cell counter (SYSMEX Haematology Analyser; Sysmex Corporation, Hyogo, Japan). Cord blood units with WBCs >7x10^6 cell/mL were diluted with 2 parts MACS buffer. The ACCUSPIN^{TM} system employs centrifuge tubes specially designed with two chambers separated by a porous high-density polyethylene barrier ("frit"). As described by the manufacturer, the lower

chamber contains HISTOPAQUE®-1077, which allows the addition of anti-coagulated whole blood without risk of mixing with the separation medium. There was no barrier when using LSM 1077. Each 50 mL tube contains 15 mL HISTOPAQUE®-1077, and separates between 15 to 30 mL of anti-coagulated diluted blood. When using LSM 1077, 25 mL of whole cord blood was gently layered on 20 mL LSM 1077. On centrifugation at 1990 rpm when using HISTOPAQUE®-1077 and 1600rpm with LSM 1077 for 30 minutes with acceleration 9 and no break, the whole blood descends through the frit to contact with the HISTOPAQUE®-1077 below the frit. The erythrocytes aggregate and the granulocytes become slightly hypertonic, increasing their sedimentation rate, pelleting at the bottom of the ACCUSPIN^{TM} tube. Lymphocytes and other mononuclear cells remain at the plasma-HISTOPAQUE®-1077 interface. This system gives a clear separation of the blood components. The aliquoted blood was centrifuged at 970 x g for 10 minutes, acceleration 9 and deceleration 1, using ACCUSPIN^{TM} tubes or at 630 x g, acceleration 9, deceleration 0 for 30 minutes if layering on LSM 1077 at 22°C, both methods in a Hettich Rotina 46R centrifuge (DJB Labcare Ltd., Newport Pagnell, Buckinghamshire, England, UK). After centrifugation MNCs appeared as a cloudy, white layer found at approximately 0.5 cm above the frit. To minimise contamination with platelets, most of the upper clear plasma was removed to 0.5 cm above the MNC layer with a sterile pastette or pipette and collected into 50 mL Falcon tubes. Collected MNCs were washed with 50 mL room temperature MACS buffer, at 630 x g for 10 minutes with acceleration 9 and break 9, at 4^{o}C in a Hettich Rotina 46R centrifuge (DJB Labcare Ltd.). Following centrifugation the supernatant was removed and washed again with

MACS buffer, this time at 350 x g for 10 minutes at 4^{o}C in a Hettich Rotina 46R centrifuge (DJB Labcare Ltd.). After centrifugation the supernatant was discarded and the fragile pellet was resuspended in 10 mL MACS buffer. An aliquot of 150 µL was used for a cell count using the SYSMEX Haematology Analyser (Sysmex Corporation). The remaining MNC suspension was topped up with 50mL and centrifuged at 350 x g for 7 minutes at 4^{o}C in a Hettich Rotina 46R centrifuge (DJB Labcare Ltd.). The supernatant was discarded.

To retrieve the CD133^{+} cells from the MNC population, MACS® Cell Separation Technology (Miltenyi Biotec Ltd.) was used **[Figure II.2].** According to the manufacturer's protocol, 100 µL FcR Blocking reagent, 300 µL MACS buffer and 100 µL CD133 MicroBeads (Miltenyi Biotec Ltd.; Cat# 130-050-801) were used per 1x10^{8} total MNCs cells and incubated for 30 minutes at 4^{o}C. After incubation, cells were washed with 20 mL MACS buffer and resuspended in 5 mL MACS buffer. Before loading the MNCs, the MACS Column was equilibrated with 5 mL MACS buffer. Then 2.5 mL of the cell suspension was loaded. The column was washed 3 times with cold (4^{o}C) MACS buffer before loading the remaining 2.5 mL of cell suspension. This procedure was repeated once. Magnetically labelled CD133^{+} cells were then flushed out upon removal of the column from the magnetic field. The purity of the isolated CD133^{+} HSCs/HSPCs was checked by flow cytometry, FACS machine BD LSRII and the viability with Topro-3 at 1:1000 dilution (Invitrogen™ Ltd., Life Technologies; Cat# T3605) **[Figure II.3]**. An aliquot of 6x10^{4} cells divided into three samples were used to assay the purity of the isolated population: 1) unstained control; 2) isotype control mIgG/2b-PE (Miltenyi Biotec Ltd.; Cat# 130-092-215); 3) CD133/2b-PE antibody (Miltenyi Biotec Ltd.; Cat# 130-090-853). A purity of

91±7.5% (n=30) UCB-CD133^{+} cells was generally obtained. Isolated cells were cryopreserved at 1x10^{6} cell/mL in 'freezy mix'. Freezy mix comprised of 90% (v/v) FBS and 10% (v/v) DMSO (Sigma Aldrich Co. LLC.). Cryovials containing cells were immediately transferred to a Mr Frosty containing room temperature isopropanol (VWR International) and stored at -80°C for 24 hours before being transferred to gaseous phase liquid nitrogen (≤150°C).

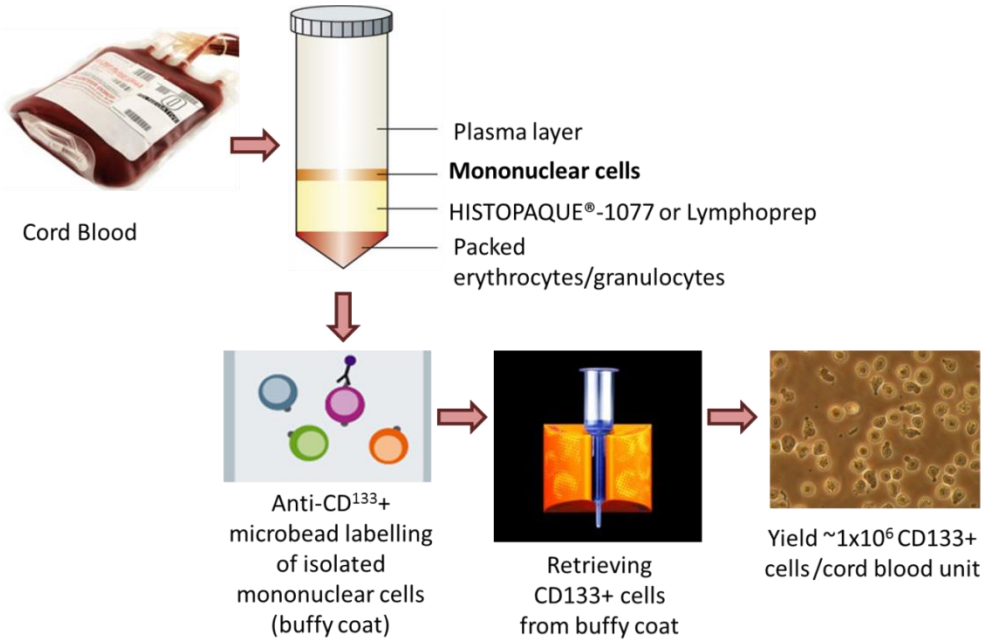

Figure II.2. Flow chart illustrating UCB-CD133^{+} cell isolation using MACS® technology.

Consented whole cord blood was obtained and separated into different blood components by density gradient centrifugation. Most mononuclear cells have densities below 1.077 g/ml and are more buoyant in HISTOPAQUE®-1077 and Lymphoprep (LSM 1077) than erythrocytes.and granulocytes. This allows for a clear separation of these blood components. To isolate CD133^{+} cells, the mononuclear cell layer was harvested and prepared for MACS® separation. From a single cord blood unit we would obtain an average yield of 1x10^{6} CD133^{+} cells. Images adapted from Miltenyi Biotec, https://www.miltenyibiotec.com/en/products-and-services/macs-cell-separation/macs-technology/microbeads_dp.aspx

II.5. Culture conditions for UCB-CD133^{+} cells

To use isolated cells in functional assays, including for hypoxic incubations or for lentiviral transductions, frozen cells were thawed in the water bath at 37^{o}C

and cultured overnight or longer in StemSpan SFEM (STEMCELL Technologies™, Cat# 09650) with four cytokines: Recombinant stem cell factor (SCF) at 100ng/ml, recombinant human thrombopoietin (TPO) at 20ng/ml, recombinant human fms-like tyrosine kinase 3 ligand (FLT-3L) at 100ng/ml and recombinant interleukin-6 (IL-6) at 100ng/ml (all cytokines from R&D Systems, Cat# 255-SC-050, 288-TP-01M, 308-FK-025 and 206-IL-050 respectively) (Rappold et al., 1999).

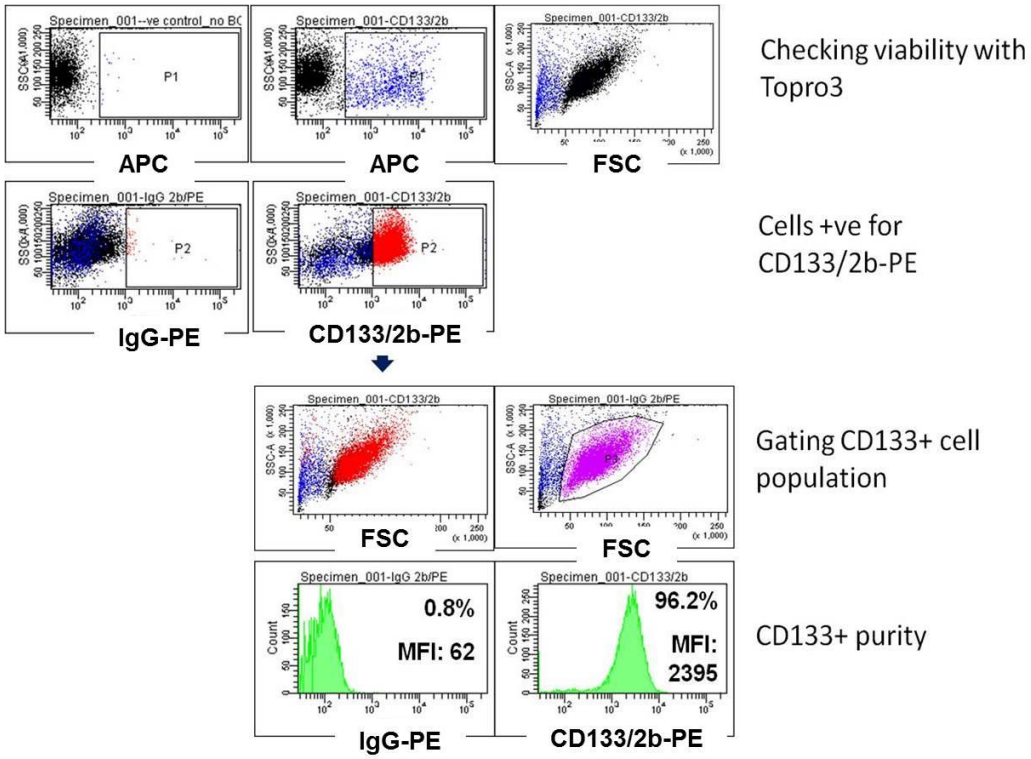

Figure II.3. Verifying purity of isolated UCB-CD133$^+$ cells.

Upon MACS separation of UCB-CD133$^+$ cells, an aliquot of cells was stained with anti-CD133$^+$-PE or mIgG2b-PE to verify the purity of the isolated HSPC population. Viability dye Topro-3 was used to determine the viable population as described in **Figure II.1**. Dead cells (blue) were identified with Topro-3 staining.

II.6. Hypoxia timecourse

KG-1 or UCB-CD133$^+$ cells were cultured in conditions described in Section-II.2 and Section-II.5 at 5x10^5 cells/mL/well using a 6-well tissue culture grade plate (BD Biosciences) and incubated under 1.5% O_2, at at 37^{o}C, 5% CO_2 and 100% humidity for periods of 4, 24, or 48 hours. Control cultures were prepared in the same culture conditions as the hypoxia cultures described above, but placed in an incubator with 20% O_2, at 37^{o}C, 5% CO_2 and 100% humidity. A total of 1x10^6 cells were used for each time point per condition. Total protein was extracted from these cells immediately after each time point, i.e. after 4, 24 or 48 hours by harvesting cells with 3 mL of cold DPBS (PAA

Laboratories GmbH). Cells were centrifuged at 1300 rpm in the Hettich Rotina 46R centrifuge (DJB Labcare Ltd.) for 3 minutes at 4^{o}C to remove growth media before adding lysis buffer (described in Section II.12). Cell lysates were used for Western blot analysis described in Section II.12.

II.7. Adhesion assays

II.7.1. Optimisation

Substrate cells (osteoblast, BMSCs and BMEC-60 cells) were used at passage 4 for each experiment, re-plated in a 96 flat-bottom black well plate (VWR International Ltd.). Confluent monolayers of either osteoblasts (1x10^{4}/well), BMSCs (2x10^{4}/well), or BMEC-60 (2x10^{4}/well), were subjected to normoxic culture (20% O_2, and 5% CO_2, and 100% at 37^{o}C humidity) for 24 hours. BMEC-60 cells were pre-stimulated with human IL-1β (10 ng/mL; BioSource International Inc., Cat# PHC0815). KG-1 or UCB-CD133^{+} cells (adhering cells) were labelled with 5 µL/1x10^{6} cells/mL 2',7'-bis-(2-carboxyl)-5(and -6)-carboxyfluoresce (BCECF-AM; Invitrogen™ Life Technologies) dye, detected at 488/530 nm (60 minutes incubation at 37^{o}C, 20% O_2, and 5% CO_2, and 100% humidity) in HBSS with Ca^{2+} and Mg^{2+}. BCECF-AM (50 µg) was reconstituted with 90 µL DMSO as per manufacturer's specification sheet. Labelled cells were washed with 5 mL HBSS with Ca^{2+} and Mg^{2+} at 300 x g in the Hettich Rotina 46R centrifuge (DJB Labcare Ltd.) and then resuspended to final concentration of 2x10^{4} cells/100 µL in HBSS with Ca^{2+} and Mg^{2+}. One hundred µL of the cell suspension was added to each well containing the monolayer of substrate cells (number of wells/substrate and per condition= 6).

To determine the optimal number of adhering cells to use for each substrate, six different concentrations of KG-1 cells were tested **[Table II.3]**. Cells were left to adhere for 1 hour under normoxic conditions (20% O_2, and 5% CO_2, and 100% at 37^{o}C humidity). Pre-adhesion fluorescence was measured using VICTOR plate reader at 485/538 nm (Perkin Elmer, Warrenville Road, Downers Grove, IL 60515, USA). Non-adherent cells were removed by removing the 100 µL of cell suspension added 1 hour before incubation, and washing with 200 µL of HBSS with Ca^{2+} and Mg^{2+} by gently pipetting up-down-up (remove/discard). Post-adhesion fluorescence was measured after washing. The percentage of adherent cells was calculated by the following formula: Results are representative of three independent experiments.

$$\%\ cell\ adhesion\ = \frac{fluorescence\ intensity\ postwash}{fluorescence\ intensity\ prewash} \times 100$$

II.7.2. Hypoxic versus normoxic adhesion

Three different hypoxic treatments were tested. Treatment 1: KG-1 cells and $CD133^{+}$ cells were pre-conditioned under hypoxia (37^{o}C, 1.5% O_2, and 5% CO_2 in air and 100% humidity) for 24 hours, labelled with BCECF-AM as described in Section II.7.1 and added to a normoxic monolayer of substrate cells as described in the optimisation protocol. Cells were left to adhere for 1 hour under normoxia (20% O_2, and 5% CO_2, and 100% at 37^{o}C humidity). Treatment 2: Substrate cells were pre-stimulated under hypoxia (37^{o}C, 1.5% O_2, and 5% CO_2 in air and 100% humidity) for 24 hours before normoxic adhering cells (labelled with BCECF-AM) were added for the 1 hour incubation. Treatment 3: Both the substrate and the adhering cells were pre-stimulated

under hypoxia (37^{o}C, 1.5% O_2, and 5% CO_2 and 100% humidity) for 24 hours. Hypoxia pre-conditioned KG-1 or CD133+ cells were BCECF-AM labelled and added to the hypoxic monolayer of substrate cells and incubated for 1 hour under normoxia (37^{o}C, 20% O_2, and 5% CO_2 and 100% humidity). The percentage of cell adhesion was calculated as shown in Section II.7.1.

Table II.3. Optimising cell adhesion to cells found in the bone marrow.

Substrate	Concentrations of adhering cells (KG-1)
BMSCs	$1x10^4$, $2x10^4$, $5x10^4$, $1x10^5$, $2x10^5$, $5x10^5$
Osteoblasts	$1x10^4$, $2x10^4$, $5x10^4$, $1x10^5$, $2x10^5$, $5x10^5$
BMEC-60	$2x10^4$, $5x10^4$, $1x10^5$, $2x10^5$

The adhesion of six different concentrations of adhering cells wasere tested to BMSCs and osteoblasts, and four concentrations to BMEC-60

II.8. Transwell migration assay

II.8.1. Optimising the assay

The migration assay was adapted from (Voermans et al., 2000). BD Falcon™ (Cat#353096, BD Biosciences™) culture inserts (transwell inserts) with 6.4mm diameters of membrane and a pore density of 3.0 µm in conjuction with Falcon™ companion tissue culture grade plate (bottom chamber) (Cat# 353504, 24 wells, BD Biosciences™), were used for the migration assay. Transwell inserts and bottom chambers were coated with 100 µL and 300 µL fibronectin at 10 µg/mL HBSS without Ca^{2+} and Mg^{2+} respectively (Sigma Aldrich®; Cat#F0895) and kept at 4^{o}C overnight. Jurkat or KG-1A cells were counted with a haemocytometer and resuspended in fresh culture media (described in Section-II.2) at $1x10^5$-$2.5x10^5$/100 µL. UCB-$CD133^+$ cells were thawed from

cryopreservation and incubated at 37^{o}C, 20% O_2, and 5% CO_2 and 100% humidity overnight in StemSpan (STEMCELL Technologies™) with cytokines IL-6, FLT-3L and SCF each at 100 ng/mL and TPO at 20 ng/mL as described in Section-II.5. The next day, fibronectin solution was removed from both chambers and allowed to air dry for ~5min. RPMI 1470 (PAA Laboratories GmbH) for KG-1A and Jurkat cells, or StemSpan (STEMCELL Technologies™) for UCB-CD133^{+} cells was prepared with chemokine SDF-1α (PeproTECH) and pipetted at 400 µL/well into the bottom chamber. Up to 3 doses of SDF-1α were tested: 100, 200 and 400 ng/mL together with a negative (-ve) control (0 ng/mL). For UCB-CD133^{+} cell migration, no cytokines were added to StemSpan media (STEMCELL Technologies™) during the migration assay, and no FBS was added to the RPMI 1470 media of Jurkat and KG-1A cells. Jurkat, KG-1A or CD133^{+} (100 µL of 1x10^{5}-2.5x10^{5}) were pipetted into the upper chamber. Triplicates of each dose were prepared. Cells were allowed to migrate for 6 hours at 37^{o}C in 20% O_2.

Flow cytometry was used to determine the % of cell migration. Transmigrated cells were harvested into FACS tubes and centrifuged at 300 x g for 5 min, at room temperature, acceleration 9 and deceleration 9. Cell pellets were mixed with the original number of CD133^{+} cells plated into the top chamber labelled with BCECF-AM as described in SectionII.7.1. For example, if 1x10^{5} cells (equalling 100%) were plated before 6 hour incubation, then 1x10^{5} BCECF-AM labelled cells/100 µL where mixed with migrated cells (non-labelled) with 300 µL FACS buffer (HBSS with 0.1% BSA). A positive control (BCECF-AM CD133^{+} labelled cells) and a negative control (non-labelled BCECF-AM

$CD133^+$ cells) were also prepared. Migrated cells were counted as a % of the labelled population negative for BCECF-AM (detected at 488/530 nm).

II.8.2. Testing effects of hypoxia pre-conditioning

Two hypoxia pre-conditioning time points were tested: 24 and 48 hours. For each hypoxic treatment a normoxic control group was also tested. Hypoxia pre-conditioning was defined by incubating cells in 1.5% O_2 at 37^{o}C, 5% CO_2 and 100% humidity, whereas normoxic conditions were defined by incubating cells in 20% O_2 at 37^{o}C, 5% CO_2 and 100% humidity. The experiment was carried out over 4 days. On DAY-0 BMEC-60 cells were plated at $2x10^4$cells/transwell insert and incubated for 72 hours) at 37^{o}C in 20% O_2, 5% CO_2 and 100% humidity. Three transwell inserts were prepared per time point, equalling a total of 6 wells per timpoint (3 for hypoxic and 3 for normoxic testing). $CD133^+$ cells were thawed from cryopreservation and cultured overnight as previously described in Section II.5 for 48 hours (time point 2) at 37^{o}C in 20% O_2, 5% CO_2 and 100% humidity. For each timepoint, $1x10^5$ of $CD133^+$ cells were used per transwell insert = $1x10^5$ cells × 6. On DAY-1, $CD133^+$ cells were thawed for the 24 hour time point (time point 1) with an additional equal number of $CD133^+$ cells to determine the number of migrating cells. These cells were stained with BCECF-AM on DAY-3 as described in Section II.8. On Day-1, $CD133^+$ cells that were thawed on DAY-0 were placed into the hypoxic incubator (37^{o}C, 1.5% O_2, and 5% CO_2 and 100% humidity) with the equal number of $CD133^+$ cells (control group) incubating in the normoxic incubator (37^{o}C, 20% O_2, and 5% CO_2 and 100% humidity). On Day-2, BMEC-60s were given fresh media (EGM-2), and $CD133^+$ cells thawed on Day-1 for the 24 hour

time point were placed in the hypoxic incubator (37^{o}C, 1.5% O_2, and 5% CO_2 and 100% humidity), joining the CD133^{+} cells that were incubating for the 48 hour time point. The respective control set was placed in the normoxic incubator. On Day-3, BMEC-60 cells were stimulated with IL-1β (BioSource International Inc., Cat# PHC0815) made up in EGM-2 at 10 ng/mL for 4 hours in 20% O_2, and 5% CO_2 at 37^{o}C and 100% humidity. BMEC-60 cells were washed two times with StemSpan (STEMCELL Technologies™) without cytokines before adding hypoxia stimulated or normoxic CD133^{+} cells at 1x10^{5} cell in StemSpan (STEMCELL Technologies™) without cytokines into the upper chamber of each well. CD133^{+} cells were allowed to migrate for 6 hours in 20% O_2, and 5% CO_2 at 37^{o}C and 100% humidity. Migrated cells were counted by flow cytometry as described earlier in Section II.8.

II.9. Plasmids and generation of lentiviral particles

II.9.1. Lentiviral vectors used

pGIPZ-CMVturboGFP.IRESPuro.shRNAmir-WRE (pGIPZ) **[Figure II.5; Table II.4]** and pLKO.1-U6shRNA.cPPT.hPGKpuro (pLKO.1) **[Figure II.6]** lentiviral vectors were purchased from Open Biosystems, Huntsville, USA (today Dharmacon, Thermo Fisher Scientific, Laffayette, USA). Viral glycoprotein envelope VSV-G, the regulatory proteins gag-pol, Δ8.91 **[Figure II.4]** and transfer vector pHR'SINcPPT.SFFVeGFP.WPRE-SEW (SFFV.eGFP.WPRE) **[Figure II.7]** were obtained from the laboratory of Professor Adrian Thrasher, UCL, London, UK.

The pGIPZ vectors included two separate shRNAs targeting HEF-1 **[Table II.5]**, a positive control vector encoding shRNA targeting GAPDH; and a non-silencing control shRNA vector**.** High titre SMARTvectorTM 2.0 lentiviral shRNA particles (SV2) were purchased from Dharmacon **[Table II.6]**. These vectors included three shRNA targeting NEDD9 (HEF-1) and a non-silencing control vector. Plasmid maps for each system are shown below. The pLKO.1 vector against HEF-1 and pLKO.1 empty control vector were purchased from Open Biosystems, Thermo Scientific, Dharmacon **[Figure II.6]**. A non-targeting pLKO.1 control vector was not available at the time. High titre lentiviral (LV)-pLKO.1 particles were purchased from Sigma Aldrich Co. **[Table II.8].**

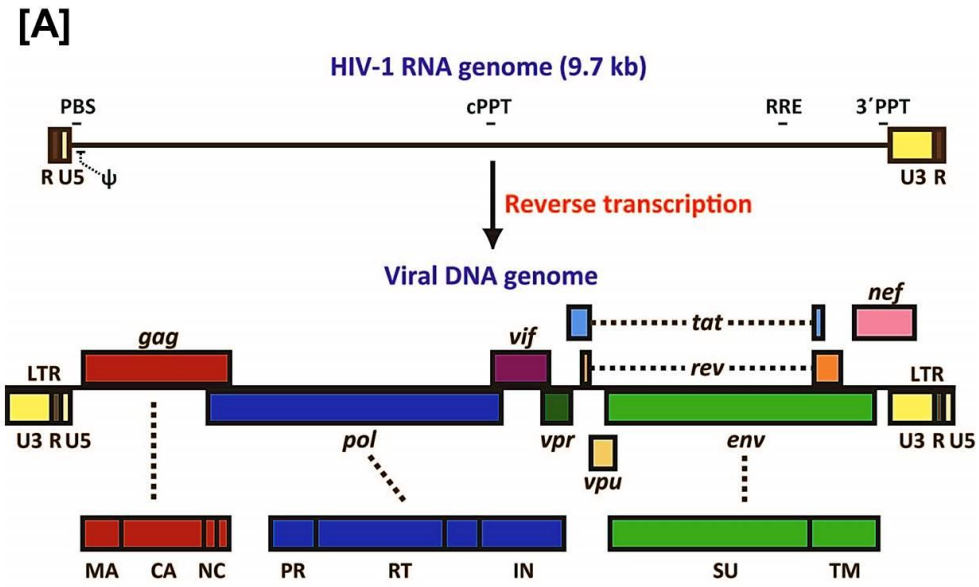

[B]

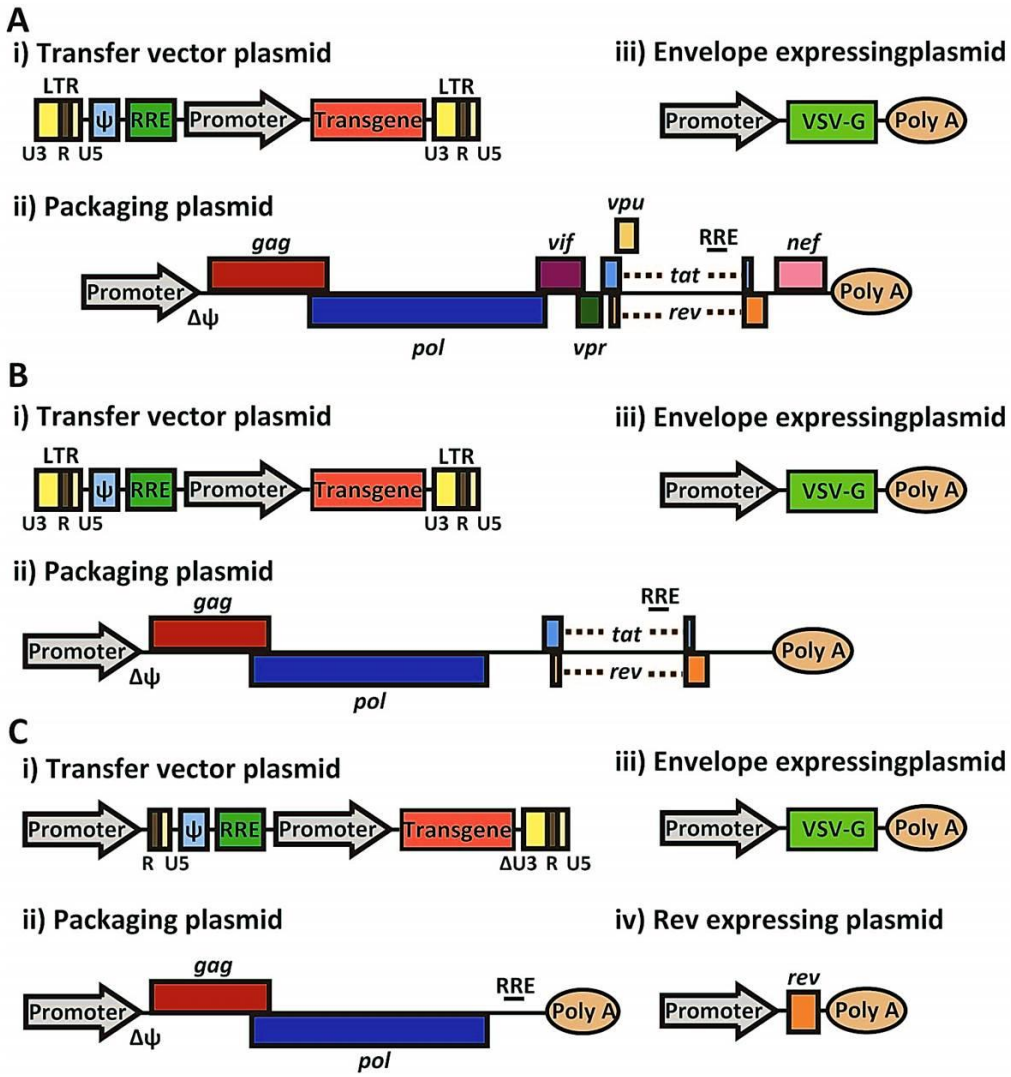
A
i) Transfer vector plasmid
LTR
ψ
RRE
Promoter
Transgene
LTR
U3 R U5
U3 R U5
iii) Envelope expressingplasmid
Promoter
VSV-G
Poly A
ii) Packaging plasmid
vpu
gag
vif
RRE
nef
tat
Promoter
Poly A
rev
Δψ
pol
vpr
B
i) Transfer vector plasmid
iii) Envelope expressingplasmid
ii) Packaging plasmid
C
i) Transfer vector plasmid
iii) Envelope expressingplasmid
ii) Packaging plasmid
iv) Rev expressing plasmid

Figure II.4. Lentiviral packaging plasmid.

[A] HIV-1 wild type vector comprising all *cis*- and *trans*-acting sequences. The first LV-vectors were generated by deleting various components in the HIV genome (Naldini et al., 1996). This resulted in a three-plasmid expression system: a packaging plasmid encoding essential genes *gag* and *pol,* to express components such as viral capsids, matrix proteins, as well as proteases, reverse transcriptase and integrases that cleave structural elements of the particles and process the vector genome for integration respectively (Logan et al., 2002). Expression of this plasmid requires the *rev* protein expressed by the second plasmid, envelope plasmid (VSV-G), a heterologous protein that broadens the tropism of the particles generated by the packaging plasmid. The transfer vector, containing *cis*-acting sequences of HIV required for packaging, reverse transcription and integration, and most importantly, a self-inactivating (SIN) configuration in the 3' LTR U3 region was the 3rd plasmid created to assemble LV-particles. [B] The packaging plasmid has undergone various modifications to improve biosafety (A, B, C). Most recently (C), regulatory genes *tat* and *rev* were eliminated. Strong constitutive promoters upstream from the transcriptional start site could replace the function of the *tat* gene. The *rev* protein is expressed *in trans* by a fourth plasmid. We used a 2nd generation packaging plasmids (B) as it works more effectively with transfer vector pHR'SINcPPT-SEW, commonly used in our laboratory. Picture credit: Yasutsugu Suzuki and Youichi Suzuki (2011). Gene Regulatable Lentiviral Vector System, Viral Gene Therapy, Dr. Ke Xu (Ed.), ISBN: 978-953-307-539-6, InTech, DOI: 10.5772/18155. Available from: http://www.intechopen.com/books/viral-gene-therapy/gene-regulatable-lentiviral-vector-system. Copyright permission 2014 granted under Open Source.

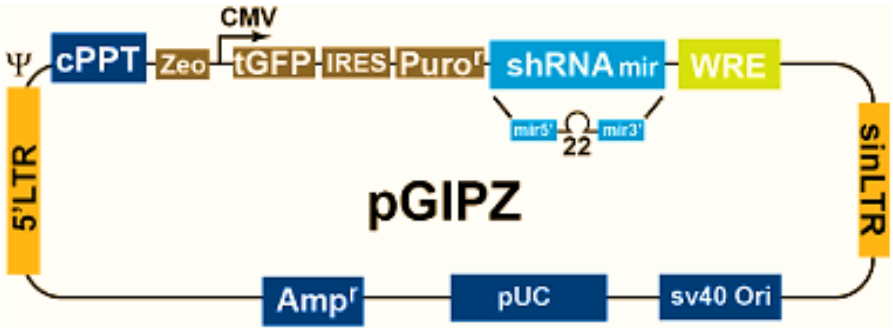

Figure II.5. pGIPZ lentivirus vector.

Transfer vector encoding expression cassette CMV-tGFP.IRES.Puro.shRNAmir[HEF-1]-WRE used to generate non-concentrated LV-particles made in house and also for high titre SV2 particles. The pGIPZ constructs encoded a miRNA-based shRNA, designed to mimic miRNA biogenesis. In contrast to the conventional RNA induced silencing pathway induced by shRNAs, shRNAmirs produce transcripts that are first processed in the nucleus by another RNase III enzyme Dorsha from pri-miRNA to pre-miRNA. Pre-miRNA is then targeted by Dicer to generate miRNA duplexes. Picture credit: Reprinted from GIPZ Lentiviral shRNA Technical Manual 2008, Open Biosystems, Thermo Scientific, Dharmacon, Resources, Copyright permission 2014 kindly granted by Thermo Scientific, http://www.thermoscientificbio.com/shrna/gipz-lentiviral-shrna/

,.

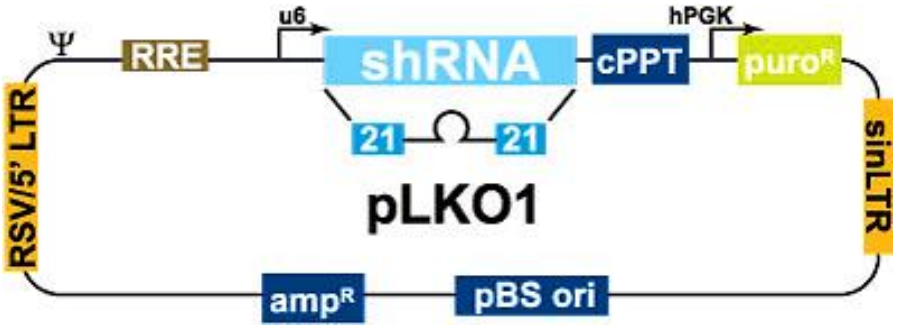

Figure II.6. pLKO.1 lentivirus vector.

Transfer vector with expression cassette encoding U6-shRNA[HEF-1].cPPT.hPGK-puro used to generate non-concentrated LV-particles made in house. The shRNA encoded in this expression cassette consisted of a siRNA sequence of 21 nucleotides, a short loop region, and the reverse complement of the siRNA sequence. U6 and hPGK are polymerase (pol)-III promoters for housekeeping genes have been successfully adapted to expression from lentiviral vectors (Logan et al., 2002). This type of shRNA is known as 'conventional' or 'simple' shRNA (Manjunath et al., 2009). Picture Credit: Reprinted from TRC Lentiviral shRNA Technical Manual 2008, Open Biosystems, Thermo Scientific, Dharmacon, Resources, Copyright permission 2014 kindly granted by Thermo Scientific, http://www.thermoscientificbio.com/shrna/trc-lentiviral-shrna/)

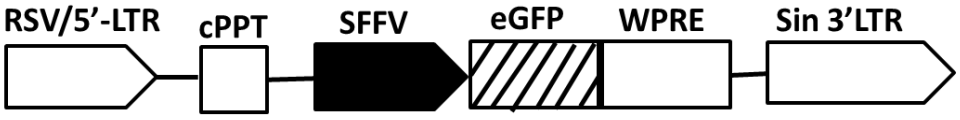

Figure II.7. pHR'SINcPPT-SEW lentiviral vector.

Transfer vector with expression cassette SFFV.eGFP.WPRE (SEW). Demaison et al. optimised this vector for haemopoietic repopulating cells. The spleen focus forming virus (SFFV) and the Woodchuck hepatitis virus posttranscriptional regulatory element (WPRE) enhanced levels of gene expression, and incorporating the HIV central polypurine tract (cPPT) increased transduction efficiency (Demaison et al., 2002).

II.9.2. Tables with lentiviral vector specifications

Tables describing each of the vectors are shown below.

Table II.4. Description of GIPZ vector elements.

Vector Element	Utility
CMV Promoter	RNA Polymerase II promoter
cPPT	Central Polypurine tract helps translocation into the nucleus of non-dividing cells
WRE	Enhances the stability and translation of transcripts
turbo GFP	Marker to track shRNAmir expression
$Puro^r$	Mammalian selectable marker
AMP^r	Ampicillin bacterial selectable marker
5'LTR	5' long terminal repeat
pUC ori	High copy replication and maintenance in *E.coli*
SIN-LTR	3' Self inactivating long terminal repeat
RRE	Rev response element
ZEO^r	Bacterial selectable marker

Utility of each element as described by Open Biosystems. Reprinted from GIPZ Lentiviral shRNA Technical Manual 2008, Open Biosystems, Thermo Scientific, Dharmacon, Resources, Copyright permission 2014 kindley granted by Thermo Scientific, http://www.thermoscientificbio.com/shrna/gipz-lentiviral-shrna/

Table II.5. Specifications of the Open Biosystems GIPZ-plasmids.

Stock code	pGIPZ Clone ID	Target Sequence	Description	Titre obtained in house (TU/mL)
RHS4430-200198735	V2LHS_198368	GCAAGGGCCTTATATGACA	Human NEDD9 shRNA, glycerol stock	8.5×10^5
RHS4430-2001251005	V2LHS_251005	GCCTTTCTGACTCTTAATA	Human NEDD9 shRNA, glycerol stock	8.5×10^5

Listed are the sequences used to target HEF-1 (NEDD9) with the shRNA GIPZ-plasmids and the viral titres obtained in house.

Table II.6. Specifications for the Dharmacon high-titre lentiviral particles.

Clone ID:

Catalog Number	Source Clone ID	Target Seq	Gene Symbol
VSH5417	SH-019466-01	AGGAACTGGCCTTTCGCAA	NEDD9
VSH5417	SH-019466-02	GCCAACAGAAGCTCTATCA	NEDD9
VSH5417	SH-019466-03	CGTCATAGAGCAGAACACA	NEDD9

Titer Results:

Source Clone ID	Titer (TU/ml)	Volume / Vial	No. Vials	Lot#
SH-019466-01	1.06×10^8	25µl	4	IV240901
SH-019466-02	1.05×10^8	25µl	4	IV240902
SH-019466-03	1.00×10^8	25µl	4	IV240903

Titre Results:

Catalogue#	Description	Titre (TU/mL)	Volume/Vial	Lot#
VSC5417	SMARTvector 2.0 non-targeting control – viral particles	5.75×10^5	25 µL	DV240901

Listed are the sequences used to target HEF-1 with the SV2 high-titre viral particles and their corresponding titres provided by the manufacturer.

Table II.7. Specifications for Open Biosystem pLKO.1 vector.

Stock code	pLKO.1 Clone ID	Target Sequence	Description
RHS3979-201737242	TRCN0000004969	CCTGAATATCTTGGCCATCAA	TRC Human NEDD9 shRNA, glycerol stock

Clone ID selected for target sequence being close to target sequence of Dharmacon siRNAs: 5'-AAAGACGGUGCCCGAUGAUU-3' and 5'-GAACAAGTGTGACGAUCUGUU-3'.

Table II.8. MISSION® Lentiviral Transduction Particles.

Gene	TRC Number/ catalogue number	Clone ID & Target sequence	Vector	TRC Version	Volume	Lot 01131228MN RESULTS
NEDD9/ HEF-1	**TRCN0000004969**	**NM_006403.2-1689s1c1 Sequence:** CCTGAATATCTTGGCCATCAA	**pLKO.1**	**TRC 1**	**1.0 mL**	**9.5×10^8 TU/mL**
Non-targeting shRNA	**SHC002H**	**N/A**	**pLKO.1**	**TRC 1**	**1.0 mL**	**1.4×10^9 TU/mL**

Listed are the specifications of the high titre viral particles purchased from Sigma Aldrich to knockdown HEF-1 in UCB-$CD133^+$ cells. Viral titres provided by the manufacturer were obtained by using a p24 antigen Elisa assay.

II.9.3. Generating lentiviral vectors and particles

LV-pGIPZ and non-concentrated LV-pLKO.1 particles were generated in house. *Ecoli* competent strains JM109 purchased from Stratagene, Agilent Technologies UK Ltd., Wokingham, UK, (Stratagene, Agilent Technologies Ltd.) were used to amplify the viral glycoprotein envelope VSV-G, the regulatory protein gag-pol Δ8.91**,** and transfer vectors pGIPZ-GAPDH, pGIPZ-HEF1A, pGIPZ-HEF1B, pGIPZ-Non-Silencing, pLKO.1-shRNA[HEF-1], and pLKO.1 empty. An aliquot of 100 µL of bacteria was gently mixed and aliquoted into pre-chilled tubes for each DNA plasmid with 0.8 µL of β-mercaptoethanol provided with the JM109 kit (Stratagene, Agilent Technologies Ltd.). Bacteria were incubated at 42^{o}C for 10 minutes and swirled every 2 minutes. Thirty ng/µL of DNA plasmid was added to each aliquot of cells and incubated for 30 minutes on ice. As control DNA, an aliquot with 1 µL of pUC18 (also provided with JM109 kit, Stratagene, Agilent Technologies Ltd.) was also prepared. To trigger the uptake of the DNA, tubes were heat-pulsed in a 42^{o}C water bath for 45 seconds. 0.9mL of SOC medium provided with JM109 kit (Stratagene, Agilent Technologies Ltd.) was added to each tube and incubated at 37^{o}C for 1 hour and shaking at 225-250 rpm in an incubator at 37^{o}C containing a shaker. Transformed mixtures were plated out on Luria Broth (LB) (Sigma Aldrich Co. LLC.) agar plates at 200 µL/plate with 100 µg/mL ampicillin (Sigma Aldrich Co. LLC.) and incubated at 37^{o}C overnight. To make up 1 L of LB the following measurments are normally required: 10 g of NaCl, 10 g of tryptone, 5 g of yeast extract and 10 g of agar. LB used for this experiment was made with LB tablets purchased from Sigma Aldrich Co. LLC. Eight tablets were disoved in deionized H_2O (dH_2O) to make up a final volume of 400 mL. The next day one colony of

each DNA plasmid was picked and inoculated into 2 mL LB and 100 µL/mL amipicillin (Sigma Aldrich Co. LLC.) for 6 to 8 hours at 37^{o}C shaking at 250 rpm in an incubator at 37^{o}C with containing a shaker. 200 µL of amplified bacteria were inoculated into an autoclaved clonical flask with LB and ampicillin and incubated overnight at 37^{o}C. To make new glycerol stocks, 1mL of each amplified plasmid/transformed *E.coli* was mixed with 200 µL glycerol (Sigma Aldrich Co. LLC.) and stored at -80^{o}C.

To extract the DNA from the amplified *E.coli*, the Invitrogen Pure Link™ HiPure Plasmid DNA Maxiprep Kit was used according to the manufacturer's procedures. HiPure Filter Maxi Columns were equilibrated with 30 mL of Equilibrium Buffer (EQ1). To harvest cells, overnight LB-culture was centrifuged at 4000x g for 10 minutes in a in a Hettich Rotina 46R bucket centrifuge (DJB Labcare Ltd.). The pellet was resuspended in 10 mL Resuspension Buffer (R3) with RNaseA until homogeneous. This mix was transferred into a 50mL centrifuge tube, mixed gently with 10 mL Lysis Buffer (L7) and incubated for 5 minutes at room temperature. Ten mL of Precipitation Buffer was added and mixed immediately until homogeneous. The precipitated lysate was transferred into the equilibrated HiPure Filter Maxi Column. The residual bacterial lysate in the HiPure Filter Maxi Column was washed with 10 mL Wash Buffer (W8) to increase the final DNA yield. When the filter stopped dripping the inner Filtration Cartridge from the column was removed immediately. The Maxi column was washed with 50 mL of Wash Buffer. 15 mL Elution Buffer (E4) was used to elute the DNA and collected in a 50 mL tube under gravity flow at room temperature. The eluted DNA was mixed well with 10.5 mL isopropanol (VWR International Ltd.) and centrifuged > 4460 x g for 60 minutes at 4^{o}C in a Hettich Rotina 46R

centrifuge (DJB Labcare Ltd.). The DNA pellets were resuspended in 5 mL 70% ethanol (VWR International Ltd.) and centrifuged at > 4460 x g for 10 minutes at 4^{o}C. The pellets were air-dried for 10 minutes. DNA ∆8.91 was resuspended in 100 µL TE buffer provided by the Invitrogen Pure Link™ HiPure Plasmid DNA Maxiprep Kit and DNA pGIPZs (transfer vector DNA) and VSV-G in 300 µL of TE buffer and incubated for 37^{o}C, shaking gently for 30 minutes and then stored overnight at 4^{o}C. The next day, DNA concentrations were measured with NanoDrop ND-1000, Spectrophotometer (Latech International, UK). Lentiviral vectors (LVs) were stored at -20^{o}C at 1mg/mL.

NHSBT SCR.SOP for LV-production was followed to assemble the LV-pGIPZ particles. HEK293FT cells cultured in conditions described in Section II.2 were co-transfected at 60-70% confluency. The transfection mix was prepared in two 15 mL Falcon tubes. Tube 1 contained 3.75 mL OptiMem medium (Invitrogen™, Life Technologies), 50 µg LV transfer vector, 17.5 µg pVSV-G, and 32.5 µg p∆8.91, and Tube 2 containing 3.75 mL OptiMem medium (Invitrogen™, Life Technologies) and 200 µL Lipofectamine 2000 (Invitrogen™, Life Technologies). Each tube was incubated for 5 minutes at room temperature and then mixed gently and incubated for another 20 minutes, also at room temperature. Transfection mix was added to the flask of HEK293FT cells containing 10 mL of DMEM (Lonza) and incubated overnight at 37^{o}C in 20% O_2, 5% CO_2 and 100% humidity. The next day, media were replaced with 10 mL fresh media as described in Section II.2. On day 3, media from the flask was harvested and centrifuged at 300 x g for 5 minutes in a Hettich Rotina 46R centrifuge (DJB Labcare Ltd.) to remove any unwanted particles. The

supernatant with the viral particles was collected and stored at -80^{o}C for subsequent experiments.

II.9.4. Titration assay to determine TU/mL

To determine the transducing units (TU) per mL of the generated lentiviral stocks HEK293Ts were seeded in a 24-well plate at 5x10^{4} in culture media (described in Section II.2) a day before transduction. The next day, with a cell confluency of no more than 40-50%, cell were transduced with five fold viral dilution stocks as recommended by Dharmacon. LV-partilcle stocks were thawed on ice and diluted with serum-free media (DMEM) in a 96-well plate. Eight wells with 80 µL of serum-free media were prepared for each viral stock. Column 1 was used to dilute the neat viral stock (20 µL) with five fold subsequent dilutions from column 2 to 8, i.e. 20 µL of well mixed dilution 1 were transferred to column 2. Dilution 2 was then mixed well (pipetting up and down 10-15 times) before transferring 20 µL of dilution 2 into column 3, and so forth. Culture media of HEK293T cells was removed from each well and replaced with 225 µL of serum free media. HEK293Ts were transduced with 25 µL of diluted virus from the original 96-well plate **[Table II.9]**, thus an additional *10 fold dilution (25 µL is 1/10th of final volume in well of 250 µL)**.** The assay was incubated for 4 hours at 37^{o}C in 100% humidity and 5% CO_2. Transduction mix was then removed and replaced with 1 mL of culture media (DMEM with 10% (v/v) FBS and 1% (v/v) P/S). Cells were cultured for 48 hours at 37^{o}C in 100% humidity and 5% CO_2.Viral titres were determined by counting GFP positive colonies by microscopic observation. Colonies of 2 dilution factors were counted for each vector to calculate an average. Number of colonies were counted per

well and multiplied by the dilution factors: For example, titre of vector SV1= number of colonies x dilution factor x *additional dilutions= 30 x 625 x *40 (x40 = *10 fold dilution x *4, where 4 adjusts to obtain TU per 1 mL rather than per 250 µL used in 24 well-plate for titration assay). This calculation was provided by titration protocol from Dharmacon.

Table II.9. Protocol provided by Dharmacon.

Well (Row A, B, C, or D)		Volume of diluted virus	Dilution Factor
Originating (96 well plate)	Destination (24 well plate)		
A1	--	25 µL	5
A2	A1	25 µL	25
A3	A2	25 µL	125
A4	A3	25 µL	625
A5	A4	25 µL	3125
A6	A5	25 µL	15625
A7	A6	25 µL	78125
A8	--	25 µL	390625

Table illustrating set up used to carry out titration of lentiviral supernatants.

II.10. Puromycin kill curve

HEK293T cells were seeded at $5x10^4$/well, and KG-1 and KG-1A at $1x10^5$ in a 24-well plate in their culture media as described in Section II.2. The next day, culture media was replaced with the culture media, however this time containing puromycin from *Streptomyces alboniger* (Version# 09D24-MM, InvivoGen) Concentrations of puromycin tested included 0.25-16 µg/mL, as recommended by Open Biosystems. Percentage of surviving cells was monitored by eye under the microscope (as described by Open Biosystem), on

day 2, before replacing with freshly prepared selective media, i.e. culture media RPMI or DMEM with puromycin. The effect of the puromycin concentration was detected on day 3 and was optimal at a concentration of 2µg/mL for HEK293T cells and 5 µg/mL for KG-1 and KG-1A cells (graphs shown in Chapter V, Section V.2.3.1 and V.2.3.2 respectively). Transduced HEK293T cells were thus selected with 2µg/mL puromycin and KG-1 and KG-1A with 5 µg/mL puromycin until cell culture reached confluency.

II.11. Lentiviral transductions

II.11.1. Transducing adherent cells

HEK293T cells were plated at a density of $5x10^4$ cells/well in 24-well in DMEM (Lonza) and 1% (v/v) P/S (PAA Laboratories GmbH), 10% (v/v) FBS (PAA Laboratories GmbH), 500 µg/mL Geneticin (GIBCO®, Invitrogen™, Life Technologies; Cat# 10131027), 0.1 mM non-essential amino acids (GIBCO®; Cat# 11140050), and 1 mM sodium pyruvate (GIBCO®; Cat# 11360039) according to the Dharmacon, Thermo Scientific transduction protocol to transduce cells the following day at 40-50% confluency. The DMEM culture media were aspirated and viral supernatant was applied at an MOI of 2 and 5 for the GIPZ-shRNA lentiviral constructs and at MOI 5 and 10 for the SV2 lentiviral constructs. MOI = multiplicity of infection:

$$volume\ of\ viral\ supernatant\ \times \frac{(TU/mL)}{number\ of\ cells\ used\ for\ infection}\ .$$

The viral supernatant was left overnight for the non-concentrated LV-particles and for 6-7 hours for the high titre LV-particles, according to the

manufacturer's protocols. Viral supernatant was replaced with fresh culture media and cells were incubated for 48 hours before examining GFP expression by optical microscopy or selecting transduced cells with 2 µg/mL puromycin (Sigma Aldrich Co. LLC.) based on puromycin kill curve described in Section II.10. Thereafter, media was replaced every 3 days and cells were left to grow until 95% confluent. GFP expression was quantified by flow cytometry analysis.

II.11.2. Transducing cells in suspension

KG-1A or KG-1 cells at $1x10^5$/100 µL were plated into a 48-well plate in serum free RPMI-1640 and mixed with 500 µL of viral supernatant (MOI of 5; viral titre of $1x10^6$ TU/Ml). Cells were incubated at 37^{o}C for 6-7 hours. 400 µL of fresh growth media (RPMI-1640 medium with 20% (v/v) FBS) was added to incubating cells and the cells cultured for an additional 72 hours to allow vector integration and expression. Cells were then selected with 5 µg/mL puromycin (Sigma Aldrich Co. LLC.) based on the puromycin kill curve described in Section II.10 to select for transduced cells.

II.11.3. Optimising transduction of UCB-CD133$^+$ cells

RetroNectin® Recombinant Human Fibronectin Fragment (Takara, ClonTech; Cat#T100B) diluted to 100 µg/mL in sterile DPBS (PAA Laboratories GmbH) was pipetted at 500 µL/well in a 48-well plate, and incubated for 2 hours at room temperature. RetroNectin® solution was removed before adding cell suspension and viral supernatant. Plated cells in 48-well plate ± RetroNectin® and transduced with MOI of 10 ($5x10^4$ cells/well) and 20 ($2.5x10^4$ cells/well); titre at $1x10^6$ TU/mL= 500 µL viral supernatant per well for both MOIs, using the

pHR'SINcPPT-SEW vector. Cells were centrifuged at 600 x g at 32°C for 90 minutes (spinoculation) in a Hettich Rotina 46R centrifuge (DJB Labcare Ltd.) and then incubated overnight at 37°C, 20% O_2, 5% CO_2 and 100% humidity. Wells were topped up with 400 µL StemSpan (Stem Cell Technologies) and the 4 cytokines (IL-6, SCF, FLT-3L and TPO; R&D Systems) as previously described in Section II.5, and incubated for 24 hours. Cells were examined by fluorescent microscopy 48 hours post-transduction and eGFP expression quantified by flow cytometry.

II.11.4. Transducing UCB-CD133$^+$ cells with high titre virus

For each construct (pLKO.1-NT and pLKO.1-shRNA[HEF-1]), $9.5x10^5$ UCB-CD133+ cells were transduced with an MOI of 50 (~$3x10^5$ cells in 200 µL StemSpan with 15 µL of high titre ($1x10^9$ TU/mL) viral supernatant/well) by spinoculation on RetroNectin® coated 24-well plates as described in Section V.2.4. Cells were harvested 48 and 96 hours post-transduction to extract total protein for Western blot (WB) analysis.

II.11.5. Transducing UCB-CD133$^+$ cells with in house made concentrated LV-pLKO.1 particles

In order to achieve high titre stocks of in house made LV-particles, Amicon® Ultra-4, 100 kDa MW filtration devices (Millipore, USA, Cat# UFC810024) were used to concentrate LV-pLKO.1 and LV-SFFV.eGFP.WPRE supernatants.

For each construct, 20 mL of viral supernatant was harvested from transfected HEK293T cells as previously described in Section II.9. According to the manufacturer's protocol, 4 mL of LV-supernatant was loaded into each filtration unit and centrifuged in swinging buckets at 4000 x g for 20 minutes at 20^{o}C in a Hettich Rotina 46R centrifuge (DJB Labcare Ltd.). Concentrated supernatants were aliquoted and stored at -80^{o}C. With only 200 µL of concentrated virus stock available, the total number of target cells was adjusted to test two different MOIs. MOIs of 200 were tested on 5x10^{4}/well, whereas twice the number of cells (1x10^{5}/well) was transduced with an MOI of 100, all on RetroNectin® coated 48-well plates as described in Section V.2.4. Cells were harvested 72 hours post-transduction

II.12. Western blotting

Western blotting is a molecular biology technique that enables detection of the presence of specific proteins in a mixture extracted from cells. The procedure involves separating protein complexes by negative charge—which correlates roughly with the molecular mass or size—using gel electrophoresis, transferring these separated proteins onto a membrane, and finally detecting proteins of interest using protein specific antibodies. A positive protein:antibody interaction is visualised as a band on a X-ray film, blotting membrane, or imaging system. To carry out Western blotting, five main stages were performed.

Stage 1: ***Extracting protein from cells.*** This involved the following steps. Cells were washed with cold (4^{o}C) DPBS (PAA Laboratories GmbH) to remove any traces of culture medium and minimise proteolysis, dephosphorylation, and

denaturation. Adherent cells (HEK283T cells) were washed twice with cold 10 mL DPBS and then removed from the plates surface using small cell scrapers (Cat#29442-202, VWR International Ltd.). Lifted cells were harvested into 15 mL falcon tubes and centrifuged at 400 x g in a Hettich Rotina 46R centrifuge (DJB Labcare Ltd.) for 3 minutes at 4^{o}C. Cells in suspension were counted prior to washing with cold DPBS and then centrifuged as adherent cells. Cell pellets were lysed using lysis buffer known as Nonidet P-40 (NP-40) Lysis Buffer **[Table II.10].** This is made up of 1% IGEPAL (Sigma Aldrich Co. LLC.; equivalent to NP-40) (non-ionic, non-denaturing reagent), 20 mM Tris-HCL (Sigma Aldrich Co. LLC.), 137 mM NaCl (Sigma Aldrich Co. LLC.), 10% glycerol (Sigma Aldrich Co. LLC.), 2 mM Na_2EDTA (Sigma Aldrich Co. LLC.), and 1x protease inhibitor cocktail (Sigma Aldrich Co. LLC.) **[Table II.11].** HEK293T cells were lysed using 100 mL per 1x10^{6} cells, which was obtained from a 95% confluent T25 (25 cm^{2}) tissue culture flask. KG-1, KG-1A and Jurkat cells were lysed using 50 uL per 1x10^{6} cells. UCB-CD133^{+} cells were lysed using 30 uL per 1x10^{6} cells. Cell pellets with added lysis buffer were kept on ice for 30 minutes and gently vortexed every 5 minutes. Lysed cells were centrifuged at top speed (15,000 rpm) using a Hettich MIKRO 200/200R centrifuge (Hettich Centrifuges Ltd., Beverly, MA, USA) for 5 minutes at 4^{o}C. Cell lysates were carefully removed (leaving a micro-pellet), aliquoted into 500 µL eppendorfs and stored at -20^{o}C until used for Western blotting Stage 2-5.

Table II.10. Protocol followed to prepare NP-40 Lysis Buffer.

Reagents	Amount used to make up 100 mL NP-40 Lysis Buffer
1% IGEPAL	1 mL
20 mM Tris-HCL	440 mg Tris HCL+ 265 mg TRIZMA base
137 mM NaCl 58.4 fw	800 mg
10% Glyerol	10 mL
2 mM Na2EDTA 372.2 fw	74.4 mg
1x Protease inhibitor cocktail added just before use	10 uL per 1 mL made up lysis buffer

Table II.11. Components of protease inhibitor cocktail (Sigma Aldrich Co. LLC.)

PROTEASE INHIBITOR COCKTAIL, SIGMA ALDRICH CO. LLC.
AEBSF—[4-(2-Aminoethyl)benzenesulfonyl fluoride hydrochloride]—serine proteases, e.g..,trypsin, chymotrypsin, plasmin, kallikrein and thrombin; Aprotinin—serine proteases, e.g., trypsin, chymotrypsin, plasmin, and kallikrein, human leukocyte elastase, but not pancreatic elastase; Bestatin hydrochlorine—aminopeptidases, e.g., leucine aminopeptidase and alanyl aminopeptidase; E-64-[N-(trans-Epoxysuccinyl)-L-leucine4-guanidinobutylamide]—cysteine proteases, e.g., calpain, papain, cathepsin B, and cathepsin L; Leupeptin hemisulfate salt—both serine and cysteine proeteases, e.g., plasmin, trypsin, papain, and cathepsin B.; Pepstatin A—acid proteases, e.g., pepsin, rennin and cathepsin D, and many microbial aspartic proteases.

Stage 2: ***Quantifying total protein***. Frozen cell lysates were thawed on ice. Bio-Rad DC™ Protein Assay (Cat# 500-0116), containing Reagent A (alkaline copper tartrate solution), Reagent B (Folin), and Reagent S (description not provided by the manufacturer; BIO-RAD Laboratories Ltd., Hemel Hempstead, Hertfordshire, UK), was used to determine the protein concentration in the extracted cell lysates. The Bio-Rad DC™ Protein Assay is a colorimetric assay where a reaction occurs between protein and copper in an alkaline medium, and the subsequent reduction of Folin reagent by the copper-

treated protein. The development of a blue colour is primarily due to the amino acids tyrosine and tryptophan, and to a lesser extent, cystine, cysteine, and histidine. To carry out the assay BSA stocks were prepared using BSA from Sigma Aldrich Co. LLC. at the following concentrations: 0.2, 0.5, 1.0, 1.5 and 2.0 mg/mL in NP-40 Lysis Buffer **[Table II.12]**. Bio-Rad reagents were aliquoted into two separate 15 mL falcon tubes: Tube1 containing Bio-Rad Reagent B and Tube2 containing mixed Bio-Rad Reagent A (1 mL) with 20 µL of Bio-Rad Reagent S. Using a clear 96 well plate, 5 µL of standard stocks were pipetted in triplicates and 5 µL of the thawed cell lysates were also plated out in triplicates. HEK293T cell lysates were diluted 1:5 in NP-60 Lysis Buffer. Then 25 µL of Bio-Rad Reagent A+S was added per well, followed by 200 µL of Bio-Rad Reagent B per well. The assay was incubated for 15 minutes at room temperature in the dark. Absorbance was read using Microplate Reader Bio-Rad (BIO-RAD Laboratories Ltd) set at 655nm. Absorbance values were interpreted in a spreadsheet using Microsoft Excel and protein concentrations were determined relative to the standard curve absorbance values obtained. The volume of cell lysate required to load 25-50 µg of total protein for Western blotting was subsequently calculated.

Table II.12. Preparing BSA stocks for standard curve.

Desired BSA concentrations mg/mL (µg/uL)	Amount in uL from BSA stock (10mg/ml)	Amount in uL of NP-40 Lysis Buffer as dilutant (µL)
2.0	200	800
1.5	150	850
1.0	100	900
0.5	50	950
0.2	20	980

Stage 3: ***Running the gel.*** NuPAGE® Bis-Tris Gels, 12% acrylamide (Invitrogen™ Ltd.) were used to separate the proteins. A maximum of 20 µL could be loaded into the NuPAGE® Bis-Tris Gels. Cell lysates (*x* µL) were prepared with 2.5 µL NuPAGE® LDS Sample Buffer (Invitrogen™ Ltd.), 1 µL NuPAGE® Reducing Agent 10x (Invitrogen™ Ltd.), and 6.5 µL dH_2O to a final volume of ~20 µL according to the manufacturers specifications (Invitrogen™ Ltd.). Prepared samples were vortexed for a few seconds, pulse spun for ~30 seconds using a Hettich MIKRO 200/200R centrifuge, and then incubated at 70^{o}C for 10 minutes on a heating block (Fisher Scientific UK Ltd., Loughborough, UK). Samples were allowed to cool down for 5 minutes and then pulse centrifuged for ~30 seconds using a Hettich MIKRO 200/200R centrifuge and where then ready for loading. Samples were loaded into the NuPAGE® Bis-Tris Gel (maximum 20 µL) with a molecular weight ladder, Full-Range Rainbow Molecular Weight Markers, Cat# RPN800E from Amersham™, GE Healthcare UK Ltd., and run at 200 volts for 48 minutes in NuPAGE® MES SDS Running Buffer (20X) (Invitrogen™ Ltd.). The running buffer is made up of 50 mM MES, 50 mM Tris Base, 0.1% (v/v) SDS, 1 mM EDTA, at pH 7.3, diluted 1:50. The gel was then transferred onto Mini iBlot® Transfer Stacks, 0.2-micron nitrocellulose (Invitrogen™ Ltd.), using Invitrogen iBlot® programme 2. Membranes were blocked with 5% (w/v) skim milk in 1x TBST (100 mM Tris HCL, 150 mM NaCl, 0.1% Tween 20, pH 7.4) [blocking buffer] for 30 minutes at room temperature after transfer.

Stage 4: ***Immunoblotting for protein of interest.*** Western blots were probed with antibodies against either mouse anti HIF-1α, clone 54/HIF-1α (BD Transduction Laboratories™) at 1:250 dilution in blocking buffer for KG-1 cells

and 1:500 dilution in blocking buffer for UCB-CD133^{+}, cells to confirm hypoxic effect or mouse monoclonal [2G9] anti-HEF-1 (Cat#ab18056, Abcam®, Cambridge UK). To evaluate equal loading of total protein per well, purified mouse anti-Actin Ab-5, clone C4/actin (BD Transduction Laboratories^{TM}) was used at dilution 1:5000 in blocking buffer. Anti-GAPDH was used to detect GAPDH in HEK293T cells (Cat# ab9485, Abcam®, Cambridge UK), and to detect α-tubulin as a loading control anti-α-tubulin at 1:4000 (Cat# ab18251, Abcam®, Cambridge UK).

Stage 5: ***Detecting immunoblotted protein by X-ray film.*** Secondary antibody, ECL anti-mouse IgG horseradish peroxidise linked (Amersham^{TM}, GE Healthcare UK Ltd., Cat#NA93IV) was used to detect the antibody with ECL Western Blot Detection Reagents (Amersham^{TM}, GE Healthcare UK Ltd., Cat#RPN2106) or SuperSignal West Dura Extended Duration Chemiluminescent Substrate (Thermo Scientific, Cat# 34076).

II.13. Densitometry analysis

To quantify Western blots, software Image Studio Light (open source, http://www.licor.com/bio/products/software/image_studio_lite/, was used. Scanned images of Western blots or already annotated diagrams in JPG format were imported by selecting ' import' and then 'other image'. An excel spreadsheet was created to export 'output data'. Under the 'shapes' tab, 'draw rectangle' was used to draw a rectangle first around loading control bands. A large enough box should be drawn to be able to use the same rectangle for all consecutive bands. Rectangle was copied (Command C) and pasted

(Command V) onto subsequent bands. Position of the rectangle was adjusted by using arrows on keyboard. Software produces 3 readings for each band: R (red), G (green), and B (blue); found at bottom of window under 'shapes'. Each of these readings represented densitometry readings using different 'filters' (channels); useful when analysing a colour image. However, Western blots were in greyscale, thus readings were the same for all three channels. For example, 45 readings were equivalent to 15 unique readings. Densitometry readings were exported by selecting the 'table' tab to 'export file' and selecting created excel spreadsheet. In excel a filter was applied using 'data' tab to select only one channel's readings to start analysing and plotting data. The curser needed to be on first row when applying 'filter' command.

In each Western blot, actin or α-tubulin protein was detected as a loading control. The loading control allowed correction of pipetting variability between samples. For example, actin or α-tubulin densitometry signal was retrieved and entered into the first 5 entries shown in **[Table II.13].** A separate column was created to normalise all data. To normalise the data, one condition, in this instance the 'Non-transduced' condition was selected as the assays control. The densitometry signal of the selected control became the denominator, e.g. $D$5, to determine a 'normalisation factor'. Thus control = Excel formula D5/$D$5 = 1. The normalisation factors of subsequent conditions were obtained using D6/$D$5 (shRNA[GAPDH]), D7/$D$5 (shRNA[HEF-1A]) etc. **[Table II.13]**. Once the normalisation factor was determined the densitometry signal of the test protein could be calculated as follows: 'Signal' (column D)/normalisation factor (column M) = normalised signal (column N). Finally, the '% of protein expression' was derived as a percentage of the 'Non-transduced' normalised

signal, e.g. Non-trans = N19/N$19, shRNA[GAPDH] = N22/N$19,…etc. Where protein levels were not compared to a control condition, i.e. Non-transduced sample, the 1st experiment was used as the 'control' (baseline) to determine the normalisation factors.

Table II.13. Example of excel spreadsheet to analyse densitometry results

	A	B	C	D	F	H	K	L	M	N	O
3	Image Name	Channel	Name	Signal	Area	Type	Protein	Condition	Normalising Factor	Normalised Signal	% Protein Expression
4	LV-Gipz anti-HEF1 in HEK293Ts. R		00001	82645	1595	Signal	Loading Control	Non-transduced	1		
7	LV-Gipz anti-HEF1 in HEK293Ts. R		00004	87640	1595	Signal	Loading Control	shRNA[GAPDH]	1.060439228		
10	LV-Gipz anti-HEF1 in HEK293Ts. R		00007	88654	1595	Signal	Loading Control	shRNA[Non-Sil]	1.072708573		
13	LV-Gipz anti-HEF1 in HEK293Ts. R		00010	91228	1595	Signal	Loading Control	shRNA[HEF-1A]	1.103853833		
16	LV-Gipz anti-HEF1 in HEK293Ts. R		00013	98158	1595	Signal	Loading Control	shRNA[HEF-1B]	1.187706455		
19	LV-Gipz anti-HEF1 in HEK293Ts. R		00016	39114	1595	Signal	GAPDH	Non-transduced		39114	100%
22	LV-Gipz anti-HEF1 in HEK293Ts. R		00019	24894	1595	Signal	GAPDH	shRNA[GAPDH]		23475	60%
25	LV-Gipz anti-HEF1 in HEK293Ts. R		00022	44142	1595	Signal	GAPDH	shRNA[Non-Sil]		41150	105%
28	LV-Gipz anti-HEF1 in HEK293Ts. R		00025	45234	1595	Signal	GAPDH	shRNA[HEF-1A]		40978	105%
31	LV-Gipz anti-HEF1 in HEK293Ts. R		00028	42964	1595	Signal	GAPDH	shRNA[HEF-1B]		36174	92%
34	LV-Gipz anti-HEF1 in HEK293Ts. R		00031	37793	1595	Signal	HEF-1	Non-transduced		37793	100%
37	LV-Gipz anti-HEF1 in HEK293Ts. R		00034	45071	1595	Signal	HEF-1	shRNA[GAPDH]		42502	112%
40	LV-Gipz anti-HEF1 in HEK293Ts. R		00037	39625	1595	Signal	HEF-1	shRNA[Non-Sil]		36939	98%
43	LV-Gipz anti-HEF1 in HEK293Ts. R		00040	39420	1595	Signal	HEF-1	shRNA[HEF-1A]		35711	94%
46	LV-Gipz anti-HEF1 in HEK293Ts. R		00043	36461	1595	Signal	HEF-1	shRNA[HEF-1B]		30699	81%
49											

II.14. Statistical analysis

Each experiment was repeated independently at least three times. Student's paired t-test or one-way ANOVA of variance was used for statistical analysis unless stated otherwise. The standard deviation (SDEV) was provided for most data, to present the variability between individual experiments in a sample, and the standard error of the mean (SEM) when wanting to show how closely the sample mean represents the population mean (Cumming et al., 2007, Nagele, 2003). All analyses were carried out using software Prism Graph 5, GraphPad Software Inc. http://www.graphpad.com/scientific-software/prism/. $P < 0.05$ was considered statistically significant.

Chapter III Optimising Functional Assays

III.1. Introduction

HSCs infused into the patient have to find their way home to the BM (homing). This involves a multistep journey of rolling, tethering, adhesion, transendothelial migration, and finally lodgement into specific niches. Homing is a multistep process, involving a repertoire of adhesion molecules and physiological cues such as chemokines and cytokines (Chiou et al., 2013). Physical forces such as shear stress also influence the activity of adhesion/migration molecules involved in the process (Christophis et al., 2011, Peled et al., 1999a). Initially, the selectin ligands on HSCs or BMEC are involved in rolling and tethering of HSCs to BMEC **[Figure III.1].** Circulating HSCs and HSPCs respond particularly to the chemoattractant SDF-1 (Watt and Forde, 2008, Wuchter et al., 2014), which is secreted by BMECs (Jo et al., 2003, Yun and Jo, 2003). SDF-1 activates integrins such as VLA-4, LFA-1, and VLA-5 on migrating HSCs/HSPCs to mediate firm adhesion to their ligands on BM endothelium (Hidalgo et al., 2001, Peled et al., 2000), as well as to extracellular matrix (Papayannopoulou et al., 1995, Papayannopoulou and Nakamoto, 1993, Rood et al., 2000b, Teixido et al., 1992). At this stage, integrins can act directly as signalling receptors, triggering “outside-in signalling”, or become activated (have increased avidity to ligand) upon engagement of cell surface receptors to chemokines and cytokines. This in turn activates downstream adaptor molecules known as “inside-out signalling” (Kinashi, 2005). These signalling events lead to structural rearrangements of the cells, enabling the cell to adhere, stop rolling, transmigrate and continue their journey. HSCs/HSPCs will enter the

BM and eventually lodge in the appropriate niche, where engraftment takes place; HSCs/HSPCs are able to self-renew and produce new progeny.

BMECs, BMSCs and osteoblasts are important niche cells, shaping HSC/HSPC fate. Osteoblasts are an integral part of the endosteal niche, able to recruit HSCs/HSPCs through Notch signalling (Weber and Calvi, 2010) as well as secreting the chemokine SDF-1 (Jung et al., 2006). Osteoblasts also express haemopoietic growth factors (Jung et al., 2005, Ponomaryov et al., 2000, Taichman and Emerson, 1994, Taichman et al., 1996) and osteopontin, a multidomain, phosphorylated glycoprotein, which modulates HSC/HSPC maintenance and proliferation (Nilsson et al., 2005). Other HSC/HSPC niche cells that contribute to the haemopoietic environment and serve as a rich source of growth factors for a variety of haemopoietic processes include perivascular stromal cells (BMSCs). These niche cells are particularly well known for their ability to maintain haemopoiesis in long-term cultures (Corselli et al., 2013, Dexter et al., 1990a, Dexter et al., 1990b, Dorshkind, 1990, Fan et al., 2013). Recently studies from Kunisaki et al. have indicated that nestin^{+} perivascular cells (Nes^{peri}) adjacent to AECs maintain HSC quiescence in mice (Kunisaki et al., 2013). Interestingly, BMSCs secrete SDF-1α more abundantly than BMEC (Yun and Jo, 2003), not surprisingly also influencing molecular activities of local and nearby HSCs/HSPCs (Kortesidis et al., 2005, Schajnovitz et al., 2011)**.**

To mimic these niches in our functional studies, the immortalised human BMEC-60 cell line and primary BMSCs and osteoblasts were used together with UCB-CD133^{+} HSCPs in *in vitro* assays. BMEC-60 cells were used for both adhesion and transwell migration assays, and BMSCs and osteoblasts for

adhesion assays only. Tests were performed to optimise the adhesion and the transwell migration assay and these are presented in this chapter.

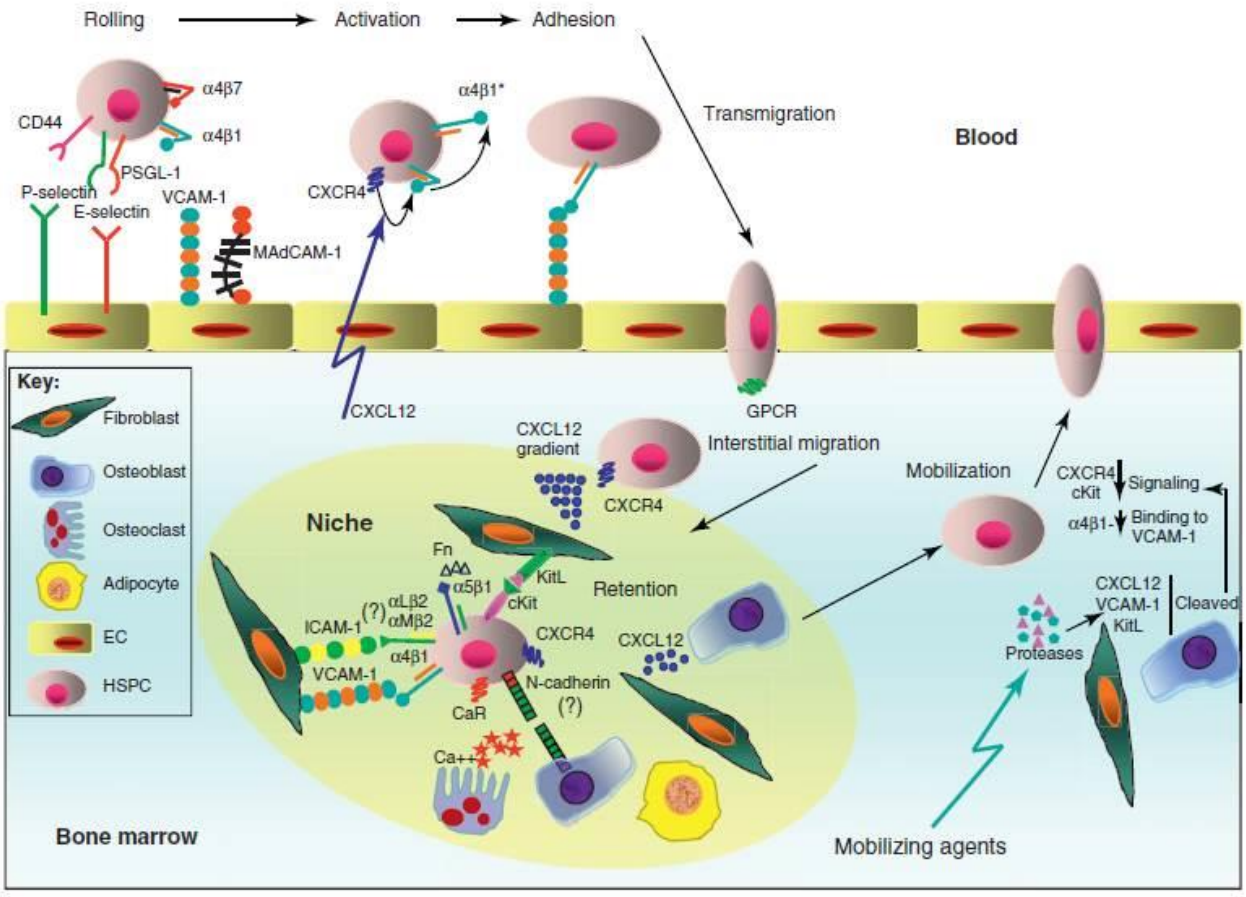

Figure III.1. Survival, homing, and successful engraftment are factors that determine the fate of transplanted HSCs and their progeny.

Homing is a multistep process mediated by an array of adhesion molecules whose action is regulated by signalling cascades. Molecular signalling events and environmental cues influence each stage. Tethering and rolling of HSPCs is mediated by an on and off binding of selectins and their ligands. Cytokines and chemokines can then be presented on the surface of substrate cells to rapidly increase the avidity of downstream integrins, or secreted in soluble form to induce changes in integrin affinity states (Levesque et al., 1995, Shamri et al., 2005, Solanilla et al., 2003).The net effect results in stimulated cells moving along (tethering) and migrating through (diapedesis) substrate cells (Kinashi, 2005). Presentation of chemokine SDF-1α on BM endothelial cells (BMEC) activates integrins such as VLA-4 on $CD34^{+}$ cells (Rood et al., 2000b). Firm adhesion is followed by cytoskeletal rearrangements to extend the leading edge of the cell, as this will enable the cell to transmigrate through the endothelium and enter the BM extra vascular space where the HSPCs interact with niche elements. Picture credit: Reprinted from Trends in Immunology, Vol 32, issue 10, Mazo I.B., Massberg S., von Andrian U.H., Hematopoietic stem and progenitor cell trafficking, pp. 493–503, Copyright 2014, with permission from Elsevier.

III.2. Results

III.2.1. Individual profiles of BM niche substrate cells

Cell surface phenotyping involving flow cytometry analysis compared the cell surface profile of BMEC-60 cells, BMSCs and osteoblasts (termed substrate cells in our functional assays) **[Figure III.2]**. The panel of mAbs to cell surface markers included: CD31 (endothelial and haemopoietic), CD14 (monocytes), CD45 (leukocytes), CD34 (progenitor cells), CD90 (adhesion molecule; Thy 1), CD29 (β1 integrin; adhesion molecule), CD44 (adhesion receptor), CD105 (endoglin, endothelial and BMSCs), CD106 (VCAM-1; activated endothelial cells), and CD166 (also known as activated leukocyte cell adhesion molecule (ALCAM); activated endothelial and BMSCs). BMEC-60s were also phenotyped after IL-1β stimulation to compare expression of adhesion molecules pre- and post-stimulation, but no differences were observed.

IL-1β stimulated BMEC-60 cells expressed high levels of CD31, were CD45 negative, and showed only low levels of CD14. Primary osteoblasts and BMSCs were negative for endothelial and haemopoietic markers CD31 and CD34, as well as for CD45 and CD14. All three cell types expressed high levels of cell adhesion molecules/receptors CD90, CD166, CD105, CD44 and CD29. Adhesion molecule CD106 (VCAM-1) was expressed only at low levels in osteoblasts and BMEC-60, and absent in BMSCs. These immortalised endothelial cells were kindly provided by Professor Ellen Van der Schoot, who confirmed their normal phenotype and showed that IL-1β stimulation induced expression of E-selectin, ICAM-1, and VCAM-1 (Rood et al., 2000a).

Stimulating these BMEC-60 cells in house with IL-1β also resulted in increased expression of VCAM-1 (CD106), although this was not statistically significant (MFI difference = 213.5; $p>0.05$). IL-1β stimulation also increased the expresson of CD29 (integrin β1; MFI difference = 6639; $p>0.05$), adhesion molecule CD166 (MFI difference = 3386; $p>0.05$), adhesion receptor CD44 (MFI difference 609.5; $p>0.05$) and antigen CD34 (MFI difference = 1825; $p>0.05$). IL-β stimulation also enhanced adhesion in our functional assay **[Figure III.5B and Figure III.6]. Figure III.3** summarises the cell surface profile as a distinctive 'fingerprint' for each cell type.

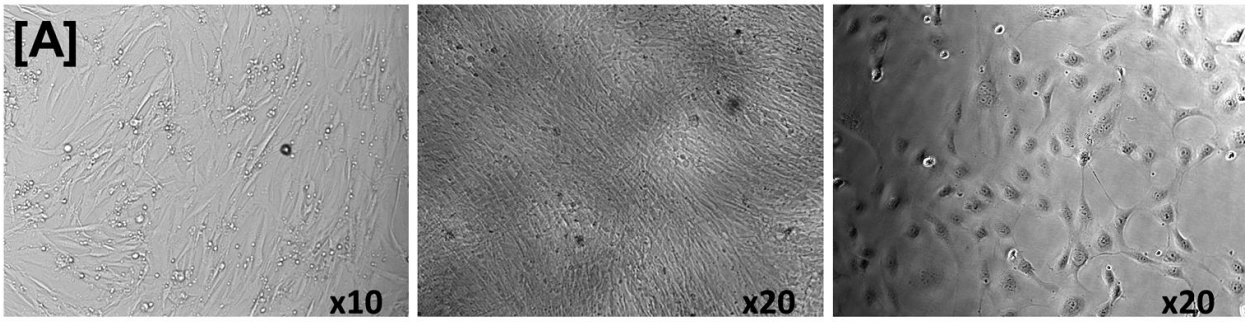
[A]
x10
x20
x20

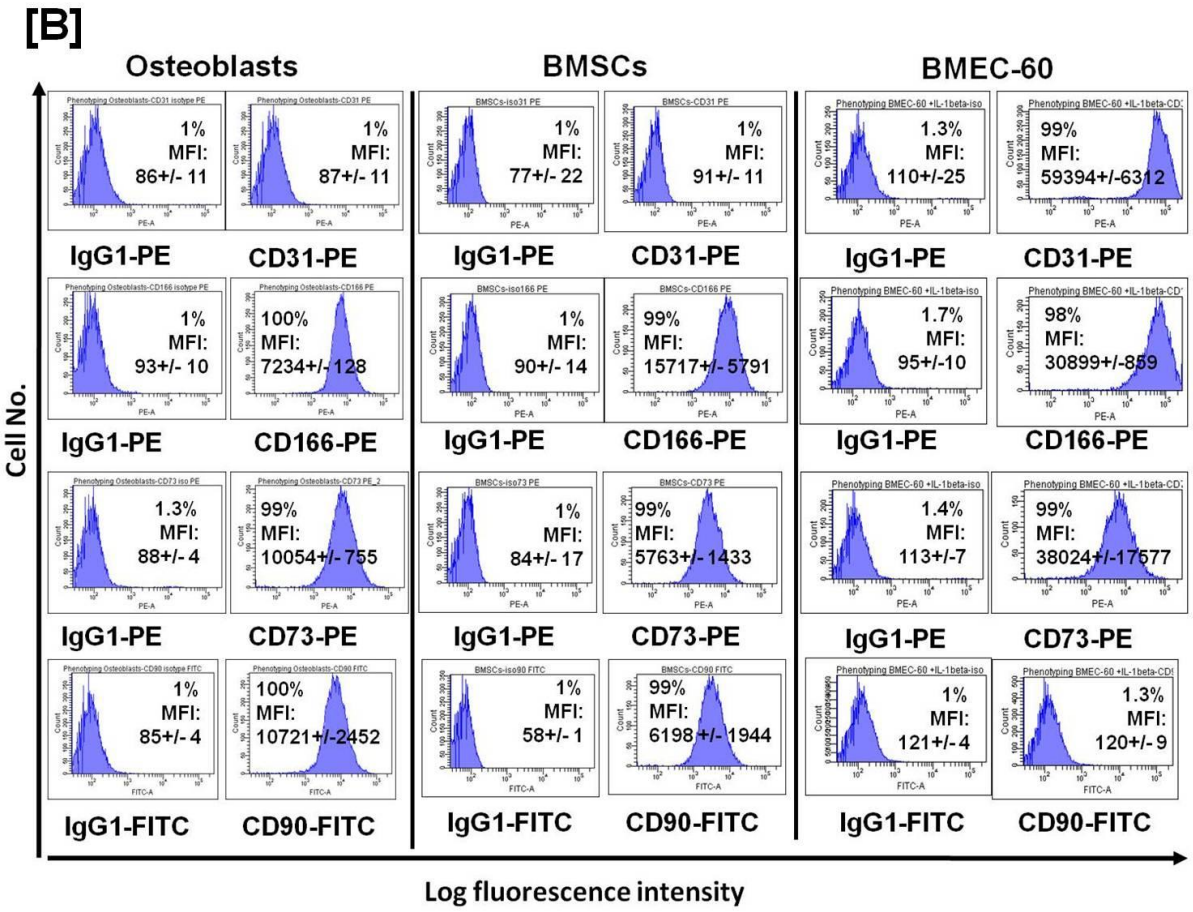
[B]
Osteoblasts
BMSCs
BMEC-60
1% MFI: 86+/- 11
IgG1-PE
1% MFI: 87+/- 11
CD31-PE
1% MFI: 77+/- 22
IgG1-PE
1% MFI: 91+/- 11
CD31-PE
1.3% MFI: 110+/-25
IgG1-PE
99% MFI: 59394+/-6312
CD31-PE
1% MFI: 93+/- 10
IgG1-PE
100% MFI: 7234+/- 128
CD166-PE
1% MFI: 90+/- 14
IgG1-PE
99% MFI: 15717+/- 5791
CD166-PE
1.7% MFI: 95+/-10
IgG1-PE
98% MFI: 30899+/-859
CD166-PE
1.3% MFI: 88+/- 4
IgG1-PE
99% MFI: 10054+/- 755
CD73-PE
1% MFI: 84+/- 17
IgG1-PE
99% MFI: 5763+/- 1433
CD73-PE
1.4% MFI: 113+/-7
IgG1-PE
99% MFI: 38024+/-17577
CD73-PE
1% MFI: 85+/- 4
IgG1-FITC
100% MFI: 10721+/-2452
CD90-FITC
1% MFI: 58+/- 1
IgG1-FITC
99% MFI: 6198+/- 1944
CD90-FITC
1% MFI: 121+/- 4
IgG1-FITC
1.3% MFI: 120+/- 9
CD90-FITC
Cell No.
Log fluorescence intensity

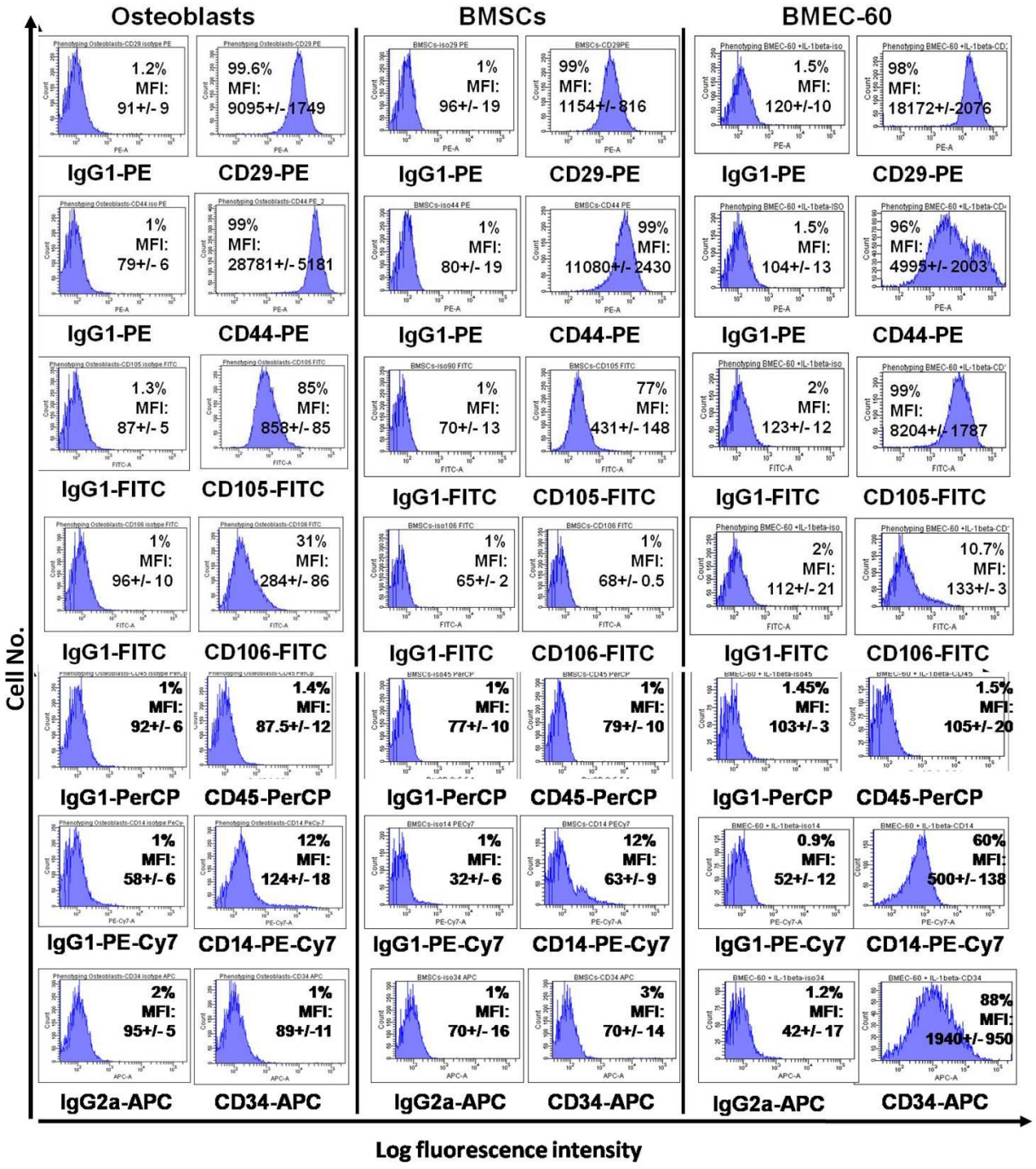

Figure III.2. BM niche cells used in adhesion assays.

[A] Microscopy images of osteoblasts [x10], BMSC [x20] and BMEC-60 [x20]. Morphology and flow cytometry analysis confirm cells express relevant adhesion molecules and of cell surface markers specific for these cell types. [B] The median fluorescence intensity (MFI) ± SEM (n=3 independent experiements) of each analysis was recorded to quantify the expression levels of the antigen identified. The % of the cell population positive for the particular marker is also presented.

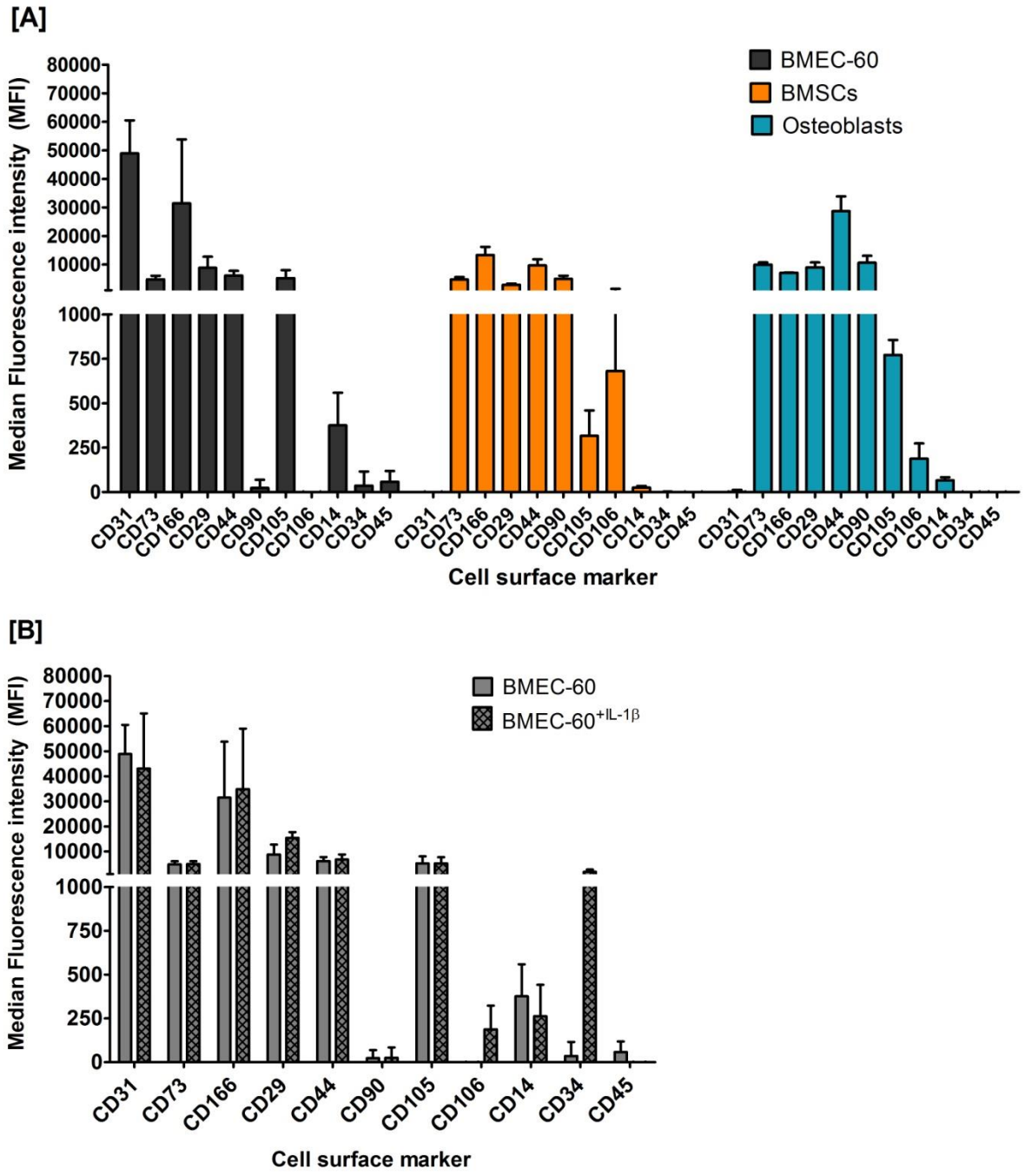

Figure III.3. Distinct 'fingerprints' of BM substrate cells.

[A] A quantitative profile based on the MFI values obtained by FACS. Bar graphs enable comparing the cell surface phenotypes of the three cell types. Values are means ± SEM of n=3 independent experiments. [B] Comparing MFI values between non-stimulated and IL-1β stimulated BMEC-60 cells. Values are means ± SEM of n=3 independent experiments.

III.2.2. KG-1 and KG-1A: models for UCB-HSPCs

As only a limited number of $CD133^+$ HSPCs can be harvested from human UCB, KG-1 and KG-1A cells were chosen as model cell lines for optimising assays as well as testing our experimental hypotheses. Both haemopoietic cell lines are derived from leukaemic myeloid cells (Furley et al., 1986) and express the progenitor marker CD34 (Fernández et al., 2000). Here we confirm CD34 expression on both cell lines and show they are negative for stem cell marker CD133. KG-1A cells have previously been reported to be negative for CD133 (Yin et al., 1997). An immortalised T-lymphocyte cell line, Jurkat, (Abraham and Weiss, 2004) was used as a negative control for both antigens, while $CD133^+CD34^+$ UCB-cells were used as the positive control **[Figure III.4]**

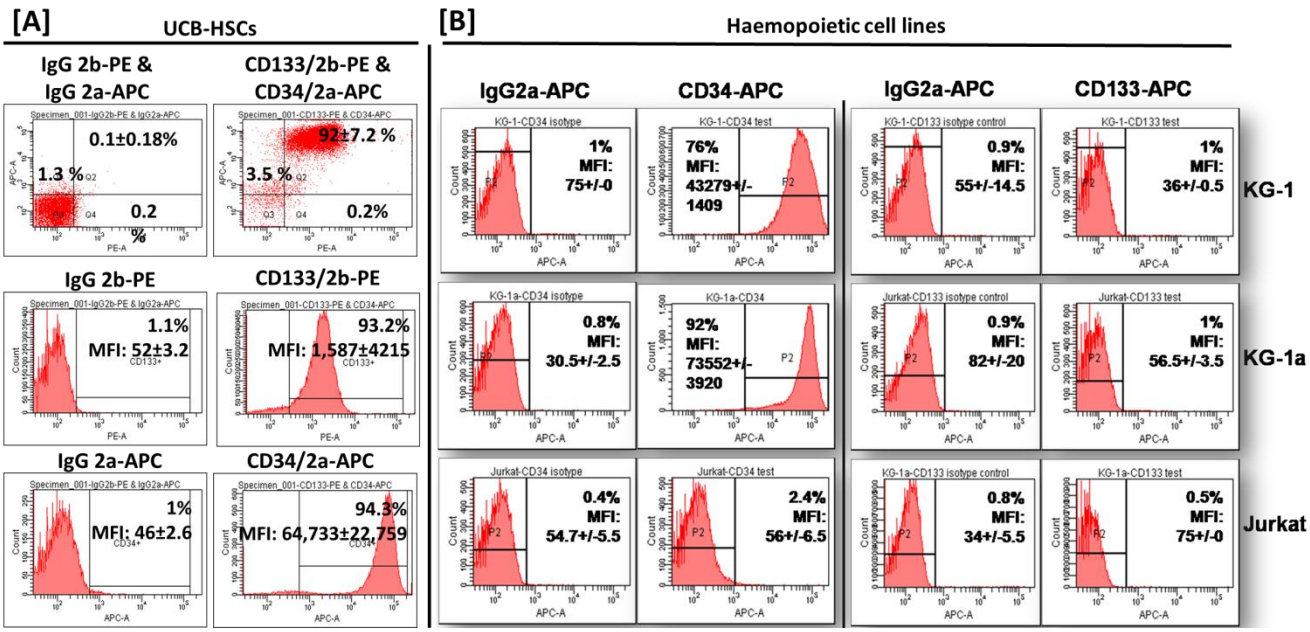

[C]

Stem cell progenitor maker

Cell type	CD133	CD34
UCB-HSCs	++	++++
KG-1	-	+++
KG-1A	-	++++
Jurkat	-	-

Figure III.4. CD34 Expression confirmed on model cell lines.

[A] HSPCs isolated using microbeads specific for $CD133^+$ antigen from human UCB. Flow cytometry analysis confirms $CD133^+CD34^+$ antigen expression. Isotype controls included IgG2b-PE and IgG2a-APC. [B] Same antibodies were used to detect these markers on KG-1, KG-1A, and Jurkat cells. Results confirm that KG-1 and KG-1A express high levels of CD34 antigens, but were negative for CD133 expression. Jurkat cells do not express CD34 nor CD133. [C] Qualitative representation of FACS results. n=3 independent batches for all ± SEM).

III.2.3. Do KG-1 cells bind to the niche cells?

Adhesion to BM niche cells (substrate cells) was first examined under normoxic conditions, i.e. 20% O_2, using KG-1 cells with regard to two variables: (1) the ratio of adhering cells to substrate cells (osteoblasts, BMSCs, and BMEC-60) and (2) BMEC-60 substrate cells pre-stimulated with IL-1β. Adhering cells (KG-1 cells) were labelled with BCECF-AM, a membrane-permeable fluorescent indicator, and then seeded onto a monolayer of one of the substrate cells for 1 hour at 37^{o}C. A percentage of cell adhesion was determined by the ratio of fluorescence intensity of adhering cells post-wash to pre-wash multiplied by 100 as follows:

$$\frac{(fluorescence\ intensity\ pre{-}wash)}{(fluorescence\ intensity\ post{-}wash)} \times 100\%.$$

A standard curve also shows a linear relationship between fluorescence intensity and KG-1 cell concentration/well **[Figure III.5A]**, and indicated the level of fluorescence intensity expected in relative light units (RLU) for a given cell count. Results showed a maximum binding of 3.5x10^4 KG-1 cells to 1x10^4 osteoblasts, i.e. a maximum of 3.5 KG-1 cells per osteoblast **[Figure III.5C]**. Similarly, a maximum of 3.75 KG-1 cells bound per BMSC cells, based on a maximum of 7.5x10^4 KG-1 cells binding to 2x10^4 BMSCs **[Figure III.5D]**. We did not test high enough concentrations to calculate the maximum cell binding capacity of the BMEC-60 substrate **[Figure III.5E]**. The data in **Figure III.5B** verify that IL-β stimulation enhances adhesion to BMEC-60. The absolute number of adhering cells was deduced from the standard curve and was consistent with the percentage adhesion shown in the plots.

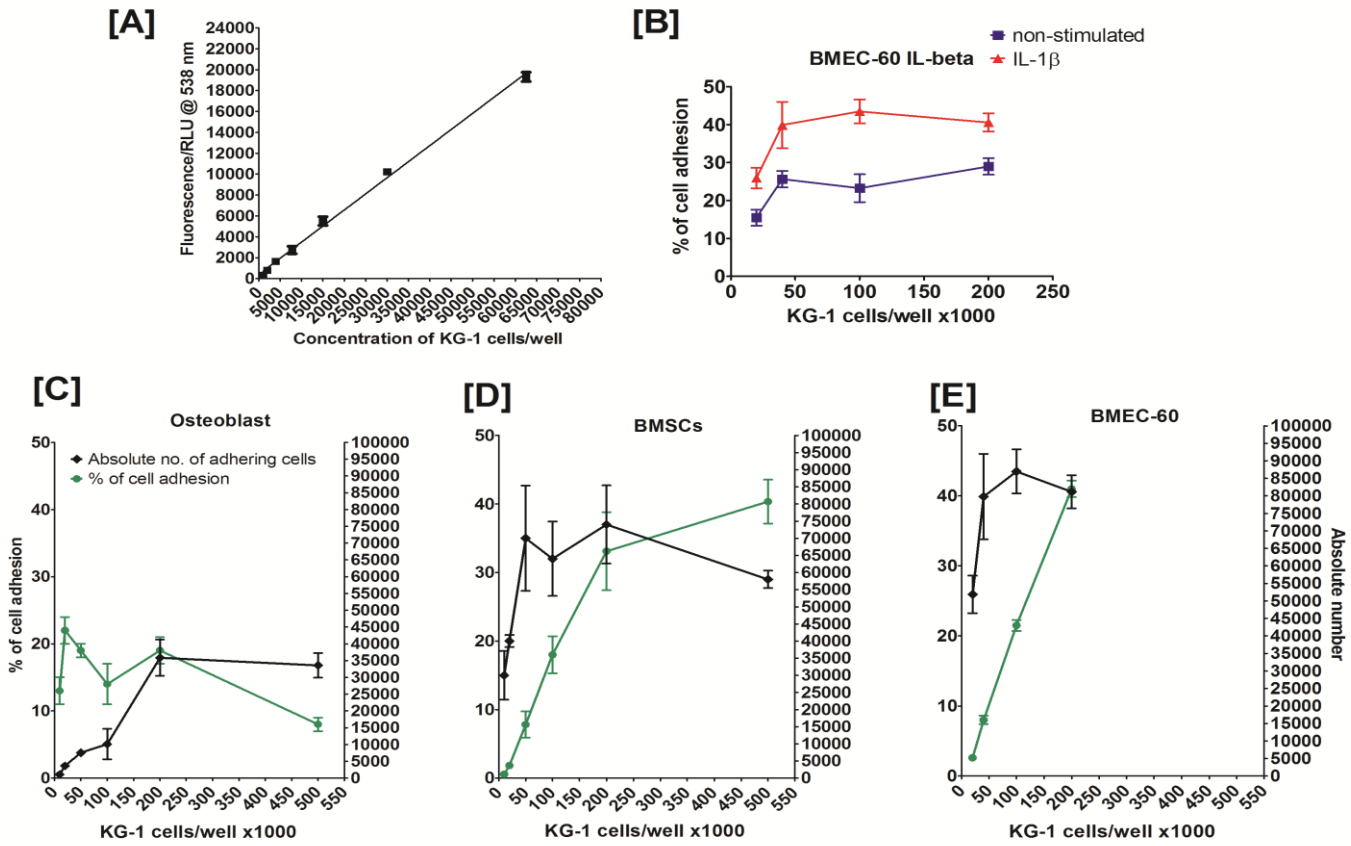

.

Figure III.5. Optimising an in vitro adhesion assay.

[A] Standard curve showing fluorescence as a function of KG-1 cell number/well. [B] % adhesion of KG-1 cells to BMEC-60 cells is enhanced by treatment with IL-1β (n=3 independent experiments). [C-D] The % of cell adhesion (black data points) as well as the absolute number of adhering cells (green data points). This comparison illustrate how increasing KG-1 cell counts (x-axis) result in the saturation of the assay, which is reflected in a decline in % of cell adhesion. [C] % adhesion of KG-1 cells to osteoblast cells peaks at $3x10^4$ to $4x10^4$ cells per $1x10^4$ osteoblasts (n=3 independent experiments). [D] The % adhesion of KG-1 cells to BMSCs peaks at $5x10^4$ to $7.5x10^4$ cells per $2x10^4$ BMSCs (n=3 independent experiments). [E] KG-1 concentration tested was not high enough to calculate the maximum binding capacity of BMEC-60 cells (n=3 independent experiments), however by $2x10^5$ the % of adhering cells is no longer increasing, suggesting KG-1 adhesion to $2x10^4$ BMEC-60/well peaks between $1x10^5$ and $2x10^5$. Values are means ± SDEV. Green line= absolute number of adhering cells; black line = % of cell adhesion.

Based on the results obtained using KG-1 cells, the adhesion of UCB-CD133^{+} cells to the three substrate cells was examined. **Figure III.6A** shows that differences between all three substrates (excluding non-stimulated BMEC-60) are not statistically significant ($p>0.05$). However, stimulating BMEC-60 clearly increases the adhesion potential of UCB-CD133^{+} cells ($p<0.0001$).

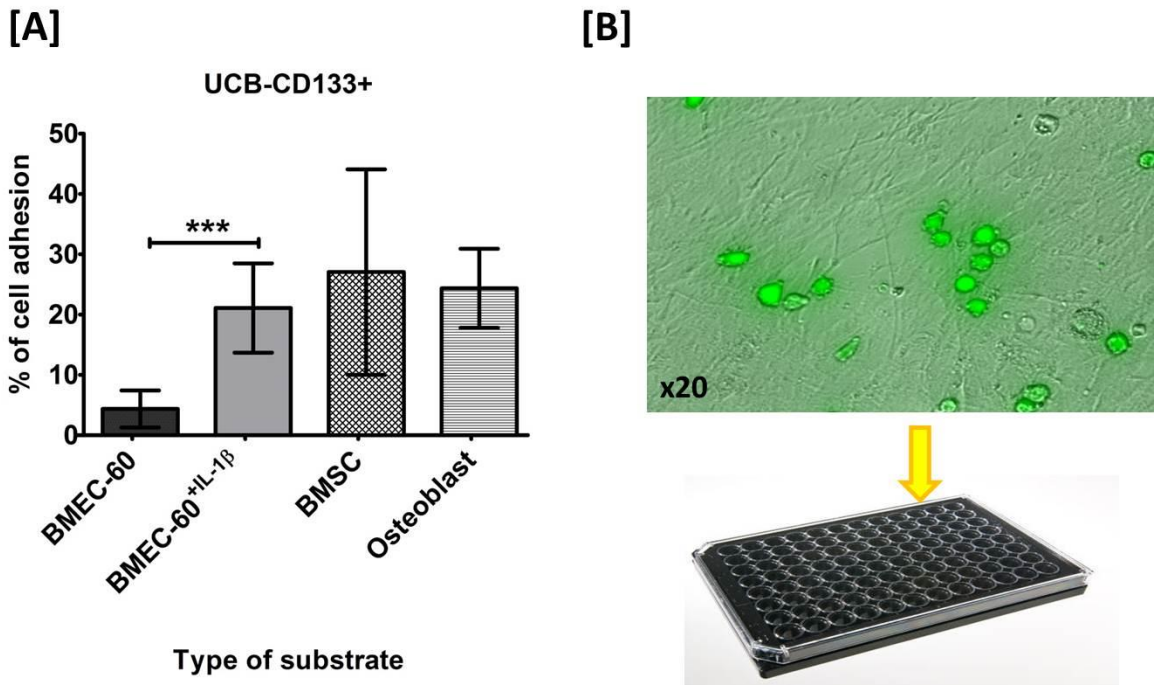

Figure III.6. UCB-CD133^{+} cell adhesion to substrate cells.

[A] Adhesion of $2x10^{4}$ UCB-CD133^{+} cells/well were tested to all three substrates, including to IL-1β stimulated BMEC-60. IL-1β stimulation significantly enhances ($p<0.0001$) the adhesion potential to BMEC-60s (4.36±3.07% vs. 21.1±7.4%). 27±17.04% of UCB-CD133^{+} adhere to BMSCs and 24.37±6.55% to osteoblasts; ± = SDEV; n= 3 independent experiments. [B] Microscopy image of adhesion of BCECF-AM (green) labelled UCB-CD133^{+} cells to osteoblasts post-wash in a 96 black-coated well plate. *** = $p<0.0001$; 1 way ANOVA followed by Dunn's Multiple Comparison Test.

III.2.4. UCB-CD133$^+$ cell migration across BMEC-60 cells

In the process of homing, HSCs/HSPCs migrate across the BM endothelium and extracellular matrix in response to the chemokine SDF-1 (Dar et al., 2006, Peled et al., 1999a, Voermans et al., 1999). Hypoxia upregulates the expression of SDF-1 in the BM and sequesters circulating HSCs/HSPCs towards this hypoxia-induced SDF-1 gradient (Ceradini et al., 2004) by binding to the receptor CXCR4 (Nagasawa et al., 1996, Zou et al., 1998). To confirm this chemotactic response of UCB-CD133$^+$ cells isolated in our laboratory, their migration towards SDF-1α was tested in the transwell migration assay **[Figure III.7]**. KG-1 cells expressed similar levels of CXCR4 as isolated UCB-CD133$^+$ cells **[Figure III.8]**. Other researchers have reported basal to low levels of CXCR4 expression on KG-1 cells (Gul et al., 2010, Mohle et al., 1998, Van Buul et al., 2003). KG-1A cells were almost negative for CXCR4 (3±2.3%), and resulted perhaps not surprisingly in their poor transmigration towards an SDF-1α gradient **[Figure III.10].**Transwell migration of UCB-CD33$^+$ cells across fibronectin was compared to KG-1A and Jurkat transmigration based on differences in CXCR4 expression. Jurkat cells expressed higher levels of CXCR4 compared to UCB-CD133$^+$ cells, and were thus used as a positive control of the CXCR4/SDF-1α signalling axis. With almost negative CXCR4 expression, KG-1A cells were used as a negative control. Transmigration of KG-1 cells was not examined, for which reasons are presented in Chapter V, Section V.2.1. Three different doses of SDF-1α were also tested to determine optimal doses in our assay and compared the percentage of transwell migration of CD34$^+$ to previously reported transwell migrations. Most surprisingly,

significantly lower transmigration of Jurkat cells was observed compared to UCB-CD133^{+} transmigration, 12.85±5% vs. 21.35±9.63% respectively at 200 ng/mL SDF-1α across fibronectin and 1.58±0.53% vs. 15.45±3.22% respectively at 100 ng/mL SDF-1α across BMEC-60 cells **[Figure III.4]**. Flow cytometry was used to determine the percentage of cell migration **[Figure III.9]**.

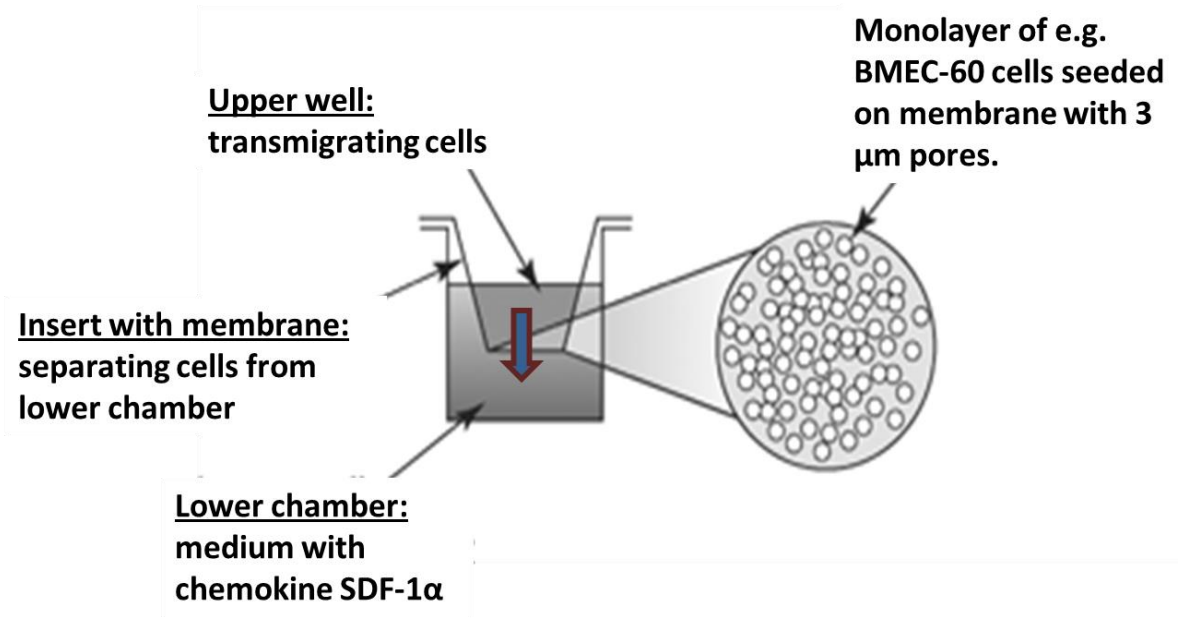

Figure III.7. Schematic illustration of transwell migration assay.

The transwell migration assay enables examining the effects experimental treatments have on the chemotaxis of transmigrating cells. The lower chamber filled with medium and the chemoattractant is separated from the target cells by a porous membrane at the bottom of the upper well (insert), stimulating the migration of cells across the membrane. To determine the optimal chemoattractant concentration for our experiment, three different doses of SDF-1α were tested. With the research objective of examining the effects of hypoxia pre-conditioned UCB-CD133^{+} cell on adhesion and migration through BMEC-60 cells, the porous membrane in the insert was also covered with a monolayer of BMEC-60s instead of fibronectin. Successfully transmigrated cells would drop into the lower chamber, and could be thus easily harvested.

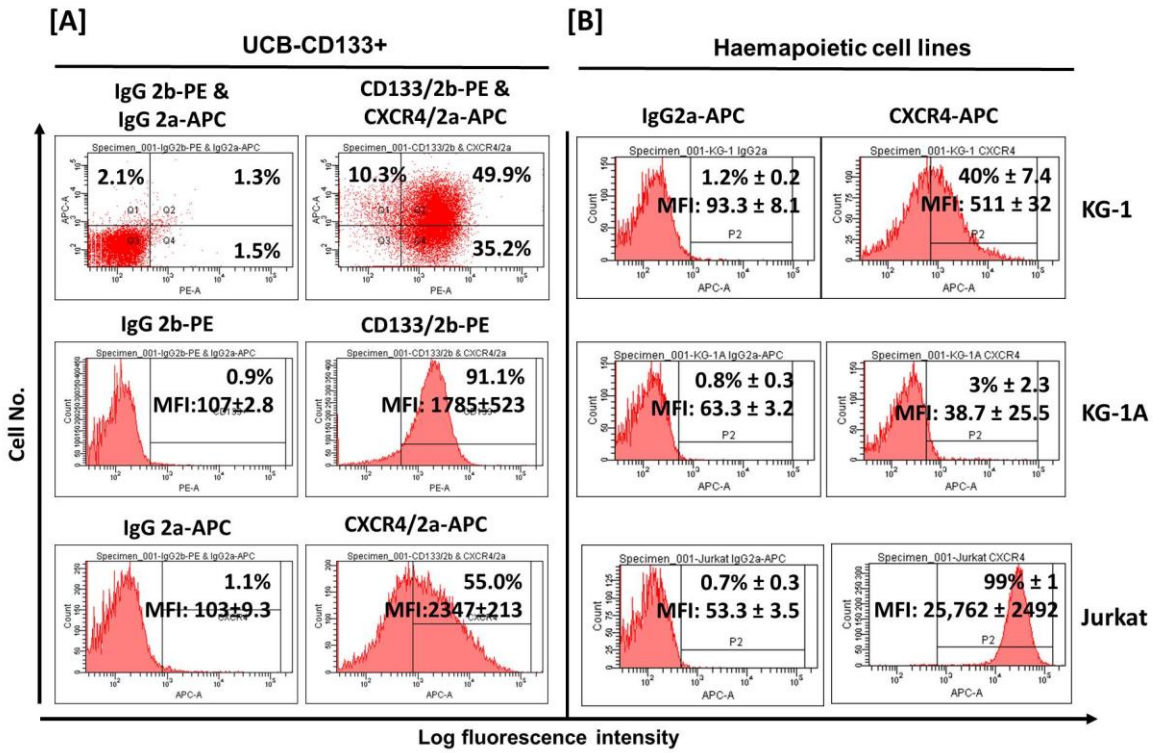

Figure III.8. CXCR4 expression of model cell lines.

Model cell lines KG-1 and KG-1A, as well as Jurkat cells were examined for cell surface expression of homing molecule CXCR4 using BD antibody CD184, clone 12G5. UCB-CD133^{+} cells were used as a +ve control. KG-1 cells expressed similar levels of CXCR4 as UCB-CD133^{+} cells, however with differences in expression levels across the populations; 40% in KG-1 and 55% in CD133^{+} cells had higher MFI readings than the remaining population, as shown by the gating. Jurkat cells expressed the highest levels of CXCR4 expression with a more homogeneous CXCR4 profile; MFI 25,762±2492 vs. 511±32 on KG-1 CXCR4^{high} and 2347±523 on CD133^{+}CXCR4^{high} cells. KG-1A cells expressed very low positive levels (3%). Values are means ± SEM; n=3 independent experiments.

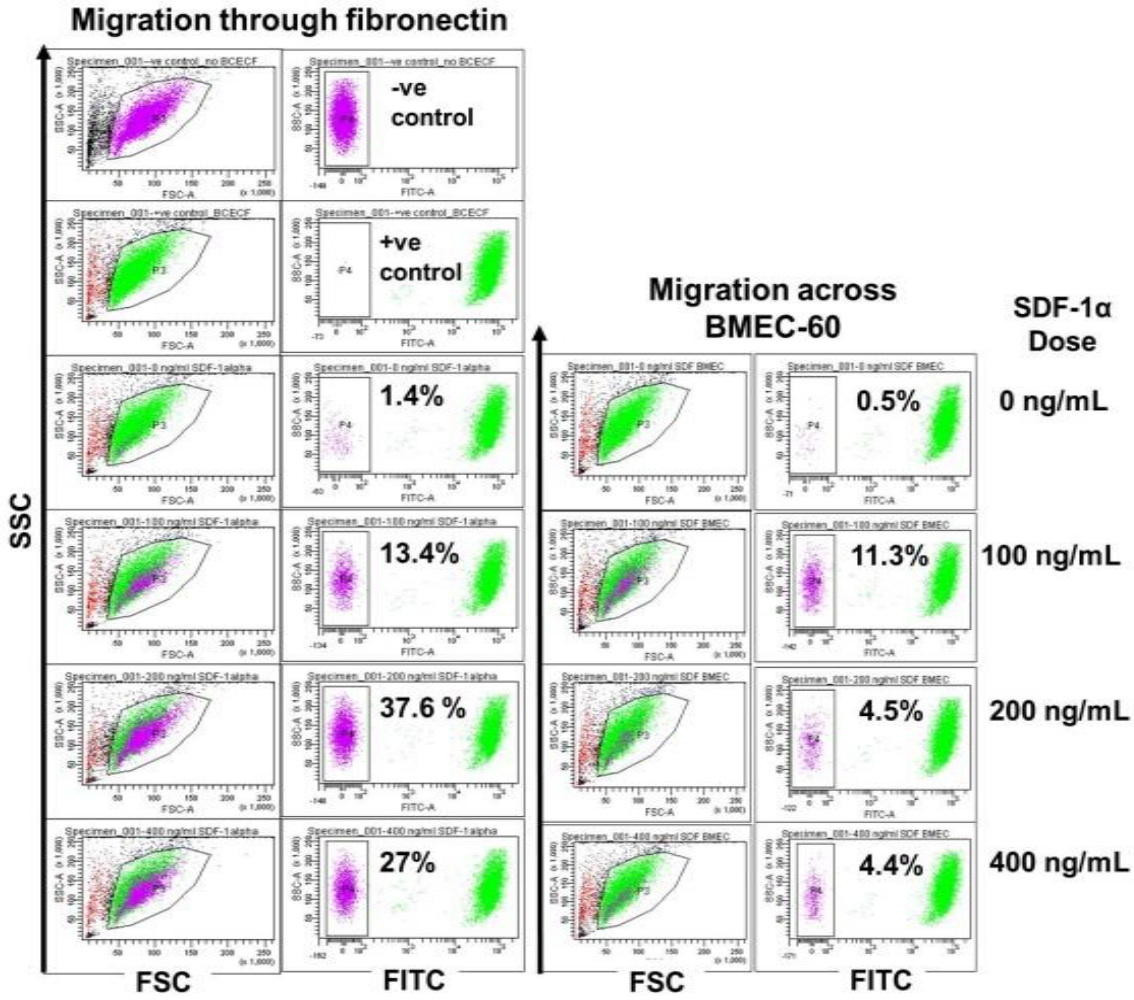

Figure III.9. Determining percentage of transmigrated cells by flow cytometry.

To quantify the increase in transmigrated cells, we used flow cytometry to calculate the percentage of migration. Jurkat, KG-1A or UCB-CD133^{+} cells (100 µL of 1x10^{5}-2.5x10^{5}) were pipetted into the upper well and allowed to transmigrate for 6 hours. Transmigrated cells were harvested into FACS tubes and mixed with the original number of UCB-CD133^{+} cells (labelled with BCECF-AM) that had been plated into the top well. For example, 1x10^{5} cells (=100%) plated before 6 hour incubation, hence 1x10^{5} BCECF-AM labelled cells where mixed with the number of cells (non-labelled) that had migrated across the membrane. Migrated cells (negative for FITC) were counted as a percentage of the labelled population. Positive control cells were labelled with BCECF-AM and negative controls were non-labelled cells.

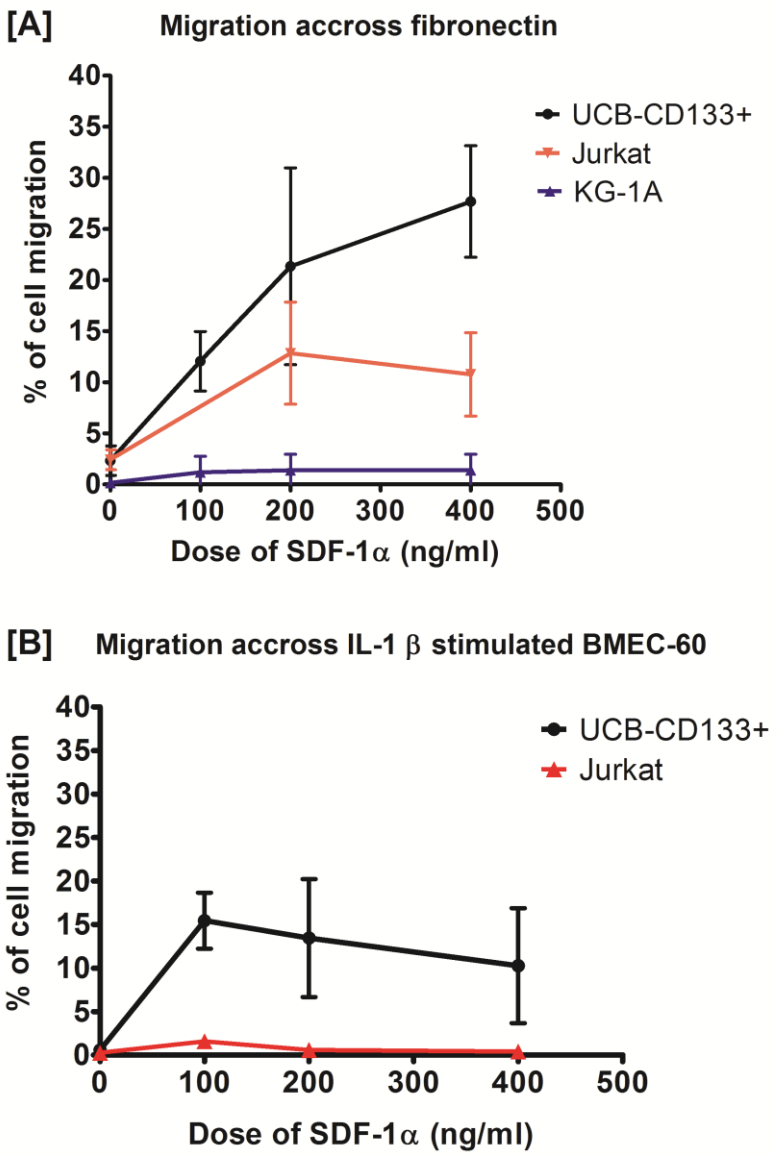

Figure III.10. Optimising UCB-CD133$^+$ cell transwell migration.

[A] A higher % of UCB-CD133$^+$ cells migrated (2.33±1.45%, 12.07±2.92%, 21.35±9.63% and 27.68±5.46% at 0,100, 200 and 400 ng/mL SDF-1α respectively) across fibronectin compared to KG-1A (0.17±0.2%, 1.2±1.56%, 1.4±1.56% and 1.4±1.56% at 0, 100, 200 and 400 ng/mL SDF-1α respectively) and Jurkat cells (2.43±0.97%, 12.85±5% and 10.78±4.09% at 0, 200 and 400 ng/mL). The difference between the lines based on linear regression is statistically significant ($p>0.0001$; n= 6 independent experiments) [B] UCB-CD133$^+$ cells migration across BMEC-60 cells peaked at 100 ng/mL SDF-1α (15.45±3.22%; 0.58±0.22%, 13.45±6.76% and 10.28±6.6 at 0, 200 and 400 ng/mL respectively). Jurkat transmigration across BMEC-60 was statistically significantly lower (0.26±28%, 1.58±0.53%, 0.58±0.32% and 0.42±0.26% at 0, 100, 200, 400 ng/mL respectively) based on linear regression analysis ($p>0.0001$; n= 4 independent experiments). ± = SDEV

III.3. Discussion

To ensure that both our functional assays were optimised adequately and offered suitable experimental conditions to test our hypothesis, we tested a number of parameters. Haemopoietic cell lines, KG-1, KG-1A and Jurkat cells, were used to optimise parameters for adhering UCB-CD133^{+} cells and three BM niche cells, BMEC-60 cells, BMSCs and osteoblasts, were validated to model the HSPCs BM niche *in vitro.* KG-1 cells proved to be a suitable model cell line for experiments on adhesion to the three substrate cells and enabled determining a suitable cell number for subsequent experiments. Cell surface markers common to BMEC-60 cells, BMSCs and osteoblasts, confirmed their phenotype as well as showing a distinct cell surface profile for each cell type. For example, BMEC-60 cells were CD45^{-}, CD34^{+}, CD31^{+}, CD105^{+}, CD106^{+}, CD14^{low} and CD90^{-}. In contrast, BMSCs and osteoblasts were CD90^{+}, CD105^{+}, CD106^{-} in BMSCs and CD106^{+} in osteoblasts, CD34^{-}, CD31^{-}, CD45^{-}, CD14^{-}. Some of the well-known adhesion molecules were also detected such as β1 integrin (CD29), CD44, and CD166. Recently, CD166 expression on osteoblasts was directly correlated high haemopoiesis enhancing activity (HEA) (Chitteti et al., 2013). However, in the same study, increasing culture conditions (> 7 days) decreased the CD166 expression and higher osteocalcin levels, indicative of a more mature population (Chitteti et al., 2013). Thus, high CD166 expression observed in osteoblasts used in our functional studies suggest a healthy phenotype with potential HEA ability (alkaline phosphatase activity is reported by Lonza in their manufacturing specification sheet). Other valuable markers could have been screened for, such as E and P-selectins expressed on BM endothelium, and cell type specific molecule osteopontin on osteoblasts,

which are other adhesion molecules involved in HSC/HSPC homing and lodgement at the endosteum (Rood et al., 2000b, Sun et al., 2013). However, profiling was restricted to antibodies already available in our laboratory, with the objective to expand the panel if functional effects were determined and worthy of further investigation.

By testing different doses of SDF-1α in the transwell migration assay, it was identified that chemotaxis of UCB-CD133^{+} cells across BMEC-60 peaked with 100 ng/mL of SDF-1α, whereas saturation point across fibronectin was not reached with the highest dose test of 400 ng/mL. This difference in dose response has been observed previously by Voermans et al., where 600-1000 ng/mL of SDF-1α was required to achieve optimal migration across fibronectin and only 30-100 ng/mL across IL-1β stimulated BMEC-60 cells (BMEC-60$^{+IL\text{-}1\beta}$) (Voermans et al., 2000). Voermans et al. obtained higher percentages of transmigrating cells using UCB-CD34^{+} cells, ~68% across fibronectin and ~50% across BMEC-60$^{+IL\text{-}1\beta}$ with 100 ng/mL SDF-1 (Voermans et al., 2000). Other transwell migration studies using UCB-CD34^{+} cells obtained 20-25% of cells transmigrating across human umbilical vein endothelial cell (HUVEC) monolayers (Leung et al., 2011). The % of transmigrated Jurkat cells showed a similar SDF-1α dose response as that of UCB-CD133^{+} cells, however fewer cells transmigrated, particularly across BMEC-60 cells. Interestingly, BMECs have been observed to internalise circulating SDF-1, translocating it back to the BM and increasing the homing of circulating or transplanted CD34^{+} cells (Dar et al., 2005). Thus, two factors might be triggering an earlier saturation point in the chemotaxis of UCB-CD133^{+} cells across BMEC-60 cells compared to that observed across fibronectin: 1) Soluble SDF-1α in the bottom chamber is

internalised by BMEC-60 cells in the membrane and presented on the apical surface of BMEC-60 cells, 2) SDF-1α produced by the BMEC-60 themselves is secreted into the lower chamber, subsequently increasing the overall dose in the bottom chamber and/or is translocated to the apical surface in the top chamber. As a result, CXCR4 presenting cells would potentially stay bound on the apical surface of BMEC-60 cells rather than transmigrating across the endothelial layer. In both cases, these phenomena would be precipitated with increasing doses of SDF-1α (due to SDF-1α secretion by the monolayer of BMEC-60 cells and the increased SDF-1α molecules pipetted into the bottom chamber). Conversely, a recent *in vitro* study, which examined the transmigration of monocytes and lymphocytes across immortalised human brain microvascular endothelial cells, observed that apical SDF-1α enhanced transmigration. Most interestingly, apical SDF-1α "selectively reduced CXCR4 MFI of transmigrating monocytes compared to the input population…" and did not alter CXCR4 expression on the lymphocytes implying that the SDF-1α/CXCR4 axis can have different effects in different cell types (Man et al., 2012). Other studies that included mathematical models to examine optimality and saturation points of chemotaxis in neuronal growth cones suggest that "each receptor also signals the number of unbound-to-bound transitions it experiences within the observation period" (the period at which it encounters the chemoattractant), which in the case of a neuronal growth cone enables the cell to estimate different concentrations across its spatial surroundings and provide direction to its migration. However, "as the concentration increases and the length of time the receptor spends unbound decreases, the growth cone essentially reaches a limit to sensing accuracy related to the number of

unbound-to-bound transitions that can occur within the observation period" (Mortimer et al., 2010), which in turn negatively impacts a directional response, i.e. the chemoreceptors become saturated and cells do not migrate (Yuan et al., 2013). These examples provide different clues as to what cellular behaviour might have occurred in the transmigration of UCB-CD133^{+} cells across BMEC-60 cells presented in **Figure III.10**. Anti-SDF-1α staining of the transwell membrane could be performed to compare SDF-1α levels, as well as anti-CXCR4 staining to compare numbers of attached Jurkat and UCB-CD133^{+} cells at higher SDF-1α concentrations. What about other SDF-1α receptors? Does SDF-1α bind exclusively to CXCR4? Other SDF-1α chemokine receptors have been reported (Balabanian et al., 2005, Bleul et al., 1996). For example, SDF-1 binding receptor CXCR7 was shown to have a ten-fold higher affinity than CXCR4 to SDF-1 (Bleul et al., 1996). However, blocking CXCR7 on CD34^{+} cells did not affect chemotaxis towards SDF-1 (CXCL12) (Hartmann et al., 2008, Tarnowski et al., 2010). Thus, potential SDF-1α binding to CXCR7 was unlikely an additional saturation factor.

Chapter IV Effects of hypoxia on UCB-CD133+ cell adhesion & migration

IV.1. Introduction

Compared to HSCPs derived from BM or mPB, UCB-derived HSPCs take a longer time to engraft. In addition, unsuccessful UCB-transplantion is associated with a low UCB cell-dose in both children and adults, which in turn also delays engraftment and immune reconstitution (Ballen et al., 2013, Rocha and Broxmeyer, 2010). Multiple approaches to improve the transplantation potential of UCB-derived HSPCs have been explored, from infusing double UCB units, to developing *in vitro* UCB expansion strategies, manipulating homing molecules expressed on $CD34^+$ cells, and to bypassing the homing process by intra-marrow injections (Ballen et al., 2013). One study found that UCB-derived human $CD34^+$ cells expressed defective PSGL-1 (ligand for P-selectins) due to incomplete post-translational modifications, which resulted in their inability to interact fully with the BM microvasculature (Hidalgo et al., 2002) **[Figure IV.1]**. However, although the rolling of human UCB-$CD34^+$ HSPCs was enhanced by fucosylation of selectin ligands on these cells, this did not improve their adhesion via integrins (Hidalgo and Frenette, 2005). More recently, five new molecules were identified to play a role in the homing of $CD34^+$ cells: CD164, CD9, CD82, Robo4 and its ligand Slit2. CD164 is a type-1 integral transmembrane sialomucin highly expressed on the human $Lin^-CD133^+CD34^+CD38^{low/-}$ and $Lin^-CD133^+CD34^-CD133^-CD38^{low/-}$ cells (Bühring et al., 1999, Watt et al., 2000). Blocking CD164 on UCB-$CD133^+$ cells greatly reduced their ability to migrate towards SDF-1α across fibronectin, and was

found to co-localise with critical homing integrins VLA-4 and VLA-5, as well as chemokine receptor CXCR4 (Forde et al., 2007). CD9 and CD82 are transmembrane proteins of the tetraspanin superfamily whose functional effects on adhesion and membrane-domain polarisation enhanced homing and engraftment (Larochelle et al., 2012, Leung et al., 2011). Robo4 and its ligand Slit2 were shown to cooperate with CXCR4 to direct HSC to specific BM niche sites, facilitating HSC lodgement in the BM (Smith-Berdan et al., 2011, Smith-Berdan et al., 2012). Most interestingly, all four molecules were associated with the SDF-1α/CXCR4 axis. As discussed in Chapter I, expression of SDF-1α and CXCR4 can be stimulated by hypoxic conditions, mediated by HIF-1α stabilisation (Ceradini et al. 2004; Semenza 2009; Staller et al. 2003).

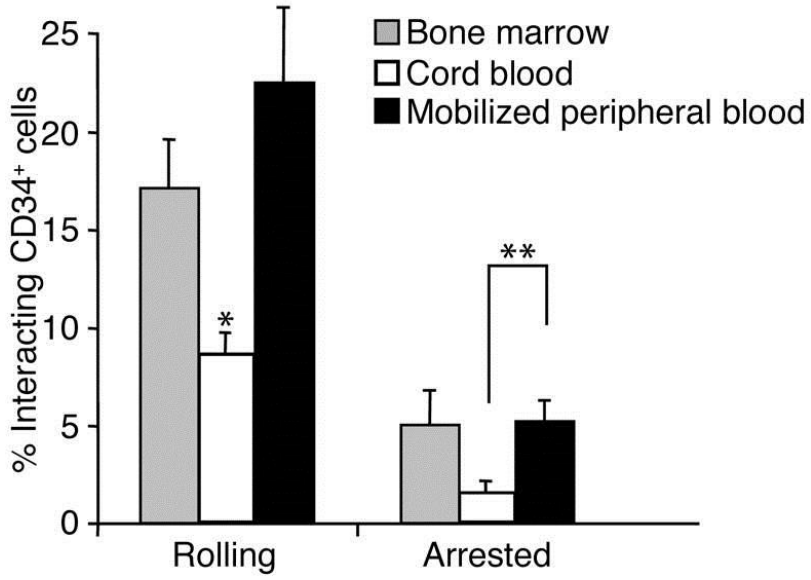

Figure IV.1. Comparative analysis of the interactions of CD34$^+$ cells with BM microvessels in NOD/SCID mice.

"Fluorescently labeled CD34$^+$ cells from steady-state human BM, mPB, or CB were injected into NOD/SCID mice, and the numbers of cells interacting (rolling or arrested) with the BM microvasculature were determined by analysis of video recordings from fluorescence intravital microscopy experiments. n = 7–10 mice and human donors. *P < 0.02 compared with BM and mPB. **P = 0.03." Reprinted from The Journal of Clinical Investigation, Hidalgo A., Weiss L.,Frenette P., Functional selectin ligands mediating human CD34(+) cell interactions with bone marrow endothelium are enhanced postnatally, 2002, pp. 559-569, Copyright 2014 with permission by the American Society of Clinical Investigation.

Table IV.1. Summary of clinical approaches to improve the engraftment potential of UCB transplantation.

Experimental and Clinical Approaches to Increase Number of CB-Cells and Improve Engraftment after UCB Transplantation
• *Increase number of cells at cord blood collection* Banking cord blood units with greater volume and high number of CD34+ cells. Perfusing the placental vessels after draining the blood from the cord.
• *Enhance homing of cord blood cells* Inhibiting the enzymatic activity of CD26/Dipeptidylpeptidase IV (DPPIV). In vivo direct injection of cord blood cells into the iliac crest (Phase II clinical trials). Fucoslation of PSGL-1. Upregulation of CXCR4 activity with dmPGE2.
• *In vitro and in vivo expansion of cord blood cells* Using of SDF-1/CXCL12 associated to Diprotin A and/or other cytokines Using Notch-ligand Delta 1 (Phase II clinical trials). Using copper chelator tetraethylenepentamine (TEPA) (Phase II clinical trials).
• *Identification of modifiable prognostic factors for engraftment* Choosing the "best" cord blood unit based on cell dose, HLA, diagnosis, screening for antibodies against HLA, quality of cord blood units. Modifying the conditioning regimen and GVHD prophylaxis.
• *Increase number of cells at infusion* Using double cord blood transplantation (on going prospective and observational studies). Using third party mobilized T cell-depleted haploidentical cells (Phase II trials).
• *Decreasing toxicity and shorten time of aplasia* Using RIC (on going prospective and observational studies).
• *Co-infusion of cord blood cells with accessory cells* Using multipotent mesenchymal stromal cells (Phase I/ II trials).

GVHD indicates graft-versus-host disease; UBC, umbilical cord blood; RIC, reduced intensity conditioning regimen.

Adapted from from Biology of Blood and Marrow Transplantation, Vol. 16, Issue 1, Rocha V. and Broxmeyer H.E., New Approaches for Improving Engraftment after Cord Blood Transplantation, pp. S126-S132, Copyright 2014 with permission from Elsevier.

Here we postulated that hypoxia or stabilisation of HIF-1α play a key role in driving signalling in HSC/HSPCs, to retain, release, or attract them to BM niche cells. Consequently, it should be possible to enhance HSPC adhesion and migration by simply exposing cells to hypoxic conditions or by ensuring that HIF-1α is stabilised in these cells. In this chapter, the effects of acute hypoxia were examined on human UCB-CD133$^+$ cells as an environmental cue that homing HSPCs encounter when entering specific niches in the BM or following G-CSF treatment to induce HSPC mobilisation. Stabilisation of transcription factor HIF-1α was first verified here as an indicator of the acute hypoxic response in adhering cells, human UCB-CD133$^+$ and KG-1 cells, and substrate cells, osteoblasts, BMSCs and BMEC-60. Subsequently, the functional effects of hypoxia vs normoxic conditions (20% O_2) on human UCB-CD133$^+$ cell adhesion to the three substrate cells, as well as their transmigration across BMEC-60 were examined.

Hypoxic conditions were defined by pre-incubating cells in 1.5% O_2 (hypoxia pre-conditioning) before allowing adhering or transmigrating cells and substrate cells to interact. Three different hypoxic treatments were tested in the adhesion assay. Treatment 1 involved pre-incubating adhering HSPCs for 24 hours in 1.5% O_2, labelling these hypoxia stimulated cells with fluorescent dye BCECF-AM, and finally adding the labelled cells to the monolayer of normoxic substrate cells for 1 hour in 20% O_2 to enable adhesion. In treatment 2, substrate cells were hypoxia pre-conditioned for 24 hours, whereas the adhering HSPCs were incubated under normoxic conditions. In treatment 3, both cells were hypoxia pre-conditioned separately for 24 hours before seeding the adhering cells onto substrate cells as previously described. A % of cell

adhesion was determined by the ratio of fluorescence intensity of adhering cells post-wash to pre-wash multiplied by 100 as defined in Chapter III. A paired t-test was used to determine whether the treatment had a statistically significant effect. A further value, “percentage gain or percentage loss” (Δ%,), is also presented here to reflect the magnitude of the treatment’s effect relative to the % adhesion in the control group. The Δ% was calculated as follows:

$$\frac{hypoxic\ KG1\ adhesion - \ normoxic\ KG1\ adhesion}{normoxic\ KG1\ adhesion} \times 100\%.$$

Using KG-1 cells as an example, hypoxic adhesion of 44% and normoxic adhesion of 41% yields a difference of 3% and Δ of 7%. A negative change, e.g. Δ-7%, is indicative of a decrease in adhesion due to hypoxia pre-conditioning. These three different treatment sets were tested to examine which of the two cell types when subjected to hypoxia affected adhesion outcome, or if changes in adhesion were dependent on both cell types being hypoxia stimulated. In other words, does hypoxia enhance the adhesion potential of the adhering cells, the substrate cells or both? The immature haemopoietic cell line, KG-1, was used initially to model the HSPC response given that human UCB $CD133^+$ cells are rare and not easy to source. Transmigration was examined by seeding hypoxia pre-conditioned human UCB-$CD133^+$ cells onto IL-1β stimulated BMEC-60 and incubating the assay for 6 hours under 20% O_2 for transmigration to take place.

IV.2. Results

IV.2.1. Stabilisation of hypoxia-inducible transcription factor

To ensure that both adhering human cells (KG-1 and UCB-CD133$^+$ cells) and human substrate cells (osteoblasts, BMSCs and BMEC-60s) were hypoxia stimulated, successful stabilisation of transcription factor HIF-1α was established in all five cell types. Western blot results show signs of HIF-1α expression in KG-1 cells after 4 hours of 1.5% O_2 incubation, reaching a steady-state after 24 to 48 hours. Noteworthy are the low HIF-1α expression levels under 5% O_2 **[Figure IV.2A-B]**. Stabilisation of HIF-1α was also confirmed in UCB-CD133$^+$ after 24 hours under 1.5% O_2 **[Figure IV.2E].** UCB-CD133$^+$ cells were cultured in StemSpan with cytokines IL-6, FLT-3L, SCF and TPO as described in Chapter II (Materials and Methods, Section II.5) for both normoxic and hypoxic incubations. KG-1 cells were also incubated for 24 hours in 75 µM and 150 µM $CoCl_2$. $CoCl_2$ can be used to induce continuous stabilisation of HIF-1α, thus a useful positive control. As a competitive inhibitor of iron, it attaches to the iron-binding site of prolyl hydroxylase (PHD) (Vengellur et al., 2005), preventing its potential interaction with oxygen, and is consequently unable to hydroxylate HIF-1α to trigger its degradation. It is often used as a hypoxia mimic for *in vitro* experiments (Dayan et al., 2009, Dulak et al., 2007, Vengellur and Lapres, 2004, Yao et al., 2008). Both concentrations of $CoCl_2$ stabilised HIF-1α, but more effectively at 150 µM **[Figure IV.2C]**. HIF-1α stabilisation was also detected in all three BM niche cells, under both 1.5%O_2 and 150µM $CoCl_2$ after 24 hours **[Figure IV.3].**

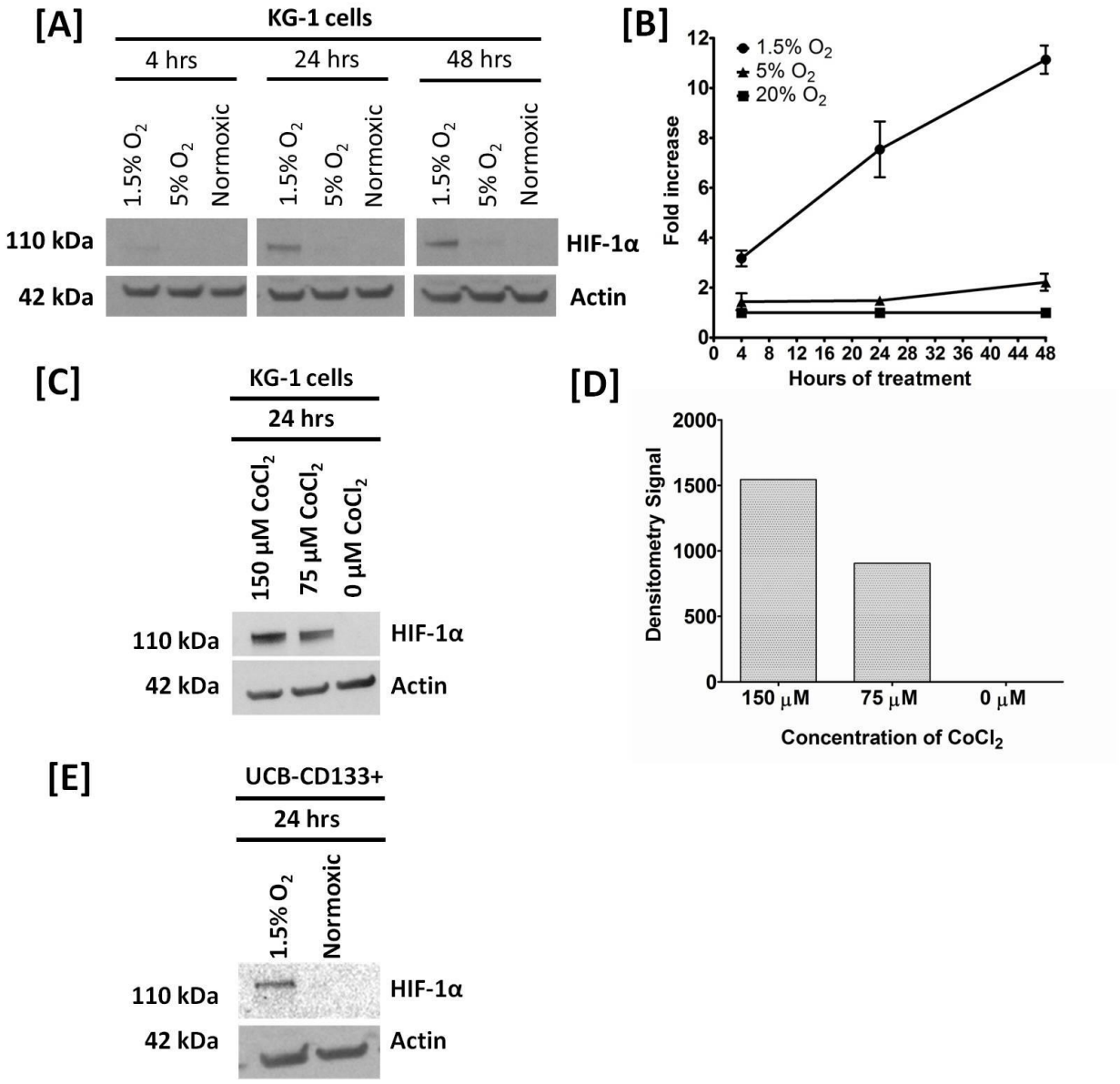

Figure IV.2. Response of adhering cells to hypoxia.

KG-1 cells were incubated under three different oxygen conditions for 4, 24 and 48 hours (hrs). Cells were harvested with cold DPBS and processed immediately to extract total protein. [A] Western blot of KG-1 cell lysates showing the effects of 1.5% O_2 and 5% O_2 compared to 20% O_2 (normoxic control) on HIF-1α at three different timepoints. With increasing exposure to 1.5% O_2, stabilisation of HIF-1α became apparent. [B] Densitometry analysis quantifying expression of HIF-1α under 1.5% O_2, 5% O_2 and normoxic conditions (n=3 independent experiments for 24 hour timepoint, mean= 7.54±1.12 SDEV; n=2 for 4 and 48 hour timepoints). [C] Treating cells with $CoCl_2$ also stabilises HIF-1α in KG-1 cells. [D] Densitometry analysis of presented Western blot shows that HIF-1α protein levels are higher under 150 µM of $CoCl_2$ compared to 75 µM (n=2 independent experiments). [E] Western blot showing stabilisation of HIF-1α in UCB-$CD133^+$ cells after 24 hrs in 1.5% O_2 (n=3 independent experiments).

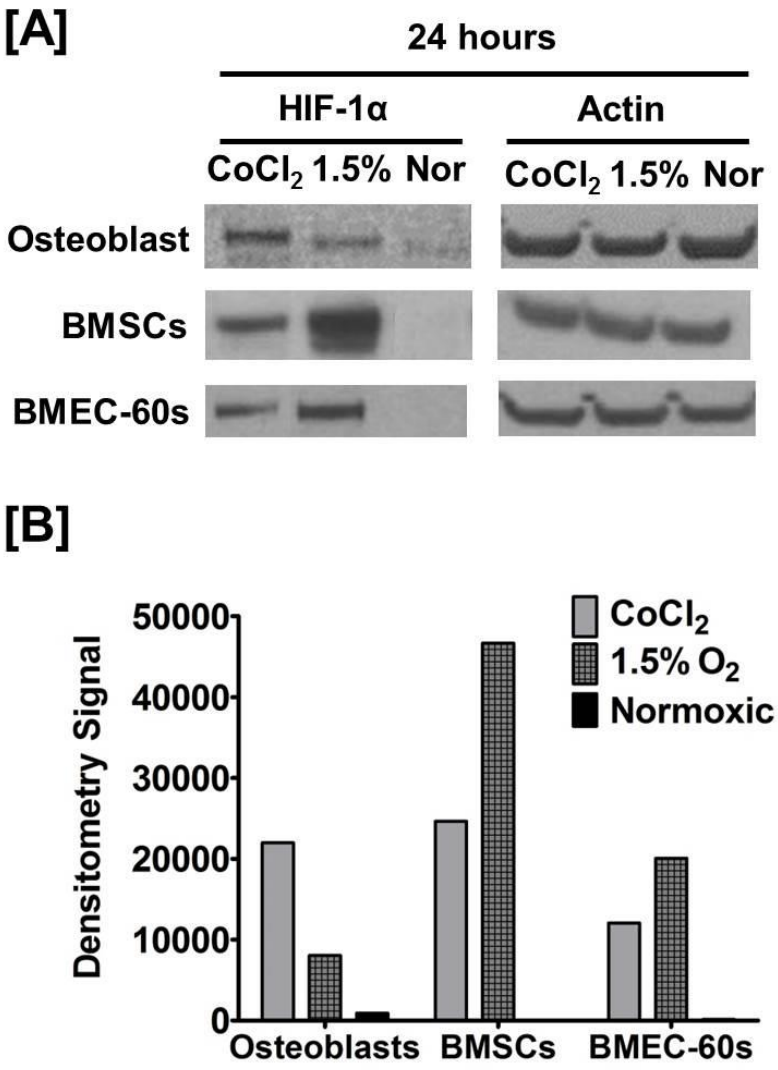

Figure IV.3. Response of BM niche cells to hypoxia.

[A] Representative Western blot confirming stabilisation of HIF-1α also occurs in substrate cells after exposing cells for 24 hours to 1.5% O_2 and 150µM $CoCl_2$ (1.5% =1.5% O_2; Nor=normoxic; Actin= loading control); (n=2 independent experiments) [B] Densitometry analysis of Western blot shown, comparing expression of HIF-1α under the effects of hypoxia and $CoCl_2$.

IV.2.2. Effects of hypoxia on adhesion to osteoblasts

Osteoblasts are reported to be exposed to severe hypoxia at the endosteum in the BM (Levesque et al., 2007, Parmar et al., 2007). In this set of experiments, the aim was to examine whether hypoxia enhances adhesion of UCB-CD133^{+} cells to osteoblasts. The effects of hypoxia on KG-1 adhesion to osteoblasts were examined first. The control test was defined by normoxic (20% O_2) conditioning of the assay. **Figure IV.4** shows that pre-incubating osteoblasts for 24 hours in 1.5% O_2 (osteoblasts$^{\text{hypoxia-stimulated (H)}}$) caused a decrease in KG-1 cell adhesion (35.20±2.48% vs. 38.87±9.87% in control). Hypoxia pre-conditioned KG-1 cells (KG-1 $^{\text{hypoxia-stimulated (H)}}$) to normoxic osteoblasts (osteoblasts^{N}) also resulted in decreased adhesion (30.84±10.91% vs. 34.28±8.35% in control). Interestingly, hypoxia pre-conditioning of both cell types (KG-1^{H} to osteoblasts^{H}) restored this effect (48.27±8.02% vs. 43.37±2.18% in control), with one of the three individual experiments showing an increase in KG-1 adhesion. Hypoxic treatments were also compared to each other, but no statistical difference was found between the three hypoxia treatment sets ($p>0.05$; data plots not shown). A trend towards increased cell adhesion was also observed for all sets of UCB-CD133^{H} to osteoblasts^{H} (25.04±2.53% vs. 22.69±4.50% in control), as well as for UCB-CD133^{H} to osteoblasts^{N} (28.88±3.31% vs. 25.75±4.32% in control), which was the inverse in KG-1^{H} to osteoblasts^{N}. Effects of hypoxia on adhesion with UCB-CD133^{N} to osteoblasts^{H} were inconclusive as changes of adhesion were different between individual experiments, i.e. no trend was observed **[Figure IV.5]**. However, it would be of interest to increase the number of individual experiments for each treatment set

and establish whether the trend towards increased adhesion due to hypoxia pre-conditioning is statistically significant.

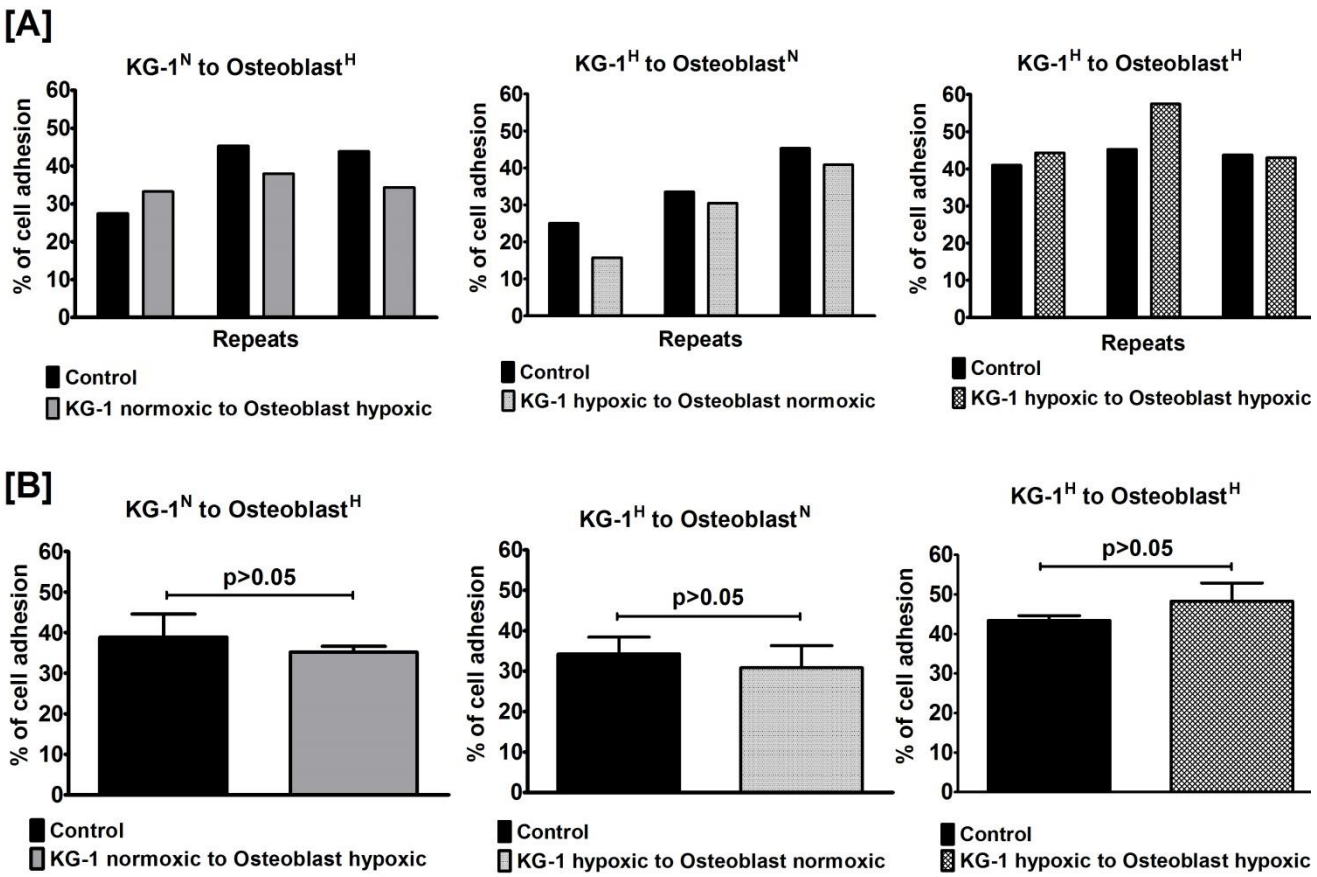

Figure IV.4. Effects of hypoxia pre-conditioning on KG-1 adhesion to osteoblasts.

[A] The adhesion assay experiment was repeated n=3 indepent times. [B] Compiled data with paired t-test. Effects were not statistically significant: Δ= -9.44% in $KG\text{-}1^{N}$ to $Osteo^{H}$ (35.20±2.48% vs. 38.87±9.87% in control, p>0.05); Δ= -10.03% in $KG\text{-}1^{H}$ to $Osteo^{N}$ (30.84±10.91% vs. 34.28±8.35% in control, p>0.05); Δ= 11.30% in $KG\text{-}1^{H}$ to $Osteo^{H}$ (48.27±8.02% vs. 43.37±2.18% in control, p>0.05). ± = SDEV; Control = 20% O_2 pre-conditioning.

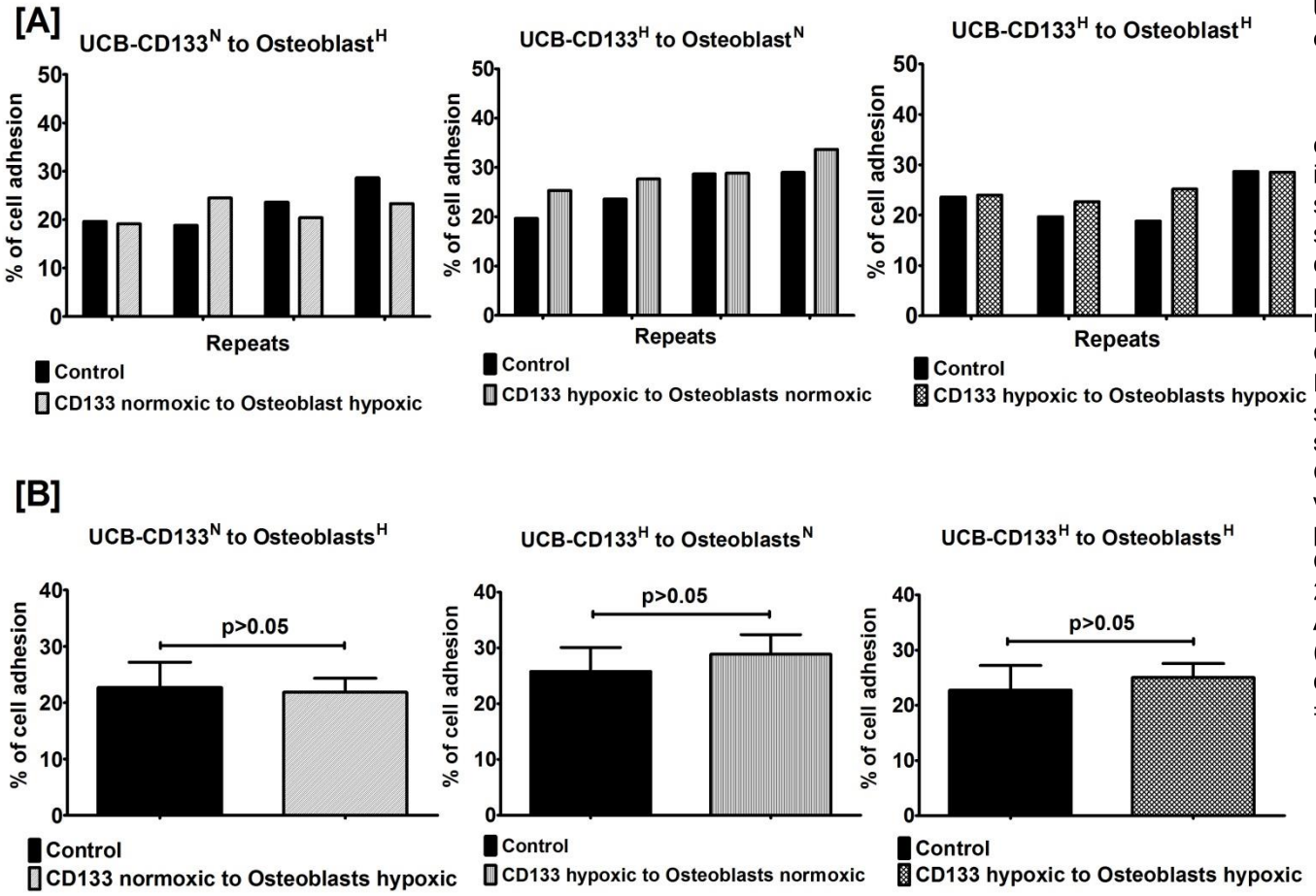

Figure IV.5. Effects of hypoxia pre-conditioning on UCB-CD133+ adhesion to osteoblasts.

[A] The adhesion assay experiment was repeated n=4 indepent times. Repeated test show hypoxia pre-conditioning stimulates increased UCB-CD133+ cell adhesion to osteoblast provided UCB-CD133+ cells are hypoxia pre-conditioned. [B] Compiled data with paired t-test. Effects were not statistically significant. Effects were not statistically significant: Δ= -3.7% in $CD133^{N}$ to $Osteo^{H}$ (21.85±2.48% vs. 22.69±4.50% in control, p>0.05); Δ= 12.15% in $CD133^{H}$ to $Osteo^{N}$ (28.88±3.51% vs. 25.75±4.32% in control, p>0.05); Δ=10.36% in $CD133^{H}$ to $Osteo^{H}$ (25.04±2.53% vs. 22.69±4.50% in control, p>0.05). ± = SDEV; Control = 20% O_2 pre-conditioning.

IV.2.3. Effects of hypoxia on adhesion to BMSCs

Because BMSCs also reside in the endosteal region and are thus exposed to hypoxia, we examined whether hypoxia had an effect on these niche cells and their interaction with HSPCs. Most interestingly, compared to the adhesion patterns observed to osteoblasts, KG-1 adhesion to BMSCs resulted in increased adhesion in all three treatments. In fact, KG-1^{N} to $BMSCs^{H}$ was statistically significant with a percentage gain 17.65% (55.66±11.28% vs. 47.31±12.91% in control, $p<0.05$) **[Figure IV.6]**. Hypoxic treatments were also compared to each other, but no statistical difference was found between the three hypoxia treatment sets ($p>0.05$; data plots not shown). Testing these treatments on UCB-$CD133^{+}$ cell adhesion to BMSCs did not replicate the statistically significant effects as for $CD133^{N}$ to $BMSC^{H}$, however, a positive trend was observed when BMSCs were hypoxia pre-conditioned (35.13±7.33% vs. 31.66±17.27% in control for $CD133^{N}$ to $BMSC^{H}$, and 40.78±19.26% vs. 35.22±25.49% in control for $CD133^{H}$ to $BMSC^{H}$) **[Figure IV.7]**.

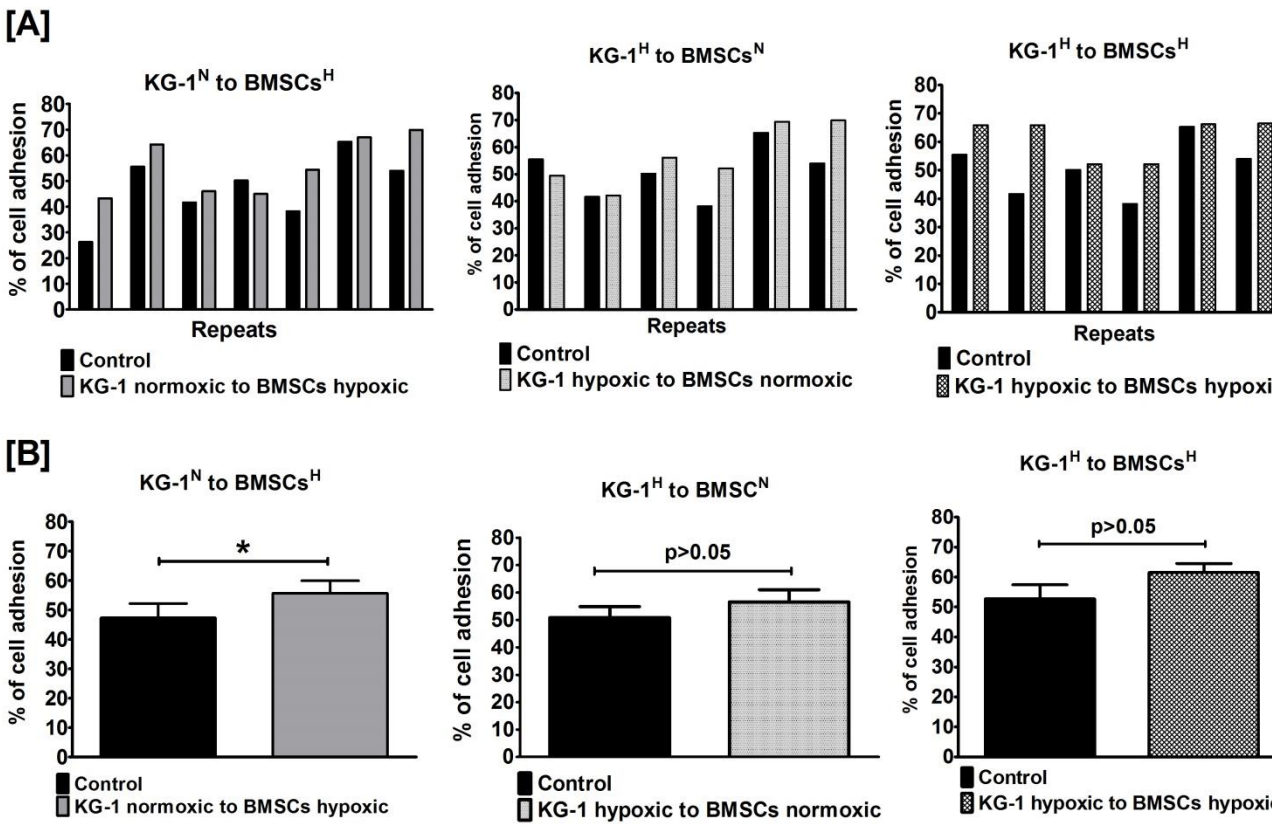

Figure IV.6. Effects of hypoxia pre-conditioning on KG-1 cell adhesion to BMSCs.

[A] The adhesion assay experiment was repeated n≈6 indepent times. Repeats of each test show that hypoxia pre-conditioning enhances adhesion in most instances. [B] Paired t-test confirms statistically significant effects. KG-1^N to $BMSC^H$ Δ%= 17.65 (55.66±11.28% vs 47.31±12.91% in control, $p<0.05$). Treatment was not statistically significant in the other two tests. In KG-1^H to $BMSCs^N$ Δ= 11.24% (56.53±11.07% vs 50.82±9.84% in control, $p>0.05$); Δ= 16.75% in KG-1^H to $BMSCs^H$ (61.53±7.24% vs 52.70±11.51% in control, $p>0.05$). ± = SDEV; Control = 20% O_2 pre-conditioning.

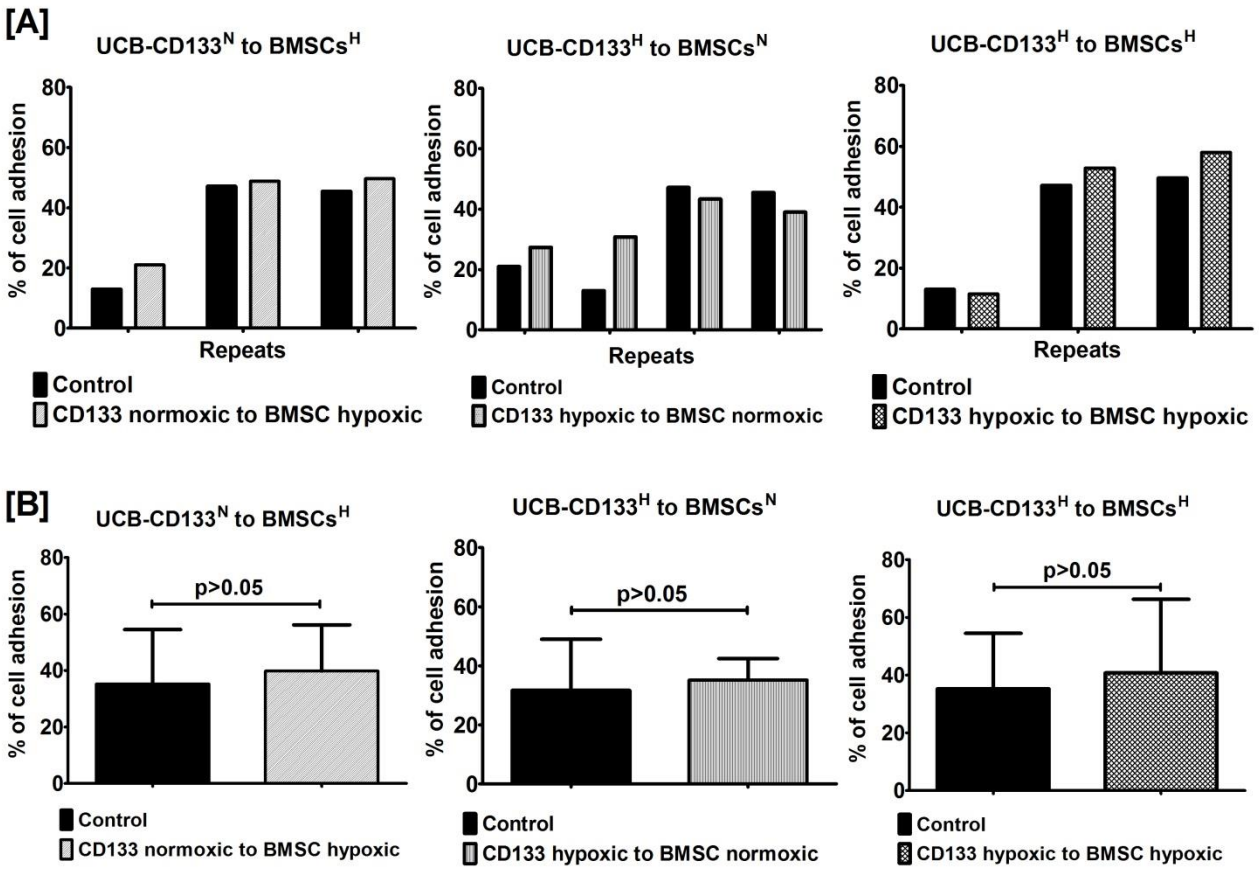

Figure IV.7. Effects of hypoxia pre-conditioning on UCB-CD133+ cells to BMSCs

[A] The adhesion assay experiment was repeated n≈3 indepent times. Repeats of each treatment set show a trend towards enhanced adhesion due to 24 hours hypoxia pre-conditioning. [B] Compiled data with paired t-test. Effects were not statistically significant in $CD133^{N}$ to $BMSCs^{H}$ (35.13±7.33% vs. 31.66±17.27% in control, p>0.05, Δ= 10.96%); $CD133^{H}$ to $BMSCs^{N}$ (39.83±16.32% vs. 35.22±19.26% in control, p>0.05, Δ= 13.08%); $CD133^{H}$ to $BMSCs^{H}$ (40.78±25.49% vs. 35.22±19.26% in control, p>0.05, Δ=15.79%). ± = SDEV; Control = 20% O_2 pre-conditioning.

IV.2.4. Effects of hypoxia on adhesion to BMEC-60

Located throughout the BM cavity, BMECs are certainly vital binding sites for HSCs and their progeny, allowing cells to enter and exit the circulatory system to maintain haemopoietic homeostasis. Since the oxygen tension within the BM is estimated to vary between 1 to 5% (Chow et al., 2001a, Chow et al., 2001b, Eliasson and Jönsson, 2010, Mohyeldin et al., 2010), potentially hypoxic HSPCs leaving the endosteal regions bind to less hypoxic normoxic BMEC. Futhermore, *in vivo* treatments with mobilising agents such as G-CSF or cytotoxic agents such as cyclophosphamide commonly used in the clinic for transplantation therapy, can result in severe hypoxia in the BM, thus also affecting BMECs of normally more oxygenated areas in the BM (Levesque et al., 2007, Winkler et al., 2010). Thus, increasing evidence that BMEC can also be subjected to a low supply of oxygen (Hooper et al., 2009, Kubota et al., 2008, Kunisaki et al., 2013, Lo Celso et al., 2009, Porter and Calvi, 2009) suggests that hypoxic HSPCs and hypoxic BMEC may also interact. The effects hypoxia pre-conditioning on UCB-CD133$^+$ cell adhesion to BMEC-60 cells was therefore also tested, as well as on KG-1 adhesion to BMEC-60.

Despite observing effects in individual experiments, after repeating the different treatment sets independently at least three times, no apparent trend was observed for UCB-CD133$^+$ cell adhesion to BMEC-60 **[Figure IV.9]**. However, statistically significant effects were observed in KG-1 cell adhesion to BMEC-60 cells **[Figure IV.8]**. Hypoxia pre-conditioning of BMEC-60 cells resulted in a statistically significantly decreased KG-1 adhesion, with Δ%= –

23.72% in KG-1^{N} to $BMEC^{H}$ (21.70±7.66% vs 28.45±7.59% in control, $p<0.005$) and Δ%= –37.38 in KG-1^{H} to $BMEC^{H}$ (18.88±5.06% vs 30.15±6.99% in control, $p<0.05$). Interestingly, stimulating BMEC-60s with IL-1β greatly restored adhesion of hypoxic KG-1 cells to similar levels as the normoxic controls or even surpassing control levels (58.08±14.45% vs 53.95±9.79% in control). These results suggest hypoxia particularly induces changes in the cell surface profile of BMEC-60s that alters their interaction with adhering cells.

Hypoxic treatments were also compared to each other. A statistically significant difference was found for hypoxia pre-conditioned KG-1 and UCB-$CD133^{+}$ cell adhesion to BMEC-60 cells stimulated with IL-1β compared with their adhesion to hypoxia pre-conditioned BMEC-60 cells ($p<0.005$) **[Figure IV.10]**. These results suggest that both cell types adhere preferentially to IL-1β stimulated cells under normoxic and hypoxic conditions.

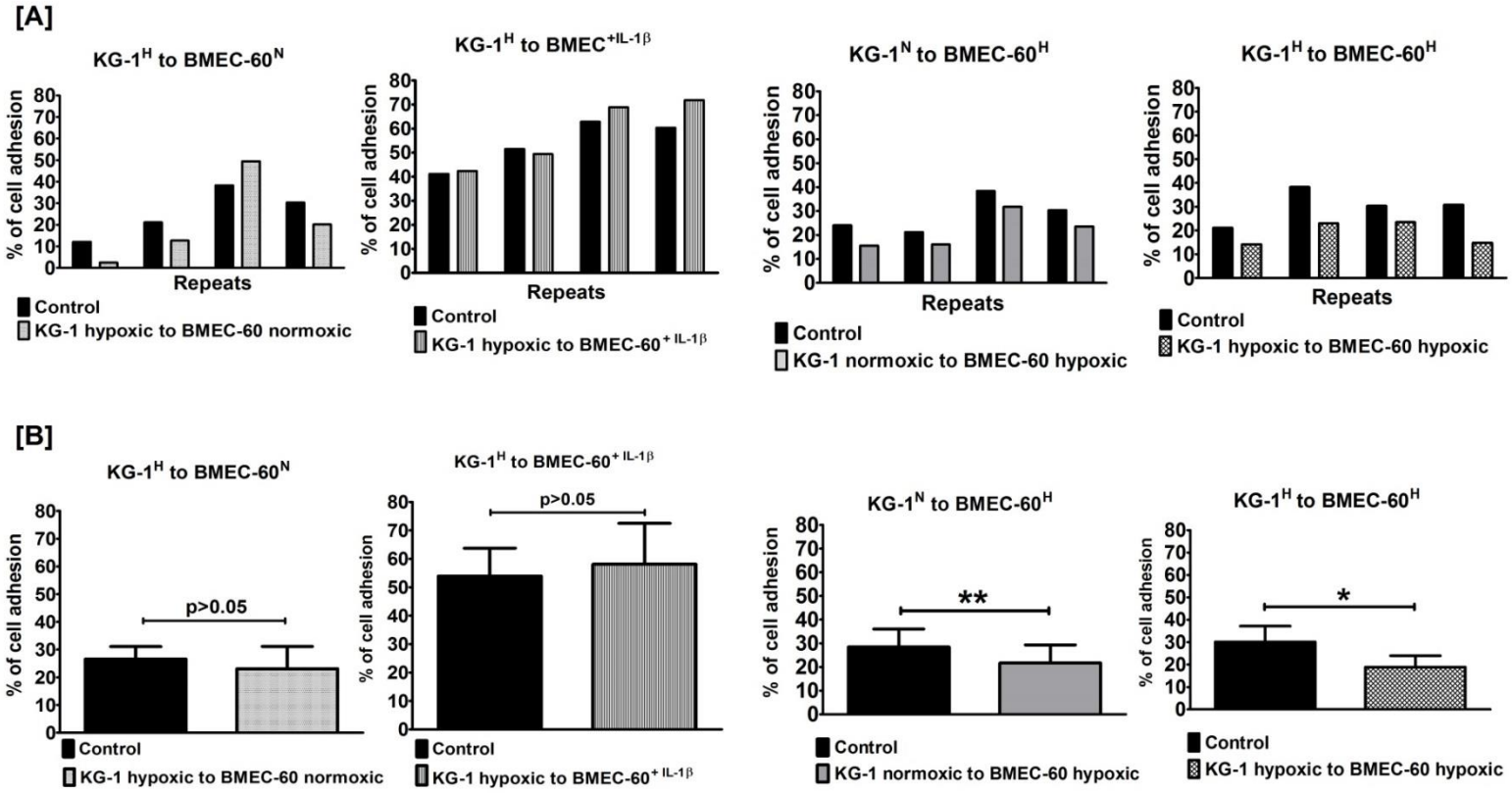

Figure IV.8. Effects of 1.5% O_2 pre-conditioning on KG-1 cell adhesion to BMEC-60.

[A] The adhesion assay experiment was repeated n=4 indepent times. Repeats for each treatment set show that hypoxia pre-conditioning results in a trend towards decreased adhesion provided BMEC-60 are not stimulated with cytokine IL-1β, which stimulates adhesion.[B] Compiled data with paired t-test. Changes in adhesion for KG-1^H to BMEC-60^N where not statistically significant (23.08±17.98% vs 26.54±10.09% in control, p>0.05, Δ%= –13). A trend towards enhanced KG-1^H adhesion to BMEC-$60^{+IL\text{-}1\beta}$ was also not statistically significant (58.08±14.45% vs 53.95±9.79% in control, p>0.05, Δ%= 7.66). However, effects were statistically significant when BMEC-60 where hypoxia pre-conditioned: Δ%= –23.72% in KG-1^N to BMEC-60^H (21.70±7.66% vs 28.45±7.59% in control, p<0.005) and Δ%= –37.38 in KG-1^H to BMEC-60^H (18.88±5.06% vs 30.15±6.99% in control, p<0.05). ± = SDEV; Control = 20% O_2 pre-conditioning.

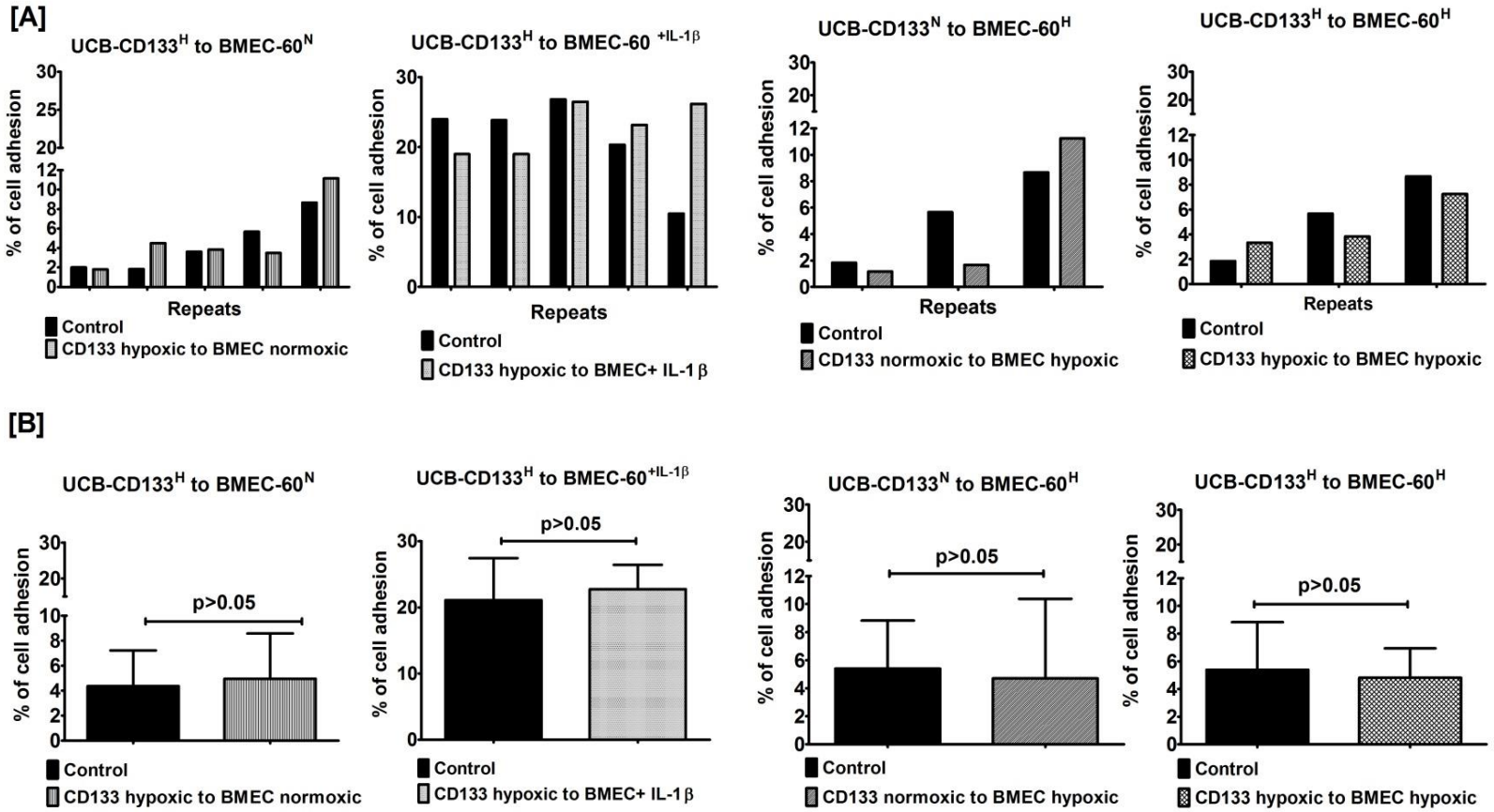

Figure IV.9. Hypoxia pre-conditioning on UCB-CD133^{+} cell adhesion to BMEC-60s.

[A] The adhesion assay experiment was repeated n=3-5 indepent times. Repeats for each treatment show an inconclusive trend in all treatment sets. [B] Compiled data with paired t-test: Δ= 13.76% in CD133^{H} to BMEC-60^{N} (4.96±2.86% vs 4.36±3.61% in control, p>0.05); Δ= 7.97% in CD133^{H} to BMEC-60$^{+IL\text{-}1\beta}$ (22.77±3.67% vs 21.09±6.35% in control, p>0.05); Δ= –12.96% in CD133^{N} to BMEC-60^{H} (4.70±5.68% vs 5.40±3.43% in control, p>0.05); Δ= –10.95% in CD133^{H} to BMEC-60^{H} (4.80±2.13% vs 5.39±3.43% in control, p>0.05). ± =SDEV; Control = 20% O_2 pre-conditioning.

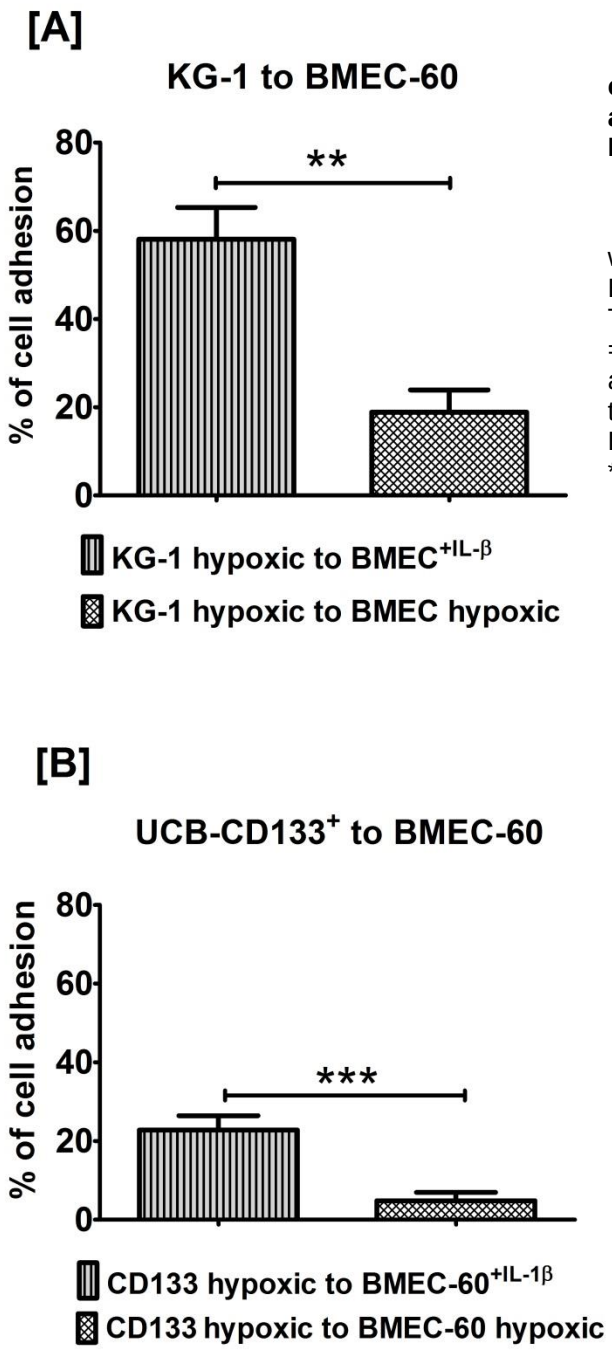

Figure IV.10. Hypoxia pre-conditioned KG-1 and UCB-CD133^{+} cells adhere preferentially to IL-1β stimulated BMEC-60 cells.

[A] KG-1^{H} cell adhesion to BMEC^{H} was compared to KG-1^{H} adhesion to BMEC$^{+IL-\beta}$ (18.88±5.06 vs. 58.08±14.45%). The difference is statistically significant (** = $p<0.005$). [B] A statistical difference was also obtained comparing CD133^{H} adhesion to BMEC^{H} with CD133^{H} adhesion to BMEC$^{+IL-\beta}$(4.80±2.13% vs. 22.77±3.67%; *** = $p<0.001$). ± = SDEV

IV.2.5. Testing effects of hypoxia on migration

Transmigration of HSCs/HSPCs across BMECs is a key stage in the homing of HSCs/HSPCs to the BM, as well as when leaving the BM during stress responses or other physiological challenges. It was thus also of interest to examine the effects of low oxygen levels/stabilisation of HIF-1α on UCB-$CD133^+$ cell migration across BMECs. Chapter III described the transwell migration assay and showed that an optimal dose of 100 ng/mL SDF-1α stimulates migration of UCB-$CD133^+$ cells across BMEC-60s. Transmigration of KG-1 cells was not examined due to results presented in Chapter IV, Section V.2.2.

Here we examined whether hypoxia pre-conditioning UCB-$CD133^+$ cells affected their transmigration across IL-1β stimulated BMEC-60 cells. Quite remarkably, although not statistically significant, hypoxia pre-conditioning for 24 hours increased the percentage of transmigrated UCB-$CD133^+$ cells dramatically (Δ%= 117%, 14.67±1.25% vs. 6.76±3.42% in normoxic control). A statistically significant effect was obtained upon 48 hour hypoxia pre-conditioning, with a Δ% of 58.65% (27.13±9.24% vs. 17.10±8.35% in normoxic control, $p<0.01$) **[Figure IV.11]**. Noteworthy is that the statistical results of the 24 hour set are based on a smaller sample size (n=3 vs 9 individual 48-hour hypoxia pre-conditioning experiments), with a p-value of the 24 hour set equalling 0.086 (comparing migration of hypoxia pre-conditioned UCB-$CD133^+$ cell to the migration of the normoxic control group). Increasing the number of individual experiments could thus become statistically significant.

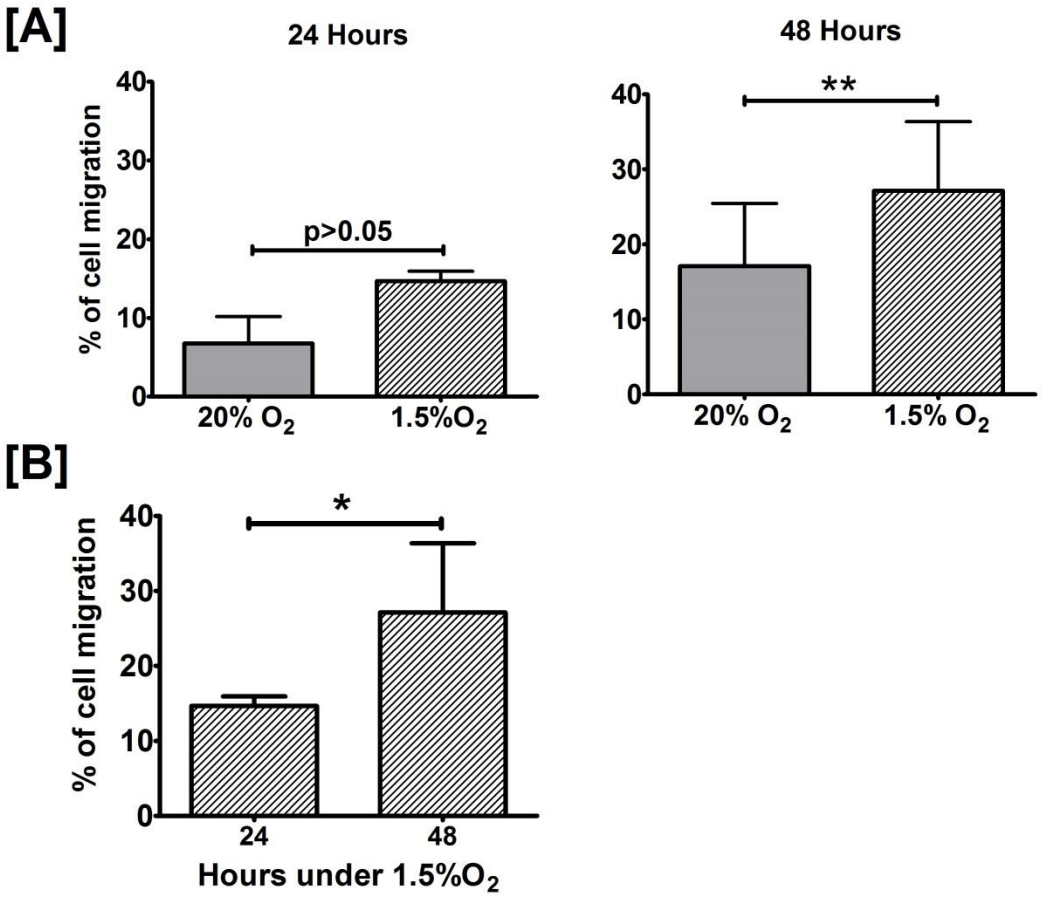

Figure IV.11. Transwell migration of hypoxia pre-conditioned UCB-CD133+ cells through BMEC-60 cells.

UCB-CD133$^+$ cells were incubated for 24 and 48 hours under 1.5% O_2 prior to their migration across a monolayer of IL-1β stimulated BMEC-60 cells. Results show a trend towards increased transmigration of 24 hour hypoxia pre-conditioning UCB-CD133$^+$ cells (14.67±1.25% vs. 6.76±3.42% in control, $p>0.05$, Δ=117%, n=3 independent experiments) and a statistically significant increased transmigration when UCB-CD133$^+$ cells were pre-conditioned for 48 hours (27.13±9.24% vs. 17.10±8.35% in control, ** = $p<0.01$; Δ=58.65%, n=9 independent experiments). [B] Increasing the incubation time under 1.5% O_2 significantly enhances the transmigration of UCB-CD133$^+$ cells (* = $p<0.05$). ± = SDEV

Given these results, effects of 1.5% O_2 pre-conditioning on adhesion of UCB-CD133$^+$ cells to BMEC-60 was re-examined, this time pre-conditioning UCB-CD133$^+$ cells for 48 hours. Strikingly, results showed a significant effect on UCB-CD133$^+$ cells adhesion to non-stimulated BMEC-60 cells, increasing adhesion by Δ77% ($p<0.001$). Interestingly hypoxia pre-conditioning had no significant effect on adhesion to IL-1β stimulated BMEC-60s (41.50±2.62% vs. 43.40±6.12% in control) **[Figure IV.12]**. This difference suggests that IL-1β signalling dominates over hypoxia induced signalling. Enhanced KG-1 cell adhesion to non-stimulated BMEC-60s vs IL-β stimulated BMEC-60 provides corroborating evidence **[Figure IV.8]**. Nonetheless, hypoxia pre-conditioning does have significant effects on the migration of UCB-CD133$^+$ cells across IL-1β stimulated cells, suggesting that hypoxia pre-conditioning activates signalling molecules that upon exposure to chemoattractants such as SDF-1α promote tethering and diapaedesis of UCB-CD133$^+$ cells **[Figure IV.12]**. These results also suggest that the length of hypoxia pre-conditioning is critical to detect significant effects, and prompts the need to re-examine effects of hypoxia pre-conditioning on adhesion to osteoblasts and BMSCs with longer hypoxia incubation times.

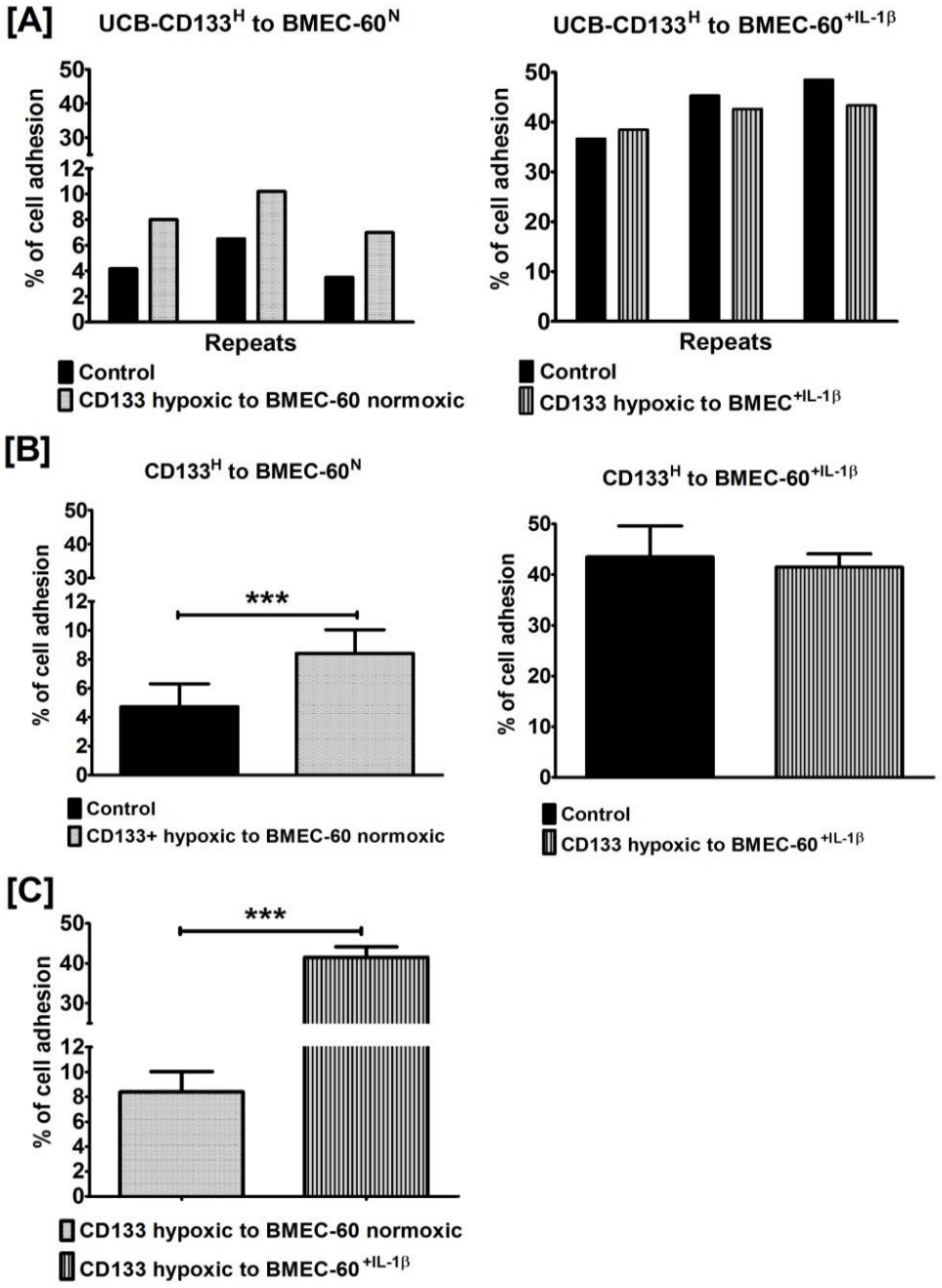

Figure IV.12. Effects of 48 hour hypoxia pre-conditioning on UCB-CD133$^+$ cell adhesion to BMEC-60s.

UCB-CD133$^+$ cells were incubated for 48 hours in 1.5% O_2, and BMEC-60s in 20% O_2. [A] Repeats for both treatment sets. [B] Compiled data with paired t-test. Pre-conditioning UCB-CD133$^+$ for 48 hours in hypoxia significantly enhances their adhesion to non-stimulated BMEC-60 (8.40±1.64% vs 4.72±1.58% in control, *** = p<0.001, Δ= 78%). No significant effects were observed on UCB-CD133^H cell adhesion to IL-1β stimulated BMEC-60 (41.50±2.62% vs 43.50±6.12% in control, p>0.05, Δ = –4.60%). [C] Hypoxia pre-conditioned UCB-CD133$^+$ adhere preferentially to IL-1β stimulated BMEC-60 (*** = p< 0.001). ±= SDEV; Control = = 20% O_2 pre-conditioning.

IV.2.6. Detecting small changes in adhesion

The main objective of Sections IV.2.2-IV.2.4 was to examine the overall effect of hypoxia on adhesion of UCB-CD133^{+} cells to BM niche cells. However, a sizeable proportion of the cells did not adhere, raising the question why not? We thus examined whether this 2nd population would adhere if given 'another chance'.

In a preliminary experiment, KG-1 and UCB-CD133^{+} cells as well as osteoblasts were pre-conditioned with 1.5% O_2 for 24 hours and allowed to interact in the adhesion assay as previously described. However, instead of discarding non-adherent cells, these were harvested and added for 1 hour to a fresh monolayer of hypoxia pre-conditioned osteoblasts. Adhesion of these cells was measured as performed with the standard assay. **Figure IV.13** shows how more than 40% of KG-1 cells did not adhere. When this non-adherent fraction (2nd population) was seeded onto a fresh monolayer of osteoblasts only a small percentage of cells adhered. However, most interestingly, the difference in KG-1 cell adhesion between the normoxic 2nd population control (6.30%) and the hypoxia pre-conditioned 2nd population (11%) was statistically significant ($p<0.01$), with a remarkable percentage change of Δ75%. When testing our 2nd population hypothesis on UCB-CD133^{+} cell adhesion to osteoblasts, we also observed a higher percentage change between hypoxia treated and the normoxic control (Δ45%) than in our standard assay (Δ15.86%). These results show that 'small' but significant increases in cell adhesion are more readily detected in a 'poorly adhering' cell population than in a cell population showing

high adhesion levels. It also highlights that statistical changes detected against a low background are not detectable with a high background.

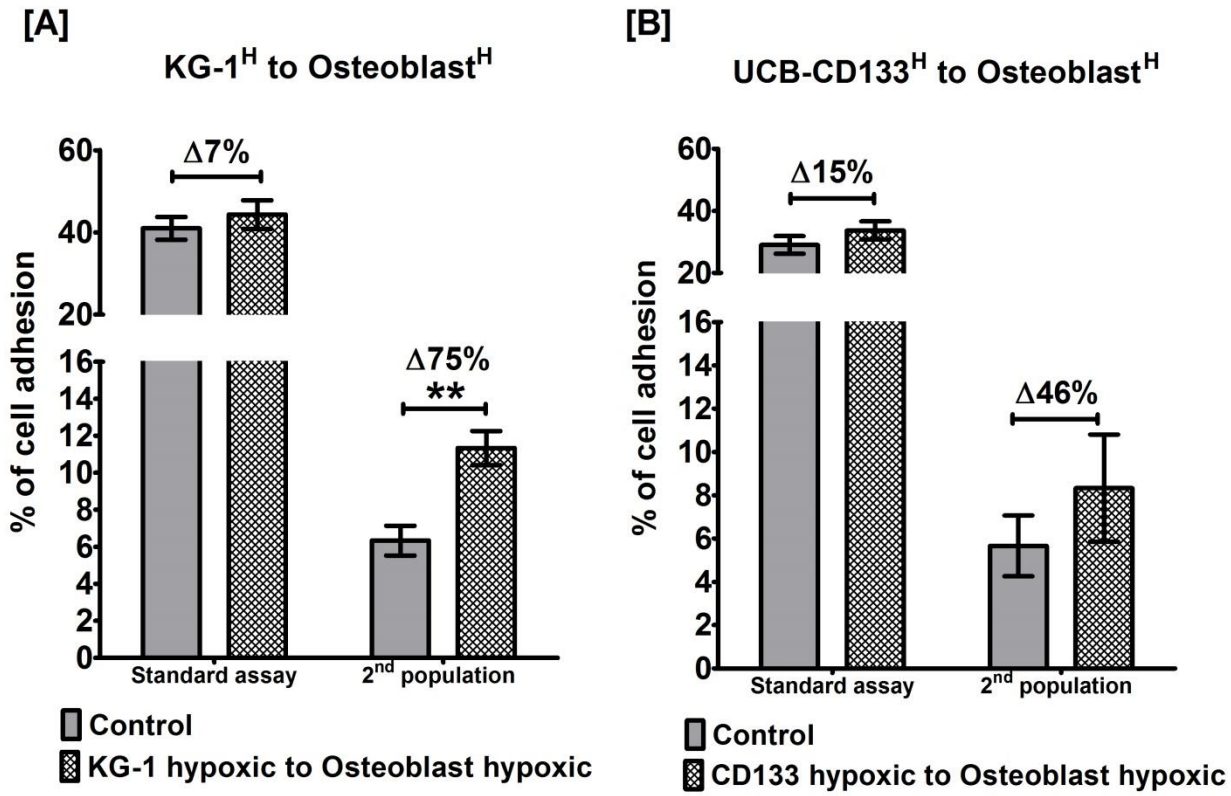

Figure IV.13. Examining effects of hypoxia on adhesion of a sub-set of UCB-CD133^{+} cells.

[A] Hypoxia pre-conditioning has a statistically significant effect ($p<0.01$) on the '2nd populations' of KG-1 cells—a change that is detected only when comparing adhesion to the 2nd population of poorly adherent normoxic cells of the standard assay. Hypoxic adhesion of 44±8.6% % and normoxic adhesion of 41±6.8% ($p>0.05$) yields Δ of 7.32%. Even more dramatically, in the 2nd population of KG-1 cells Δ is 77%.(11±2.3% vs. 6.3±2%; ($p>0.05$). [B] This is also observed for the 2nd populations of UCB-CD133+ cell where Δ% is 45% compared (adhesion 8.3±6.1% vs. 5.7±3.4% in control, $p>0.05$) to Δ15% (adhesion 33.6±7.23% vs. 29±7.01%, $p>0.05$) in the standard assay. ± = SDEV; Control= 20% O_2 pre-conditioning.

IV.2.7. Hypoxia cell surface profiling of UCB-CD133$^+$ cells

Given the statistically significant enhanced transmigration of UCB-CD133$^+$ cells due to 1.5% O_2 pre-conditioning, it was of interest to examine the effect hypoxia had on the expression of cell surface adhesion molecules. UCB-CD133$^+$ cells pooled from at least three different donors were exposed to 1.5% O_2 for 48 hours under the culture conditions previously described and then incubated with one of the following antibodies: VLA-5 (CD49e), VLA-4 (CD49d), ICAM-1 (CD54), VCAM-1 (CD106), CD105 (endoglin), LFA-1 (CD11a), β1 integrin (CD29), β2 integrin (CD18), α5-β3 integrin (CD61), E-selectin (CD62e), CD44, CXCR4, JAM-A and CD164. VLA-4 integrin and its ligand VCAM-1 (VLA-4 /VCAM-1) are perhaps the most well-known adhesion molecules involved in the firm adhesion of HSCs/HSPCs to the BMEC, with endothelial selectins and molecules such as β2-integrin/ICAM-1 and LFA-1/β2-integrin required for initial tethering and rolling (Mazo et al., 2011). CXCR4 is currently 'the king' of the homing ligands for they bind SDF-1α, making it thus of paramount interest to examine the effect on its expression upon 48 hour 1.5% O_2 pre-conditioning. Adhesion receptor CD44 co-localises with CXCR4 for cells to migrate towards chemokine SDF-1 (Avigdor et al., 2004) and was observed to interact on UCB-CD34$^+$ cells with MSCs by fluorescence microscopy (Wagner et al., 2008), thus another homing/adhesion molecule particularly attractive to examine. Expression of JAM-A and CD164 were also assessed as these are candidate molecules that have recently joined the homing-molecule repertoire (Forde et al., 2007, Stellos et al., 2010). With upregulation of endoglin on endothelial cells and α5-β3 integrin on melanoma cells upon exposure to hypoxic conditions

(Cowden Dahl et al., 2005, Li et al., 2003), it was of interest to also examine their response on UCB-CD133$^+$ cells.

Flow cytometry analysis revealed no statistically significant effect ($p>0.05$) of the 48 hour hypoxic (1.5% O_2) treatment on any of the molecules detected compared to the normoxic control (20% O_2) with the exception of VLA-4 **[Figure IV.14]**. Hypoxia pre-conditioning statistically significantly decreased the cell surface expression of VLA-4 on UCB-CD133$^+$ cells ($p<0.05$). Interestingly, for all other examined molecules any differences observed were also towards decreased expression. CD164 was the only molecule where its expression was positively stimulated by hypoxia pre-conditioning. Interestingly, other studies show that CXCR4 also interacts with CD164 on the surface of HSPCs in response to SDF-1 presentation (Forde et al., 2007), with CD164 most likely acting to upregulate the expression of CXCR4 (Huang et al., 2013). Most unexpected was the negative effect (although not statistically significant) observed on homing ligand and hypoxia-regulated CXCR4.

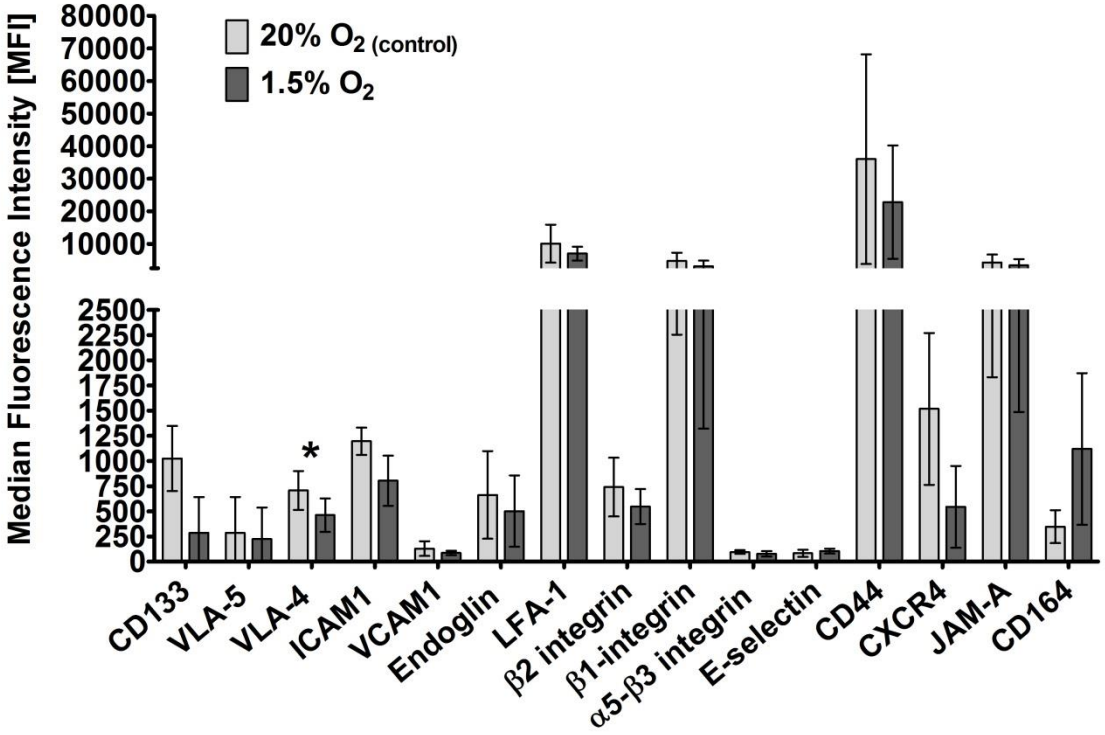

Figure IV.14. Effects of hypoxia on the expression of adhesion molecules on UCB-CD133$^+$ cells.

Cell staining was performed on UCB-CD133$^+$ cells exposed to 1.5% O_2 for 48 hours and compared to cell staining of the normoxic control (48 hours in 20% O_2). Immunofluorescence detection by flow cytometry analysis shows that hypoxia pre-conditioning had no significant statistical effect ($p>0.05$) on most of the adhesion markers. A decrease in VLA-4 expression was the exception ($p<0.05$); using paired t-test (n=3 independent experiments; error bars= SDEVs).

IV.3. Discussion

A hypoxic microenvironment has for some time been associated with the regulation of haemopoiesis as well as HSC/HSPC maintenance and function (Cipolleschi et al., 1993, Danet et al., 2003, Hermitte et al., 2006, Ivanovic et al., 2000, Ivanovic et al., 2004, Levesque et al., 2007, Suda et al., 2011, Winkler et al., 2010). Quite remarkably, only recently has attention shifted to studying direct effects of hypoxia on the fate of HSCs in the BM (Andrade et al., 2013, Ceradini et al., 2004, Eliasson et al., 2010, Iriuchishima et al., 2011, Ong et al., 2010, Shima et al., 2009, Takubo et al., 2010). More specifically as described here, this includes the role of hypoxia on the interaction of HSCs/HSPCs with major BM cell types, notably osteoblasts, BMSCs, and BMECs. Very low oxygen levels (~1.3%) have been reported to occur at the endosteum (Levesque et al., 2007, Parmar et al., 2007), one of the site that attracts HSCs/HSPCs (Kunisaki et al., 2013, Lo Celso et al., 2009, Xie et al., 2009). More recent studies by Nombela-Arrieta et al. suggest that HSPCs at least in mice, naturally express HIF-1α, and that this is independent of the location of these cells within the BM, spleen or circulating blood (Nombela-Arrieta et al., 2013). Further studies to define the actual oxygen tension within the BM will be required to confirm these new observations. A major thrust of this DPhil project was to ascertain the role of severe hypoxia as a means of stabilising HIF-1α expression on HSC/HSPC fate in the BM, specifically examining the effects on their adhesion and transmigration.

In the first set of experiments we show for the first time that HIF-1α can be expressed in KG-1 cells, by exposing these cells for a minimum of 4 hours to

1.5% O_2. Stabilisation of HIF-1α was confirmed in UCB-CD133$^+$ cells, as previously reported by Danet et al. (Danet et al., 2003) and our group (Martin-Rendon et al., 2007). This hypoxia pre-conditioning (24 hours) or stabilisation of HIF-1α appeared to have only a small effect on adhesion between UCB-CD133$^+$ cells and substrate cells. Although a trend towards increased adhesion was observed in UCB-CD133$^+$ cell adhesion to BMSCs, no distinct patterns were observed in their adhesion particularly to BMEC-60s and only minimal to osteoblast. The BMSCs that were used are capable of supporting haemopoiesis (according to the manufacturer's specifications sheets, Lonza, Wokingham Ltd.), however, these have not been specifically separated into recently described BMSCs located in the two vascular niches of murine BM, which at least in mice contain nestin$^+$LepR$^-$NG2$^+$ and nestin^{low}LepR$^+$NG2$^-$ BMSCs adjacent to the arteriolar and sinusoidal endothelial niche cells respectively. Nestin$^+$LepR$^-$NG2$^+$ arteriolar niche cells were identified to promote HSC quiescence (Kunisaki et al., 2013). Further studies might thus be conducted with more defined BMSC subsets. Similarly, even though osteoblasts undoubtedly influence HSC/HSPC function (Levesque et al., 2010), the presence of neighbouring niche components might be required to fully detect hypoxic effects associated with adhesion to hypoxic osteoblasts (Lane et al., 2011). Inconclusive adhesion patterns can also be viewed as a mismatch between two cell types adapted to different environments; depending on the physiological state of the cells, crosstalk will trigger different cellular actions. Hence, trends were more apparent when UCB-CD133$^+$ cells and substrate cells were both hypoxia pre-conditioned. On the other hand, although only small differences were observed between normoxic controls and hypoxia treated cells,

the “percentage gain” also presented with these results provides an alternative way of interpreting our observations, and show that the impact of hypoxia pre-conditioning targets specifically lower adhesion percentages **[Figure IV.15]**. Interestingly, dramatic changes due to hypoxia were detectable with greater sensitivity when testing our 2^{nd} population hypothesis, and while the small number of adhering cells in the 2^{nd} population might just reflect ‘spillage’ of normally adhering cells (due to non-specific removal during the assay), the fact remains that a large proportion of UCB-$CD133^{+}$ cells did not adhere despite given another chance. The 2^{nd} population of UCB-$CD133^{+}$ and KG-1 cells can be thus viewed as a more sensitive method to detect changes in cell adhesion otherwise not detected in our standard assay and raises the following questions: Is there a phenotypic difference between the two populations? Can longer exposures to hypoxia change the fate or cell surface phenotype of otherwise non-adhering UCB-$CD133^{+}$ cells, i.e enable them to adhere?

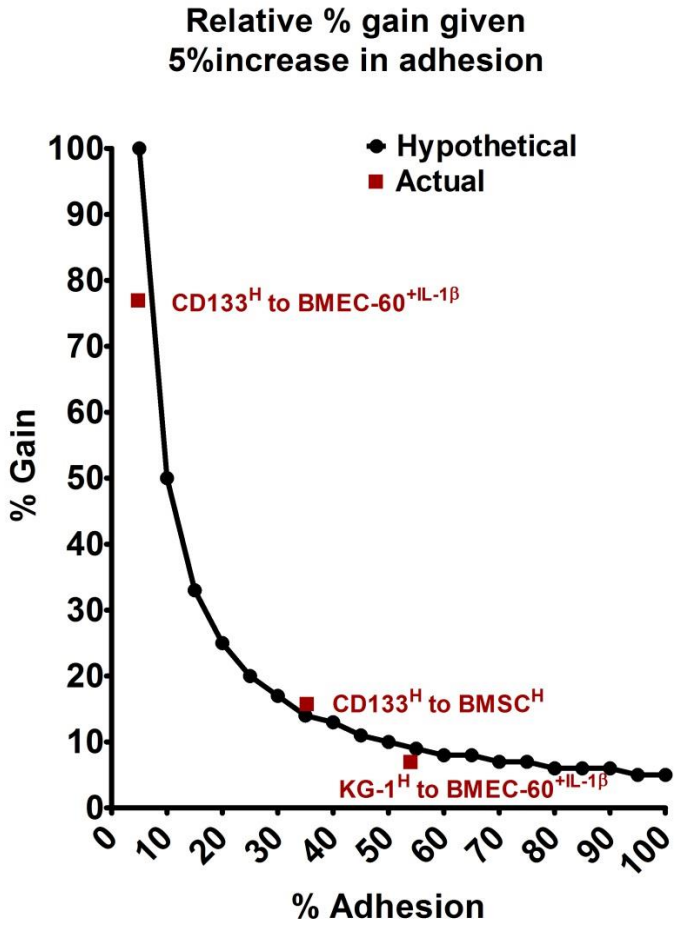

Figure IV.15. Percentage gain reflects the magnitude of increased cell adhesion

This figure illustrates the significance in determining the % gain rather than simply accepting the mean difference between the control and treatment group. Here hypothetical increases in 5% cell adhesion are plotted against their respective % gain, and show an inverse relationship: As the % of adhesion increases, the magnitude i.e the % gain based on a mean difference of 5% decreases. Three data point from our results are also plotted as an example. The % gain obtained for e.g. UCB-CD133^{H} to BMEC-60$^{+IL\text{-}1\beta}$ where the average adhesion was 8.4% vs. 4.72% in the normoxic control= 3.68% mean difference, translates to a % gain of 78%. In contrast, UCB-CD133^{H} to BMSC^{H} with an average adhesion of 40.78% vs. 35.22% in the normoxic control= 5.56% mean difference, translates only to a % gain of 15.79%. The % gain becomes even smaller for KG-1^{H} to BMEC-60$^{+IL\text{-}1\beta}$, where the average adhesion was 58.08% vs. 53.95% in the normoxic control= 4.13% mean difference and translating to a % gain of 7.66%. The mean difference clearly does not always reflect significant changes in cell adhesion due to hypoxia pre-conditioning.

A few studies address some of these questions. Peled et al. identified that only 20 to 25% of UCB-CD34^{+} cells migrated towards SDF-1α in a transwell migration assay and also found that this population was comprised of significantly more primitive CD34^{+}CD38^{-} cells than the non-migrating population

of CB-CD34^{+} cells (Peled et al., 1999b). Wagner et al. found that more primitive HSPCs (CD34^{+}CD38^{-} vs CD34^{+}CD38^{+}) and slower dividing fractions versus faster dividing fractions of CD34^{+}CD38^{-} adhered significantly more to MSCs (Wagner et al., 2007). Alakel et al. show that adherent HSCs/HSPCs isolated from mPB included more cells with a less differentiated phenotype, CD34^{+}CD133^{+}, CD34^{+}CD38^{-}, and CD133^{+}CD38^{-}, compared to non-adhering HSCs/HSPCs from the same source (Alakel et al., 2009). Regarding the role of hypoxia on HSC/HSPC fate, LTR-HSCs isolated directly from the endosteal region (endCD150^{+}CD48^{-}LSK) in mice exhibited superior proliferation capacity and homing efficiency compared to LT-HSCs isolated from the central BM cavity (Grassinger et al., 2010), which is further supported by Winkler et al., who show that the most potent HSC niches, harbouring HSCs/HSPCs capable of serial transplantation, are “enriched with locally secreted factors and low oxygen tension due to negligible blood flow” (Winkler et al., 2010). Results presented here, show that increasing exposure to hypoxia from 24 to 48 hours improved adhesion of UCB-CD133^{+} cells to non-stimulated, normoxic BMEC-60s as well as their transmigration towards the chemokine SDF-1α. Therefore, hypoxia appears to indeed change the fate of otherwise poorly adhering UCB-CD133^{+} cells and favour their migration. Hypothetically it implies a significant difference between adhesion/homing molecules or their stability, and suggests hypoxia or stabilisation of HIF-1α can play a direct role in modulating cell surface phenotypes necessary for the adhesion and migration of transplanted UCB-CD133^{+} cells. Additional experiments using the 2nd population adhesion assay might confirm the fundamental problem encountered during HSCT of UCB-CD34^{+} HSCs/HSPCs: poor engraftment of specific HSC/HSPC subsets,

and propose hypoxia pre-conditioning as a non-invasive treatment to improve the homing and engraftment of UCB-HSCs/HSPCs.

When examining the effects of hypoxia on cell surface adhesion molecules, changes on some markers were observed. Particularly striking was the statistically significant decrease in surface expression of homing molecule VLA-4, which is involved in firm adhesion of HSCs/HSPCs to the endothelium. In line with current dogma, enhanced migration towards SDF-1α might be expected to correlate with a decrease in firm adhesion via VLA-4 to VCAM-1 on endothelial cells. These observations demonstrate that adhesion is clearly a multi-factorial process. Future studies might examine whether functional receptors rather than merely the expression of these receptors determines their role in adhesion (Lundell et al., 1996, Lundell et al., 1997).

The adhesive interactions under the influence of hypoxia to the substrate cells evidently differ between UCB-CD133$^+$ and KG-1 cells. This is most apparent in their adhesion patterns to BMEC-60s, where hypoxia significantly decreased KG-1 cell adhesion in all treatments except when BMEC-60s were IL-1β stimulated. Even KG-1 adhesion patterns to BMSCs were significantly more influenced by hypoxia pre-conditioning than UCB-CD133$^+$ cell adhesion to these substrate cells. These results are perhaps indicative of the phenotypic variations between UCB-CD133$^+$ cell populations from different donors, a major factor likely to be affecting transplantation outcome. KG-1 and KG-1A cells on the other hand are immortalised cells derived from adult acute leukaemic cells, the phenotype of which is less likely to differ between batches, reducing experimental variability, consequently providing more consistent and robust

conclusions. It might also be expected that leukaemic cells possess adhesion and migration properties that differ from normal cells or that UCB cells differ from adult cells. As highlighted earlier, the statistically significant effects hypoxia had on KG-1 to BMEC-60 provided supporting evidence that IL-1β stimulation shifts the dominance among adhesion pathways towards one not prevalent in non-stimulated BMEC-60 nor elicited by priming the adhering cells (UCB-$CD133^+$) for 48 hour under hypoxic conditions. KG-1 cells were indeed a valuable model cell line but have their stated limitations as models for normal HSCs/HSPCs and may be more significantly used when defining the interaction of leukaemic cells with the BM niche.

Results obtained for the transwell migration assay were conceivably the most exciting, with statistically significant increased migration when pre-treating UCB-$CD133^+$ cells for 48 hour in 1.5% O_2, which also led to re-examining effects of hypoxia on adhesion between UCB-$CD133^+$ cells and BMEC-60s that resulted in statistically significant enhanced adhesion to non-stimulated BMEC-60 cells. No observed changes in adhesion to IL-1β activated BMEC-60 cells supports previous studies that hypoxia pre-conditioning enhances the migration of UCB-$CD133^+$ cells by releasing cells from firm adhesion in the perivascular niche (Levesque et al., 2007). Furthermore, hypoxia induced signalling might be time-dependent, even though relevant homing molecules have been upregulated at the mRNA level (Martin-Rendon et al., 2007).

The main drawback of UCB-derived HSCT is the limited number of HSCs that reach the BM to repopulate a recipient's haemopoietic system. Infusing higher doses of $CD34^+$ (>$3x10^7$ NC/Kg or >$2x10^5$ $CD34^+$ cells/Kg before

freezing) (Gluckman et al., 2011) has been correlated with better patient survival, thus various methods to increase cell dose have been adopted and continue being developed. For example, transplantation of two cord blood units has been practised (Stanevsky et al., 2010), whilst other groups have focused on *ex-vivo* expansion of UCB-HSCs (Csaszar et al., 2012, Delaney et al., 2010, Dorrell et al., 2000, Moore and Hoskins, 1994, North et al., 2007). Our data so far provide a platform to further analyse the apparent role of hypoxia or at least the stabilisation of HIF-1α on the fate of HSCs/HSPCs and their(Lord et al., 2007) migration within the BM niche. The challenge will be to simulate the hypoxic microenvironment as may be found in the BM, i.e. provide continuous low oxygen levels during the experiments and a representative substrate. Perhaps using small molecules to stabilise HIF-1α expression will be an alternative approach (Forristal and Levesque, 2013). Since the experiments in this thesis were completed, a number of interesting effects of HIF-1α stabilisation on murine HSPCs have been described. Firstly, as mentioned earlier in Chapter I, Section I.5, Singh et al. reported that the loss of PHD2 modulates the self-renewal capacity of murine HSPCs and MPPs, and that this was a HIF-1α dependent event (Singh et al., 2013). Forristal et al. found that injecting mice with PHD protein inhibitors, DMOG and FG-4497, HIF-1α was increased in the BM and more HSPCs were in G_0 phase of the cell cycle. If these small molecules were injected into mice prior to sublethal irradiation of 9.0 Gy and subsequent BM transplantation, enhanced HSC and blood cell recovery was observed (Forristal et al., 2013). Speth et al. have further shown that dmPGE2 and DMOG treatment of murine HSPCs for 2-4 hours transiently stabilises HIF-1α, leading to upregulation of CXCR4 and subsequent enhanced

migration *in vitro* of HSPCs to SDF-1, as well as enhanced overnight homing and LTR engraftment (over 6 months) *in vivo* (Speth et al., 2014)

The bi-dimensional setting in our adhesion assays might be the caveat of these *in vitro* studies, as they do not provide the same tissue organisation to mimic *in vivo* settings (De Barros et al., 2010). On the other hand, to fully disentangle specific roles of components in a complex system, confounding factors that could otherwise cloud the results should be minimal.

With the *in vitro* data provided here, we hypothesise that hypoxia pre-conditioning or maintaining HIF-1α expression can enhance the homing and engraftment of UCB-derived HSCs/HSPCs to the BM and reduce the need to infuse higher doses of UCB-HSCs. Forty eight hour hypoxia pre-conditioning of UCB-$CD133^+$ cells resulted in 58.65% more cells transmigrating through activated BMEC-60s. In the next chapter, we examine the potential role the intracellular scaffolding protein HEF-1, which was identified in a microarray study undertaken in our laboratory (Martin-Rendon et al., 2007). HEF-1 was amongst a number of genes in UCB-$CD133^+$ cells upregulated at the mRNA level after exposing these cells to 1.5% O_2 for 24 hours. As described in Chapter I, HEF-1 is currently known to enhance the migration and invasion of cancer cells, thus its upregulation in UCB-$CD133^+$ in response to hypoxia could imply a functional role in migration of HSCs/HSPCs.

Chapter V Studies to dissect the function of HEF-1 in hypoxia and its role in the HSPC Niche

V.1. Introduction

The first objective of this DPhil project was to determine the functional effects of hypoxia on adhesion and migration of human UCB-CD133$^+$ cells. Chapter IV shows that pre-conditioning UCB-CD133$^+$ cells for 48 hours with 1.5% O_2 significantly enhances their adhesion to BM niche cells BMEC-60 (non-stimulated), as well as their transmigration towards the chemokine SDF-1α. These findings suggest that the priming of UCB-HSPCs with 1.5% O_2 or stabilising the expression of transcription factor HIF-1α in these cells prior to their administration into patients could improve the number of UCB-HSPCs reaching and lodging in the BM. To further support these results, another objective of this project was to identify hypoxia regulated molecules that are driving these changes in adhesion and transmigration. Using microarray analysis, our laboratory identified 161 genes upregulated by hypoxia in human UCB-CD133$^+$, including relevant homing and engraftment molecules such as chemokine SDF-1α, VEGF-A, VLA-4, CD133, KIT, Tie1 and GATA2 (Martin-Rendon et al., 2007). Amongst the other genes not previously described in HSC/HSPCs as being upregulated by hypoxia was the scaffolding molecule HEF-1.

HEF-1 has already been reported to play a role in chemokine inside-out induced migration of T-cells (Regelmann et al., 2006), as well as in cancer cell migration, invasion and proliferation (reviewed in Chapter I, Section I.7). To

determine if HEF-1 signalling plays a role in hypoxia induced UCB-CD133^{+} cell adhesion to and across BMEC-60 cells, two molecular functions were examined. First, the effects of hypoxia were examined on HEF-1 expression in human haemopoietic cell lines KG-1 and UCB-CD133^{+} cells. Secondly, lentiviral-mediated RNA interference (RNAi) was tested as a tool to silence endogenous HEF-1 expression (knockdown). This chapter particularly presents the different steps taken to optimise the protocol for HEF-1 knockdown in UCB-CD133^{+} cells.

Small non-coding RNA molecules (~20-30 nucleotides) produced from double-stranded RNA (dsRNA) precursors target complementary portions of messenger RNA (mRNA) to regulate gene expression (Davidson and Mccray, 2011, Mittal, 2004). The short dsRNAs are expressed as inverted repeat sequences forming small hairpin RNAs (shRNAs) and are cleaved by Dicer (an endonuclease belonging to the RNase-III family) into small RNA duplexes known as small interfering RNAs (siRNAs). Gene silencing occurs when the generated siRNA duplexes are sequestered by the RNA-induced silencing complexes (RISCs), which together with an Argonaut protein (the catalytic component of RISC), Dicer and dsRNA-binding domain (dsRBD) containing protein TRPB, form the RISC-loading complex. Two features are critical for efficient and successful loading of the siRNAs: length of the duplex and presenting 5’ and 3’ ends with particular charactistics—a monophosphate group and dinucleotide overhangs respectively (Jinek and Doudna, 2009). Upon loading, the non-guide (passenger) strand is cleaved by the Argonaut protein and released, leaving a 5’-3’ guide strand able to base pair with complementary RNA sequences (target RNA). This enables the Argonaut protein to slice up the targeted RNA, as a result decreasing endogenous expression of the targeted

gene. Cells use this molecular machine to inhibit viral infection; antiviral siRNA sequences (antisense oligonucleotides) bind complementary viral RNA transcripts to trigger cleavage by the RISC complex (Haasnoot et al., 2007).

Two other classes of small regulatory RNAs can also induce gene silencing: microRNAs (miRNAs) and PIWI-interacting RNAs (piRNAs). piRNAs are ~23-31 nucleotides that silence transposons in animal germ cells, the biological mechanisms of which are still being elucidated (Mani and Juliano, 2013). miRNAs, however, are small non-coding sequences encoded in the genome that induce gene silencing in a similar manner to siRNAs, involving Dicer and the RISC machinery. Transcribed as primary transcripts (pri-miRNAs), Drosha (nucleus based RNase III enzyme) and its cofactor DGCR8 process pri-miRNAs into stem loop precursors (pre-miRNA) (Jinek and Doudna, 2009, Manjunath et al., 2009). Pre-miRNA are subsequently exported to the cytoplasm and targeted by Dicer and RISCs to regulate gene expression. The pri-miRNA processing stage of this RNAi pathway has also been adopted in shRNA gene silencing technology, where shRNAmir generate pre-miRNAs, subsequently leading to degradation of the targeted mRNA **[Figure V.1]** (Silva et al., 2005, Stegmeier et al., 2005).

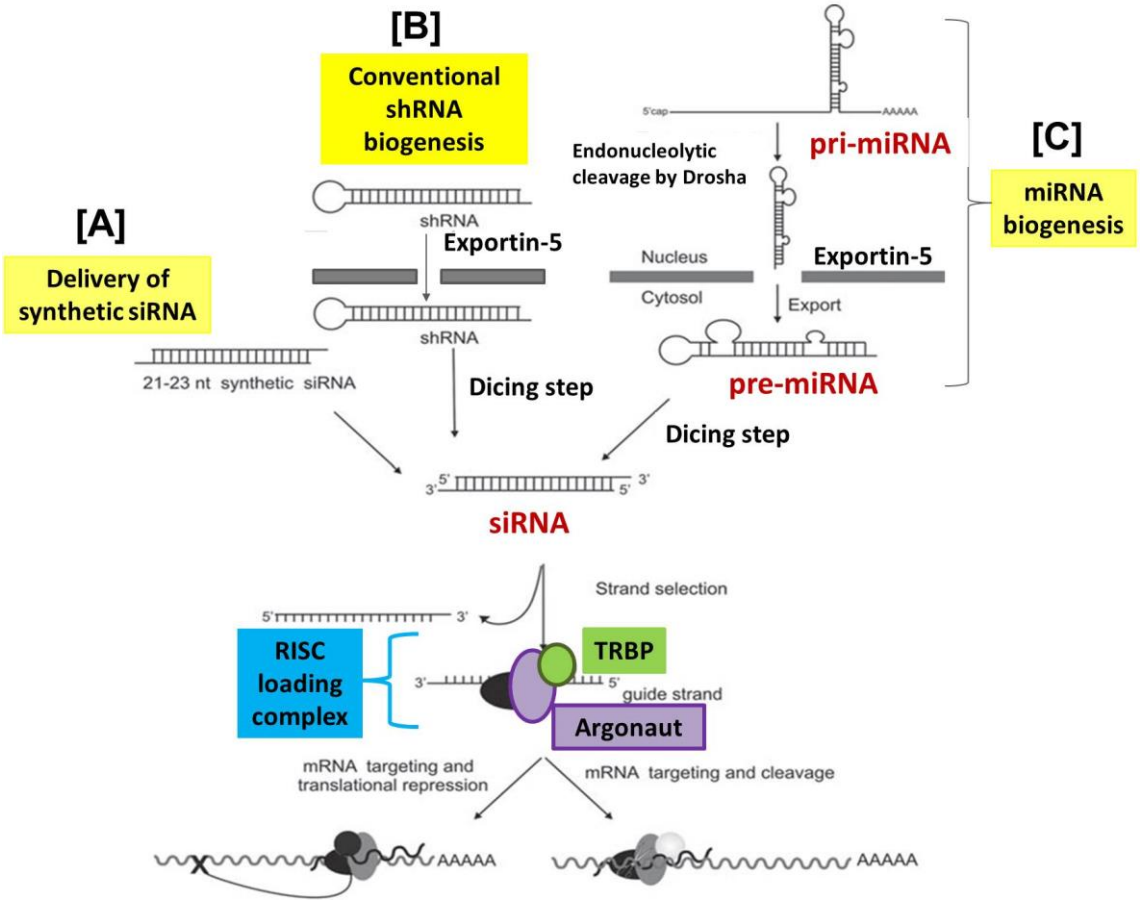

Figure V.1. Harnessing RNAi pathways for therapy.

Biochemical and structural biology studies have provided advanced understanding on small RNA biogenesis, further developing RNAi strategies for therapeutic and research applications. Chemically synthesized siRNAs enter the RNAi pathway post-Dicer cleavage, with RISCs sequestering the guide strand for mRNA targeting and cleavage. [A] This approach is quick and efficient, but only for some cell types and gene silencing is a short lived event. [B] Delivering LV-vectors encoding shRNAs offers long-term gene silencing. shRNAs are incorporated into the host genome, transcribed and exported into the cytoplasm by Exportin-5 to be synthesized into siRNA duplexes, ultimately targeting and cleaving mRNA. [C] The endogenous miRNA pathway benefits from an additional processing step before continuing in the cytoplasm. Upon transcription of the miRNA, Drosh-DGCR8 complex cleaves the hairpin of the pri-miRNA into nucleotide intermediates (pre-miRNA) before their subsequent translocation into the cytoplasm. (Manjunath et al., 2009). Picture adapted from Springer, Methods in Molecular Biology (Clifton, N.J.), Vol. 506, 2009, Chapter 15, pp. 207-219, Scherr M., Venturini L., and Eder M., Knock-down of gene expression in hematopoietic cells, Figure 1, with kind permission from Springer Science and Business Media.

The discovery of RNAi in eukaryotes has been widely adopted as a molecular tool for gene function analysis. Co-transfecting mammalian cells with exogenous double stranded 21-22 nucleotide RNAs (siRNA duplexes) induces sequence specific gene silencing within 24 hours of transfection (Elbashir et al., 2001). While the effects of siRNA duplexes are observed fairly quickly, they are often short lived due to siRNA degradation or dilution upon cell division (Manjunath et al., 2009). To examine loss of gene function over time, exogenous siRNA duplexes can be generated intracellulary by cloning the precursor shRNA into an expression vector, frequently using non-replicating recombinant viral vectors. A major advantage of viral vectors over non-viral gene delivery tools is their ability to stably integrate the dsRNA into the host genome, enabling gene function to be examined in long-term *in vitro* and *in vivo* studies (Davidson and Mccray, 2011, Segura et al., 2013). Lentiviral vectors (LVs) are a particularly suitable delivery system of synthetic shRNAs, most importantly for their ability to penetrate the intact nuclear membrane of non-dividing cells (Cooray et al., 2012, Naldini et al., 1996, Reiser et al., 1996, Rubinson et al., 2003).

The majority of LVs used to functionally silence genes in human cells are based on the human immunodeficiency virus type 1 (HIV-1) (Cooray et al., 2012). Other vector systems include non-primate lentiviruses such as equine infectious anemia virus (EIAV) and feline immunodeficiency virus (FIV) (Rohll et al., 2002). However, the basic biology of HIV replication has been characterised more extensively, making genetically modified HIV-based vectors for transforming animal cells safely and with high performance capacity. For example, transcriptional enhancers and promoters encoded in the U3 region of

long-terminal repeats (LTRs) have been deleted, creating self-inactivating LTRs (SIN). Conversely, to prevent accidental recombination of viral sequences that could create a replication-competent virus, packaging of the viral RNA and genes required for virion production and infection have been distributed onto different viral vectors (constructs) (De Palma and Naldini, 2002, Ulrich, 2005). Today, up to four HIV-based vectors ("third-generation" HIV-derived vectors) are combined in a transient co-transfection in permissive cell lines to generate LV-particles: 1) A core packaging construct that expresses the core proteins and enzymes, such as *gag* and *pol* genes, essentials for viral replication, reverse transcription and integration, 2) the *Rev* expression vector, essential for expression of packaging construct, 3) an envelope construct, most often with the G protein envelope of the vesicular stomatitis virus (VSV-G), providing stability and broad tropism, and finally 4) a transfer vector, containing *cis*-acting sequences required for optimal packaging, reverse transcription, and integration of the exogenous RNA sequence (transgene) into the host's genome (De Palma and Naldini, 2002, Logan et al., 2002, Segura et al., 2013) **[Figure V.2]**.The transgene is part of an 'expression cassette', which contains the promoter to drive the transcription of the encoded RNA. Post-transcriptional regulatory elements can also be incorporated to enhance expression of the transgene, such as the Woodchuck hepatitis virus post-transcriptional regulatory element (WPRE). A reporter transgene and an antibiotic resistant gene are additional components that are often included in the expression cassette, as it enables the measurement of transducing activity and viral efficiency.

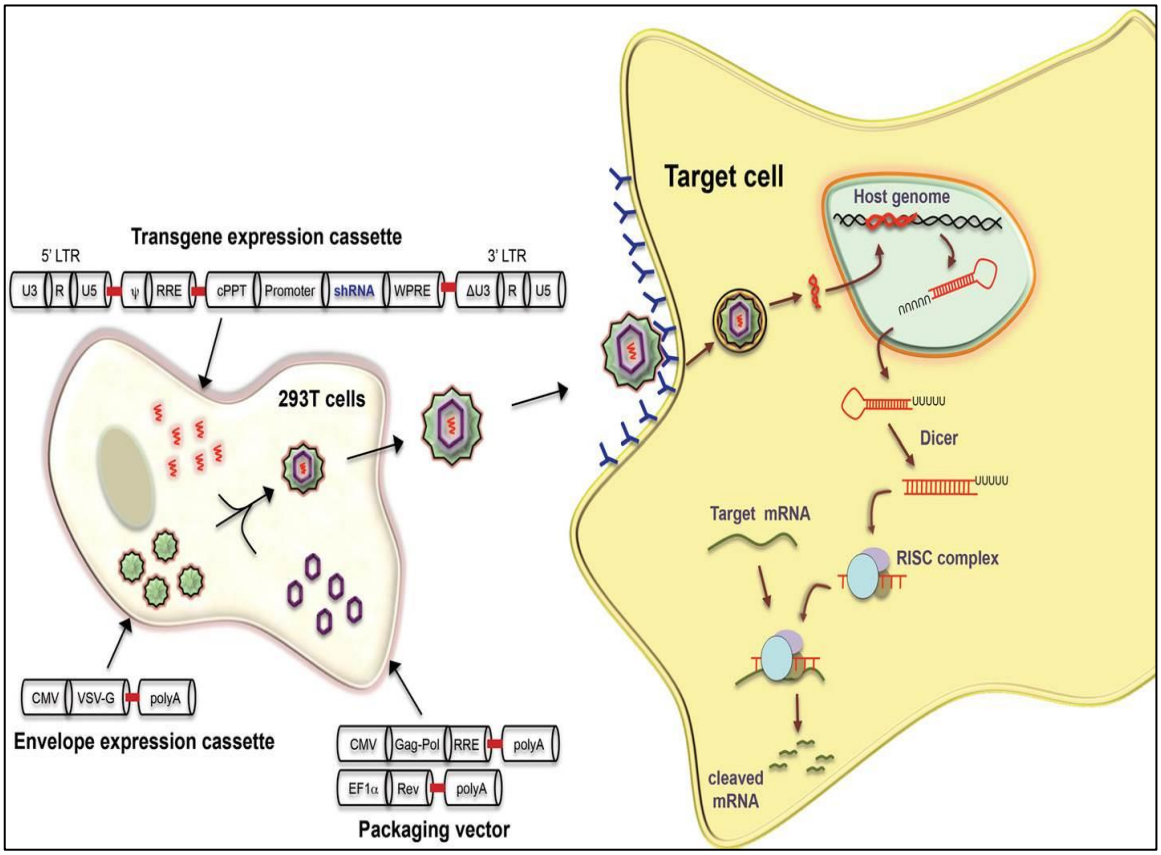

Figure V.2. Schematic drawing illustrating the generation of LV-particles by three-plasmid expression.

Human embryonic kidney 293T (HEK293T) cells transfected with a packaging vector, an envelope vector such as VSV-G, and a transfer vector containing HIV-1 cis-acting sequences and an expression cassette for transgenes such as green fluorescent protein (GFP) and/or an shRNA against e.g. HEF-1. LV-particles secreted into the media transduce target cells such as UCB-CD133^{+} cells. Target cells are transduced when the transgene is incorporated into the cell's genome and subsequently transcribed. The incorporation and expression of e.g. an shRNA sequence results in the degradation of complementary mRNA. Picture credit: Reprinted from Advanced Drug Delivery Reviews, 2009, Vol. 61, Issue 9, Manjunath N., Wu H., Subramanya S.,Shankar P., Lentiviral delivery of short hairpin RNAs, pp. 732-745, Copyright 2014 with permission from Elsevier.

Haemopoietic stem and progenitor cells, i.e. UCB-$CD34^{+}133^{-}$ and UCB-$CD34^{+}133^{+}$, from both UCB and mPB have been readily transduced with lentiviral-based vectors (Case et al., 1999, Evans et al., 1999, Robbins et al., 2006, Scherr et al., 2009, Schomber et al., 2004, Woods et al., 2001). However, despite their extensive application, developing a working protocol comprises a number of experimental steps that can become exceedingly time-consuming. Cloning and developing a transfer vector that carries the desired expression cassette, generating LV-stocks, quality control of the LV-stocks, and finally transducing the selected target cell are all individual stages that require testing, optimisation and validation (Demaison et al., 2002, Kim et al., 2010b, Woods et al., 2001). Transduction efficiencies in HSCs/HSPC, for example, rarely exceed 60% (Kim et al., 2010b, Robbins et al., 2006, Scherr et al., 2009), and there has been little success in expanding HSC/HSPC re-populating cells *ex vivo*, limiting the number of days these cells can be maintained in culture to increase yield of transduced cells (Hofmeister et al., 2007, Magnusson et al., 2013). The viral titre, i.e. the vector concentration in the transduction medium, is one of the critical factors determining transduction efficiency of HSCs/HSPCs *in vitro.* To be able to transduce cells with high titre virus, harvested viral supernatants generated using standard methods are concentrated by ultracentrifugation to change concentrations from ~10^{6} (non-concentrated titre) to >10^{8} TU/mL (high titre) (Segura et al., 2013); the higher the concentration of viral particles, the higher the probability that vector and target cells come into contact (De Palma and Naldini, 2002).

On the other hand, although non-viral gene delivery methods have been engineered as an alternative, they can be equally challenging. In fact, chemical

approaches tend to be even more inefficient at introducing genetic material into non-dividing cells, and physical delivery methods such as electropermeabilisation (Nucleofection™), even though used on “difficult-to-transfect cells”, inflict heavy cellular trauma, initiating apoptotic or programmed cell death (Mellott et al., 2013). As a consequence, the remaining number of viable and genetically modified cells is often insufficient to carry out research. Thus LVs, despite their limitations, have the potential to transduce non-dividing cells with greater efficacy.

Increased transmigration of hypoxia pre-conditioned UCB-CD133^{+} cells towards the chemokine SDF-1α provide very exciting findings for further homing and engraftment studies of UCB- HSPCs. The next objective was thus to determine whether changes in HEF-1 expression is directly coupled with changes in UCB-CD133^{+} cell adhesion and migration across BMEC-60 cells. For this a suitable knockdown system and protocol had to be developed and optimised. We thus pursued using LVs to insert shRNA sequences for long-term HEF-1 knockdown in UCB-CD133^{+} cells.

V.2. Results

V.2.1. HEF-1 expression in haemopoietic cell lines

Protein expression of HEF-1 has not been previously reported in KG-1 and KG-1A cells. With the view to use these haemopoietic cell lines to test and optimise the transduction efficiency of lentiviral particles to knockdown HEF-1 in UCB-CD133^{+} cells, HEF-1 protein expression was tested for in both cell types. Total protein was extracted from both KG-1 and KG-1A for Western blot analysis. HEF-1 activity (regulating migration) has previously been examined in Jurkat cells and was thus used as a positive control (Van Seventer et al., 2001). As described in Chapter 1, Section I.7, HEF-1 has a molecular weight of 93 kDa and becomes phosphorylated at its tyrosine residues by integrins and other stimuli. For example, phosphorylation of HEF-1 has been observed following ligation of T- and B-cell antigen receptors (Manié et al., 1997, Ohashi et al., 1998), as well as after β1-integrin crosslinking via FAK and Src family tyrosine kinases (Tachibana et al., 1997). There are two phosphorylated (p) isoforms of HEF-1 that can be detected by Western blot analysis, a p105 kDa and a p115 kDa isoform. The p115 kDa isoform is usually only detected in adherent cells (Zheng and Mckeown-Longo, 2002), where the process of cell adhesion regulates the conversion of p105[HEF-1] to p115[HEF-1]. This can be observed experimentally by detaching and then re-plating suspended cells (Zheng and Mckeown-Longo, 2006); hyper-phosphorylated 115 kDa[HEF-1] being 'activated' HEF-1 protein that is recruited to focal adhesion sites during cell attachment (O'neill and Golemis, 2001, Singh et al., 2007). Although KG-1, KG-1A and UCB-CD133^{+} cells are cells in suspension, they are continuously colliding and

stimulating cell surface receptors **[Figure V.3]**. Thus "outside in" signalling could be affecting the regulation of pHEF-1 isoforms. The abundance of the p105[HEF-1] and p115[HEF-1] appears to be cell cycle regulated, with protein expression being particularly abundant following initiation of cell division (G1/S-phase) (Law et al., 1998). Other post-translationally processes include cleaving of full length HEF-1 by caspases during mitosis and apoptosis, giving rise to specific forms p55 (Law et al., 1998) and p28 (Law et al., 2000) respectively. Thus, depending during what cellular activity cells are lysed for Western blot analysis, different forms of HEF-1 can be detected.

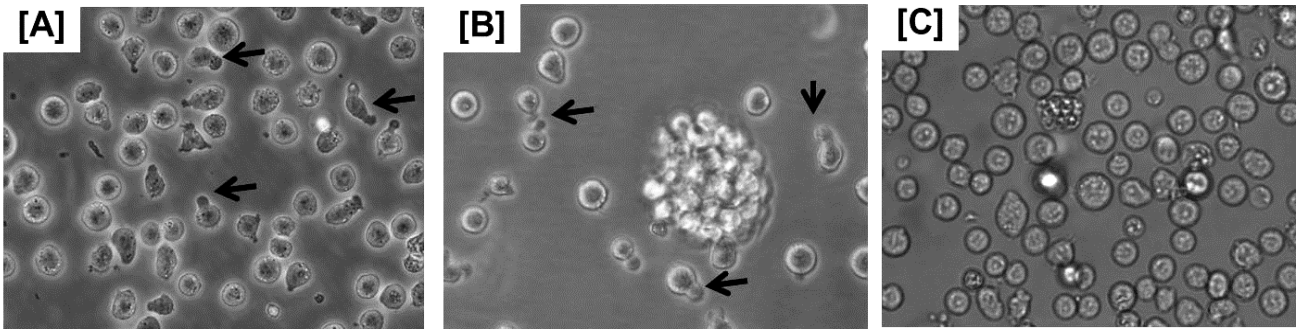

Figure V.3. Cells in suspension are in continuous motion.

[A] UCB-CD133^{+} cells (x40), [B] KG-1A (x40) and [C] KG-1 (x40) were interacting with their microenvironment or colliding with other cells in suspension. Arrows show extended lamellipodia on some of the cells. Elongation of lamellipodia requires rearrangement of the actin micro-skeleton (Gardel et al., 2010), recruiting various molecules to focal adhesion sites, including scaffolding protein HEF-1 (Fashena et al., 2002).

Total protein was extracted from KG-1, KG-1A and Jurkat cells at the same passage (passage 4) to compare HEF-1 protein levels between cell lines. Western blot results in **Figure V.4A** show that the p105 kDa form was expressed in all three cell lines, with 93 kDa protein detected mainly in KG-1 cells. Based on densitometry analysis, there was no statistically significant differences in protein expression between cells lines ($p>0.05$) **[Figure V.4]**.

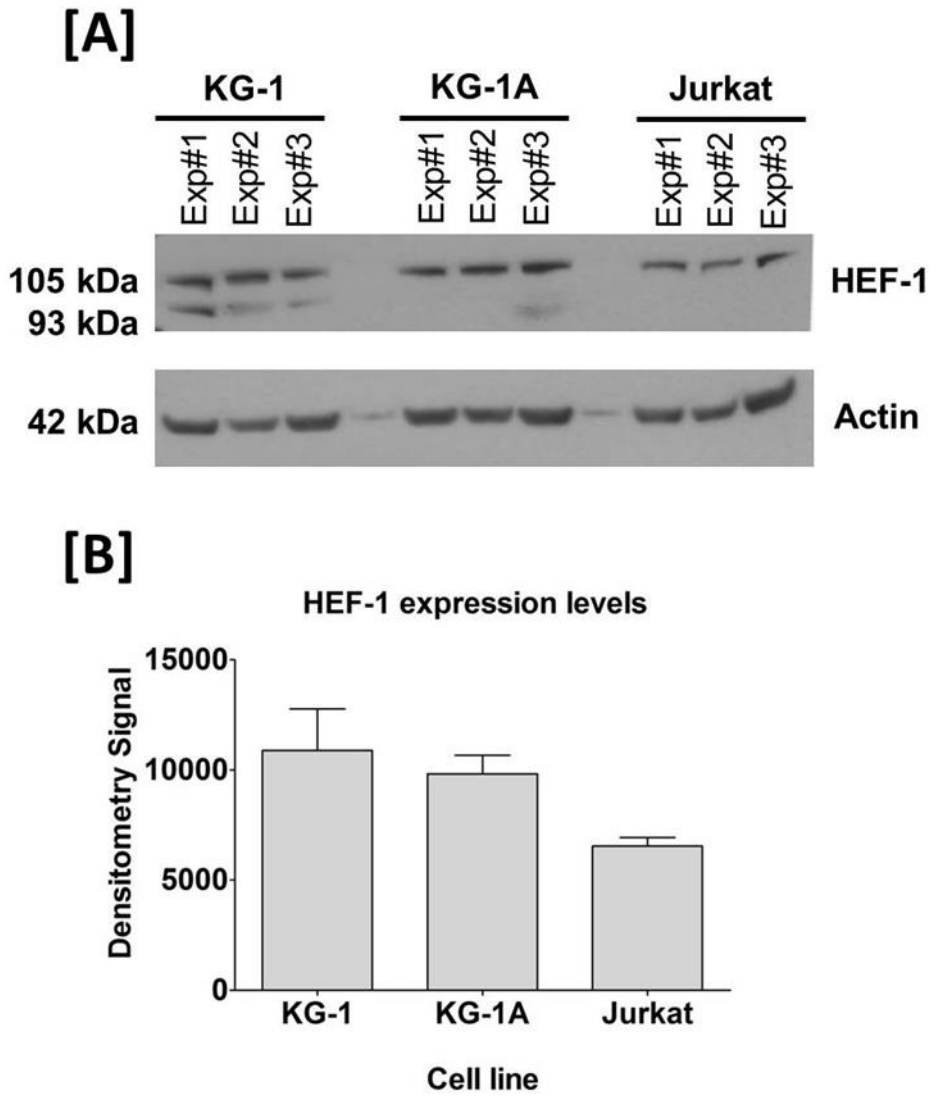

Figure V.4. Detecting HEF-1 protein in haemopoietic cell lines.

[A] Total protein of haemopoietic cell lines at passage 4, KG-1, KG-1A and Jurkat cells, was extracted in three separate instances for Western blot analysis. Loading 50 µg of total protein for all cell lines, HEF-1 was detected using mouse monoclonal [2G9] anti-HEF-1 antibody (abcam Cat# ab18056) in all three cell lines. The p105 kDa form was detected in all cell lines, whereas the non-phosphorylated of 93 kDa was mainly detected in KG-1 cells [B] Densitometry analysis showing p105 kDa HEF-1 levels expressed in each cell line. Differences in expression levels are not statistically significant (densitometry signals: KG-1=10877±1888, KG-1A=9822±844, Jurkat=6546±387; n= 3 independent experiments ±SEM, $p>0.05$, one-way Anova followed by Bonferroni's Multiple Comparison Test). Actin protein (loading control) was used to deduce the normalisation factor described in Ch 2 Section II.13.

V.2.2. Effects of hypoxia on HEF-1 expression

Hypoxia pre-conditioning had a positive effect on UCB-CD133^{+} cell migration across stimulated BMEC-60 cells. It was thus of interest to ascertain

the observed up-regulation of HEF-1 mRNA (Martin-Rendon et al., 2007) due to 1.5% O_2 conditioning at the protein level. UCB-CD133$^+$ cells pooled from at least three different donors were cultured in StemSpan with the four cytokines IL-6, SCF, FLT-3L and TPO (described in Chapter 2, Section II.5) and exposed to 1.5% O_2 for 4, 24, and 48 hours, as performed for HIF-1α stabilisation tests presented in Chapter 4, Section IV.2.1. This hypoxia timecourse experiment was also tested on KG-1 cells as a comparison. At each time-point, cells were harvested quickly with cold DPBS and lysed with the lysis buffer as described in Chapter 2, Section II.12, for total protein extractions. Using Western blot analysis HEF-1 protein expressions at the given time-points were revealed. **Figure V.6** shows that HEF-1 protein levels increased with increasing incubation time in 1.5% O_2, with a statistically significant difference after 48 hours (densitometry signal of p105 kDa = 74,515±23,701 vs. 26282±12,268 in normoxic controls, 2.8 fold increase; p93 kDa = 48,077±7,875 vs.17,270±14,134, 2.7 fold increase; $p<0.05$). In contrast, 1.5% O_2 pre-conditioning had no effects on HEF-1 expression in KG-1 cells compared to the normoxic controls **[Figure V.5B]**.

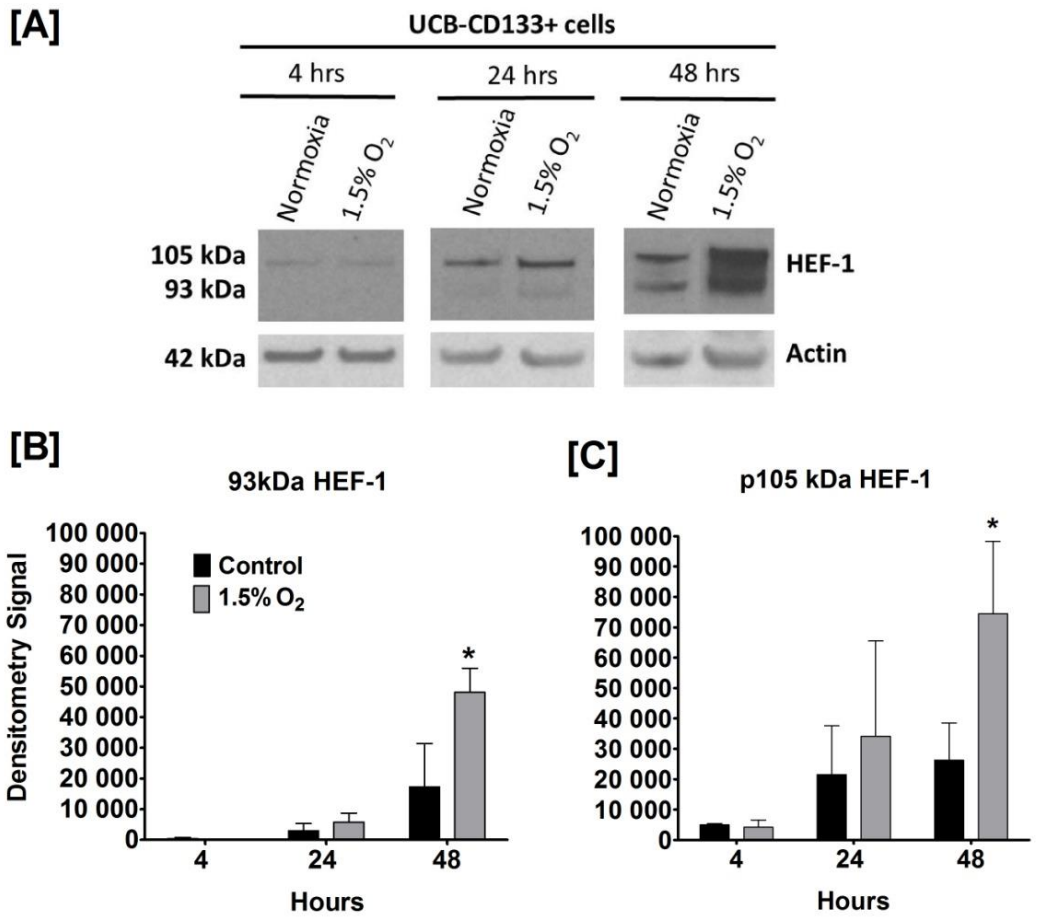

Figure V.5. Effects of 1.5% O_2 on UCB-CD133$^+$ cells.

UCB-CD133$^+$ cells pooled from at least 3 different donors were exposed to 1.5% O_2 and 20% O_2 (control) for 4, 24 and 48 hours. [A] Western blot showing expression levels of HEF-1 isoforms p105 and 93kDa, for each condition. [B-C] Densitometry analysis revealing highest expression levels at 48 hours of hypoxic treatment (fold increase at 48 hrs: 93kDa= 2.7, 105kDa= 2.8 fold, * = $p<0.05$; fold increase at 24 hrs: 93 kDa=1.95, 105 kDa= 1.58, $p>0.05$; fold increase at 4 hrs: 93 kDa=0.38, 105 kDa=0.85, $p>0.05$). N=3 independent experiments; ±SDEV; paired t-test; Actin protein (loading control) was used to deduce the normalisation factor described in Ch.2I, Section II.13.

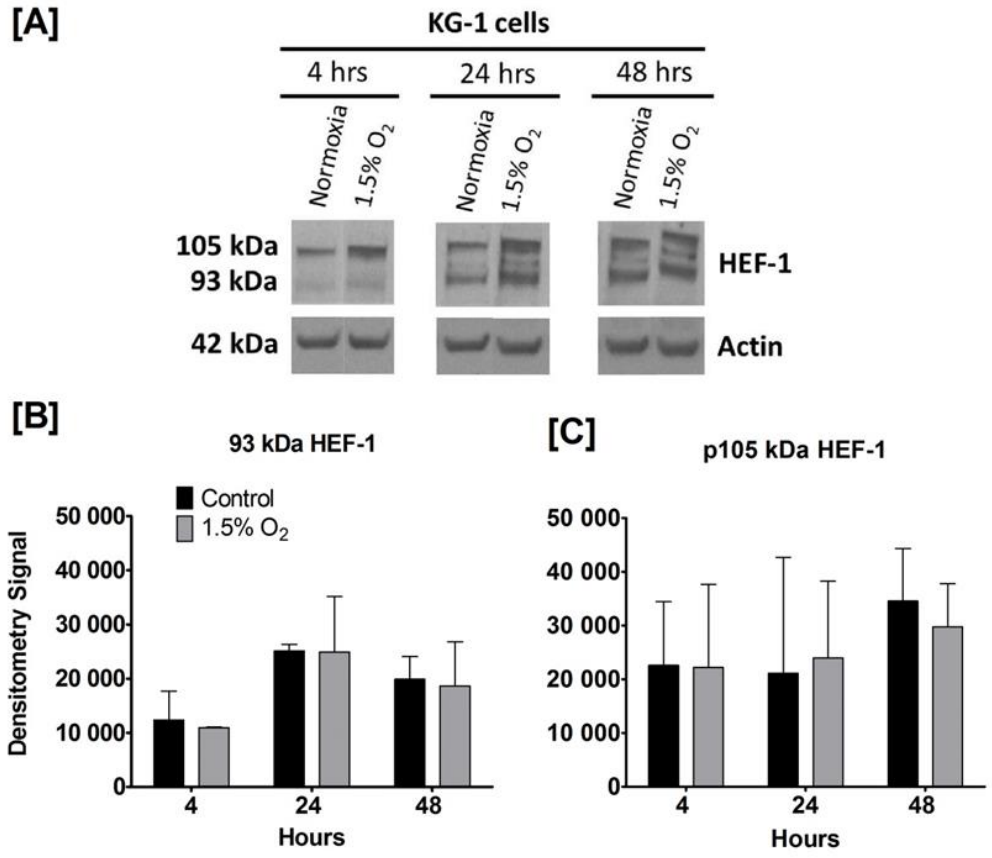

Figure V.6. Effects of hypoxia on HEF-1 expression in KG-1 cells.

KG-1 cells were exposed to 1.5% O_2 or 20% O_2 (control) for 4, 24 and 48 hours. [A] Western blot showing expression levels of HEF-1 isoforms p105 and 93kDa, for each condition. [B-C] Densitometry analysis revealed that hypoxia pre-conditioning has no effect on HEF-1 expression: 93 kDa = 0.88 fold increase at 4hrs, 0.99 at 24hrs, and 0.93 at 48hrs; 105 kDa = 0.98 fold increase at 4hrs, 1.13 at 24hrs, and 0.93 at 48hrs. N=3 independent experiments; ±SDEV; paired t-test $p>0.05$; Actin protein (loading control) was used to deduce the normalisation factor described in Ch 2, Section II.14.

V.2.3. Identifying a suitable LV-knockdown vector

V.2.3.1. Pilot studies on the pGIPZ vector

To determine if HEF-1 is involved in the hypoxia migration of UCB-CD133$^+$ cells presented in Chapter IV, attempts were made to knockdown HEF-1. Two different lentiviral vectors (LV) were tested in for their ability to silence HEF-1. The approach was to first test the vectors in a single experiment (pilot study) in

human embryonic kidney 293T (HEK293T) cells, as this cell line is easily transfected and transduced, as well as used to generate LV-particles. HEF-1 had also been previously detected in these cells in our laboratory. The first LV to be tested was the pGIPZ vector from Open Biosystem, Thermo Scientific, Dharmacon (Dharmacon). When this research began, this was the only off the shelf LV available that encoded our gene of interest, human HEF-1. In addition, this vector encoded the reporter gene turbo-green fluorescent protein (tGFP), which would help to evaluate vector performance as well as tracking individual cells in our functional assays. The vectors also contained an antibiotic resistant gene against puromycin, which would enable selecting for transduced cell if required. Thus, in a pilot study, LV-particles were generated using a three-plasmid expression system. pGIPZ vectors encoding shRNAmirs against HEF-1 were combined with the viral glycoprotein envelope VSV-G and the regulatory protein gag-pol Δ 8.91. Three pGIPZ knockdown vectors were tested: two containing a distinct shRNA sequence against HEF-1 (shRNA[HEF-1A] and shRNA[HEF-1B]) [Chapter 2, Section II.9.2] and one vector containing an shRNA against housekeeping gene GAPDH as a positive control (+ve).

Fresh non-concentrated viral supernatants were tested on HEK293T cells to obtain viral titres, by following the titration protocol provided by Dharmacon [Chapter II, Section II.9.4]. Viral titres of ~$8.5x10^5$ TU/mL were obtained per construct, and were then tested on permissive HEK293T cells at a multiplicity of infection (MOI) of 2. MOI denote the number of virions added in a transduction per number of target cells, and is calculated as follows:

$$volume\ of\ viral\ supernatant\ x\ \frac{TU/mL}{number\ of\ cells}.$$

Thus, in this instance, an MOI of 2 was equivalent to a 2:1 ratio of virus to the number of target cells. Increasing the MOI increases the chances of infecting target cells with at least one or more virion.

Using flow cytometry analysis, transduction efficacy was determined by measuring the percentage of tGFP +ve cells. Median fluorescent intensity (MFI) values quantified the intensity of tGFP expression. With an MOI of 2, transduction efficiency ranged between 21% and 37% in these transduced HEK293T cells **[Figure V.8]**. To increase the percentage of infected cells, an MOI of 5 was also tested. To remove non-transduced cells and obtain a 'purer' transduced population, transduced HEK293T cells were selected for their ability to grow in the presence of puromycin. A puromycin kill curve was performed to determine the optimal puromycin concentration for selection **[Figure V.7]**. Cells of both transductions were cultured in media containing 2 µg/mL puromycin, which was the optimal concentration determined in the kill curve. After five days in puromycin, a highly enriched tGFP+ve population was acquired for both transductions. However, flow cytometry results revealed two tGFP+ve cell populations for cells transduced at MOI of 2, reflecting heterogeneity of viral infection, compared with a single tGFP+ve population for cells transduced with an MOI of 5 **[Figure V.8].** The copy number per cell could have been assessed by quantitative-PCR (q-PCR). However, this was not done as the results below showed no knockdown of HEF-1 using this LV vector. In addition, MFI values of cells transduced with an MOI of 5 were 15 fold higher than MFI readings of cells transduced with an MOI of 2.

To determine HEF-1 knockdown, the total protein was extracted from cells transduced with an MOI of 5 for Western blot analysis. As HEF-1 isoforms p105 and p115 were so close to each other, total HEF1 protein (p115 + p105) was determined by densitometry analysis. The 93 kDa isoform was not detected from this cell lysate.

Western blot results demonstrate that shRNAs against HEF-1 were unsuccessful at targeting HEF-1 **[Figure V.9A]**. Densitometry analysis revealed the following HEF-1 protein expression levels: shRNA-Non-sil = 98%, shRNA-HEF-1A = 94%, shRNA-HEF1B = 81% vs **[Figure V.9B]**. Although the lower HEF-1 expression observed with shRNA-HEF-1B was suggestive of a decrease in HEF-1 protein compared to Non-sil control, similar decreased expression levels of the housekeeping gene GAPDH in the same cell lysate make this difference not significant (**Δ=** –17.34% vs **Δ = –**12.38%) **[Figure V.9C]**. Successful knockdown was achieved using an shRNA against GAPDH (positive control; 60% vs 103% in the Non-Sil control; **Δ=** –42%) **[Figure V.9],** validating the technique. The Δ% was calculated as follows: $(\mathrm{KD} - C)/C)$, where knockdown (KD) = % of HEF-1 expression observed in cells transfected with a shRNA, and C= % of HEF-1 in Non-Silencing (Non-Sil) control. Negative value represents the % of decreased protein expression.

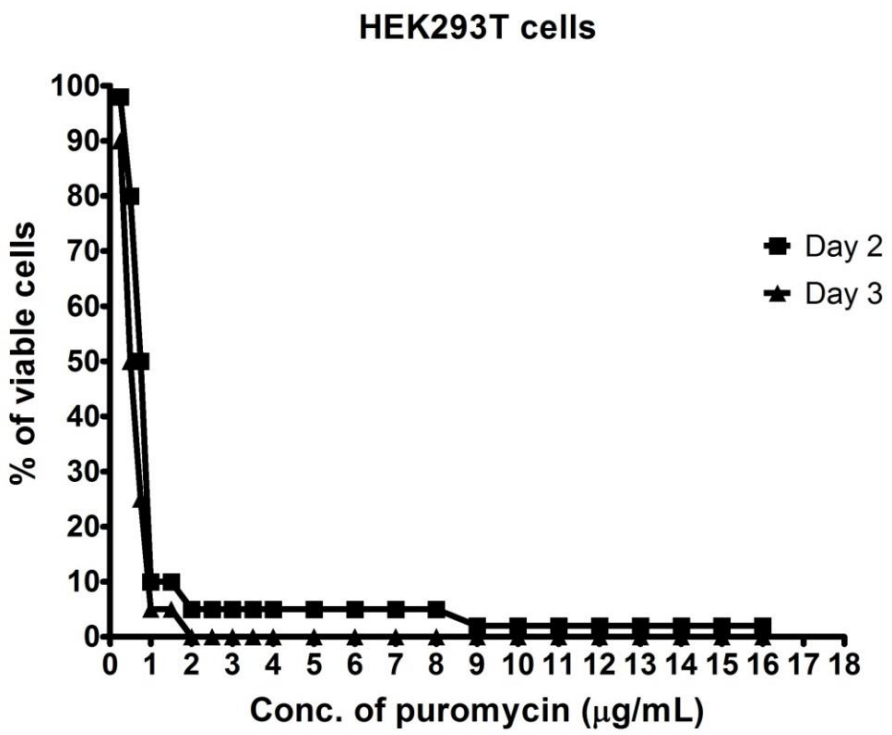

Figure V.7. Puromycin kill curve of HEK293T cells

HEK293T cells were cultured in the presence of puromycin to determine the optimal concentration for selection. Concentrations between 0.25-16 µg/mL were tested as recommended by Open Biosystems. Total cell death was observed on day 3 with 2 µg/mL puromycin. This concentration was used to select for successfully transduced HEK293T cells.

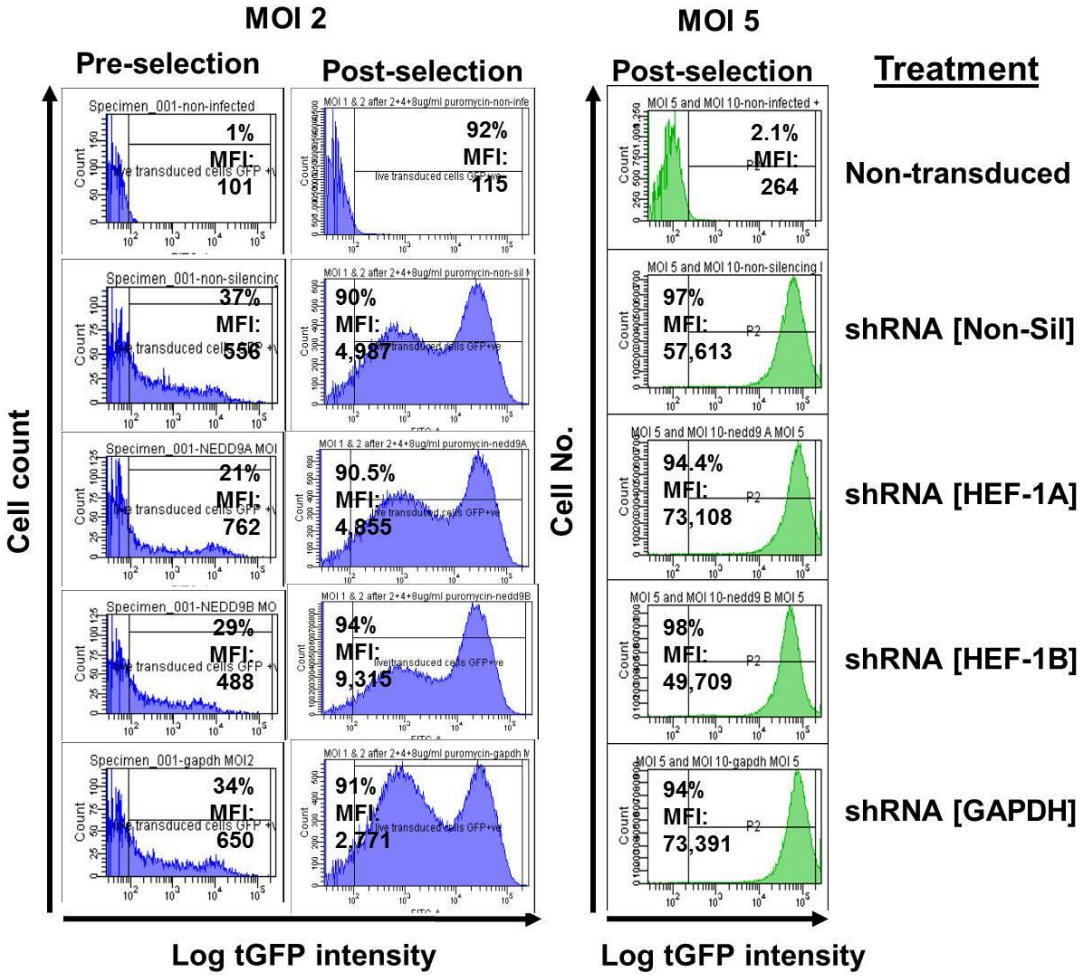

Figure V.8. Pilot study assessing transduction efficacy of pGIPZ vectors after puromycin selection.

Two MOIs were tested on HEK293T cells using pGIPZ-LV particles. Transduced cells were selected with 2µg/mL puromycin for 5 days. HEF-1A and HEF-1B represent two different preparation of viral particles containing different HEF-1 shRNA sequences. Post-selection resulted in highly enriched tGFP+ve populations for all treatments (>90%), i.e transductions with either LV-particles containing shRNA-Non-silencing, shRNA[HEF-1A], shRNA[HEF-1B], and shRNA[GAPDH]. TurboGFP intensity is represented by the MFI values indicated next to the histograms, with a significantly higher tGFP intensity in cells transduced with an MOI of 5.

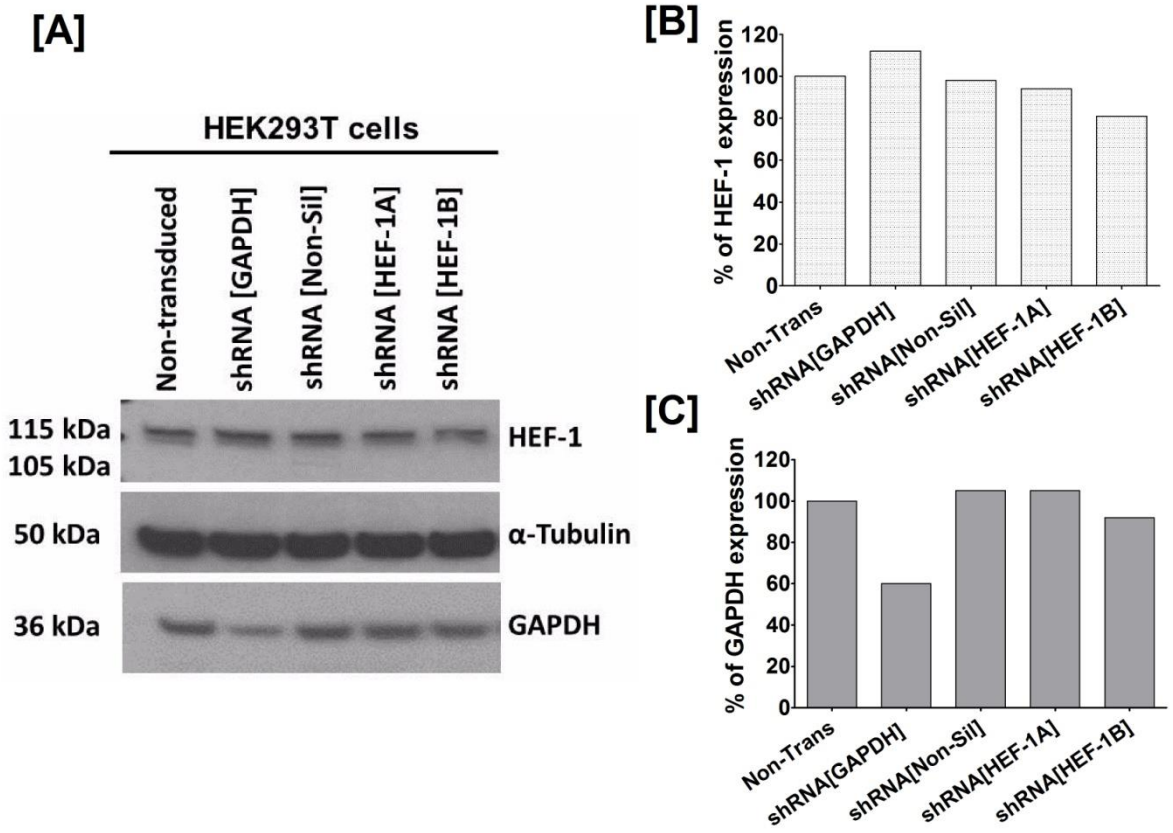

Figure V.9. Pilot study showed that LV-particles encoding pGIPZ with shRNA against HEF-1 did not knockdown HEF-1.

[A] Total protein was extracted from tGFP +ve cells to evaluate effects of shRNAs shown at the top of each Western blot lane. Western blots show successful knockdown of the +ve control, shRNA[GAPDH]. Isoforms p105[HEF-1] and p115[HEF-1] were detected in all treatments, thus no HEF-1 knockdown was achieved using shRNA[HEF-1A] and shRNA[HEF-1B]. [B] Densitometry analysis based on total HEF-1 protein (p105+p115). HEF-1 levels with the following pGIPZ vectors compared to Non-Trans control (100% expression): shRNA-[GAPDH] = 112%, shRNA[Non-sil] 98%, shRNA[HEF-1A] = 94%, shRNA[HEF-1B] = 81%. [C] Densitometry analysis. GAPDH levels with the following pGIPZ vectors compared to Non-Trans control (100% expression): shRNA[GAPDH]= 60%, shRNA[Non-sil] 105%, shRNA[HEF-1A] = 105%, shRNA[HEF-1B] = 92%. Data normalised to non-transduced (Non-Trans) cells after correcting for protein loading based on levels of α-tubulin.

As knockdown against HEF-1 was not detected with these in house made LV-particles, three new shRNA sequences (SV2-NEDD9-1, SV2-NEDD9-2 and SV2-NEDD9-3) using the same pGIPZ constructs were purchased from the same manufacturer (Dharmacon, Chapter 2, Section II.9.2 provides sequences). However, this time high titre particles (SMARTvector 2.0 lentiviral shRNA particles) were purchased. To increase the transduction efficiency in this pilot study, HEK293T cells were transduced at an MOI of 20. Forty-eight hours post-tranduction, tGFP expression was detected by fluorescence microscopy, and the transduction efficacy by flow cytometry. Dharmacon high titre LV-particles transduced 6% of cells with the non-silencing control, 45% with SV2-NEDD9-1, 50% with SV2-NEDD9-2 and 37% with the SV2-NEDD9-3 construct. MFI readings of tGFP +ve cells were high for all four constructs **[Figure V.10A]**. Transduced cells were selected for their ability to grow in the presence of puromycin (2µg/mL) as previously described and used for Western blot analysis. Although visual interpretation of the blot might indicate HEF-1 knockdown with the SV2-NEDD9-1 construct, low detection levels of HEF-1 protein for the non-silencing control, hindered quantification and comparison **[Figure V.10B].** To validate these observations, Western blot analysis and/or transductions would have to be repeated. However, because the transduction efficiencies obtained using these high titre SV2-particles were lower than expected, based on vector concentrations of ~1x10^{8} TU/mL, titre values provided by the manufacturer were tested. Significantly lower titre values were detected than those provided by the manufacturer's information sheet **[Figure V.10C]**. This was repeated twice and also corroborated by an independent worker in our laboratory. Given these titre

results, further troubleshooting experiments were not carried out. Instead, another lentiviral vector was considered: The pLKO.1 vector.

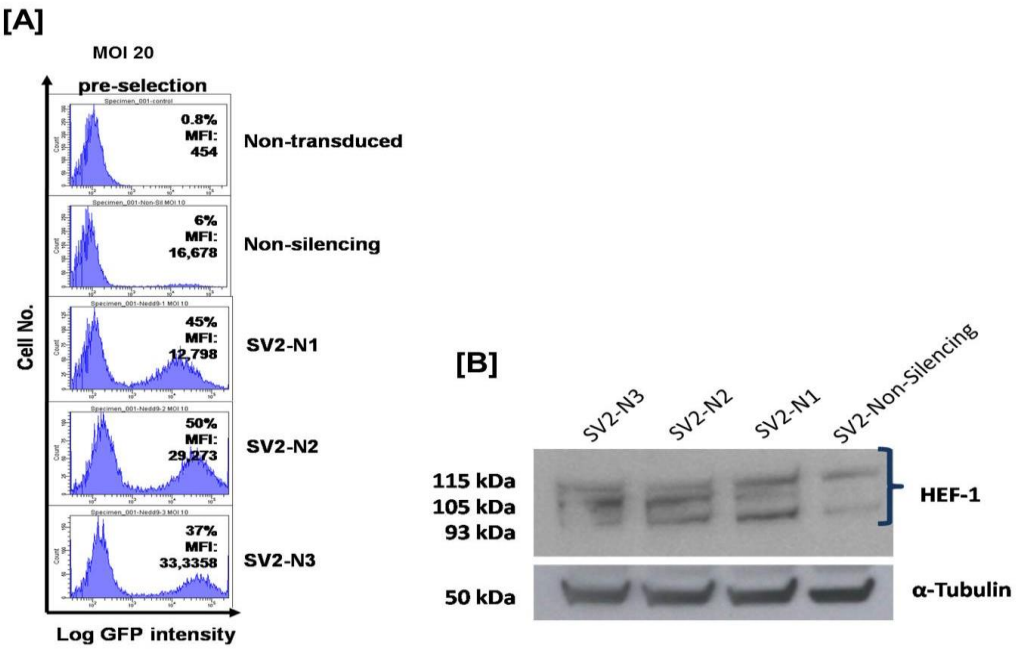

[C]

Source clone ID	Description	Titre (TU/mL) Dharmacon	MOI based on Dharmacon titre	Titre (TU/mL) SCRL	MOI based on SCRL titre
SH-019466-01	SV2-NEDD9-1 (N1)	1.06 x 10^8	20	1.3 x 10^5	0.026
SH-019466-02	SV2-NEDD9-2 (N2)	1.05 x 10^8	20	5.75 x 10^5	0.115
SH-019466-03	SV2-NEDD9-3 (N3)	1.00 x 10^8	20	1.01 x 10^6	0.2
S-0050001-01	SV2 non-targeting	5.17 x 10^8	20	2.95 x 10^5	0.059

Figure V.10. Flow cytometry analysis quantifying transduction efficacy of SV2 LV-particles.

HEK293T cells were transduced with LV-vectors encoding three new short-hairpins against target gene HEF-1, SV2-N1, SV2-N2, and SV2-N3. [A] Transduction efficacy of LV-particles targeting HEF-1 ranged between 37-50%, and 6% for non-silencing control vector. [B] Transduced cells were selected using 2 µg/mL puromycin prior to extracting total protein for Western blot analysis. Isoforms detected were p115[HEF1], p105[HEF-1] and 93[HEF-1]. Lower HEF-1 protein levels detected in the non-silencing control suggests the scrambled shRNA encoded in this construct is targeting HEF-1, thus not an appropriate control; consequently, deducing %Δ was not possible. [C] Validation of SV2 titres purchased from Dharmacon, Thermo Scientific. An end-point titration assay was carried out according to Dharmacon's protocol. Six dilutions of the viral stocks were tested on HEK293T cells and 48 hours post-transduction, cells were examined for tGFP+ve colonies. TU/mL values determined were >1000 fold lower than values received from the manufacturer. Based on new titre values from our laboratory (SCRL), corrected MOI values are shown in this table.

V.2.3.2. The pLKO.1 vector is a suitable LV-vector for HEF-1 knockdown studies

The pLKO.1 vector has previously been used to knockdown HEF-1 in murine melanoma cells lines by Regelman et al. (Regelmann et al., 2006). In 2009, data were published where the pLKO.1 vector had also been used to transduce UCB-derived HSCs/HSPCs (Kranc et al., 2009). We thus decided to assess the potential of this vector to knockdown human HEF-1 in UCB-CD133^{+} cells. Key differences between the pGIPZ and the pLKO.1 vector are listed in **Table V.1**.

The pGIPZ vector encodes a number of elements that should improve shRNA production and outcome, as well as facilitate easier identification of transduced cells. Firstly, the shRNAs expressed by this vector mimic human microRNA-30 (mirRNA-30) primary transcripts (pri-miRNA), allowing the shRNA to enter the mirRNA pathway. Inducing gene silencing via the mirRNA pathway became an attractive alternative, as this produced siRNAs that resembled more closely endogenous RNAi substrates for Dicer processing. Conventional shRNA transcripts often do not provide the typical 3' dinucleotide overhang created by Drosha cleaving. This can lower shRNA transcript stability or impair their translocation into the cytoplasm by Exportin 5; un-processed shRNA transcripts accumulate in the nucleus and become toxic. Conversely, very efficient overhangs may saturate Exportin 5 (Boudreau et al., 2008, Davidson and Mccray, 2011, Silva et al., 2005, Stegmeier et al., 2005). Secondly, pGIPZ vectors contain an internal ribosomal entry site (IRES). This element enables two proteins to be expressed in a single transcript. Rather than depending on

an additional 5'cap, ribosomes can bind and initiate translation at a second, internal site in the vector, expressing e.g. reporter gene tGFP and the puromycin resistant gene simultaneously (bicistronic expression cassette). More significantly, a bicistronic expression cassette may prevent competition or interference between two otherwise adjacent promoters (Ben-Dor et al., 2006).

The main disadvantage using the pLKO.1 vector has been the lack of a reporter gene. However, certain vector elements in the pLKO.1 vector provide advantages. The pLKO.1 vector encodes the U6 and hPGK promoters, which have been reported as being very efficient promoters at transducing primary human $CD34^+$ UCB progenitors (Roelz et al., 2010). Another recent study demonstrated better transduction efficiency when using the human cytomegalovirus (CMV) promoter (Varma et al., 2011). Successful viral gene delivery can also be affected by the size of the transgene (Kreiss et al., 1999), and large LVs result in lower titre preparations (Leuci et al., 2011). The smaller vector size of the pLKO.1 vector may thus improve viral packaging, and consequently quality of generated viral titres.

Table V.1. Differences between pGIPZ and pLKO.1 vector.

Vector Elements	pGIPZ	pLKO.1
shRNA	2nd generation: microRNA-adapted shRNA (based on miR-30)	1st generation: Simple stem-loop shRNA
Transgenes	TurboGFP & puromycin	puromycin
Transcription regulators	IRES	N/A
Internal promoters	CMV	U6 & hPGK
Enhancers	WPRE	none
Plasmid size	11.8 kb	7.1 kb

Six vector elements distinguish the pGIPZ from the pLKO.1 vector. Possessing a reporter gene is particularly useful for functional studies, but a smaller vector size might be transferred more easily. shRNAmir are modelled on the miRNA hairpin pre-cursors (pri-miRNAs) as Drosha-DGCR8 processing is key to subsequent stages in the pathway; two nucleotide 3' overhangs created by Drosha on the pre-miRNAs provide critical substrates for Exportin-5 and Dicer (Boudreau et al., 2008). Traditional shRNAs (first-generation) only mimic pre-miRNA, often containing an inadequate flanking sequence for Exportin-5 or Dicer recognition, which can result in toxic levels of shRNAs (Davidson and Mccray, 2011, Manjunath et al., 2009). Diagrams of the constructs are presented in Chapter II, Section II.9.1.

Five new shRNAs were available for the pLKO.1 vector. All five shRNA HEF-1 target sequences were identified within the sequence of the full length HEF-1 transcripts, NCBI Reference Sequence NM_006403.3 (Transcript variant 1) and NM_001142393.1 (Transcript variant 3). One of the five HEF-1 targeting shRNA sequences [covering nucleotides (NT) 1703-1723 in Transcript variant 1, and NT 1897-1918 in Transcript variant 3] was in close proximity to an siRNA target sequence previously used in our laboratory in mesenchymal stem cells (covering NT 1770-1789 in Transcript variant 1, and NT 1965-1984 in Transcript variant 3) [the appendix provides more details on the screening process]. The vector encoding this shRNA (pLKO.1-U6.shRNA[HEF-1.puro) was purchased and tested for knockdown (Cat# RHS3979-9573754, oligo ID: TRCN0000004969, Open Biosystems).

As a pilot study, HEK293T cells were transfected with the pLKO.1 plasmid containing the shRNA encoding HEF-1 target sequence CCTGAATATCTTGGCCATCAA. After 24 hours, cells were harvested, washed with fresh growth media, and re-plated and incubated for an additional 24 and 48 hours (a total of 48 and 72 hour incubations respectively). Given that HEK293T cells are adhering cells, harvesting and re-plating these cells was thought to prompt the recruitment of HEF-1 at focal adhesion sites, consequently triggering the activation and expression of endogenous HEF-1 (as discussed in Section V.2.2). Western blot analysis revealed successful HEF-1 knockdown after 72 hours post-transfection of the 93kDa HEF-1 isoform (49.5%), whereas reduced protein expression of the active forms, p105 kDa (93.1%) and p115 kDa (19%), were visible by 24 hours **[Figure V.11].** The increase of p115[HEF-1] at 48 hours might reflect the activity of HEF-1 at focal

adhesion sites. Altough HEF-1 mRNA is being targeted by the RISC complex for degradation, it is simultaneously being recruited to focal adhesion sites, which requires the conversion of p105 to p115. Thus, further reducing isoforms 93[HEF-1] and 105[HEF-1]. With positive HEF-1 knockdown results using the pLKO.1 vector in this pilot study on HEK293T cells, LV-particles were made in house by three-way plasmid transfection of HEK293T cells as discussed in Section V.1. Non-concentrated LV-particles were then tested on model cell line KG-1 and KG-1A with an MOI of 5, based on previous studies on these cell lines (Szyda et al., 2006). Transduced cells were selected for their ability to grow in puromycin (5 µg/mL) based on a puromycin kill curve **[Figure V.12].** Non-transduced cells were also selected in puromycin over the 5 day selection process (as shown in **Figure V.12**) and served as a baseline. The survival of cells was estimated by microscopic observation (described in Chapter II, Section II.10). Compared to the non-transduced cell population, 90% of transduced KG-1A cells survived puromycin selection. KG-1 cells were transduced less effectively, with 60% cell survival. Most excitingly, Western blots confirmed HEF-1 knockdown in both KG-1 and KG-1A cells **[Figure V.13].** Given the higher transduction efficiency obtained for KG-1A cells, transductions using LV-pLKO.1 particles were repeated in three more independent experiments. Western blot results presented in **Figure V.14** confirm successful stable long-term HEF-1 knockdown.

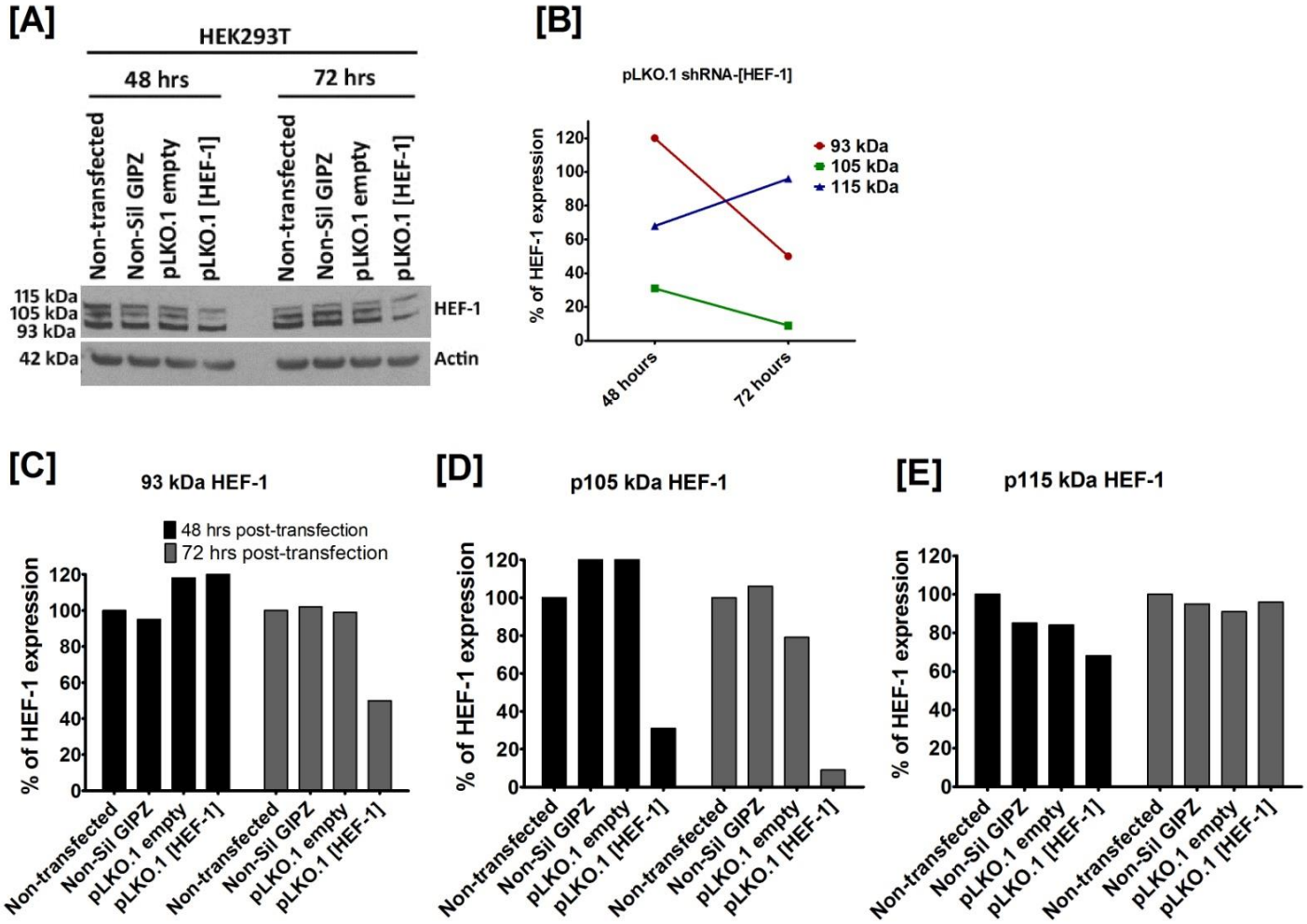

Figure V.11. HEF1 knockdown in HEK293T cells.

[A] Western blotting showing HEF-1 knockdown (n=1). Densitometry analysis was used to quantify Western blotting results [B] Effects of RNAi using pLKO.1shRNA-[HEF-1] vector on HEF-1 isoforms 93, p105, and p115 (normalised data). The % change (Δ%) was deduced from the densitometry data. At 48 hours 93 kDa, Δ =1.7%; 105 kDa, Δ = –93.1%; 115 kDa Δ = –19.0%. At 72 hours 93 kDa Δ = –49.5%; 105 kDa Δ = –88.6%; 115 kDa, Δ = 5.5%. Negative values represent the % of decreased protein expression. [C-E] Plotted densitometry results. Actin protein (loading control) was used to deduce the normalisation factor described in Chapter II, Section II.13.).

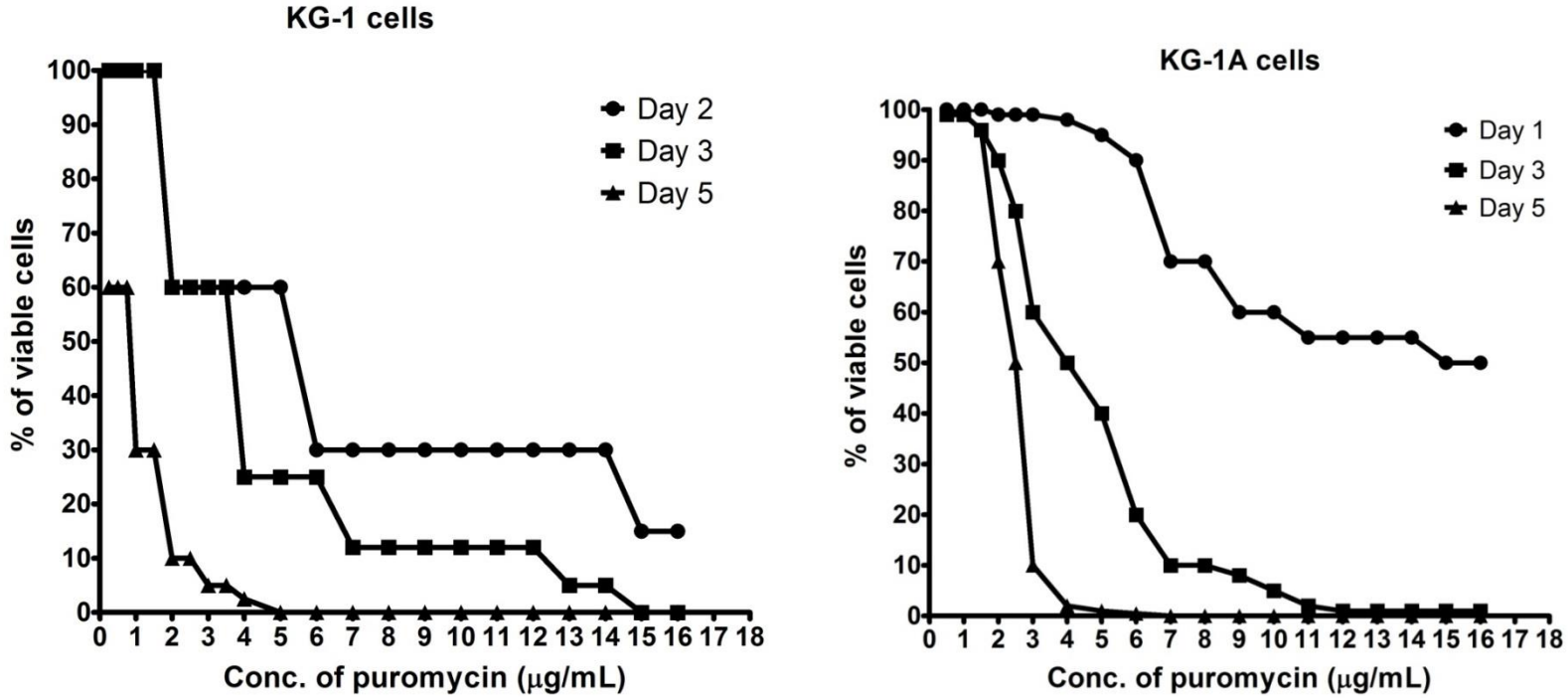

Figure V.12. Puromycin kill curve on KG-1 cells and KG-1A cells.

Cells ($1x10^5$/well) were cultured in a 24-well plate to determine the optimal concentration for selection of successfully transduced KG-1 and KG-1A cells. A range of 0.25-16 μg/mL of puromycin was tested with an optimal concentration determined at 5 μg/mL observed on day 5.

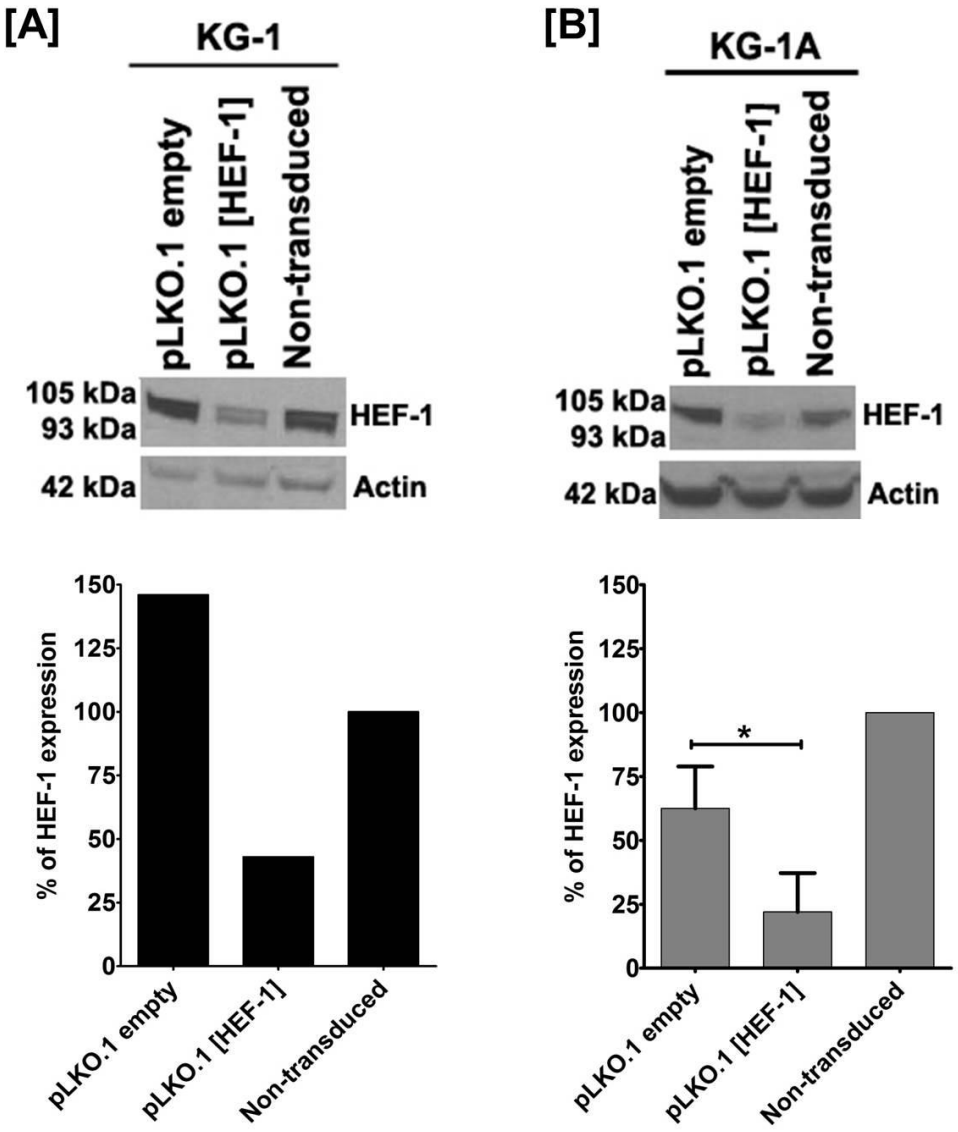

Figure V.13. HEF-1 knockdown in model cell lines using pLKO.1 vector.

KG-1 and KG-1A cells were successfully transduced with non-concentrated LV-pLKO.1 particles with an MOI of 5. Cells containing the pLKO.1 vector survived puromycin selection and were harvested for Western blot analysis after 5 days of puromycin selection. [A] HEF-1 silencing in KG-1 cells transduced with pLKO.1-shRNA[HEF-1] and corresponding densitometry analysis confirming a Δ% –70.5% knockdown (146%, pLKO.1-empty vs. 43%, pLKO.1[HEF-1]). Both the 93 kDa and p105 kDa protein forms were detected. (n=1) [B] HEF-1 silencing in KG-1A cells and densitometry analysis confirming a Δ% –64.8 knockdown (22±15.2% vs 65±16.4% in pLKO.1 empty). (n= 4 independent experiments). Actin protein (loading control) was used to deduce the normalisation factor described in Ch.II, Section II.13.

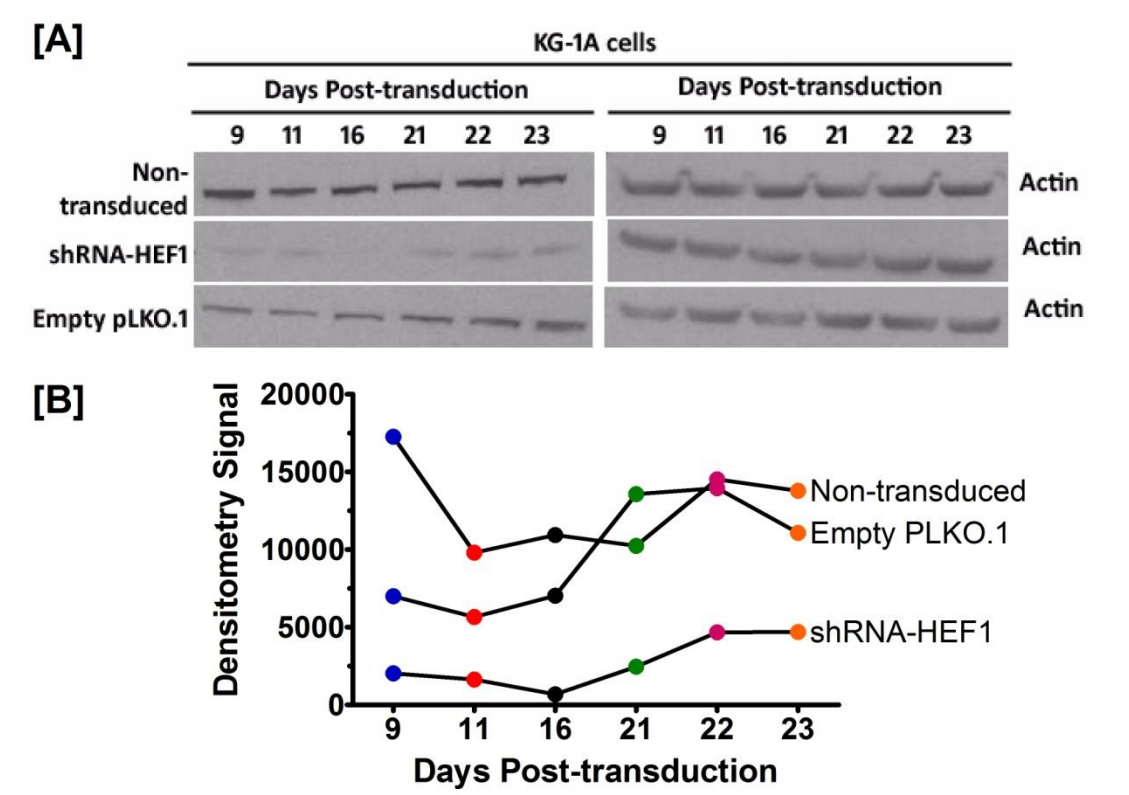

Figure V.14. Long-term HEF-1 knockdown in KG-1A cells.

[A] Western blots show decreased levels of p105[HEF-1] protein using LV-pLKO.1 particles on a 3rd batch of KG-1A cells. Total protein of puromycin selected cells was harvested at different timepoints. [B] Densitometry analysis confirmed decreased levels of HEF-1 protein compared to empty pLKO.1 control vector at each time point. Actin protein (loading control) was used to deduce the normalisation factor described in Ch.II, Section II.13.

As part of this pilot study on the pLKO.1 vector, the effects of stable long-term knockdown in KG-1A (KG-1A^{-HEF1}) cells was tested in an adhesion assay to BMEC-60 cell, described in Chapter III, Section III.2.3. KG-1A^{-HEF1} adhesion was tested to both IL-1β stimulated and non-stimulated BMEC-60 cells. Quite remarkably, consistently decreased adhesion to non-stimulated BMEC-60 cells was achieved (8.44±2.88% vs 14.23±4.74% in the non-transduced control; **Δ= –** 40.7%) **[Figure V.15A]**, which was statistically significant ($p<0.005$) **[Figure V.15B]**. Interestingly, adhesion of KG-1A^{-HEF1} to stimulated BMEC-60 varied between transduced batches, observing consistently decreased adhesion only in transduced KG-1A batch #3 **[Figure V.15C]** making compiled data not statistically significantly different (45.06±8.8% vs. 47.65±3.64% adhesion in non-transduced cells, $p>0.05$) **[Figure V.15D].** KG-1A^{-HEF1} transmigration across BMEC-60 cells was not tested as these cells did not migrate under normal conditions (data presented in Chapter III, Section III.2.4).

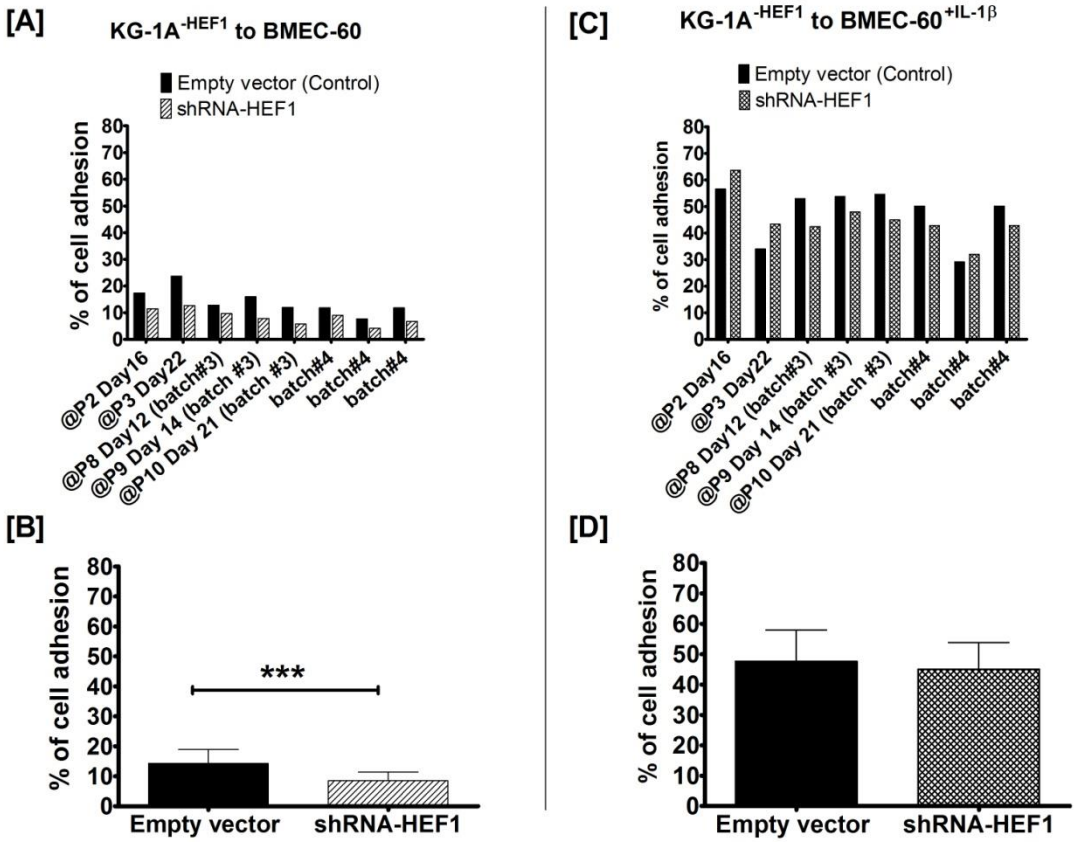

Figure V.15. HEF-1 knockdown affects adhesion of KG-1A cells to BMEC-60.

Adhesion of three different batches of transduced KG-1A cells with LV-pLKO.1-shRNA[HEF-1] particles to BMEC-60 cells was tested (n=8) using the adhesion assay previously described in Chapter III, Section III.2.3. [A] HEF-1 knockdown in all three batches of transduced KG-1A cells decreased adhesion to non-stimulated BMEC-60. [B] Compiled data of KG-1A-HEF1 adhesion to non-stimulated BMEC-60 result in a mean percentage adhesion of 8.44±2.88% vs 14.23±4.74% in the non-transduced control (*** =$p<0.005$ paired t-test); Δ= – 40.7% [C] Effects of HEF-1 knockdown were not consistent between batches of KG-1A-HEF1 cell adhesion to IL-1β stimulated BMEC-60. [D] Overall effects of HEF-1 knockdown on KG-1A adhesion to stimulated BMEC-60 were not statistically significant ($p>0.05$), 45.06±8.8% vs. 47.65±3.64% in non-transduced control; Δ= – 5.4%. ± =SDEV

V.2.4. Optimising conditions for transduction of UCB-CD133$^+$ cells

With positive functional effects obtained in KG-1A adhesion to BMEC-60 cells, transducing UCB-CD133$^+$ cells with LV-pLKO.1 particles was next attempted. In order to obtain high transduction efficiencies in UCB-CD133$^+$ cells, three assay conditions that are often used in transduction protocols for difficult to transduce cells were tested: 1) transduction on recombinant fibronectin fragment CH-296 (RetroNectin®, Takara) coated plates 2) spinoculation and 3) high titre viral supernatant (Hanenberg et al., 1996, Laje et al., 2010, Moritz et al., 1996).

Viral particles bind to the heparin binding domain II of fibronectin fragment CH-296, whilst adhesion molecule VLA-4 and/or VLA-5 on target cells interact with the CS1 and/or C-domain of the CH-296 fragment to facilitate the molecular interaction between virions and cells (Takara, www.clontech.com) **[Figure V.16].** Similarly, spinoculation has also been widely used to transduce non-dividing cells. Pioneering studies suggested ultracentrifugal inoculation enhanced viral transductions by increasing viral concentration; the gravity force required for viral sedimentation is ~50,000 x g (Guo et al., 2011). Interestingly, Guo et al. also observed that centrifugation at 300 x g triggered changes in actin and cofilin activity, facilitating viral DNA integration in resting T cells (Guo et al., 2011). Thus, actin remodelling might be an important step for viral entry into the cytoplasm of non-dividing cells (Valencia and Hutt-Fletcher, 2012). Finally, as discussed earlier in this chapter, viral titres increased from 10^5 - 10^7

(non-concentrated stocks) to ~10^9 TU/mL (high titre) permits transducing a larger population of cells per assay with MOIs >20.

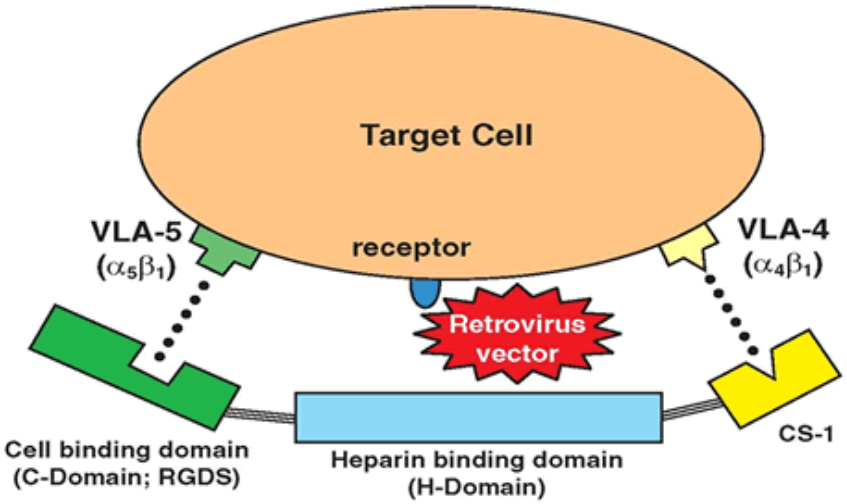

Figure V.16. Fibronectin fragment CH-296 facilitates viral gene transfer.

RetroNectin (CH-296) is a ~63 kDa protein that contains a central bindin domain (C-Domain), a high affinity heparin-binding domain II and CS1 site within the alternatively spliced IIICS region of human fibronectin. RetroNectin improves the transduction efficacy of lentiviral particles by binding to both virions and target cells, bringing virus and cell into contact. Picture credit: Reprinted from CloneTech Takara Bio Company© found at http://www.clontech.com/takara/GB/Products/Molecular_Biology/Gene_Transfer_and_Expression/RetroNectin_Reagent_and_Precoated_Dishes?sitex=10040:22372:US Copyright permission 2014 kindly given by Clonetech.

The effects of RetroNectin® and spinoculation were first examined using non-concentrated viral particles (method described in Chapter II, Section II.11.2). UCB-$CD133^+$ cells derived from at least three different donors were pooled and pre-stimulated overnight in StemSpan and cytokine cocktail SCF, FLT-3L, TPO and IL-6, [as described in Chapter II, Section II.5]. Because the pLKO.1 vector used did not encode a reporter gene to easily evaluate and compare transduction efficacies, UBC-$CD133^+$ cells were first transduced with LV-particles containing LV-pHR'SINcPPT-SEW with an *enhanced*-GFP reporter gene [expression cassette SFFV.eGFP.WPRE (SEW)]. Two MOIs (titre at $1x10^6$ TU/mL), 10 and 20, were tested in the presence and absence of

RetroNectin®. $CD34^+$ cells are often transduced at MOIs between 10 and 3000 (Haas et al., 2000). Others have reported successful transduction of $CD34^+$ using MOIs <1 (Zielske and Gerson, 2002). In light of our successful transductions in KG-1 and KG-1A cells with an MOI of 5, a 2 and 4 fold higher MOI were tested in this experiment. Examining cells by confocal microscopy after treatment showed that RetroNectin® and spinoculation caused UCB-$CD133^+$ cells to evenly distribute across the well [**Figure V.17A**]. Cells were harvested 48 hours post-transduction, to measure eGFP intensity by flow cytometry. Results show that spinoculating cells on RetroNectin® enhanced transduction efficacies. A 1.2-fold increase was observed with an MOI of 10, 55.6% using RetroNectin® vs 46.1% without RetroNectin® (Δ = 20%), and 1.18-fold increase with an MOI 20, 57.3% using RetroNectin® vs 48.4% without (Δ = 18%) **[Figure V.17C].** On the basis of these results, UCB-$CD133^+$ cells were spinoculated on RetroNectin® pre-coated plates in all subsequent transductions.

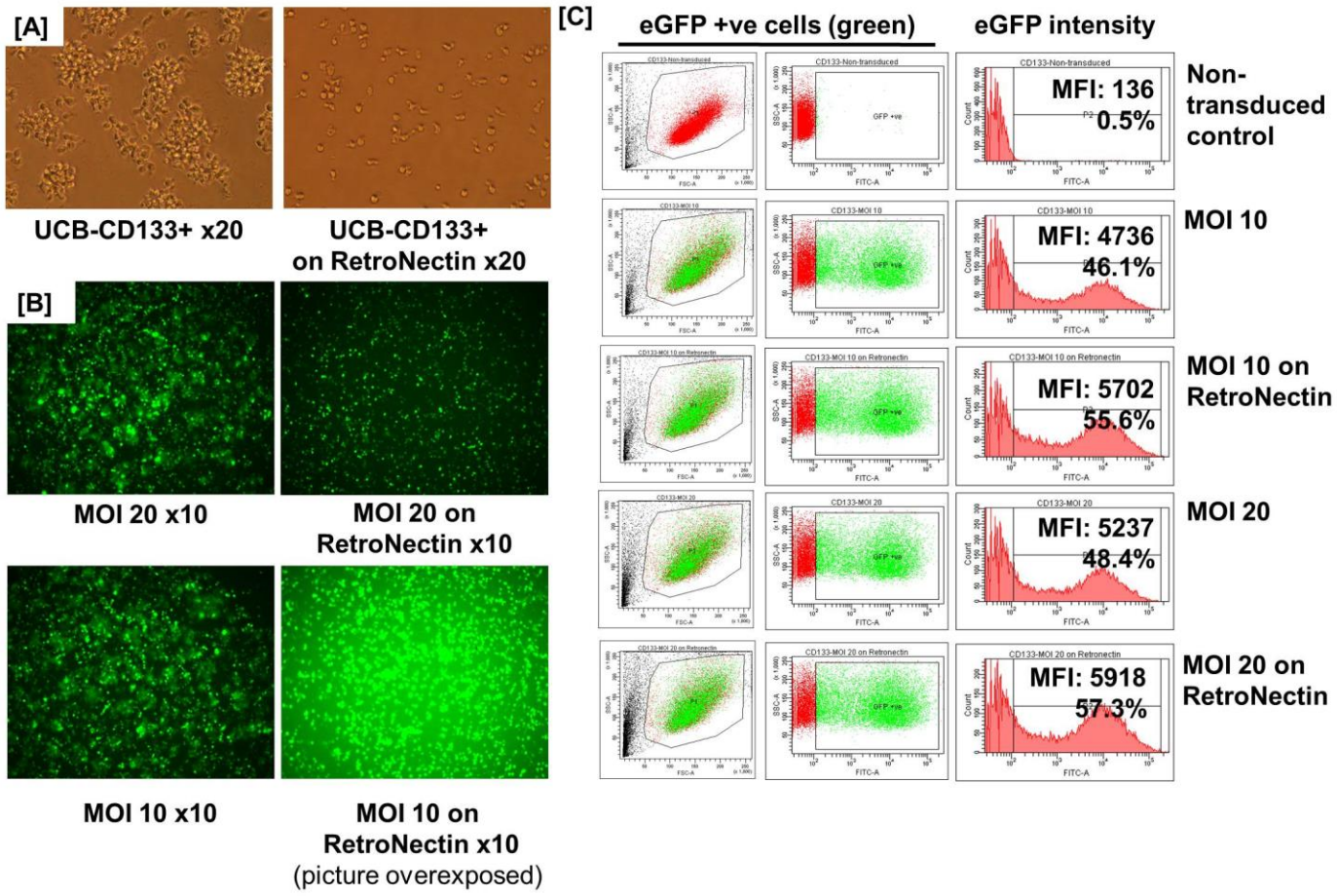

Figure V.17. Optimising transduction efficacy of UCB-CD133^{+} cells.

[A] UCB-CD133+ cells were seeded onto RetroNectin® coated plates and centrifuged at 600x g for 90 minutes at 32^{o}C. The presence of RetroNectin® caused cells to distribute evenly across the well. UCB-CD133^{+} cells were spinoculated with non-concentrated LV-particles encoding expression cassette SFFV.eGFP.WPRE. [B] eGFP expression was observed under the microscope with both MOIs (10 and 20), 48hrs post-transduction. [C] Cells were harvested for flow cytometry analysis to quantify transduction efficacy. MFIs and % of eGFP+ve cells revelead that RetroNectin® enhanced transduction efficacy; MOI of 10 Δ = 20% and MOI 20 Δ=18%.

V.2.5. Concentrating LV-pLKO.1 particles

In the previous section, spinoculating UCB-CD133$^+$ cells on RetroNectin® coated wells provided conditions that enhanced transduction efficiency. However, the % of transduced cells assessed by flow cytometry was still <60%. Given that these transductions were performed with non-concentrated LV-particles, high titre LV-pLKO.1 particles containing the desired shRNA sequence [CCTGAATATCTTGGCCATCAA] were purchased from Sigma Aldrich in an attempt to further increase the % of transduced UCB-CD133$^+$ cells. High titre LV-pLKO.1 particles from Sigma Aldrich were tested on UCB-CD133$^+$ cells using an MOI of 50 (×10 the MOI used on KG-1A cells). Forty-eight and 96 hours post-transduction, HEF-1 knockdown was examined by Western blot. Disappointingly, Western blot results revealed unsuccessful knockdown **[Figure V.18]**. Because the LV-pLKO.1 particles did not encode a reporter gene to identify (e.g. by flow cytometry) the % of transduced cells, transduced UCB-CD133$^+$ cells were instead selected with puromycin (5μg/mL) to evaluate transduction efficacy. Most (98%, based on trypan blue counts) cells died after 5 days in puromycin selection, indicative of poor transduction efficacy. An alternative method would be to determine transduction efficiency with q-PCR.

Having successfully transduced KG-1A cells with non-concentrated LV-pLKO.1 particles, the high titre LV-pLKO.1 particles from Sigma Adrich were tested on KG-1A and HEK293T cells with an MOI of 5 and 10. Transduction efficacy was assessed by puromycin selection. Compared to control cultures,

cells selected in puromycin did not survive treatment **[Figure V.19]**, indeed suggesting a problem with the high titre viral stocks.

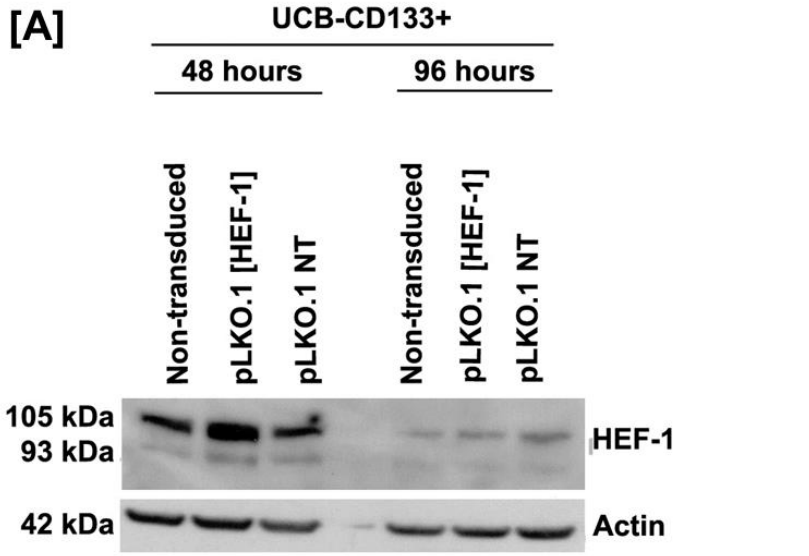

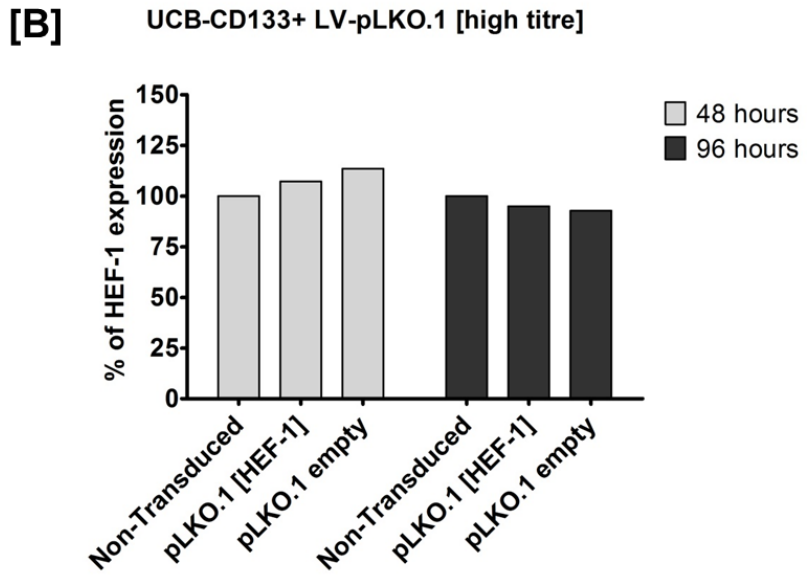

Figure V.18. Unsuccessful HEF-1 knockdown using high titre LV-particles from SIGMA.

UCB-CD133^{+} cells were transduced at MOI of 50 based on a viral titre of 1x10^{9} TU/mL. Cells were transduced by centrifugal inoculation (spinoculation) on RetroNectin® coated wells. [A] HEF-1 knockdown was examined by Western blot 48 and 96 hours post-transduction. HEF-1 knockdown was not apparent for either timepoint. [B] Densitometry analysis confirmed negative knockdown results of Western blot. N= 1 independent experiment.

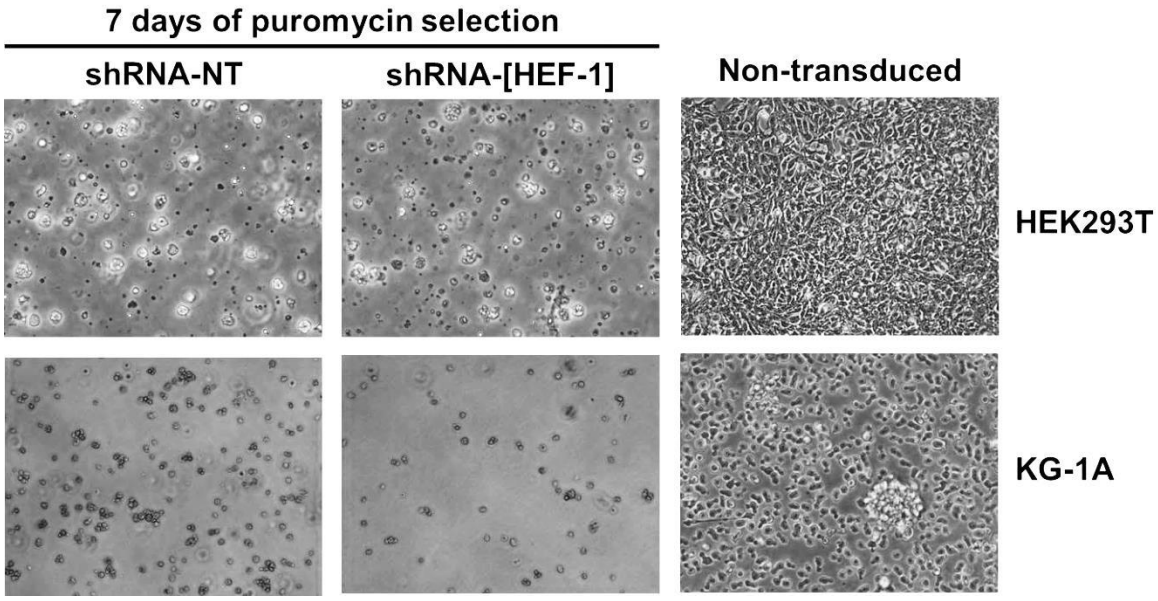

Figure V.19. Evaluating high titre LV-pLKO.1 particles from Sigma Aldrich.

HEK293T and KG-1A cells transduced with Sigma Aldrich LLC. Co. high titre viral particles were cultured in the presence of puromycin to select for transduced cells. After 7 days, no viable cells were observed. Microscope observations were supported with trypan blue staining (not shown).

With a final attempt to transduce UCB-CD133^{+} cells with high titre lentiviral stocks, pLKO.1 viral supernatants were concentrated in house using Millipore ultracentrifugation devices, Amicon© Ultra-4. Viral supernatant containing expression cassette SFFV.eGFP.WPRE was also concentrated, with a starting titre of 1x10^{6} TU/mL. Each Amicon© Ultra-4 centrifugal filter unit concentrated 4 mL of viral supernatant to a final volume of 40 µL, producing ×100 viral stocks. A total volume of 20 mL was concentrated for each vector construct, generating 200 µL of total concentrated viral stock per construct. Concentrated stocks containing the SFFV.eGFP.WPRE expression cassette were tested first, as this vector had worked in transductions presented in [Section V.2.4]. UCB-CD133^{+} cells were transduced with an MOI 100 and 200 [method described in Chapter II, Section II.11.5] and compared to transductions with non-concentrated viral

supernatant using an MOI of 10. Transduction efficiencies based on the eGFP intensity were compared 72 hours post-transduction by flow cytometry. Results show that transduction efficacy was significantly increased using concentrated stocks. With an MOI of 100, there was a 3.2 fold increase in both the percentage of transduced cells (58.7% vs 18.1% with an MOI of 10; Δ = 224%) and the intensity of eGFP (MFI of 26,962 vs. 8,332 in MOI 10). Most interestingly, although transduction with an MOI of 200 also resulted in an increased number of transduced cells (35.5% vs 18.1% = 1.9 fold; Δ = 96%) and MFI (17,277 vs 8,332), this was lower than the improvement observed using an MOI of 100 **[Figure V.20]**. This experiment will need to be repeated to confirm that the working concentrated LV-pHR'SINcPPT-SEW supernatant generated with Amicon Ultra-4 centrifugal filters is a reproducible method, and most importantly, tested on LV-particles containing the pLKO.1-shRNA[HEF-1] vector. Unfortunately, due to time constraints, these experiments could not be conducted.

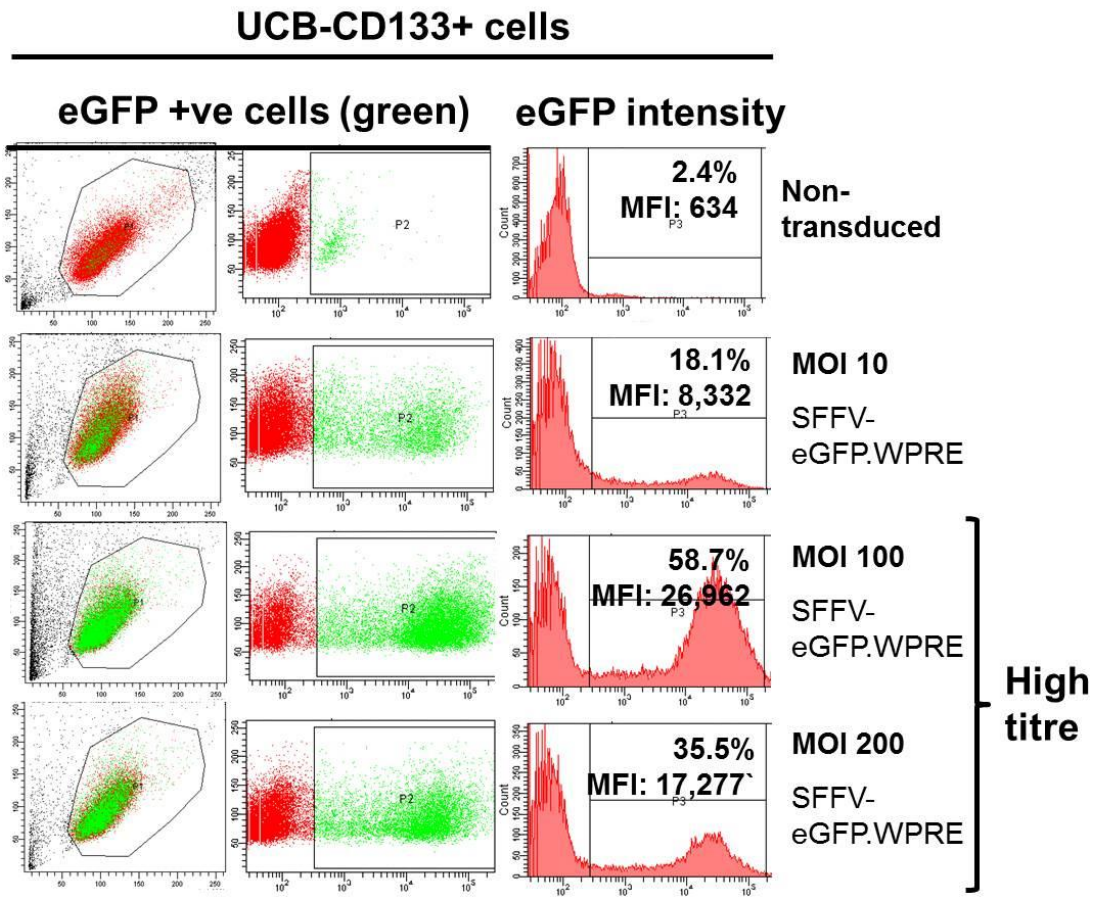

Figure V.20. Using high titre LV-pHR'SINcPPT-SEW particles improves transduction efficacy in UCB-CD133^{+} cells.

An MOI of 10 was tested with the non-concentrated virus and MOIs of 100 and 200 with the high titre virus obtained using Amicon® filters. Flow cytometry analysis showed that enhanced-GFP (eGFP) expression (green scatter plots) and the % of transduced cells were significantly improved with the concentrated viral stocks, particularly with an MOI of 100 (72 hours post-transduction; MOI of 100 = 58.7% vs 18.1% with an MOI of 10, Δ = 224%; MOI of 200 = 35.5% vs 18.1% = 1.9 fold; Δ = 96%). N= 1 independent experiment.

V.3. Discussion

The aim in this last results chapter was to deduce a potential correlation between the hypoxia induced HEF-1 up-regulation in UCB-CD133^{+} cells and their enhanced transmigration towards SDF-1α across BMEC-60 cells, as presented in Chapter IV. To achieve this, pilot studies were performed to identify a suitable lentiviral silencing vector. Successful HEF-1 knockdown was achieved in haemopoietic cell lines KG-1 and KG-1A using the lentiviral pLKO.1-shRNA[HEF-1] vector (LV-pLKO.1), with reproducible results confirmed in KG-1A cells. To knockdown HEF-1 in UCB-CD133^{+} cells with the LV-pLKO.1 vector, high titre LV-pLKO.1 particles were ordered from Sigma Aldrich. However, these particles proved to be faulty, and concentrated stocks were instead generated in house using Amicon Ultra-4 centrifugal filters. With no reporter gene in the pLKO.1 vector, another vector (LV-pHR'SINcPPT-SEW) was tested first to define optimal transduction conditions for UCB-CD133^{+} cells. Transduction efficiencies were increased up to 3.2 fold with these concentrated LV-pHR'SINcPPT-SEW stocks. Further work will require confirming these results, and testing this concentration method on the LV- pLKO.1 particles, as well as detecting HEF-1 knockdown in UCB-CD133^{+} cells.

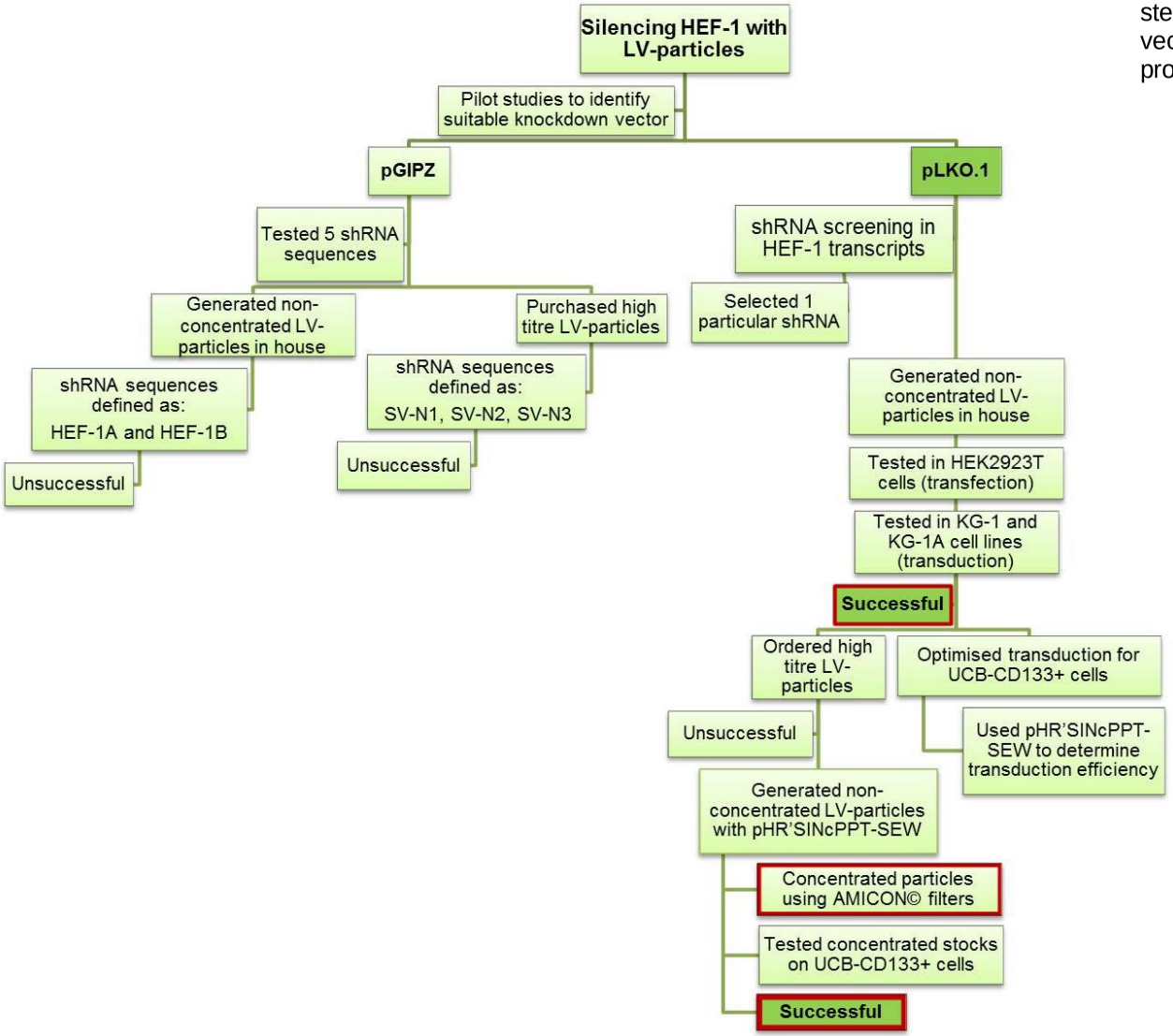

Figure V.21. Flow chart illustrating steps taken to identify a suitable LV-vector and develop a transduction protocol for UCB-CD133^{+} cells.

Lentiviral vectors are clearly a potent class of viral vectors once a suitable gene silencing vector and transduction protocol have been identified. Obtaining desirable titres compromise *in vitro* and small animal *in vivo* studies, and is not surprisingly a major challenge for clinical application (Segura et al., 2013). The concentration of viral particles (TU/mL) does affect the potency of viral stocks, hence the production of high titre stocks to enhance infection outcome. However, vector quantity alone is not sufficient; quality and concentration of *active* particles is an equally crucial component of suitable LV-stocks. Different methods are used to determine the transducing activity (vector infectivity) of viral supernatants, often resulting in great variation between different laboratories (Follenzi and Naldini, 2002). The high titre values provided by Sigma Aldrich for instance, base TU/mL on immunosorbent determination of Gag capsid protein p24 concentrations. p24 is a major structural component of the HIV-1 core, consequently of all HIV-1 derived vectors. However, although p24 levels are indicative of LV-particle content in the viral stock, not all ELISA test differentiate between assembled and disassembled p24 protein, and more importantly, vector infectivity. A p24 assay can provide a closer estimation of vector stock quality in conjunction with an end-point titration [(TU/mL)/(ng p24/mL)=TU/ng24]. End-point titration alone is confounded by Brownian motion (the random moving of particles suspended in solution) (Chuck et al., 1996, De Palma and Naldini, 2002). To validate the transduction efficiency of the high titre viral stocks purchased from Sigma Aldrich, given the absence of a reporter gene in the pLKO.1 construct, other quantitation methods such as qPCR and Southern blot would reveal pLKO.1 vector integration. In fact, both of these two methods are desirable quality assessments that should be carried out to continue this work. In light of our transduction experiments on UCB-CD133^{+} cells using LV-pHR'SINcPPT-SEW, it might be desirable to incorporate expression cassette SFFV.eGFP.WPRE, into the

pLKO.1-shRNA[HEF-1] construct to design a bicistronic expression cassette, or vice versa **[Figure V.22]**. This would enable detecting transduced UCB-CD133^{+} cells in our functional studies.

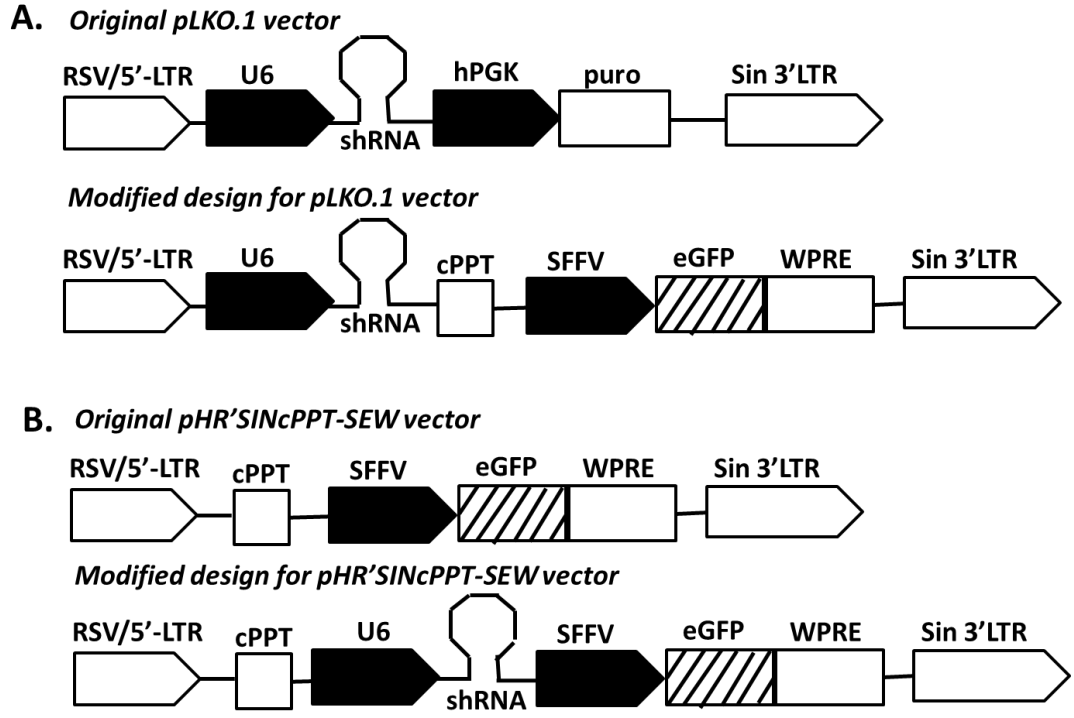

Figure V.22.Schematic representation of potential LV-transfer vector designs for HEF-1 knockdown studies.

[A] To be able to detect transduced UCB-CD133+ cells using the pLKO.1-shRNA[HEF-1]vector amongst non-transduced cells, we propose replacing expression cassette hPGK.puro with SFFV.eGFP.WPRE encoded in LV-vector pHR'SINcPPT-SEW. In addition, incorporating cPPT should further enhance transduction efficiencies. [B] Alternatively, expression cassette U6.shRNA of the pLKO.1 vector could be sub-cloned into transfer vector pHR'SINcPPT-SEW, given our successful transduction results on UCB-CD133^{+} cells using this vector—using this LV-vector might be more appropriate.

Concentrating in house generated LV- vector pHR'SINcPPT-SEW stocks using Amicon® centrifugal filter devices offered an alternative approach to purchasing, testing and troubleshooting additional high titre LV-stocks. Concentrated stocks did result in enhanced transduction efficiencies compared to transductions using non-concentrated stocks. Interestingly, increasing the MOI from 100 to 200 resulted in a lower efficiency, suggesting that cell density is also a critical factor. UCB-CD133^{+} cells were transduced with the same LV- vector pHR'SINcPPT-SEW stock

concentration, yet with different total cell counts to test different MOIs. Concentration of viral particles and target cells appear to be critical parameters for successful and efficient transduction, rather than basing transductions on an MOI value. Increasing the MOI when the vector concentration is held constant requires to either increasing the volume of viral supernatant in order to increase the number of virions per target cell, or decrease the total number of target cells, consequently lowering cell density (Haas et al., 2000). Palma and Naldini regard the MOI an “arbitrary definition” (De Palma and Naldini, 2002). Based on our preliminary results using the in house concentrated pHR’SINcPPT-SEW LV-particles, a series of UCB-CD133^{+} cell densities whilst keeping the LV-particles concentration constant and vice versa would be worth testing, to determine the optimal transduction conditions irrespective of MOI. Furthermore, an additional condition that might be worth testing to enhance transduction efficiency is the presence of cationic liposomes (Konopka et al., 1991), such as lipofectamine. The combination of “physical means” to enhance the contact between LV-particles and UCB-CD133^{+} cells may have synergistic effects (Liu et al., 2000a).

Only one out of six shRNA sequences tested resulted in successful HEF-1 knockdown. These are not uncommon results as high-throughput screening methods used by industry do not validate gene silencing efficacy of individual hairpins. Furthermore, algorithms designed to predict potent siRNAs cannot ensure to be effective for shRNA selection, as transcription and shRNA or pre-miRNA processing will affect the final configuration of the generated RNA duplexes. Advances in expanding and validating lentiviral libraries are being continuously developed to optimise hit selection of vector expressed shRNAs and minimise non-specific effects (Bassik et al., 2009, Fellmann et al., 2011, Pan et al., 2012). In the meantime, simply

testing a number of clones is the fastest and simplest approach. It would, however, be desirable to identify a second shRNA vector also directed at silencing HEF-1, as a positive control, and/or rescuing the loss-of-function phenotype by expressing a modified version of the target gene that has silent mutations in the shRNA-target region. Nonetheless, functional changes due to HEF-1 knockdown were observed with the single shRNA tested in this project.

HEF-1 is a multifunctional scaffolding protein studied predominantly in cancer cells, but also in B- and T-cells of the immune system (reviewed earlier in this chapter, as well as in Chapter I, Section I.7). In these systems, HEF-1 acts a migration 'enhancer', precipitating the invasion of metastatic cells and facilitating chemokine induced trafficking of lymphocytes. The significantly increased HEF-1 protein expression detected in UCB-CD133^{+} cells with increasing exposure to 1.5% O_2, suggests an apparent role of HEF-1 signalling in HSCs/HSPCs found in the hypoxic microenvironments of the BM. At the molecular level, it implies that stabilisation of HIF-1α (data shown in Chapter IV, Section IV.2.1) regulates HEF-1 expression via the HRE of the HEF-1 promoter (Kim et al., 2010a). Thus, HEF-1 certainly emerges as a prime signalling molecule to investigate in HSCs/HSPCs.

To confirm this hypothesis, future studies could inhibit HIF activity during hypoxia pre-conditioning or negatively target the HRE element of the HEF-1 promoter. In the study by Rehn et al., the HRE for VEGF was mutated in mouse model VEGF$^{\delta/\delta}$, which prevented HIF binding. This not only reduced hypoxia regulated VEGF expression on highly purified HSC/HSPCs, but also impaired their repopulation capacity. The study thus confirmed that either HSCs/HSCPs reside in hypoxic microenvironments in the BM or that HIF-1α is stabilised in these cells, and that

VEGF is hypoxia or at least HIF-1α regulated to sustain haemopoiesis (Rehn et al., 2011).

HIF certainly plays a major role in regulating genes vital to HSCs/HSPCs maintenance; sustaining cell quiescence and a primitive phenotype (Eliasson et al., 2010, Forristal et al., 2013, Miharada et al., 2012, Singh et al., 2013), regulating metabolic requirements (Miharada et al., 2012, Simsek et al., 2010, Takubo et al., 2013), as well as protecting HSCs/HSPCs from stress-induced cellular senescence *in vivo* (Rouault-Pierre et al., 2013, Takubo et al., 2010). As a multifunctional scaffolding adaptor protein, it would be of interest to elucidate the precise molecular mechanisms that regulate hypoxia induced HEF-1 expression in HSCs/HSPCs. We provide first time data suggesting a functional role in migration towards SDF-1α across BM endothelial cells **[Figure V.23].** Testing HEF-1 knockdown vectors on UCB-CD133^{+} cell migration towards chemokine SDF-1α in the quest to improving the homing and engraftment of UCB-HSCs/HSPCs would be thus of paramount interest.

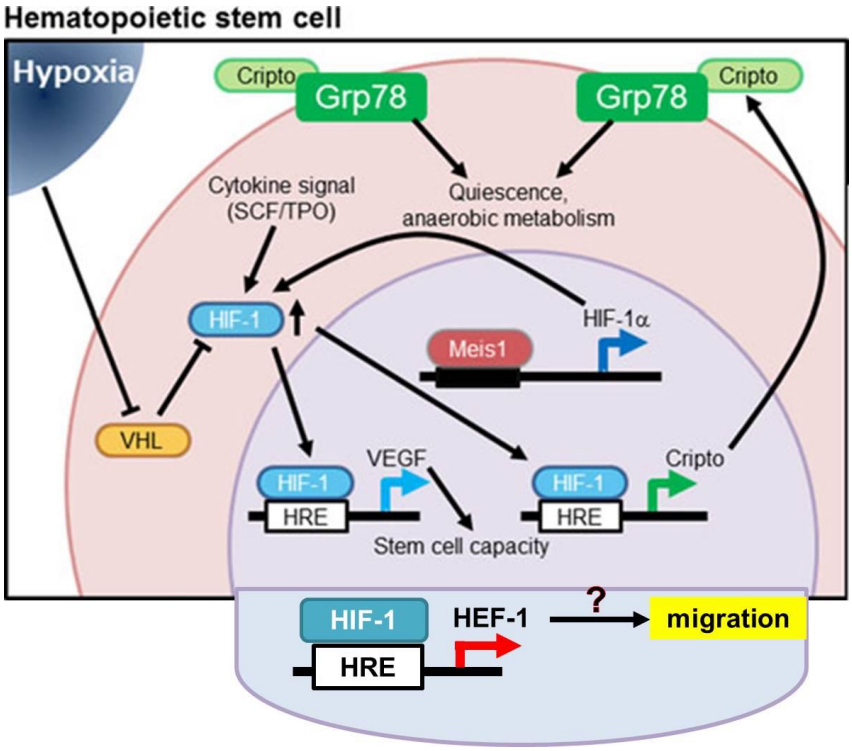

Figure V.23. Example of genes with an HRE region for HIF-1 regulation.

Adapted from: (Takubo and Suda, 2012) Reprinted from International Journal of Hematology, Takubo K., and Suda T., Roles of the hypoxia response system in hematopoietic and leukemic stem cells, 2012, pp. 478–483, Copyright 2014 with permission from Springer.

Successful HEF-1 knockdown was attained in haemopoietic cell lines KG-1 and KG-1A using the lentiviral pLKO.1-shRNA[HEF-1] vector (LV-pLKO.1), with reproducible results confirmed in KG-1A cells. Effects of long-term HEF-1 knockdown on KG-1A adhesion to BMEC-60 cells was also observed, suggesting a potential role of HEF-1 in $CD34^+$ expressing cell adhesion to endothelial cells in the BM. Unfortunately, due to time constraints, we were unable to test the effects of HEF-1 knockdown in UCB-$CD133^+$ cell adhesion and transmigration. However having identified a suitable knockdown expression cassette and transduction protocol provides a valuable platform for future HEF-1 studies in UCB-$CD133^+$ cells. Most importantly, UCB-$CD133^+$ were successfully transduced with LV-particles for the first time in our laboratory. Future work will involve fine tuning this protocol so that HEF-1 knockdown can be assessed for functional effects in human UCB-$CD133^+$ cells.

Chapter VI General Summary

As part of NHSBT's long term objective to enhance the homing and engraftment potential of UCB-derived HSCs/HSPC, this DPhil project had two main aims: 1) To investigate whether hypoxic conditions as found in the human BM, which up-regulate HIF-1α, affect the adhesion and transmigration potential of UCB-HSCs/HSPCs to BM niche cells and 2) given the effects found on migration, to examine whether hypoxia regulated scaffolding protein HEF-1, which plays a role in migration in other cell types, has a functional role in hypoxia induced UCB-HSC/HSPC transmigration. This thesis presents the findings obtained, and the tools and techniques used to achieve these aims. To conclude, this last chapter summarises the highlights of my work and briefly discusses how results obtained not only bring into light new research opportunities in BM biology but also propose a novel approach to tackle the difficulties in transplanting UCB-HSCs/HSPCs.

With the notion that there are hypoxic microenvironments in the BM and the increasing evidence that hypoxia regulated transcription factor HIF-1α plays a key role in mediating molecular signalling in HSC/HSPC, it was of interest to examine the effects of hypoxia pre-conditioning on UCB-derived $CD133^{+}$ cell adhesion to BM niche cells and their transmigration across BMEC-60 cells. These results are presented in Chapter IV. Changes in adhesion due to hypoxic incubations appeared at first to be minimal. However, targeting cells, that initially adhered poorly to niche cells, revealed significant functional changes of which the magnitude of change was better appreciated with the percentage gain (Δ%) calculated. The adhesion and transwell migration assay are perhaps not best at mimicking the 3D environment encountered *in vivo*, however, they do reflect conditions and tools that can be applied in the clinic, to prepare UCB-HSCs or HSCs/HSPCs derived from other sources for

HSCT therapy. To consolidate our findings for potential therapeutic use, it will be of interest to elucidate the phenotype of the more poorly adhering UCB-HSCs/HSPCs and carry out future homing studies particularly with this cell population. There is increasing evidence that co-infusing other progenitor cells such as more mature HSCs/HSPCs (Bautista et al., 2009, Sebrango et al., 2010) and niche supporting cells, such as MSCs, improve transplantation outcome (Hengxiang et al., 2013, Kim et al., 2013, Kita et al., 2011, Klein et al., 2013). In fact, some studies suggest that the main advantage of infusing two CB units is that one of the units contributes to haemopoiesis in the first three months, rather than sustaining long term haemopoiesis; it “completely disappears” (Stanevsky et al., 2010). However, this impression is being challenged as infusing two units has increased the incidence of GVHD in some series and is very costly (Kurtzberg, 2011). Thus, it will be equally important to investigate whether improving the adhesion and/or transmigration of these ‘weakly’ adhering HSCs/HSPCs would actually improve the long-term outcome of the transplant.

Understanding what molecular and extracellular conditions impact the physiology of HSC/HSPC is paramount to improving transplantation of UCB-HSCs/HSPCs. Results presented in Chapter V confirm that exposure to 1.5% $O_{2,}$ with up-regulated HEF-1 mRNA levels (Martin-Rendon et al., 2007), indeed increases HEF-1 protein levels. From the studies presented in Chapter IV that 24-48 hour hypoxia pre-conditioning of UCB-CD133^{+} cells enhanced their transmigration towards SDF-1α across stimulated BMEC-60 provided promising correlating observations. A ~2-fold increase in transmigration was coupled with a ~2- fold increase in HEF-1 protein expression. To investigate the role of HEF-1 in this UCB-CD133^{+} hypoxia induced transmigration, LV-gene silencing was optimised to silence HEF-1 protein

expression in KG-1 and KG-1A cells. Future work will require confirming successful HEF-1 knockdown in UCB-CD133^{+} cells and perhaps incorporate a reporter gene into the pLKO.1 vector to be able to track transduced UCB-HSCs/HSPCs in our migration assays or other functional *in vitro* and *in vivo* studies.

In a single preliminary co-localisation experiment **[Figure VI.1A]**, immunofluorescence staining of HEF-1 and CXCR4 indicated that HEF-1 was recruited to the same location after stimulating UCB-CD133^{+} cells with SDF-1α molecules presented on fibronectin coated wells. Fluorescence intensity of both proteins was strongest at the leading edge (lamellipodia) of the cells. Co-immunoprecipitation or co-localisation assays such as Fluorescence Resonance Energy Transfer (FRET) would ultimately confirm direct molecular interactions. However, these initial observations suggest that active HEF-1 may localises to sites of integrin-dependent attachment to extracellular matrix in response to the chemokine SDF-1α **[Figure VI.1B]**.

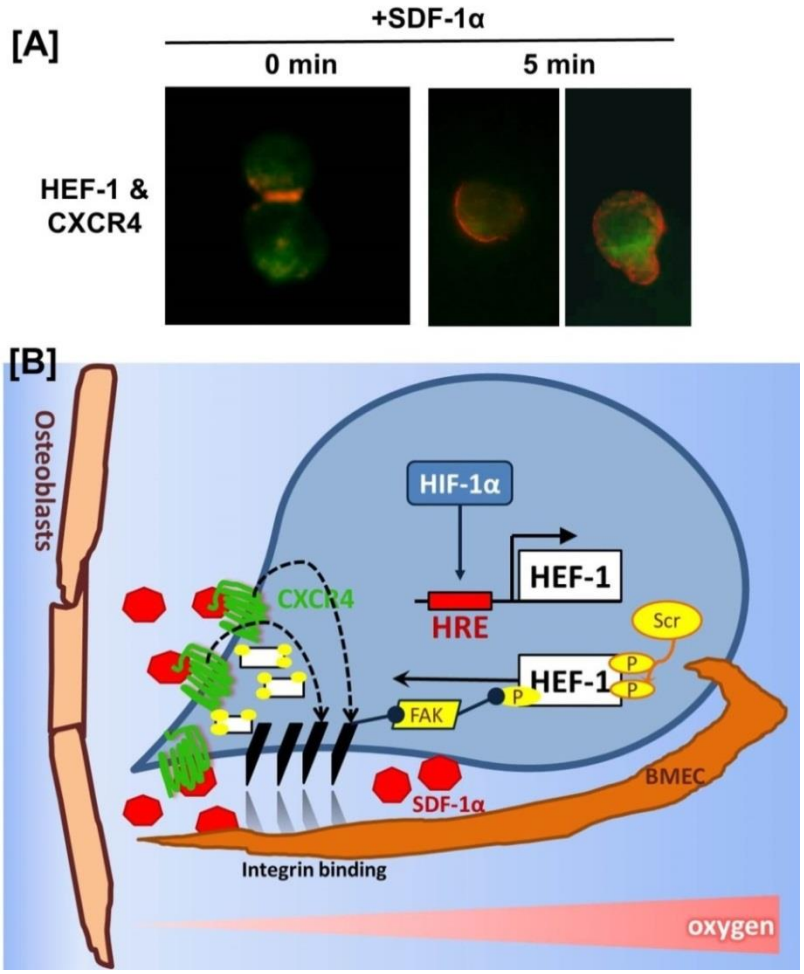

Figure VI.1. Effects of SDF-1 stimulation on CXCR4 and HEF-1 localisation.

UCB-CD133^{+} cells were seeded at different timepoints on fibronectin coated with chemokine SDF-1α. Paraformaldehyde (4%) was used to stop the reaction and cells were incubated with primary CXCR4 (Ab2074, BD) and HEF-1 ([2G9] ab18056, abcam) antibody, and then with fluorescently tagged secondary antibodies for immunofluorescence detection. [A] Localisation of CXCR4 (orange staining) is clearly seen at the junction of two cells at 0 minutes of SDF-1α stimulation, and concentrated with HEF-1 (green) at the leading edge of the cell after 5 minutes. [B] A schematic diagram illustrating how HIF-1α induced upregulation of HEF-1 might be involved in the SDF-1α/CXCR4 signalling axis: SDF-1α stimulation modulates LFA-1, VLA-4, and VLA-5 integrin-dependent adhesion to BMECs and extracellular matrix on immature human CD133^{+}CD34^{+} cells. The stabilisation of HIF-1α due to low oxygen tension or other stimuli results in the increased expression of HEF-1 protein. Perhaps, FAK becomes activated upon integrin activation of LFA-1, VLA-4, and/or VLA-5, which then, together with Scr phosphorylate and induces HEF-1 signalling. pHEF-1 is sequestered to the leading edge of a migrating cell, at focal adhesion sites, to interact with Crk to enhance activation of Rac and Rap1, which regulate cell attachment or drive cellular movement.

Although it remains unclear what microenvironmental factors or location in the BM governs the hypoxic status and stabilisation of HIF-1α in HSCs/HSPCs, there is clear evidence that both hypoxia and HIF-1α expression play important roles in HSC/HSPC maintenance (Forristal et al., 2013, Jing et al., 2011, Miharada et al.,

2011, Nombela-Arrieta et al., 2013, Rehn et al., 2011, Singh et al., 2013, Speth et al., 2014, Takubo et al., 2010). We postulate that HIF-1α regulated protein HEF-1 is also a key player in HSC/HSPC maintenance, being particularly upregulated in migrating cells. Other roles could include regulating the cell cycle of HSCs/HSPCs as HEF-1 has been linked with transforming growth factor-beta (TGF-β). TGF-β1, TGF-β2, TGF-β3, latent TGF-β1, Activin-A, and Nodal were found to inhibit cytokine-mediated lipid raft clustering in HSCs/HSPCs (Yamazaki et al., 2009), which is essential to trigger HSCs/HSCPs to re-enter the cell cycle. It is well established that that HSCs/HSPCs are in a quiescent (G_0) or slow cycling (G_0/G_1) state when they home to the BM (Giet et al., 2002, Larochelle et al., 2012, Yong et al., 2002). TGF-β was also found to maintain and increase the expression of CD34 membrane antigen, which is associated with a HSC/HSPC phenotype (Batard et al., 2000). In contrast, HEF-1 has been reported to positively regulate cell cycle progression, with HEF-1 depletion leading to mitotic timing defects (Dadke et al., 2006, Pugacheva and Golemis, 2005). Most interestingly, TGF-β was found to regulate the proteasomal degradation of HEF-1 through TGF-β downstream effector Smad3 (Liu et al., 2000b), but was also able to increase the expression of HEF-1 in a dose dependent manner (Zheng and Mckeown-Longo, 2002). Finally, like HEF-1, TGF-β is hypoxia regulated (Hung et al., 2013, Zhang et al., 2003a), thus a potential molecular relationship between the two molecules associated with the cell cycle of HSCs/HSPCs might exist.

This DPhil project aimed to provide a novel approach to enhance the homing and engraftment potential of UCB-$CD34^+CD133^+$ cells by examining the role of hypoxia and hypoxia up-regulated protein HEF-1 on their adhesion to BM niche cells and transmigration across BM endothelial cells. The low yield of HSCs/HSPCs obtained from UCB-units coupled with their longer engraftment time greatly

compromises UCB transplantation, particularly in adults, and hence, the pressing interest in developing a method to expand cell numbers *in vitro*. A recent study designed a stirred multiwell bioreactor for expanding UCB-$CD34^+$ cells under continuous and constant low oxygen concentrations (Luni et al., 2011). Our findings propose subjecting $CD34^+CD133^+$ cells to 1.5% O_2 or to small molecules that upregulate or stabilise HIF-1α prior to their infusion into patients, with the prospect of increasing the number of UCB-derived HSCs/HSPC reaching the BM. Such treatment offers clinical interventions without the need to genetically manipulate cells for HSCT therapy; an alternative approach more likely to obtain ethical approval and lower costs in HSCT therapy.

While finalising the writing of this thesis, a study was published that measured the oxygen levels in the BM of mice (mentioned in Chapter I, Section I.5) (Spencer et al., 2014). The researchers confirm that the BM is indeed hypoxic, recording intravascular oxygen levels of ~20.4 mmHg and ~13.3 mmHg in the extravascular space (mean oxygen levels of 13.3 mmHg, 1.8%). As postulated in mathematical models by Chow et al. (Chow et al., 2001a, Chow et al., 2001b), a “steep lateral gradient away from blood vessels” was observed (Spencer et al., 2014). However, quite remarkably, Spencer et al. found the oxygen gradient to be in the inverse direction as previously depicted. The oxygen tension decreased with increasing distance away from the endosteum, with smaller vessels (<15 μm in diameter) located closest to the endosteum (0-20 μm) showing higher oxygen levels than wider vessels located further away from the endosteum (>40 μm); 22.7 mmHg (3.0%) versus 19.5 mmHg (2.6%), respectively.

This study also confirmed that $nestin^+$ cells (discussed in Chapter I, Section I.4 and Chapter III, Section III.2.3) were mainly perivascular as previously observed

(Kunisaki et al., 2013), to which transplanted LSK-HSCs attached preferentially (Spencer et al., 2014). Oxygen levels were found higher in nestin^{+} vessels than in nestin^{-} vessels (22.8 mmHg vs 17.6 mmHg). Furthermore, the “vascular network map” examined by Spencer et al. showed that nestin^{+} vessels were upstream of and drained into sinusoidal vessels. Therefore, it is conceivable that HSC/HSPCs encounter changes in oxygen concentrations while they circulate through these different vessels with concomitant exposure to changes in SDF gradients. This would likely regulate intracellular signalling pathways and modulate HSCs/HSPCs migration and ultimately determin their lodgment in distinct BM niches. The *in vitro* enhanced transmigration of hypoxia pre-conditioned UCB-CD133^{+} cells across BMEC-60, demonstrated in this thesis, depicts in part these potential cellular dynamics. This new study thus provides corroborative evidence that investigating the role and effects of hypoxia on the homing and engraftment UCB-HSCs is of paramount interest to improving HSCT therapy.

APPENDIX

IDENTIFYING THE SHRNA SEQUENCE ENCODED IN THE PLKO.1 VECTOR IN HEF-1 TRANSCRIPTS

Amino acid sequences shown below were retrieved from Ensemble! genome browser encoding Transcript NEDD9-001 ENST00000379446..

Also reported as Transcript variant 1, mRNA NM_006403.3 in NCBI (pubmed) and Transcript variant 1, RefSeq Summary (NM_006403) in UCSC Browser.

TRANSCRIPT VARIANT 1 NM_006403.3:

The shRNA targeting sequence is found 68 NT based upstream of the siRNA target sequence previously used in SCRL (our lab) on mesenchymal stem cells (NT 1703-1723 vs 1770-1789 respectively)

Amino acid sequence in pLKO.1 vector: CCTGAATATCTTGGCCATCAA is highlighted in red in HEF-1 sequences shown below. siRNA sequence CAAAGACGGTGCCCGATGA is highlighted in green. Other highlighted regions are shown as found on Ensemble! genome browser (http://www.ensembl.org/index.html).

shRNA targets mRNA coding for the serine rich region of HEF-1 (amino acid region 512-519) (Briknarová et al., 2005). Briknaronva et al. showed for the first time the structure of a functional domain of the Cas-family protein, with the serine-rich region bearing a strong structural similarity to four-helix bundles found in other adhesion components like FAK.

```
                                                          R
  1 ACAACAGTGAGCTCAGAGACTTGAGGGAGGCGCTGCGACTGACAAGCGGCTCTGCCCGGG
    ............................................................
    ............................................................

      Y           R     Y   R                      **          M
 61 ACCTTCTCGCTTTCATCTAGCGCTGCACTCAATGGAGGGGCGGGCACCGCAGTGCTTAAT
    ............................................................
    ............................................................

                                  M                   W
121 GCTGTCTTAACTAGTGTAGGAAAACGGCTCAACCCACCGCTGCCGAAATGAAGTATAAGA
```

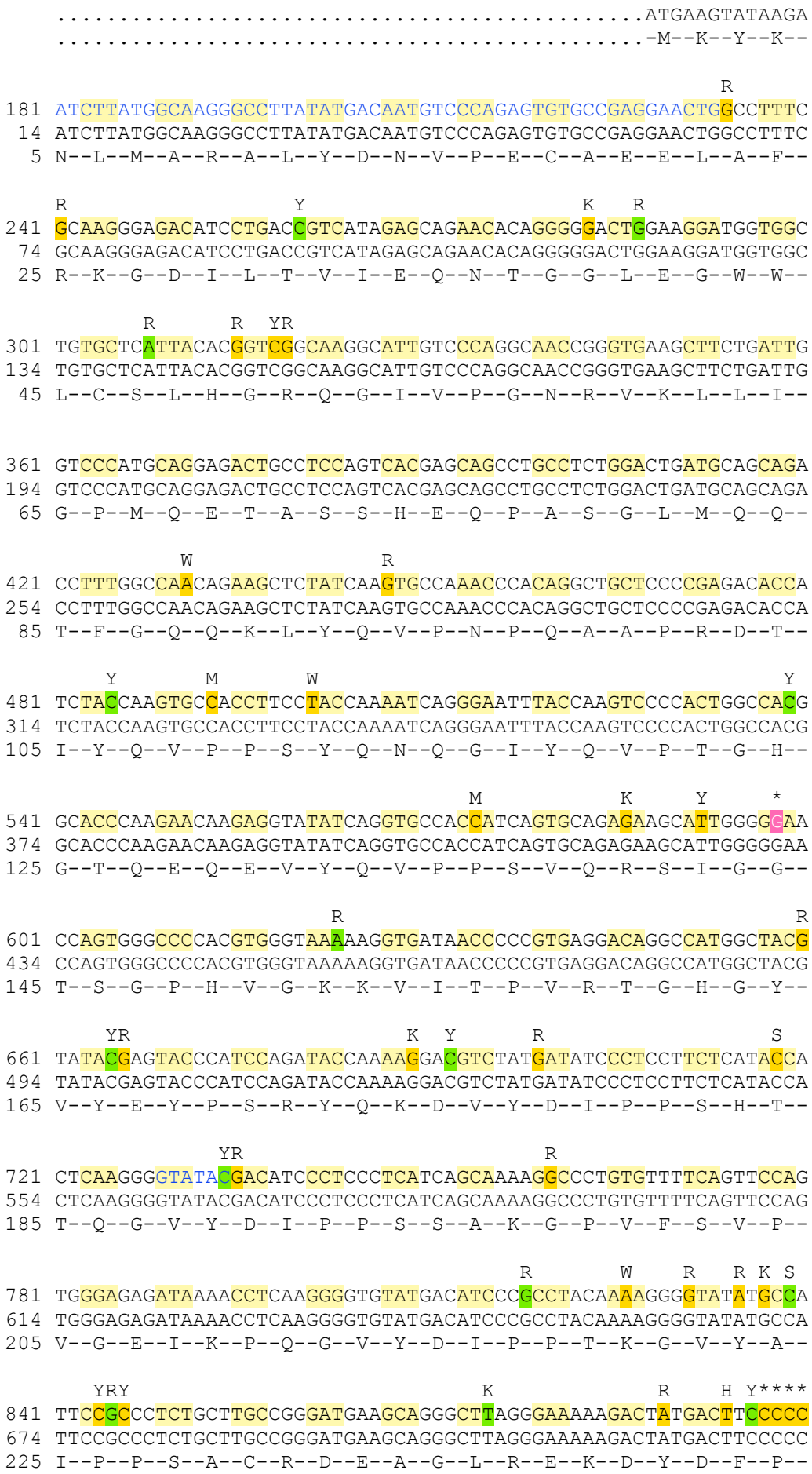
.....ATGAAGTATAAGA
.....-M--K--Y--K--
R
181 ATCTTATGGCAAGGGCCTTATATGACAATGTCCCAGAGTGTGCCGAGGAACTGGCCTTTC
14 ATCTTATGGCAAGGGCCTTATATGACAATGTCCCAGAGTGTGCCGAGGAACTGGCCTTTC
5 N--L--M--A--R--A--L--Y--D--N--V--P--E--C--A--E--E--L--A--F--
R Y K R
241 GCAAGGGAGACATCCTGACCGTCATAGAGCAGAACACAGGGGGACTGGAAGGATGGTGGC
74 GCAAGGGAGACATCCTGACCGTCATAGAGCAGAACACAGGGGGACTGGAAGGATGGTGGC
25 R--K--G--D--I--L--T--V--I--E--Q--N--T--G--G--L--E--G--W--W--
R R YR
301 TGTGCTCATTACACGGTCGGCAAGGCATTGTCCCAGGCAACCGGGTGAAGCTTCTGATTG
134 TGTGCTCATTACACGGTCGGCAAGGCATTGTCCCAGGCAACCGGGTGAAGCTTCTGATTG
45 L--C--S--L--H--G--R--Q--G--I--V--P--G--N--R--V--K--L--L--I--
361 GTCCCATGCAGGAGACTGCCTCCAGTCACGAGCAGCCTGCCTCTGGACTGATGCAGCAGA
194 GTCCCATGCAGGAGACTGCCTCCAGTCACGAGCAGCCTGCCTCTGGACTGATGCAGCAGA
65 G--P--M--Q--E--T--A--S--S--H--E--Q--P--A--S--G--L--M--Q--Q--
W R
421 CCTTTGGCCAACAGAAGCTCTATCAAGTGCCAAACCCACAGGCTGCTCCCCGAGACACCA
254 CCTTTGGCCAACAGAAGCTCTATCAAGTGCCAAACCCACAGGCTGCTCCCCGAGACACCA
85 T--F--G--Q--Q--K--L--Y--Q--V--P--N--P--Q--A--A--P--R--D--T--
Y M W Y
481 TCTACCAAGTGCCACCTTCCTACCAAAATCAGGGAATTTACCAAGTCCCCACTGGCCACG
314 TCTACCAAGTGCCACCTTCCTACCAAAATCAGGGAATTTACCAAGTCCCCACTGGCCACG
105 I--Y--Q--V--P--P--S--Y--Q--N--Q--G--I--Y--Q--V--P--T--G--H--
M K Y *
541 GCACCCAAGAACAAGAGGTATATCAGGTGCCACCATCAGTGCAGAGAAGCATTGGGGCAA
374 GCACCCAAGAACAAGAGGTATATCAGGTGCCACCATCAGTGCAGAGAAGCATTGGGGGAA
125 G--T--Q--E--Q--E--V--Y--Q--V--P--P--S--V--Q--R--S--I--G--G--
R R
601 CCAGTGGGCCCCACGTGGGTAAAAAGGTGATAACCCCCGTGAGGACAGGCCATGGCTACG
434 CCAGTGGGCCCCACGTGGGTAAAAAGGTGATAACCCCCGTGAGGACAGGCCATGGCTACG
145 T--S--G--P--H--V--G--K--K--V--I--T--P--V--R--T--G--H--G--Y--
YR K Y R S
661 TATACGAGTACCCATCCAGATACCAAAAGGACGTCTATGATATCCCTCCTTCTCATACCA
494 TATACGAGTACCCATCCAGATACCAAAAGGACGTCTATGATATCCCTCCTTCTCATACCA
165 V--Y--E--Y--P--S--R--Y--Q--K--D--V--Y--D--I--P--P--S--H--T--
YR R
721 CTCAAGGGGTATACGACATCCCTCCCTCATCAGCAAAAGGCCCTGTGTTTTCAGTTCCAG
554 CTCAAGGGGTATACGACATCCCTCCCTCATCAGCAAAAGGCCCTGTGTTTTCAGTTCCAG
185 T--Q--G--V--Y--D--I--P--P--S--S--A--K--G--P--V--F--S--V--P--
R W R R K S
781 TGGGAGAGATAAAACCTCAAGGGGTGTATGACATCCCGCCTACAAAAGGGGTATATGCCA
614 TGGGAGAGATAAAACCTCAAGGGGTGTATGACATCCCGCCTACAAAAGGGGTATATGCCA
205 V--G--E--I--K--P--Q--G--V--Y--D--I--P--P--T--K--G--V--Y--A--
YRY K R H Y****
841 TTCCGCCCTCTGCTTGCCGGGATGAAGCAGGGCTTAGGGAAAAAGACTATGACTTCCCCC
674 TTCCGCCCTCTGCTTGCCGGGATGAAGCAGGGCTTAGGGAAAAAGACTATGACTTCCCCC
225 I--P--P--S--A--C--R--D--E--A--G--L--R--E--K--D--Y--D--F--P--

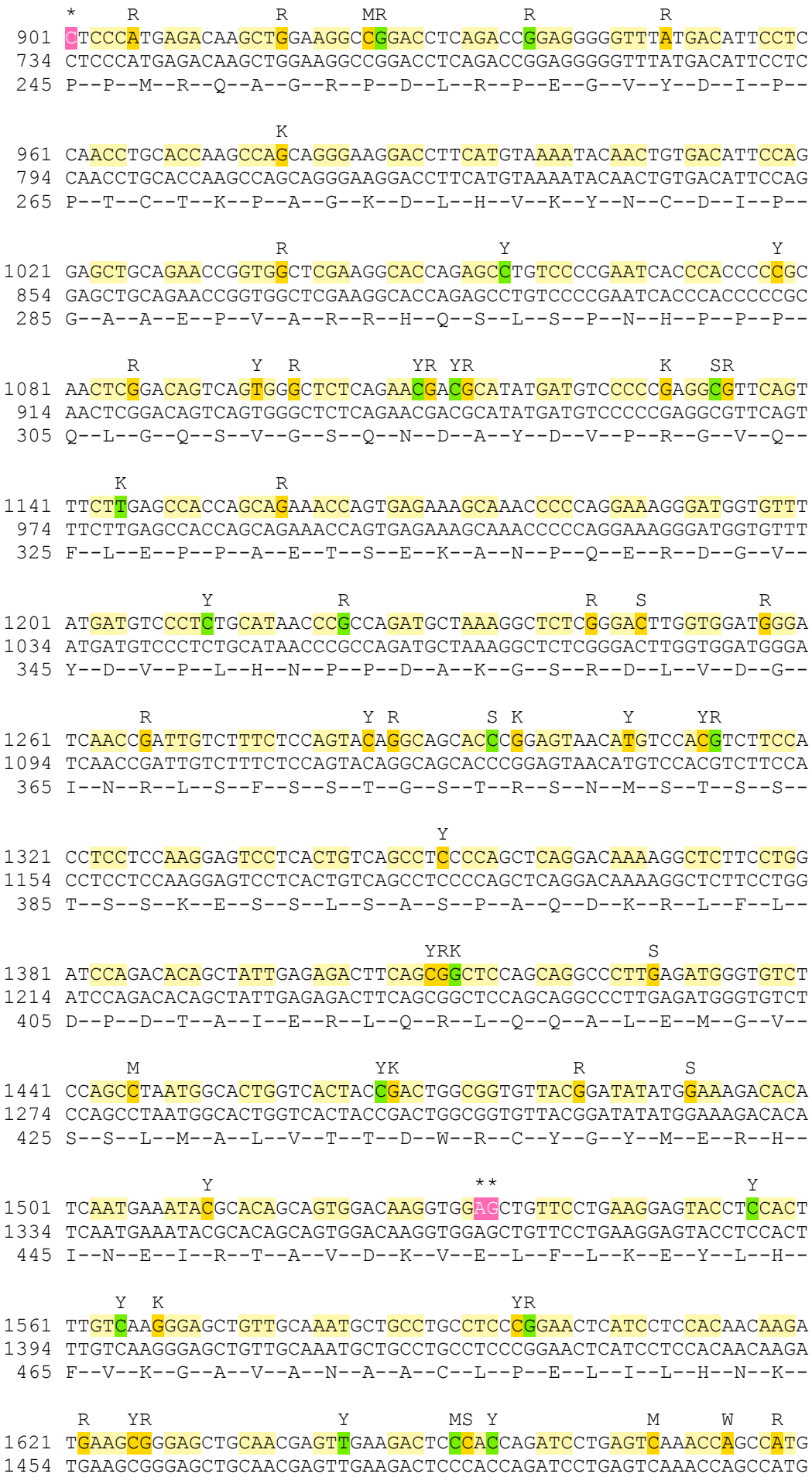
* R R MR R R
901 CTCCCATGAGACAAGCTGGAAGGCCGGACCTCAGACCGGAGGGGGTTTATGACATTCCTC
734 CTCCCATGAGACAAGCTGGAAGGCCGGACCTCAGACCGGAGGGGGTTTATGACATTCCTC
245 P--P--M--R--Q--A--G--R--P--D--L--R--P--E--G--V--Y--D--I--P--
K
961 CAACCTGCACCAAGCCAGCAGGGAAGGACCTTCATGTAAAATACAACTGTGACATTCCAG
794 CAACCTGCACCAAGCCAGCAGGGAAGGACCTTCATGTAAAATACAACTGTGACATTCCAG
265 P--T--C--T--K--P--A--G--K--D--L--H--V--K--Y--N--C--D--I--P--
R Y Y
1021 GAGCTGCAGAACCGGTGGCTCGAAGGCACCAGAGCCTGTCCCCGAATCACCCACCCCCGC
854 GAGCTGCAGAACCGGTGGCTCGAAGGCACCAGAGCCTGTCCCCGAATCACCCACCCCCGC
285 G--A--A--E--P--V--A--R--R--H--Q--S--L--S--P--N--H--P--P--P--
R Y R YR YR K SR
1081 AACTCGGACAGTCAGTGGGCTCTCAGAACGACGCATATGATGTCCCCCGAGGCGTTCAGT
914 AACTCGGACAGTCAGTGGGCTCTCAGAACGACGCATATGATGTCCCCCGAGGCGTTCAGT
305 Q--L--G--Q--S--V--G--S--Q--N--D--A--Y--D--V--P--R--G--V--Q--
K R
1141 TTCTTGAGCCACCAGCAGAAACCAGTGAGAAAGCAAACCCCCAGGAAAGGGATGGTGTTT
974 TTCTTGAGCCACCAGCAGAAACCAGTGAGAAAGCAAACCCCCAGGAAAGGGATGGTGTTT
325 F--L--E--P--P--A--E--T--S--E--K--A--N--P--Q--E--R--D--G--V--
Y R R S R
1201 ATGATGTCCCTCTGCATAACCCGCCAGATGCTAAAGGCTCTCGGGACTTGGTGGATGGGA
1034 ATGATGTCCCTCTGCATAACCCGCCAGATGCTAAAGGCTCTCGGGACTTGGTGGATGGGA
345 Y--D--V--P--L--H--N--P--P--D--A--K--G--S--R--D--L--V--D--G--
R Y R S K Y YR
1261 TCAACCGATTGTCTTTCTCCAGTACAGGCAGCACCCGGAGTAACATGTCCACGTCTTCCA
1094 TCAACCGATTGTCTTTCTCCAGTACAGGCAGCACCCGGAGTAACATGTCCACGTCTTCCA
365 I--N--R--L--S--F--S--S--T--G--S--T--R--S--N--M--S--T--S--S--
Y
1321 CCTCCTCCAAGGAGTCCTCACTGTCAGCCTCCCCAGCTCAGGACAAAAGGCTCTTCCTGG
1154 CCTCCTCCAAGGAGTCCTCACTGTCAGCCTCCCCAGCTCAGGACAAAAGGCTCTTCCTGG
385 T--S--S--K--E--S--S--L--S--A--S--P--A--Q--D--K--R--L--F--L--
YRK S
1381 ATCCAGACACAGCTATTGAGAGACTTCAGCGGCTCCAGCAGGCCCTTGAGATGGGTGTCT
1214 ATCCAGACACAGCTATTGAGAGACTTCAGCGGCTCCAGCAGGCCCTTGAGATGGGTGTCT
405 D--P--D--T--A--I--E--R--L--Q--R--L--Q--Q--A--L--E--M--G--V--
M YK R S
1441 CCAGCCTAATGGCACTGGTCACTACCGACTGGCGGTGTTACGGATATATGGAAAGACACA
1274 CCAGCCTAATGGCACTGGTCACTACCGACTGGCGGTGTTACGGATATATGGAAAGACACA
425 S--S--L--M--A--L--V--T--T--D--W--R--C--Y--G--Y--M--E--R--H--
Y ** Y
1501 TCAATGAAATACGCACAGCAGTGGACAAGGTGGAGCTGTTCCTGAAGGAGTACCTCCACT
1334 TCAATGAAATACGCACAGCAGTGGACAAGGTGGAGCTGTTCCTGAAGGAGTACCTCCACT
445 I--N--E--I--R--T--A--V--D--K--V--E--L--F--L--K--E--Y--L--H--
Y K YR
1561 TTGTCAAGGGAGCTGTTGCAAATGCTGCCTGCCTCCCGGAACTCATCCTCCACAACAAGA
1394 TTGTCAAGGGAGCTGTTGCAAATGCTGCCTGCCTCCCGGAACTCATCCTCCACAACAAGA
465 F--V--K--G--A--V--A--N--A--A--C--L--P--E--L--I--L--H--N--K--
R YR Y MS Y M W R
1621 TGAAGCGGGAGCTGCAACGAGTTGAAGACTCCCACCAGATCCTGAGTCAAACCAGCCATG
1454 TGAAGCGGGAGCTGCAACGAGTTGAAGACTCCCACCAGATCCTGAGTCAAACCAGCCATG

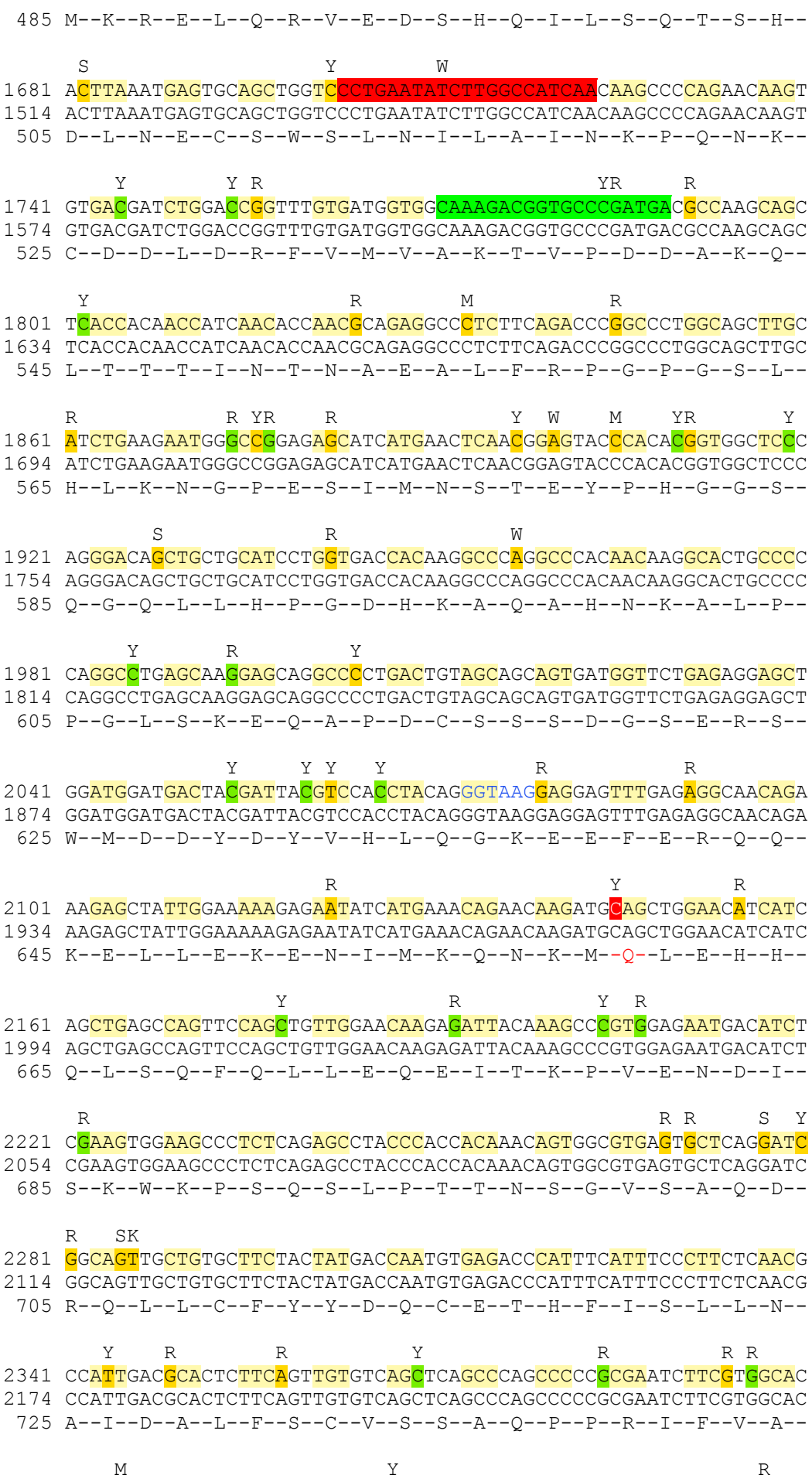
485 M--K--R--E--L--Q--R--V--E--D--S--H--Q--I--L--S--Q--T--S--H--
S Y W
1681 ACTTAAATGAGTGCAGCTGGTCCCTGAATATCTTGGCCATCAACAAGCCCCAGAACAAGT
1514 ACTTAAATGAGTGCAGCTGGTCCCTGAATATCTTGGCCATCAACAAGCCCCAGAACAAGT
505 D--L--N--E--C--S--W--S--L--N--I--L--A--I--N--K--P--Q--N--K--
Y Y R YR R
1741 GTGACGATCTGGACCGGTTTGTGATGGTGGCAAAGACGGTGCCCGATGACGCCAAGCAGC
1574 GTGACGATCTGGACCGGTTTGTGATGGTGGCAAAGACGGTGCCCGATGACGCCAAGCAGC
525 C--D--D--L--D--R--F--V--M--V--A--K--T--V--P--D--D--A--K--Q--
Y R M R
1801 TCACCACAACCATCAACACCAACGCAGAGGCCCTCTTCAGACCCGGCCCTGGCAGCTTGC
1634 TCACCACAACCATCAACACCAACGCAGAGGCCCTCTTCAGACCCGGCCCTGGCAGCTTGC
545 L--T--T--T--I--N--T--N--A--E--A--L--F--R--P--G--P--G--S--L--
R R YR R Y W M YR Y
1861 ATCTGAAGAATGGGCCGGAGAGCATCATGAACTCAACGGAGTACCCACACGGTGGCTCCC
1694 ATCTGAAGAATGGGCCGGAGAGCATCATGAACTCAACGGAGTACCCACACGGTGGCTCCC
565 H--L--K--N--G--P--E--S--I--M--N--S--T--E--Y--P--H--G--G--S--
S R W
1921 AGGGACAGCTGCTGCATCCTGGTGACCACAAGGCCCAGGCCCACAACAAGGCACTGCCCC
1754 AGGGACAGCTGCTGCATCCTGGTGACCACAAGGCCCAGGCCCACAACAAGGCACTGCCCC
585 Q--G--Q--L--L--H--P--G--D--H--K--A--Q--A--H--N--K--A--L--P--
Y R Y
1981 CAGGCCTGAGCAAGGAGCAGGCCCCTGACTGTAGCAGCAGTGATGGTTCTGAGAGGAGCT
1814 CAGGCCTGAGCAAGGAGCAGGCCCCTGACTGTAGCAGCAGTGATGGTTCTGAGAGGAGCT
605 P--G--L--S--K--E--Q--A--P--D--C--S--S--S--D--G--S--E--R--S--
Y Y Y R R
2041 GGATGGATGACTACGATTACGTCCACCTACAGGGTAAGGAGGAGTTTGAGAGGCAACAGA
1874 GGATGGATGACTACGATTACGTCCACCTACAGGGTAAGGAGGAGTTTGAGAGGCAACAGA
625 W--M--D--D--Y--D--Y--V--H--L--Q--G--K--E--E--F--E--R--Q--Q--
R Y R
2101 AAGAGCTATTGGAAAAAGAGAATATCATGAAACAGAACAAGATGCAGCTGGAACATCATC
1934 AAGAGCTATTGGAAAAAGAGAATATCATGAAACAGAACAAGATGCAGCTGGAACATCATC
645 K--E--L--L--E--K--E--N--I--M--K--Q--N--K--M--Q--L--E--H--H--
Y R Y R
2161 AGCTGAGCCAGTTCCAGCTGTTGGAACAAGAGATTACAAAGCCCGTGGAGAATGACATCT
1994 AGCTGAGCCAGTTCCAGCTGTTGGAACAAGAGATTACAAAGCCCGTGGAGAATGACATCT
665 Q--L--S--Q--F--Q--L--L--E--Q--E--I--T--K--P--V--E--N--D--I--
R R R S Y
2221 CGAAGTGGAAGCCCTCTCAGAGCCTACCCACCACAAACAGTGGCGTGAGTGCTCAGGATC
2054 CGAAGTGGAAGCCCTCTCAGAGCCTACCCACCACAAACAGTGGCGTGAGTGCTCAGGATC
685 S--K--W--K--P--S--Q--S--L--P--T--T--N--S--G--V--S--A--Q--D--
R SK
2281 GGCAGTTGCTGTGCTTCTACTATGACCAATGTGAGACCCATTTCATTTCCCTTCTCAACG
2114 GGCAGTTGCTGTGCTTCTACTATGACCAATGTGAGACCCATTTCATTTCCCTTCTCAACG
705 R--Q--L--L--C--F--Y--Y--D--Q--C--E--T--H--F--I--S--L--L--N--
Y R R Y R R R
2341 CCATTGACGCACTCTTCAGTTGTGTCAGCTCAGCCCAGCCCCCGCGAATCTTCGTGGCAC
2174 CCATTGACGCACTCTTCAGTTGTGTCAGCTCAGCCCAGCCCCCGCGAATCTTCGTGGCAC
725 A--I--D--A--L--F--S--C--V--S--S--A--Q--P--P--R--I--F--V--A--
M Y R

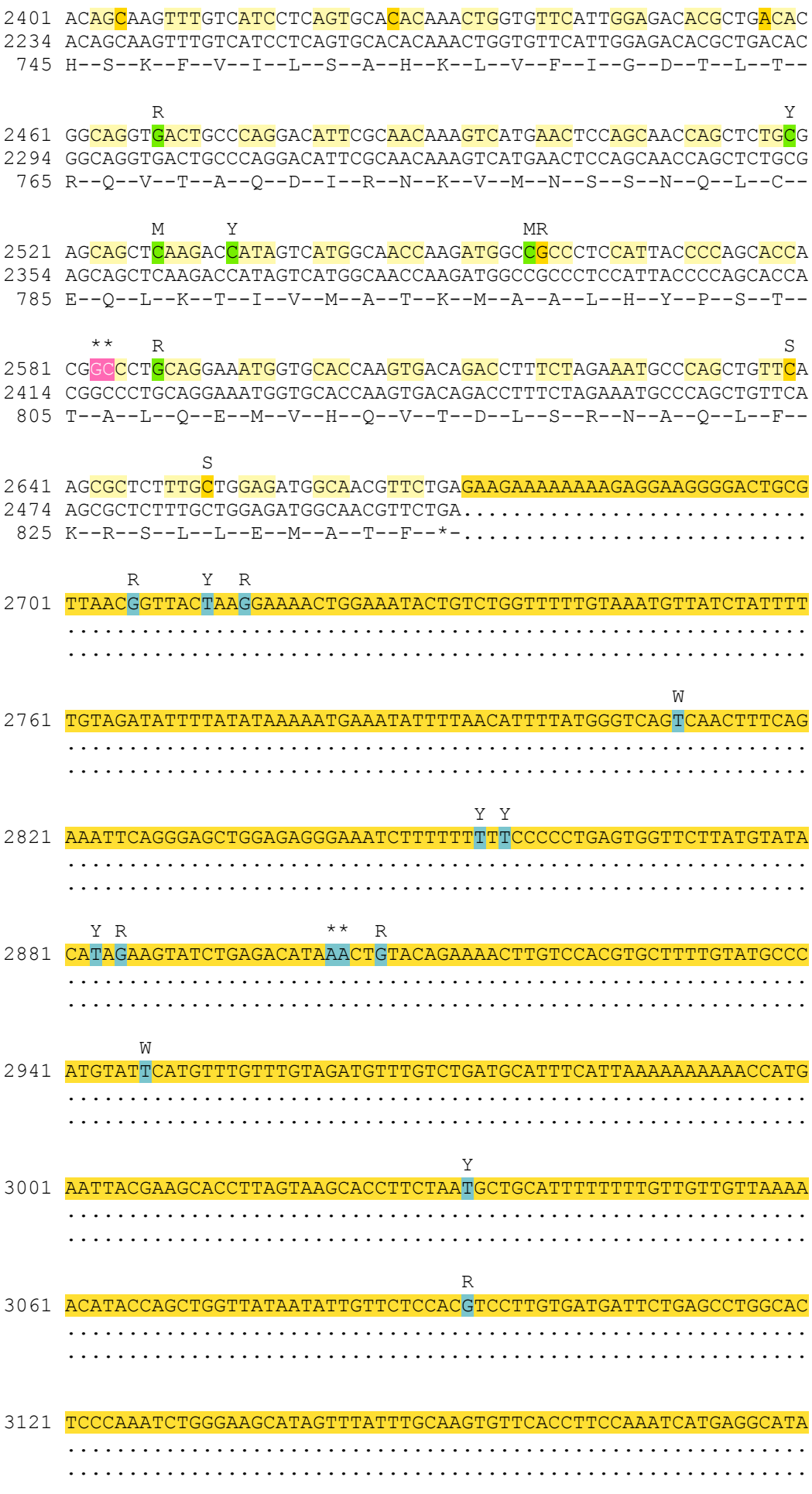
2401 ACAGCAAGTTTGTCATCCTCAGTGCACACAAACTGGTGTTCATTGGAGACACGCTGACAC
2234 ACAGCAAGTTTGTCATCCTCAGTGCACACAAACTGGTGTTCATTGGAGACACGCTGACAC
745 H--S--K--F--V--I--L--S--A--H--K--L--V--F--I--G--D--T--L--T--
2461 GGCAGGTGACTGCCCAGGACATTCGCAACAAAGTCATGAACTCCAGCAACCAGCTCTGCG
2294 GGCAGGTGACTGCCCAGGACATTCGCAACAAAGTCATGAACTCCAGCAACCAGCTCTGCG
765 R--Q--V--T--A--Q--D--I--R--N--K--V--M--N--S--S--N--Q--L--C--
2521 AGCAGCTCAAGACCATAGTCATGGCAACCAAGATGGCCGCCCTCCATTACCCCAGCACCA
2354 AGCAGCTCAAGACCATAGTCATGGCAACCAAGATGGCCGCCCTCCATTACCCCAGCACCA
785 E--Q--L--K--T--I--V--M--A--T--K--M--A--A--L--H--Y--P--S--T--
2581 CGGCCCTGCAGGAAATGGTGCACCAAGTGACAGACCTTTCTAGAATGCCCAGCTGTTCA
2414 CGGCCCTGCAGGAAATGGTGCACCAAGTGACAGACCTTTCTAGAAATGCCCAGCTGTTCA
805 T--A--L--Q--E--M--V--H--Q--V--T--D--L--S--R--N--A--Q--L--F--
2641 AGCGCTCTTTGCTGGAGATGGCAACGTTCTGAGAAGAAAAAAAAAGAGGAAGGGGACTGCG
2474 AGCGCTCTTTGCTGGAGATGGCAACGTTCTGA.....
825 K--R--S--L--L--E--M--A--T--F--*-.....
2701 TTAACGGTTACTAAGGAAAACTGGAAATACTGTCTGGTTTTTGTAAATGTTATCTATTTT
2761 TGTAGATATTTTATATAAAAATGAAATATTTTAACATTTTATGGGTCAGTCAACTTTCAG
2821 AAATTCAGGGAGCTGGAGAGGGAAATCTTTTTTTTTCCCCCTGAGTGGTTCTTATGTATA
2881 CATAGAAGTATCTGAGACATAAACTGTACAGAAAACTTGTCCACGTGCTTTTGTATGCCC
2941 ATGTATTCATGTTTGTTTGTAGATGTTTGTCTGATGCATTTCATTAAAAAAAAAACCATG
3001 AATTACGAAGCACCTTAGTAAGCACCTTCTAATGCTGCATTTTTTTTGTTGTTGTTAAAA
3061 ACATACCAGCTGGTTATAATATTGTTCTCCACGTCCTTGTGATGATTCTGAGCCTGGCAC
3121 TCCCAAATCTGGGAAGCATAGTTTATTTGCAAGTGTTCACCTTCCAAATCATGAGGCATA

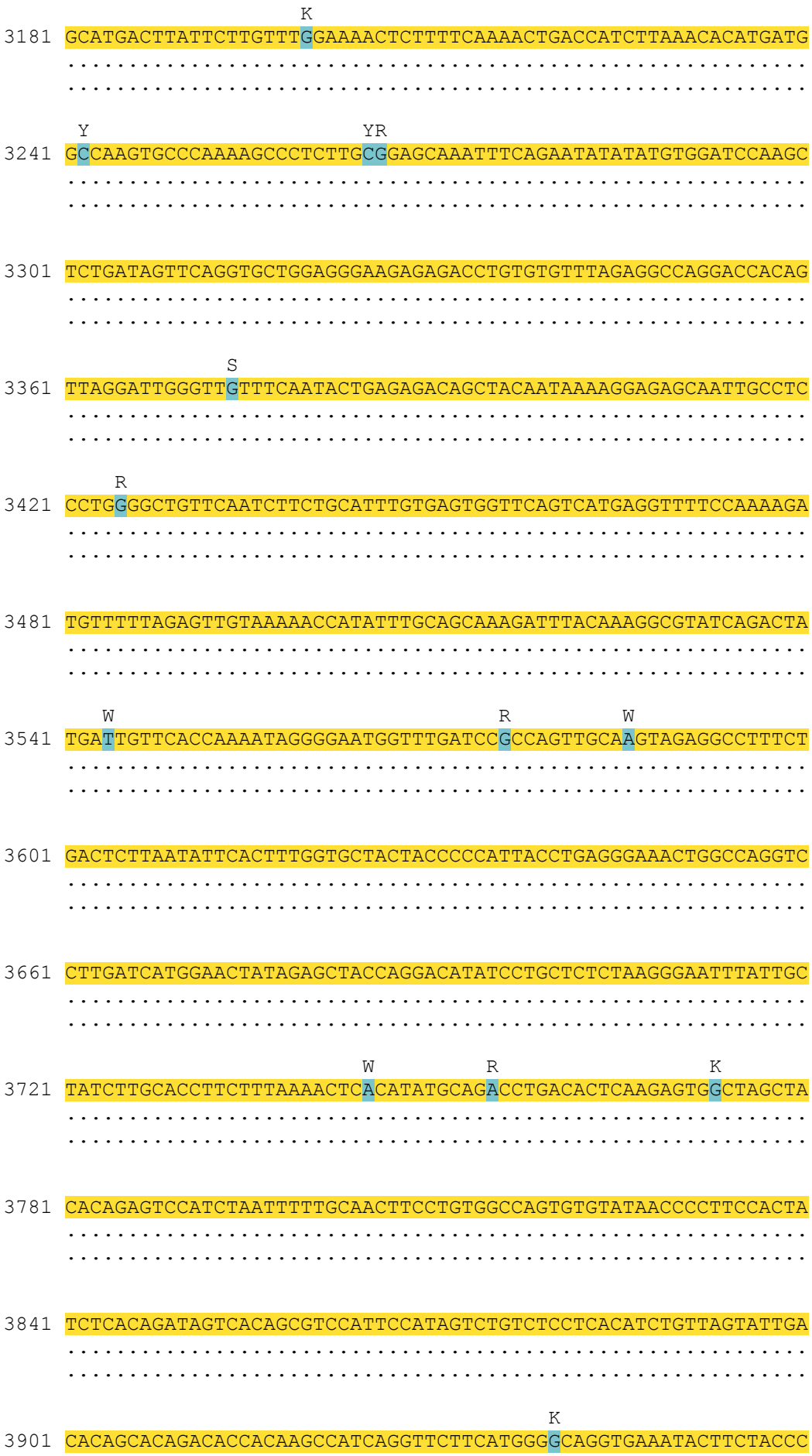
K
3181 GCATGACTTATTCTTGTTTGGAAAACTCTTTTCAAAACTGACCATCTTAAACACATGATG
Y
YR
3241 GCCAAGTGCCCAAAAGCCCTCTTGCGGAGCAAATTTCAGAATATATATGTGGATCCAAGC
3301 TCTGATAGTTCAGGTGCTGGAGGGAAGAGAGACCTGTGTGTTTAGAGGCCAGGACCACAG
S
3361 TTAGGATTGGGTTGTTTCAATACTGAGAGACAGCTACAATAAAAGGAGAGCAATTGCCTC
R
3421 CCTGGGGCTGTTCAATCTTCTGCATTTGTGAGTGGTTCAGTCATGAGGTTTTCCAAAAGA
3481 TGTTTTTAGAGTTGTAAAAACCATATTTGCAGCAAAGATTTACAAAGGCGTATCAGACTA
W
R
W
3541 TGATTGTTCACCAAAATAGGGGAATGGTTTGATCCGCCAGTTGCAAGTAGAGGCCTTTCT
3601 GACTCTTAATATTCACTTTGGTGCTACTACCCCCATTACCTGAGGGAAACTGGCCAGGTC
3661 CTTGATCATGGAACTATAGAGCTACCAGGACATATCCTGCTCTCTAAGGGAATTTATTGC
W
R
K
3721 TATCTTGCACCTTCTTTAAAACTCACATATGCAGACCTGACACTCAAGAGTGGCTAGCTA
3781 CACAGAGTCCATCTAATTTTTGCAACTTCCTGTGGCCAGTGTGTATAACCCCTTCCACTA
3841 TCTCACAGATAGTCACAGCGTCCATTCCATAGTCTGTCTCCTCACATCTGTTAGTATTGA
K
3901 CACAGCACAGACACCACAAGCCATCAGGTTCTTCATGGGGCAGGTGAAATACTTCTACCC


Y
R
3961 CATGGGTAAATGTATTCACATATTACCAAGAGAAGAAGCACATTATCTATGATCTTTTGG
*
4021 CCCAGTTCTTATTTAGCATTTTTATTCCAGCCTACTTGGAAACATGTTTTTATTTGCAAT
R
4081 ATATGCCTGACTGAATTAAGCTTGCTTGTTTTAAACAACCAAATCATTGGAACAGAAAAG
R
W
M
***
4141 GATTTAAAAAACAAGAATGCATGATCTCAGAGTGATTAAAAAAAAATCAGTGGAAATAAA
4201 TGATCATAGAAGGTGCTTTTCAAAACAACTGCTATTATAATTCTCAAAGTCCTACTCTGC
4261 CAAAAGAAGATTAAAAGTCATACATTACATTACAAGGAAATGTTCATGTGGGAAGAGGGT
4321 TGCTGAAAATCAACAACGCTTGAAGTTAAAAAGTGTGTCTTTGTAGATTTCATTGTATAA
Y
4381 TGTGTATTTCTTAGGAGATGGCTGACTTGATTGATCTACGCTAAGTGGAGACATTTCACA
R
4441 TTTTTAAAACCAAATGTTCAATCTGTATTACTCTTTGCCGTCTTGTATGTAGAGGCTATT
4501 TTTAAATCATTAAATTTTTAGATCTCTGTTTTCATA

TRANSCRIPT VARIANT 3 mRNA NM_001142393.1

Amino acid sequence shown below was retrieved from Ensemble! encoding Transcript NEDD9-002 ENST00000504387, also reported as Transcript variant 3, mRNA NM_001142393.1in NCBI (pubmed) and Transcript variant 1, RefSeq Summary (NM_006403) in UCSC Browser.

The shRNA targeting sequence is found 68 NT bases upstream of an siRNA target sequence previously used in our lab (SCRL) on mesenchymal stem cells [NT 1897-1918 vs NT 1965-1984 respectively.

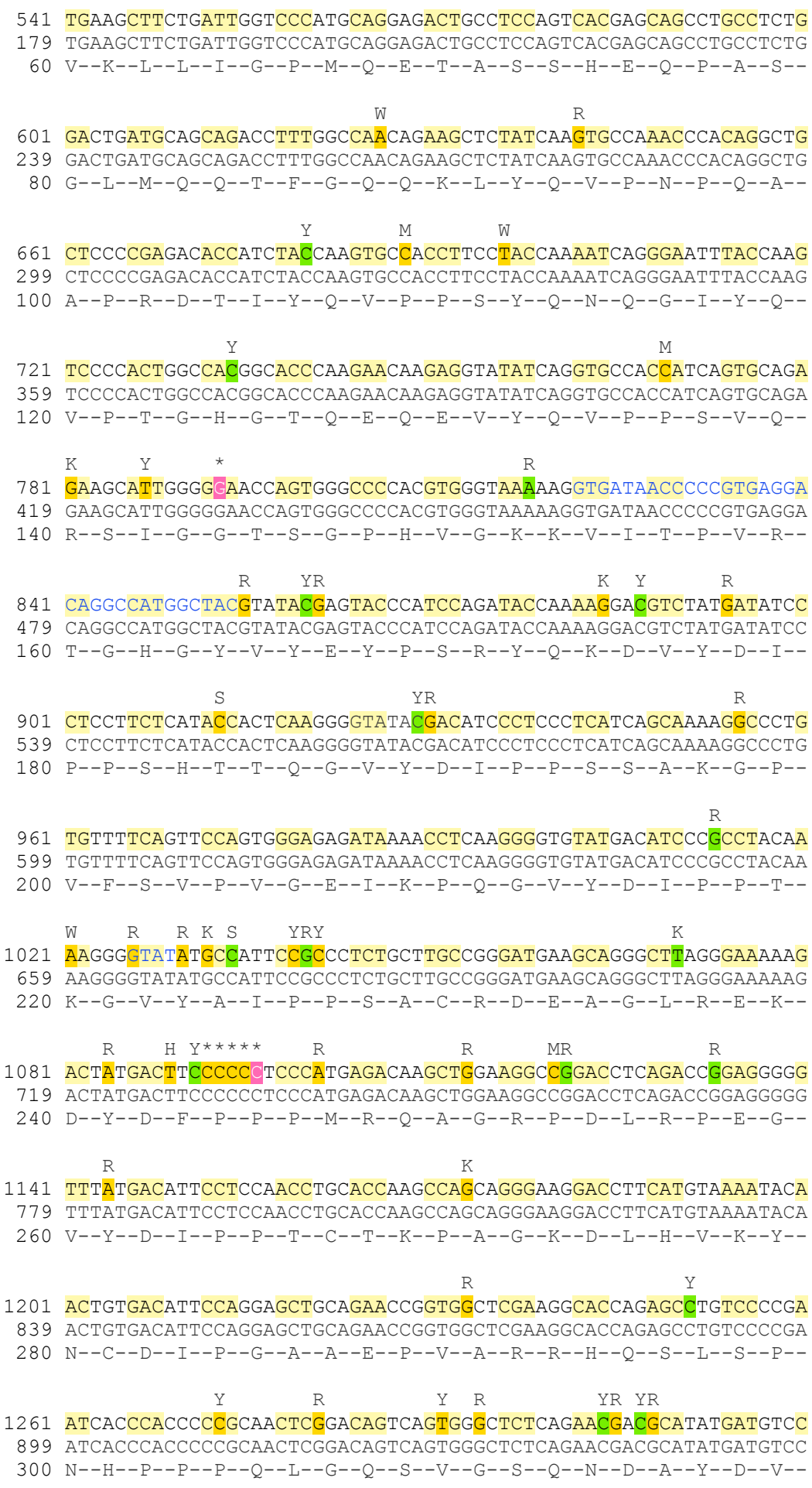
541 TGAAGCTTCTGATTGGTCCCATGCAGGAGACTGCCTCCAGTCACGAGCAGCCTGCCTCTG
179 TGAAGCTTCTGATTGGTCCCATGCAGGAGACTGCCTCCAGTCACGAGCAGCCTGCCTCTG
60 V--K--L--L--I--G--P--M--Q--E--T--A--S--S--H--E--Q--P--A--S--
601 GACTGATGCAGCAGACCTTTGGCCAACAGAAGCTCTATCAAGTGCCAAACCCACAGGCTG
239 GACTGATGCAGCAGACCTTTGGCCAACAGAAGCTCTATCAAGTGCCAAACCCACAGGCTG
80 G--L--M--Q--Q--T--F--G--Q--Q--K--L--Y--Q--V--P--N--P--Q--A--
661 CTCCCCGAGACACCATCTACCAAGTGCCACCTTCCTACCAAAATCAGGGAATTTACCAAG
299 CTCCCCGAGACACCATCTACCAAGTGCCACCTTCCTACCAAAATCAGGGAATTTACCAAG
100 A--P--R--D--T--I--Y--Q--V--P--P--S--Y--Q--N--Q--G--I--Y--Q--
721 TCCCCACTGGCCACGGCACCCAAGAACAAGAGGTATATCAGGTGCCACCATCAGTGCAGA
359 TCCCCACTGGCCACGGCACCCAAGAACAAGAGGTATATCAGGTGCCACCATCAGTGCAGA
120 V--P--T--G--H--G--T--Q--E--Q--E--V--Y--Q--V--P--P--S--V--Q--
781 GAAGCATTGGGGGAACCAGTGGGCCCCACGTGGGTAAAAAGGTGATAACCCCCGTGAGGA
419 GAAGCATTGGGGGAACCAGTGGGCCCCACGTGGGTAAAAAGGTGATAACCCCCGTGAGGA
140 R--S--I--G--G--T--S--G--P--H--V--G--K--K--V--I--T--P--V--R--
841 CAGGCCATGGCTACGTATACGAGTACCCATCCAGATACCAAAAGGACGTCTATGATATCC
479 CAGGCCATGGCTACGTATACGAGTACCCATCCAGATACCAAAAGGACGTCTATGATATCC
160 T--G--H--G--Y--V--Y--E--Y--P--S--R--Y--Q--K--D--V--Y--D--I--
901 CTCCTTCTCATACCACTCAAGGGGTATACGACATCCCTCCCTCATCAGCAAAAGGCCCTG
539 CTCCTTCTCATACCACTCAAGGGGTATACGACATCCCTCCCTCATCAGCAAAAGGCCCTG
180 P--P--S--H--T--T--Q--G--V--Y--D--I--P--P--S--S--A--K--G--P--
961 TGTTTTCAGTTCCAGTGGGAGAGATAAAACCTCAAGGGGTGTATGACATCCCGCCTACAA
599 TGTTTTCAGTTCCAGTGGGAGAGATAAAACCTCAAGGGGTGTATGACATCCCGCCTACAA
200 V--F--S--V--P--V--G--E--I--K--P--Q--G--V--Y--D--I--P--P--T--
1021 AAGGGGTATATGCCATTCCGCCCTCTGCTTGCCGGGATGAAGCAGGGCTTAGGGAAAAAG
659 AAGGGGTATATGCCATTCCGCCCTCTGCTTGCCGGGATGAAGCAGGGCTTAGGGAAAAAG
220 K--G--V--Y--A--I--P--P--S--A--C--R--D--E--A--G--L--R--E--K--
1081 ACTATGACTTCCCCCCTCCCATGAGACAAGCTGGAAGGCCGGACCTCAGACCGGAGGGGG
719 ACTATGACTTCCCCCCTCCCATGAGACAAGCTGGAAGGCCGGACCTCAGACCGGAGGGGG
240 D--Y--D--F--P--P--P--M--R--Q--A--G--R--P--D--L--R--P--E--G--
1141 TTTATGACATTCCTCCAACCTGCACCAAGCCAGCAGGGAAGGACCTTCATGTAAAATACA
779 TTTATGACATTCCTCCAACCTGCACCAAGCCAGCAGGGAAGGACCTTCATGTAAAATACA
260 V--Y--D--I--P--P--T--C--T--K--P--A--G--K--D--L--H--V--K--Y--
1201 ACTGTGACATTCCAGGAGCTGCAGAACCGGTGGCTCGAAGGCACCAGAGCCTGTCCCCGA
839 ACTGTGACATTCCAGGAGCTGCAGAACCGGTGGCTCGAAGGCACCAGAGCCTGTCCCCGA
280 N--C--D--I--P--G--A--A--E--P--V--A--R--R--H--Q--S--L--S--P--
1261 ATCACCCACCCCCGCAACTCGGACAGTCAGTGGGCTCTCAGAACGACGCATATGATGTCC
899 ATCACCCACCCCCGCAACTCGGACAGTCAGTGGGCTCTCAGAACGACGCATATGATGTCC
300 N--H--P--P--P--Q--L--G--Q--S--V--G--S--Q--N--D--A--Y--D--V--

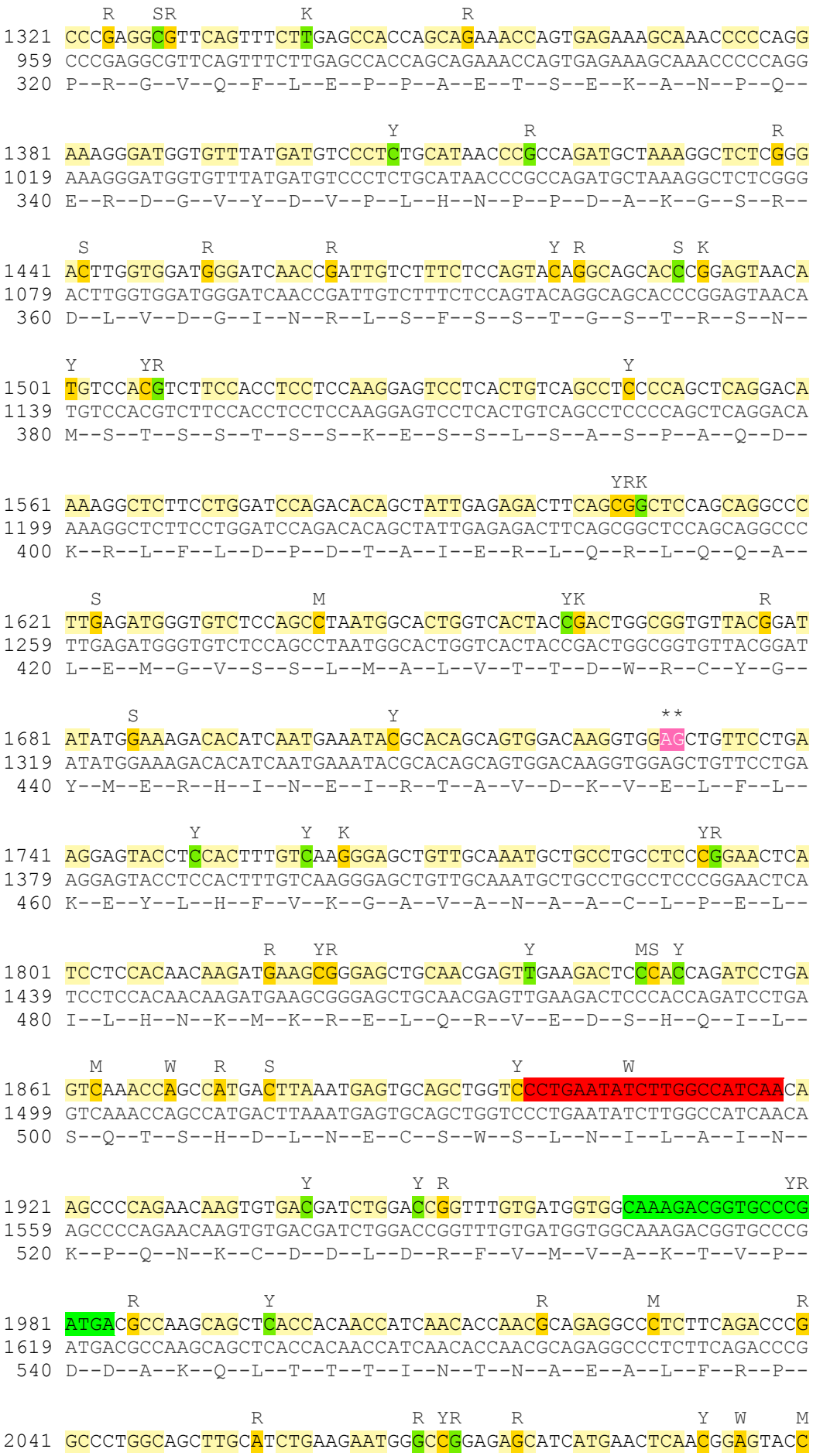

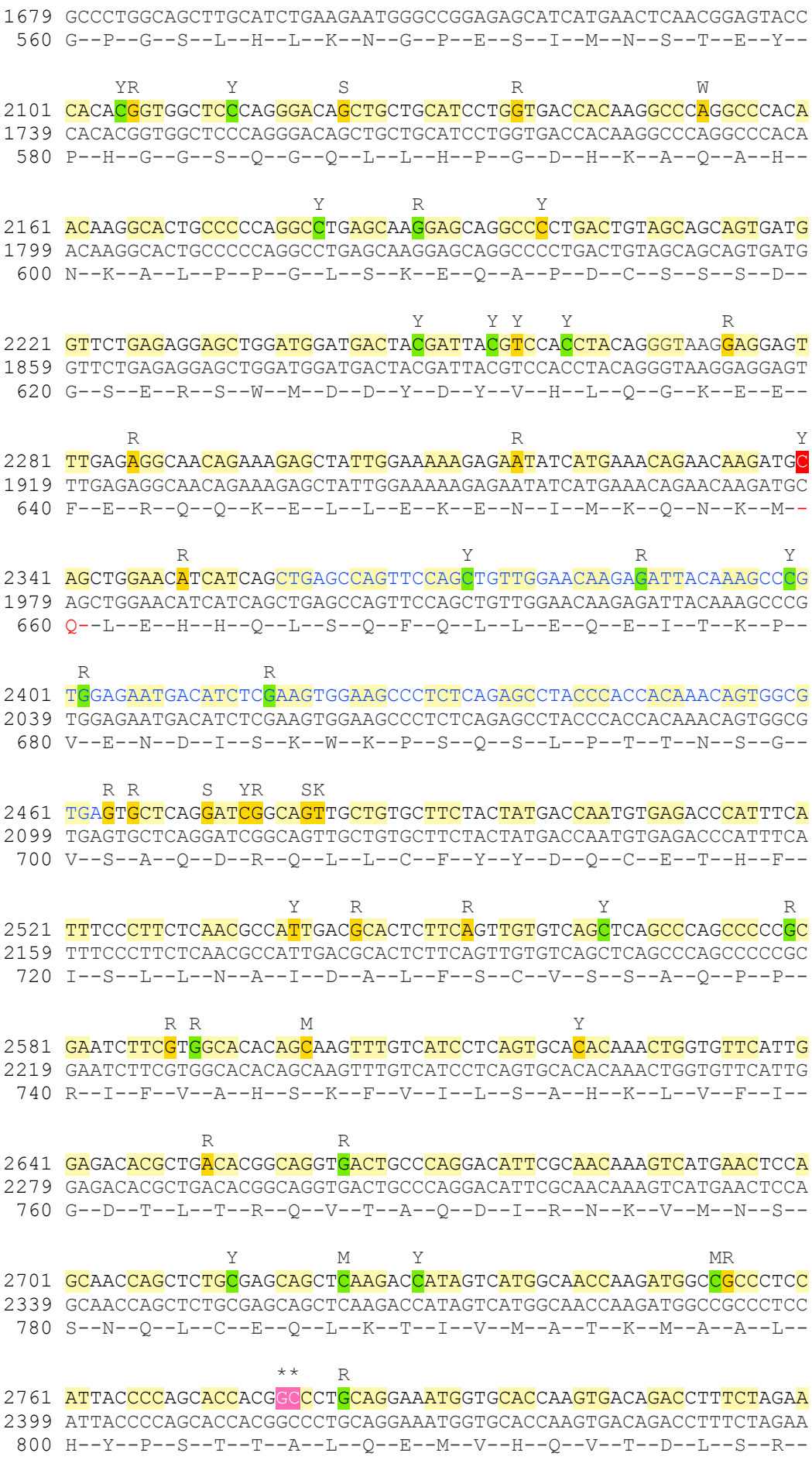
1679 GCCCTGGCAGCTTGCATCTGAAGAATGGGCCGGAGAGCATCATGAACTCAACGGAGTACC
560 G--P--G--S--L--H--L--K--N--G--P--E--S--I--M--N--S--T--E--Y--
YR Y S R W
2101 CACACGGTGGCTCCCAGGGACAGCTGCTGCATCCTGGTGACCACAAGGCCCAGGCCCACA
1739 CACACGGTGGCTCCCAGGGACAGCTGCTGCATCCTGGTGACCACAAGGCCCAGGCCCACA
580 P--H--G--G--S--Q--G--Q--L--L--H--P--G--D--H--K--A--Q--A--H--
Y R Y
2161 ACAAGGCACTGCCCCCAGGCCTGAGCAAGGAGCAGGCCCCTGACTGTAGCAGCAGTGATG
1799 ACAAGGCACTGCCCCCAGGCCTGAGCAAGGAGCAGGCCCCTGACTGTAGCAGCAGTGATG
600 N--K--A--L--P--P--G--L--S--K--E--Q--A--P--D--C--S--S--S--D--
Y Y Y R
2221 GTTCTGAGAGGAGCTGGATGGATGACTACGATTACGTCCACCTACAGGGTAAGGAGGAGT
1859 GTTCTGAGAGGAGCTGGATGGATGACTACGATTACGTCCACCTACAGGGTAAGGAGGAGT
620 G--S--E--R--S--W--M--D--D--Y--D--Y--V--H--L--Q--G--K--E--E--
R R Y
2281 TTGAGAGGCAACAGAAAGAGCTATTGGAAAAAGAGAATATCATGAAACAGAACAAGATGC
1919 TTGAGAGGCAACAGAAAGAGCTATTGGAAAAAGAGAATATCATGAAACAGAACAAGATGC
640 F--E--R--Q--Q--K--E--L--L--E--K--E--N--I--M--K--Q--N--K--M--
R Y R Y
2341 AGCTGGAACATCATCAGCTGAGCCAGTTCCAGCTGTTGGAACAAGAGATTACAAAGCCCG
1979 AGCTGGAACATCATCAGCTGAGCCAGTTCCAGCTGTTGGAACAAGAGATTACAAAGCCCG
660 Q--L--E--H--H--Q--L--S--Q--F--Q--L--L--E--Q--E--I--T--K--P--
R R
2401 TGGAGAATGACATCTCGAAGTGGAAGCCCTCTCAGAGCCTACCCACCACAAACAGTGGCG
2039 TGGAGAATGACATCTCGAAGTGGAAGCCCTCTCAGAGCCTACCCACCACAAACAGTGGCG
680 V--E--N--D--I--S--K--W--K--P--S--Q--S--L--P--T--T--N--S--G--
R R S YR SK
2461 TGAGTGCTCAGGATCGGCAGTTGCTGTGCTTCTACTATGACCAATGTGAGACCCATTTCA
2099 TGAGTGCTCAGGATCGGCAGTTGCTGTGCTTCTACTATGACCAATGTGAGACCCATTTCA
700 V--S--A--Q--D--R--Q--L--L--C--F--Y--Y--D--Q--C--E--T--H--F--
Y R R Y R
2521 TTTCCCTTCTCAACGCCATTGACGCACTCTTCAGTTGTGTCAGCTCAGCCCAGCCCCCGC
2159 TTTCCCTTCTCAACGCCATTGACGCACTCTTCAGTTGTGTCAGCTCAGCCCAGCCCCCGC
720 I--S--L--L--N--A--I--D--A--L--F--S--C--V--S--S--A--Q--P--P--
R R M Y
2581 GAATCTTCGTGGCACACAGCAAGTTTGTCATCCTCAGTGCACACAAACTGGTGTTCATTG
2219 GAATCTTCGTGGCACACAGCAAGTTTGTCATCCTCAGTGCACACAAACTGGTGTTCATTG
740 R--I--F--V--A--H--S--K--F--V--I--L--S--A--H--K--L--V--F--I--
R R
2641 GAGACACGCTGACACGGCAGGTGACTGCCCAGGACATTCGCAACAAAGTCATGAACTCCA
2279 GAGACACGCTGACACGGCAGGTGACTGCCCAGGACATTCGCAACAAAGTCATGAACTCCA
760 G--D--T--L--T--R--Q--V--T--A--Q--D--I--R--N--K--V--M--N--S--
Y M Y MR
2701 GCAACCAGCTCTGCGAGCAGCTCAAGACCATAGTCATGGCAACCAAGATGGCCGCCCTCC
2339 GCAACCAGCTCTGCGAGCAGCTCAAGACCATAGTCATGGCAACCAAGATGGCCGCCCTCC
780 S--N--Q--L--C--E--Q--L--K--T--I--V--M--A--T--K--M--A--A--L--
** R
2761 ATTACCCCAGCACCACGGCCCTGCAGGAAATGGTGCACCAAGTGACAGACCTTTCTAGAA
2399 ATTACCCCAGCACCACGGCCCTGCAGGAAATGGTGCACCAAGTGACAGACCTTTCTAGAA
800 H--Y--P--S--T--T--A--L--Q--E--M--V--H--Q--V--T--D--L--S--R--


S S
2821 ATGCCCAGCTGTTCAAGCGCTCTTTGCTGGAGATGGCAACGTTCTGAGAAGAAAAAAAAG
2459 ATGCCCAGCTGTTCAAGCGCTCTTTGCTGGAGATGGCAACGTTCTGA.....
820 N--A--Q--L--F--K--R--S--L--L--E--M--A--T--F--*-.....
R Y R
2881 AGGAAGGGGACTGCGTTAACGGTTACTAAGGAAAACTGGAAATACTGTCTGGTTTTTGTA
2941 AATGTTATCTATTTTTGTAGATATTTTATATAAAAATGAAATATTTTAACATTTTATGGG
W Y Y
3001 TCAGTCAACTTTCAGAAATTCAGGGAGCTGGAGAGGGAAATCTTTTTTTTTCCCCCTGAG
Y R ** R
3061 TGGTTCTTATGTATACATAGAAGTATCTGAGACATAAACTGTACAGAAAACTTGTCCACG
W
3121 TGCTTTTGTATGCCCATGTATTCATGTTTGTTTGTAGATGTTTGTCTGATGCATTTCATT
3181 AAAAAAAAAACCATGAATTACGAAGCACCTT

REFERENCES

Abraham, R. & Weiss, A. 2004. Jurkat T Cells and Development of the T-Cell Receptor Signalling Paradigm. *Nature Reviews Immunology,* 4, 4, 301-308.

Adams, G. B., Chabner, K. T., Alley, I. R., Olson, D. P., Szczepiorkowski, Z. M., Poznansky, M. C., Kos, C. H., Pollak, M. R., Brown, E. M. & Scadden, D. T. 2006. Stem Cell Engraftment at the Endosteal Niche Is Specified by the Calcium-Sensing Receptor. *Nature,* 439, 7076, 599-603.

Alakel, N., Jing, D., Muller, K., Bornhauser, M., Ehninger, G. & Ordemann, R. 2009. Direct Contact with Mesenchymal Stromal Cells Affects Migratory Behavior and Gene Expression Profile of Cd133+ Hematopoietic Stem Cells During Ex Vivo Expansion. *Experimental Hematology,* 37, 4, 504-513.

Andrade, P., De Soure, A., Dos Santos, F., Paiva, A., Cabral, J. & Da Silva, C. 2013. Ex Vivo Expansion of Cord Blood Haematopoietic Stem/Progenitor Cells under Physiological Oxygen Tensions: Clear-Cut Effects on Cell Proliferation, Differentiation and Metabolism. *Journal of Tissue Engineering and Regenerative Medicine*, 222-263.

Austin, E., Guttridge, M., Pamphilon, D. & Watt, S. 2008. The Role of Blood Services and Regulatory Bodies in Stem Cell Transplantation. *Vox Sanguinis,* 94, 1, 6-17.

Avigdor, A., Goichberg, P., Shivtiel, S., Dar, A., Peled, A., Samira, S., Kollet, O., Hershkoviz, R., Alon, R., Hardan, I., Ben-Hur, H., Naor, D., Nagler, A. & Lapidot, T. 2004. Cd44 and Hyaluronic Acid Cooperate with Sdf-1 in the Trafficking of Human Cd34+ Stem/Progenitor Cells to Bone Marrow. *Blood,* 103, 8, 2981-2989.

Balabanian, K., Lagane, B., Infantino, S., Chow, K., Harriague, J., Moepps, B., Arenzana-Seisdedos, F., Thelen, M. & Bachelerie, F. 2005. The Chemokine Sdf-1/Cxcl12 Binds to and Signals through the Orphan Receptor Rdc1 in T Lymphocytes. *The Journal of Biological Chemistry,* 280, 42, 35760-35766.

Ballen, K. K., Gluckman, E. & Broxmeyer, H. E. 2013. Umbilical Cord Blood Transplantation: The First 25 Years and Beyond. *Blood,* 122, 4, 491-498.

Bassik, M., Lebbink, R., Churchman, L., Ingolia, N., Patena, W., Leproust, E., Schuldiner, M., Weissman, J. & Mcmanus, M. 2009. Rapid Creation and Quantitative Monitoring of High Coverage Shrna Libraries. *Nature Methods,* 6, 6, 443-445.

Batard, P., Monier, M. N., Fortunel, N., Ducos, K., Sansilvestri-Morel, P., Phan, T., Hatzfeld, A. & Hatzfeld, J. A. 2000. Tgf-(Beta)1 Maintains Hematopoietic Immaturity by a Reversible Negative Control of Cell Cycle and Induces Cd34 Antigen up-Modulation. *Journal Cell Science,* 113 (Pt 3), 383-390.

Baum, C., Weissman, I., Tsukamoto, A., Buckle, A. & Peault, B. 1992. Isolation of a Candidate Human Hematopoietic Stem-Cell Population. *Proceedings of the National Academy of Sciences of the USA,* 89, 7, 2804-2808.

Bautista, G., Cabrera, J., Regidor, C., Forés, R., García-Marco, J., Ojeda, E., Sanjuán, I., Ruiz, E., Krsnik, I., Navarro, B., Gil, S., Magro, E., De Laiglesia, A., Gonzalo-Daganzo, R., Martín-Donaire, T., Rico, M., Millán, I. & Fernández, M. 2009. Cord Blood Transplants Supported by Co-Infusion of Mobilized Hematopoietic Stem Cells from a Third-Party Donor. *Bone Marrow Transplantation,* 43, 5, 365-373.

Beckmann, J., Scheitza, S., Wernet, P., Fischer, J. & Giebel, B. 2007. Asymmetric Cell Division within the Human Hematopoietic Stem and

Progenitor Cell Compartment: Identification of Asymmetrically Segregating Proteins. *Blood,* 109, 12, 5494-5501.

Ben-Dor, I., Itsykson, P., Goldenberg, D., Galun, E. & Reubinoff, B. 2006. Lentiviral Vectors Harboring a Dual-Gene System Allow High and Homogeneous Transgene Expression in Selected Polyclonal Human Embryonic Stem Cells. *Molecular Therapy: The Journal of the American Society of Gene Therapy,* 14, 2, 255-267.

Benveniste, P., Frelin, C., Janmohamed, S., Barbara, M., Herrington, R., Hyam, D. & Iscove, N. 2010. Intermediate-Term Hematopoietic Stem Cells with Extended but Time-Limited Reconstitution Potential. *Cell Stem Cell,* 6, 1, 48-58.

Berra, E., Benizri, E., Ginouvès, A., Volmat, V., Roux, D. & Pouysségur, J. 2003. Hif Prolyl-Hydroxylase 2 Is the Key Oxygen Sensor Setting Low Steady-State Levels of Hif-1alpha in Normoxia. *The EMBO journal,* 22, 16, 4082-4090.

Bhatia, M., Bonnet, D., Murdoch, B., Gan, O. & Dick, J. 1998. A Newly Discovered Class of Human Hematopoietic Cells with Scid-Repopulating Activity. *Nature Medicine,* 4, 9, 1038-1045.

Bhatia, M., Wang, J., Kapp, U., Bonnet, D. & Dick, J. 1997. Purification of Primitive Human Hematopoietic Cells Capable of Repopulating Immune-Deficient Mice. *Proceedings of the National Academy of Sciences of the USA,* 94, 10, 5320-5325.

Bleul, C., Farzan, M., Choe, H., Parolin, C., Clark-Lewis, I., Sodroski, J. & Springer, T. 1996. The Lymphocyte Chemoattractant Sdf-1 Is a Ligand for Lestr/Fusin and Blocks Hiv-1 Entry. *Nature,* 382, 6594, 829-833.

Boudreau, R., Monteys, A. & Davidson, B. 2008. Minimizing Variables among Hairpin-Based Rnai Vectors Reveals the Potency of Shrnas. *RNA (New York, N.Y.),* 14, 9, 1834-1844.

Bouton, A., Riggins, R. & Bruce-Staskal, P. 2001. Functions of the Adapter Protein Cas: Signal Convergence and the Determination of Cellular Responses. *Oncogene,* 20, 44, 6448-6458.

Branemark, P. 1961a. Effect of Nicotinic Acid and Histamine on Capillary Circulation of Bone Marrow in Rabbit. *Acta Haematologica,* 25, 1, 71-79.

Branemark, P. 1961b. Experimental Investigation of Microcirculation in Bone Marrow. *Angiology,* 12, 7, 293-305.

Briknarová, K., Nasertorabi, F., Havert, M., Eggleston, E., Hoyt, D., Li, C., Olson, A., Vuori, K. & Ely, K. 2005. The Serine-Rich Domain from Crk-Associated Substrate (P130cas) Is a Four-Helix Bundle. *The Journal of Biological Chemistry,* 280, 23, 21908-21914.

Bruneau, S., Woda, C., Daly, K., Boneschansker, L., Jain, N., Kochupurakkal, N., Contreras, A., Seto, T. & Briscoe, D. 2012. Key Features of the Intragraft Microenvironment That Determine Long-Term Survival Following Transplantation. *Frontiers in Immunology,* 3, 54, 1-13.

Bühring, H., Seiffert, M., Bock, T., Scheding, S., Thiel, A., Scheffold, A., Kanz, L. & Brugger, W. 1999. Expression of Novel Surface Antigens on Early Hematopoietic Cells. *Annals of the New York Academy of Sciences,* 872, 25-39.

Butler, J., Nolan, D., Vertes, E., Varnum-Finney, B., Kobayashi, H., Hooper, A., Seandel, M., Shido, K., White, I., Kobayashi, M., Witte, L., May, C., Shawber, C., Kimura, Y., Kitajewski, J., Rosenwaks, Z., Bernstein, I. & Rafii, S. 2010. Endothelial Cells Are Essential for the Self-Renewal and Repopulation of Notch-Dependent Hematopoietic Stem Cells. *Cell Stem Cell,* 6, 3, 251-264.

Calloni, R., Cordero, E. A., Henriques, J. & Bonatto, D. 2013. Reviewing and Updating the Major Molecular Markers for Stem Cells. *Stem Cells and Development,* 22, 9, 1455-1476.

Calvi, L. M., Adams, G. B., Weibrecht, K. W., Weber, J. M., Olson, D. P., Knight, M. C., Martin, R. P., Schipani, E., Divieti, P., Bringhurst, F. R., Milner, L. A., Kronenberg, H. M. & Scadden, D. T. 2003. Osteoblastic Cells Regulate the Haematopoietic Stem Cell Niche. *Nature,* 425, 6960, 841-846.

Cancelas, J., Lee, A., Prabhakar, R., Stringer, K., Zheng, Y. & Williams, D. 2005. Rac Gtpases Differentially Integrate Signals Regulating Hematopoietic Stem Cell Localization. *Nature Medicine,* 11, 8, 886-891.

Case, S., Price, M., Jordan, C., Yu, X., Wang, L., Bauer, G., Haas, D., Xu, D., Stripecke, R., Naldini, L., Kohn, D. & Crooks, G. 1999. Stable Transduction of Quiescent Cd34(+)Cd38(-) Human Hematopoietic Cells by Hiv-1-Based Lentiviral Vectors. *Proceedings of the National Academy of Sciences of the USA,* 96, 6, 2988-2993.

Ceradini, D. J., Kulkarni, A. R., Callaghan, M. J., Tepper, O. M., Bastidas, N., Kleinman, M. E., Capla, J. M., Galiano, R. D., Levine, J. P. & Gurtner, G. C. 2004. Progenitor Cell Trafficking Is Regulated by Hypoxic Gradients through Hif-1 Induction of Sdf-1. *Nature Medicine,* 10, 8, 858-864.

Chandel, N. S., Mcclintock, D. S., Feliciano, C. E., Wood, T. M., Melendez, J. A., Rodriguez, A. M. & Schumacker, P. T. 2000. Reactive Oxygen Species Generated at Mitochondrial Complex Iii Stabilize Hypoxia-Inducible Factor-1α During Hypoxia: A Mechanism of O2 Sensing. *Journal of Biological Chemistry,* 275, 33, 25130-25138.

Chang, J.-X., Gao, F., Zhao, G.-Q. & Zhang, G.-J. 2012. Role of Nedd9 in Invasion and Metastasis of Lung Adenocarcinoma. *Experimental and Therapeutic Medicine,* 4, 5, 795-800.

Cheuk, D. 2013. Optimal Stem Cell Source for Allogeneic Stem Cell Transplantation for Hematological Malignancies. *World Journal of Transplantation,* 3, 4, 99-112.

Chiou, Y.-W., Lin, H.-K., Tang, M.-J., Lin, H.-H. & Yeh, M.-L. 2013. The Influence of Physical and Physiological Cues on Atomic Force Microscopy-Based Cell Stiffness Assessment. *PLoS ONE,* 8, 10, 1-12.

Chitteti, B. R., Cheng, Y.-H., Kacena, M. A. & Srour, E. F. 2013. Hierarchical Organization of Osteoblasts Reveals the Significant Role of Cd166 in Hematopoietic Stem Cell Maintenance and Function. *Bone,* 54, 1, 58-67.

Chow, D. C., Wenning, L. A., Miller, W. M. & Papoutsakis, E. T. 2001a. Modeling Po(2) Distributions in the Bone Marrow Hematopoietic Compartment. I. Krogh's Model. *Biophysical Journal,* 81, 2, 675-684.

Chow, D. C., Wenning, L. A., Miller, W. M. & Papoutsakis, E. T. 2001b. Modeling Po(2) Distributions in the Bone Marrow Hematopoietic Compartment. Ii. Modified Kroghian Models. *Biophysical Journal,* 81, 2, 685-696.

Christophis, C., Taubert, I., Meseck, G., Schubert, M., Grunze, M., Ho, A. & Rosenhahn, A. 2011. Shear Stress Regulates Adhesion and Rolling of Cd44+ Leukemic and Hematopoietic Progenitor Cells on Hyaluronan. *Biophysical Journal,* 101, 3, 585-593.

Chuck, A., Clarke, M. & Palsson, B. 1996. Retroviral Infection Is Limited by Brownian Motion. *Human Gene Therapy,* 7, 13, 1527-1534.

Cipolleschi, M., Dello Sbarba, P. & Olivotto, M. 1993. The Role of Hypoxia in the Maintenance of Hematopoietic Stem Cells. *Blood,* 82, 7, 2031-2037.

Conneally, E., Cashman, J., Petzer, A. & Eaves, C. 1997. Expansion in Vitro of Transplantable Human Cord Blood Stem Cells Demonstrated Using a Quantitative Assay of Their Lympho-Myeloid Repopulating Activity in Nonobese Diabetic-Scid/Scid Mice. *Proceedings of the National Academy of Sciences of the USA,* 94, 18, 9836-9841.

Cooray, S., Howe, S. J. & Thrasher, A. J. 2012. Chapter Three - Retrovirus and Lentivirus Vector Design and Methods of Cell Conditioning. *In:* Theodore, F. (ed.) *Methods in Enzymology.* Amsterdam: Elsevier Inc.

Corselli, M., Chin, C., Parekh, C., Sahaghian, A., Wang, W., Ge, S., Evseenko, D., Wang, X., Montelatici, E., Lazzari, L., Crooks, G. & Péault, B. 2013. Perivascular Support of Human Hematopoietic Stem/Progenitor Cells. *Blood,* 121, 15, 2891-2901.

Cowden Dahl, K., Robertson, S., Weaver, V. & Simon, M. 2005. Hypoxia-Inducible Factor Regulates Alphavbeta3 Integrin Cell Surface Expression. *Molecular Biology of the Cell,* 16, 4, 1901-1912.

Csaszar, E., Kirouac, D., Yu, M., Wang, W., Qiao, W., Cooke, M., Boitano, A., Ito, C. & Zandstra, P. 2012. Rapid Expansion of Human Hematopoietic Stem Cells by Automated Control of Inhibitory Feedback Signaling. *Cell Stem Cell,* 10, 2, 218-229.

Cumming, G., Fidler, F. & Vaux, D. L. 2007. Error Bars in Experimental Biology. *The Journal of Cell Biology,* 177, 1, 7-11.

Cyranoski, D. 2013. Stem Cells: Egg Engineers. *Nature,* 500, 7463, 392-394.

D'aprile, A., Scrima, R., Quarato, G., Tataranni, T., Falzetti, F., Di Ianni, M., Gemei, M., Del Vecchio, L., Piccoli, C. & Capitanio, N. 2014. Hematopoietic Stem/Progenitor Cells Express Myoglobin and Neuroglobin: Adaptation to Hypoxia or Prevention from Oxidative Stress? *Stem Cells (Dayton, Ohio)*, 1-18.

Dadke, D., Jarnik, M., Pugacheva, E. N., Singh, M. K. & Golemis, E. A. 2006. Deregulation of Hef1 Impairs M-Phase Progression by Disrupting the Rhoa Activation Cycle. *Molecular Biology of the Cell,* 17, 3, 1204-1217.

Danet, G. H., Pan, Y., Luongo, J. L., Bonnet, D. A. & Simon, M. C. 2003. Expansion of Human Scid-Repopulating Cells under Hypoxic Conditions. *The Journal of Clinical Investigation,* 112, 1, 126-135.

Dar, A., Goichberg, P., Shinder, V., Kalinkovich, A., Kollet, O., Netzer, N., Margalit, R., Zsak, M., Nagler, A., Hardan, I., Resnick, I., Rot, A. & Lapidot, T. 2005. Chemokine Receptor Cxcr4-Dependent Internalization and Resecretion of Functional Chemokine Sdf-1 by Bone Marrow Endothelial and Stromal Cells. *Nature Immunology,* 6, 10, 1038-1046.

Dar, A., Kollet, O. & Lapidot, T. 2006. Mutual, Reciprocal Sdf-1/Cxcr4 Interactions between Hematopoietic and Bone Marrow Stromal Cells Regulate Human Stem Cell Migration and Development in Nod/Scid Chimeric Mice. *Experimental Hematology,* 34, 8, 967-975.

Davidson, B. & Mccray, P. 2011. Current Prospects for Rna Interference-Based Therapies. *Nature Reviews Genetics,* 12, 5, 329-340.

Dayan, F., Bilton, R. L., Laferriere, J., Trottier, E., Roux, D., Pouyssegur, J. & Mazure, N. M. 2009. Activation of Hif-1alpha in Exponentially Growing Cells Via Hypoxic Stimulation Is Independent of the Akt/Mtor Pathway. *Journal of Cellular Physiology,* 218, 1, 167-174.

De Barros, A., Takiya, C., Garzoni, L., Leal-Ferreira, M., Dutra, H., Chiarini, L., Meirelles, M., Borojevic, R. & Rossi, M. 2010. Osteoblasts and Bone Marrow Mesenchymal Stromal Cells Control Hematopoietic Stem Cell Migration and Proliferation in 3d in Vitro Model. *PLoS ONE,* 5, 2, 1-13.

De Palma, M. & Naldini, L. 2002. Transduction of a Gene Expression Cassette Using Advanced Generation Lentiviral Vectors. *Methods in Enzymology,* 346, 514-529.

Delaney, C., Heimfeld, S., Brashem-Stein, C., Voorhies, H., Manger, R. L. & Bernstein, I. D. 2010. Notch-Mediated Expansion of Human Cord Blood

Progenitor Cells Capable of Rapid Myeloid Reconstitution. *Nature Medicine,* 16, 2, 232-236.

Demaison, C., Parsley, K., Brouns, G., Scherr, M., Battmer, K., Kinnon, C., Grez, M. & Thrasher, A. 2002. High-Level Transduction and Gene Expression in Hematopoietic Repopulating Cells Using a Human Immunodeficiency [Correction of Imunodeficiency] Virus Type 1-Based Lentiviral Vector Containing an Internal Spleen Focus Forming Virus Promoter. *Human Gene Therapy,* 13, 7, 803-813.

Deramaudt, T. B., Dujardin, D., Hamadi, A., Noulet, F., Kolli, K., De Mey, J., Takeda, K. & Rondé, P. 2011. Fak Phosphorylation at Tyr-925 Regulates Cross-Talk between Focal Adhesion Turnover and Cell Protrusion. *Molecular biology of the cell,* 22, 7, 964-975.

Dexter, T., Coutinho, L., Spooncer, E., Heyworth, C., Daniel, C., Schiro, R., Chang, J. & Allen, T. 1990a. Stromal Cells in Haemopoiesis. *Ciba Foundation Symposium,* 148, 76-95.

Dexter, T., Heyworth, C., Spooncer, E. & Ponting, I. 1990b. The Role of Growth Factors in Self-Renewal and Differentiation of Haemopoietic Stem Cells. *Philosophical Transactions of the Royal Society of London. Series B, Biological Sciences,* 327, 1239, 85-98.

Dick, J. 1996. Normal and Leukemic Human Stem Cells Assayed in Scid Mice. *Seminars in Immunology,* 8, 4, 197-206.

Ding, L. & Morrison, S. 2013. Haematopoietic Stem Cells and Early Lymphoid Progenitors Occupy Distinct Bone Marrow Niches. *Nature,* 495, 7440, 231-235.

Ding, L., Saunders, T., Enikolopov, G. & Morrison, S. 2012. Endothelial and Perivascular Cells Maintain Haematopoietic Stem Cells. *Nature,* 481, 7382, 457-462.

Dorrell, C., Gan, O., Pereira, D., Hawley, R. & Dick, J. 2000. Expansion of Human Cord Blood Cd34(+)Cd38(-) Cells in Ex Vivo Culture During Retroviral Transduction without a Corresponding Increase in Scid Repopulating Cell (Src) Frequency: Dissociation of Src Phenotype and Function. *Blood,* 95, 1, 102-110.

Dorshkind, K. 1990. Regulation of Hemopoiesis by Bone Marrow Stromal Cells and Their Products. *Annual Review Immunology,* 8, 111-137.

Doulatov, S., Notta, F., Laurenti, E. & Dick, John e. 2012. Hematopoiesis: A Human Perspective. *Cell Stem Cell,* 10, 2, 120-136.

Dulak, J., Loboda, A., Jazwa, A. & Jozkowicz, A. 2007. Comment On "A Novel Role of Hypoxia-Inducible Factor in Cobalt Chloride- and Hypoxia-Mediated Expression of Il-8 Chemokine in Human Endothelial Cells". *Journal of Immunology (Baltimore, Md. : 1950),* 178, 8, 4707.

Dyke, D. V., Anger, H. O., Yano, Y. & Bozzini, C. 1965. Bone Blood Flow Shown with F18 and the Positron Camera. *American Journal of Physiology -- Legacy Content,* 209, 1, 65-70.

Eapen, M., Rubinstein, P., Zhang, M.-J., Stevens, C., Kurtzberg, J., Scaradavou, A., Loberiza, F., Champlin, R., Klein, J., Horowitz, M. & Wagner, J. 2007. Outcomes of Transplantation of Unrelated Donor Umbilical Cord Blood and Bone Marrow in Children with Acute Leukaemia: A Comparison Study. *Lancet,* 369, 9577, 1947-1954.

Ehninger, A. & Trumpp, A. 2011. The Bone Marrow Stem Cell Niche Grows Up: Mesenchymal Stem Cells and Macrophages Move In. *The Journal of Experimental Medicine,* 208, 3, 421-428.

Elbashir, S., Harborth, J., Lendeckel, W., Yalcin, A., Weber, K. & Tuschl, T. 2001. Duplexes of 21-Nucleotide Rnas Mediate Rna Interference in Cultured Mammalian Cells. *Nature,* 411, 6836, 494-498.

Eliasson, P. & Jönsson, J.-I. 2010. The Hematopoietic Stem Cell Niche: Low in Oxygen but a Nice Place to Be. *Journal of Cellular Physiology,* 222, 1, 17-22.

Eliasson, P., Rehn, M., Hammar, P., Larsson, P., Sirenko, O., Flippin, L., Cammenga, J. & Jönsson, J.-I. 2010. Hypoxia Mediates Low Cell-Cycle Activity and Increases the Proportion of Long-Term-Reconstituting Hematopoietic Stem Cells During in Vitro Culture. *Experimental Hematology,* 38, 4, 301-31000.

Ellis, S. L., Grassinger, J., Jones, A., Borg, J., Camenisch, T., Haylock, D., Bertoncello, I. & Nilsson, S. K. 2011. The Relationship between Bone, Hemopoietic Stem Cells, and Vasculature. *Blood,* 118, 6, 1516-1524.

Evans, J., Kelly, P., O'neill, E. & Garcia, J. 1999. Human Cord Blood Cd34+Cd38- Cell Transduction Via Lentivirus-Based Gene Transfer Vectors. *Human Gene Therapy,* 10, 9, 1479-1489.

Fan, X., Gay, F., Ong, S.-Y., Ang, J., Chu, P., Bari, S., Lim, T. & Hwang, W. 2013. Mesenchymal Stromal Cell Supported Umbilical Cord Blood Ex Vivo Expansion Enhances Regulatory T Cells and Reduces Graft Versus Host Disease. *Cytotherapy,* 15, 5, 610-619.

Fashena, S., Einarson, M., O'neill, G., Patriotis, C. & Golemis, E. 2002. Dissection of Hef1-Dependent Functions in Motility and Transcriptional Regulation. *Journal of Cell Science,* 115, Pt 1, 99-111.

Fellmann, C., Zuber, J., Mcjunkin, K., Chang, K., Malone, C., Dickins, R., Xu, Q., Hengartner, M., Elledge, S., Hannon, G. & Lowe, S. 2011. Functional Identification of Optimized Rnai Triggers Using a Massively Parallel Sensor Assay. *Molecular Cell,* 41, 6, 733-746.

Fernández, M., Simon, V. & Minguell, J. 2000. Production of Soluble Cd34 by Human Myeloid Cells. *British Journal of Haematology,* 111, 2, 426-431.

Follenzi, A. & Naldini, L. 2002. Generation of Hiv-1 Derived Lentiviral Vectors. *Methods in Enzymology,* 346, 454-465.

Forde, S., Tye, B. J., Newey, S. E., Roubelakis, M., Smythe, J., Mcguckin, C. P., Pettengell, R. & Watt, S. M. 2007. Endolyn (Cd164) Modulates the Cxcl12-Mediated Migration of Umbilical Cord Blood Cd133+ Cells. *Blood,* 109, 5, 1825-1833.

Forristal, C. & Levesque, J.-P. 2013. Targeting the Hypoxia-Sensing Pathway in Clinical Hematology. *Stem Cells Translational Medicine,* 3, 2, 135-140.

Forristal, C., Winkler, I., Nowlan, B., Barbier, V., Walkinshaw, G. & Levesque, J.-P. 2013. Pharmacologic Stabilization of Hif-1α Increases Hematopoietic Stem Cell Quiescence in Vivo and Accelerates Blood Recovery after Severe Irradiation. *Blood,* 121, 5, 759-769.

Fung, Y. C. & Zweifach, B. W. 1971. Microcirculation - Mechanics of Blood Flow in Capillaries. *Annual Review of Fluid Mechanics,* 3, 189-210.

Furley, A., Reeves, B., Mizutani, S., Altass, L., Watt, S., Jacob, M., Van Den Elsen, P., Terhorst, C. & Greaves, M. 1986. Divergent Molecular Phenotypes of Kg1 and Kg1a Myeloid Cell Lines. *Blood,* 68, 5, 1101-1107.

Fürst, D., Müller, C., Vucinic, V., Bunjes, D., Herr, W., Gramatzki, M., Schwerdtfeger, R., Arnold, R., Einsele, H., Wulf, G., Pfreundschuh, M., Glass, B., Schrezenmeier, H., Schwarz, K. & Mytilineos, J. 2013. High-Resolution Hla Matching in Hematopoietic Stem Cell Transplantation: A Retrospective Collaborative Analysis. *Blood,* 122, 18, 3220-3229.

Gallacher, L., Murdoch, B., Wu, D. M., Karanu, F. N., Keeney, M. & Bhatia, M. 2000. Isolation and Characterization of Human Cd34(-)Lin(-) and Cd34(+)Lin(-) Hematopoietic Stem Cells Using Cell Surface Markers Ac133 and Cd7. *Blood,* 95, 9, 2813-2820.

Gardel, M., Schneider, I., Aratyn-Schaus, Y. & Waterman, C. 2010. Mechanical Integration of Actin and Adhesion Dynamics in Cell Migration. *Annual Review of Cell and Developmental Biology,* 26, 315-333.

Gezer, D., Vukovic, M., Soga, T., Pollard, P. & Kranc, K. 2014. Genetic Dissection of Hypoxia Signalling Pathways in Normal and Leukaemic Stem Cells. *Stem Cells (Dayton, Ohio)*, 1-11.

Giet, O., Van Bockstaele, D., Di Stefano, I., Huygen, S., Greimers, R., Beguin, Y. & Gothot, A. 2002. Increased Binding and Defective Migration across Fibronectin of Cycling Hematopoietic Progenitor Cells. *Blood,* 99, 6, 2023-2031.

Gluckman, E., Ruggeri, A., Volt, F., Cunha, R., Boudjedir, K. & Rocha, V. 2011. Milestones in Umbilical Cord Blood Transplantation. *British Journal of Haematology,* 154, 4, 441-447.

Goodell, M. A., Brose, K., Paradis, G., Conner, A. S. & Mulligan, R. C. 1996. Isolation and Functional Properties of Murine Hematopoietic Stem Cells That Are Replicating in Vivo. *The Journal of Experimental Medicine,* 183, 4, 1797-1806.

Görgens, A., Radtke, S., Horn, P. & Giebel, B. 2013a. New Relationships of Human Hematopoietic Lineages Facilitate Detection of Multipotent Hematopoietic Stem and Progenitor Cells. *Cell Cycle (Georgetown, Tex.),* 12, 22, 3478-3482.

Görgens, A., Radtke, S., Möllmann, M., Cross, M., Dürig, J., Horn, P. & Giebel, B. 2013b. Revision of the Human Hematopoietic Tree: Granulocyte Subtypes Derive from Distinct Hematopoietic Lineages. *Cell Reports,* 3, 5, 1539-1552.

Grassinger, J., Haylock, D. N., Williams, B., Olsen, G. H. & Nilsson, S. K. 2010. Phenotypically Identical Hemopoietic Stem Cells Isolated from Different

Regions of Bone Marrow Have Different Biologic Potential. *Blood,* 116, 17, 3185-3196.

Guitart, A., Subramani, C., Armesilla-Diaz, A., Smith, G., Sepulveda, C., Gezer, D., Vukovic, M., Dunn, K., Pollard, P., Holyoake, T., Enver, T., Ratcliffe, P. & Kranc, K. 2013. Hif-2α Is Not Essential for Cell-Autonomous Hematopoietic Stem Cell Maintenance. *Blood,* 122, 10, 1741-1745.

Gul, H., Marquez-Curtis, L. A., Jahroudi, N., Larratt, L. M. & Janowska-Wieczorek, A. 2010. Valproic Acid Exerts Differential Effects on Cxcr4 Expression in Leukemic Cells. *Leukemia Research,* 34, 2, 235-242.

Guo, J., Wang, W., Yu, D. & Wu, Y. 2011. Spinoculation Triggers Dynamic Actin and Cofilin Activity That Facilitates Hiv-1 Infection of Transformed and Resting Cd4 T Cells. *Journal of Virology,* 85, 19, 9824-9833.

Haas, D., Case, S., Crooks, G. & Kohn, D. 2000. Critical Factors Influencing Stable Transduction of Human Cd34(+) Cells with Hiv-1-Derived Lentiviral Vectors. *Molecular Therapy: The Journal of the American Society of Gene Therapy,* 2, 1, 71-80.

Haasnoot, J., Westerhout, E. & Berkhout, B. 2007. Rna Interference against Viruses: Strike and Counterstrike. *Nature Biotechnology,* 25, 12, 1435-1443.

Handgretinger, R. & Kuçi, S. 2013. Cd133-Positive Hematopoietic Stem Cells: From Biology to Medicine. *Advances in Experimental Medicine and Biology,* 777, 99-111.

Hanenberg, H., Xiao, X., Dilloo, D., Hashino, K., Kato, I. & Williams, D. 1996. Colocalization of Retrovirus and Target Cells on Specific Fibronectin Fragments Increases Genetic Transduction of Mammalian Cells. *Nature Medicine,* 2, 8, 876-882.

Hanna, J., Wernig, M., Markoulaki, S., Sun, C.-W., Meissner, A., Cassady, J., Beard, C., Brambrink, T., Wu, L.-C., Townes, T. & Jaenisch, R. 2007. Treatment of Sickle Cell Anemia Mouse Model with Ips Cells Generated from Autologous Skin. *Science (New York, N.Y.),* 318, 5858, 1920-1923.

Harris, D. T., Schumacher, M. J., Locascio, J., Besencon, F. J., Olson, G. B., Deluca, D., Shenker, L., Bard, J. & Boyse, E. A. 1992. Phenotypic and Functional Immaturity of Human Umbilical Cord Blood T Lymphocytes. *Proceedings of the National Academy of Sciences,* 89, 21, 10006-10010.

Hartmann, T., Grabovsky, V., Pasvolsky, R., Shulman, Z., Buss, E., Spiegel, A., Nagler, A., Lapidot, T., Thelen, M. & Alon, R. 2008. A Crosstalk between Intracellular Cxcr7 and Cxcr4 Involved in Rapid Cxcl12-Triggered Integrin Activation but Not in Chemokine-Triggered Motility of Human T Lymphocytes and Cd34+ Cells. *Journal of Leukocyte Biology,* 84, 4, 1130-1140.

Hayashi, K., Ogushi, S., Kurimoto, K., Shimamoto, S., Ohta, H. & Saitou, M. 2012. Offspring from Oocytes Derived from in Vitro Primordial Germ Cell-Like Cells in Mice. *Science (New York, N.Y.),* 338, 6109, 971-975.

Hengxiang, W., Zhidong, W., Xiaoli, Z., Li, D., Ling, Z., Hongmin, Y. & Zikuan, G. 2013. Hematopoietic Stem Cell Transplantation with Umbilical Cord Multipotent Stromal Cell Infusion for the Treatment of Aplastic Anemia—a Single-Center Experience. *Cytotherapy,* 15, 9, 1118-1126.

Hermitte, F., Brunet De La Grange, P., Belloc, F., Praloran, V. & Ivanovic, Z. 2006. Very Low O2 Concentration (0.1%) Favors G0 Return of Dividing Cd34+ Cells. *Stem Cells (Dayton, Ohio),* 24, 1, 65-73.

Hess, D., Meyerrose, T., Wirthlin, L., Craft, T., Herrbrich, P., Creer, M. & Nolta, J. 2004. Functional Characterization of Highly Purified Human Hematopoietic Repopulating Cells Isolated According to Aldehyde Dehydrogenase Activity. *Blood,* 104, 6, 1648-1655.

Hess, D., Wirthlin, L., Craft, T., Herrbrich, P., Hohm, S., Lahey, R., Eades, W., Creer, M. & Nolta, J. 2006. Selection Based on Cd133 and High Aldehyde Dehydrogenase Activity Isolates Long-Term Reconstituting Human Hematopoietic Stem Cells. *Blood,* 107, 5, 2162-2169.

Hidalgo, A. & Frenette, P. 2005. Enforced Fucosylation of Neonatal Cd34+ Cells Generates Selectin Ligands That Enhance the Initial Interactions with Microvessels but Not Homing to Bone Marrow. *Blood,* 105, 2, 567-575.

Hidalgo, A., Sanz-Rodriguez, F., Rodriguez-Fernandez, J. L., Albella, B., Blaya, C., Wright, N., Cabanas, C., Prosper, F., Gutierrez-Ramos, J. C. & Teixido, J. 2001. Chemokine Stromal Cell-Derived Factor-1alpha Modulates Vla-4 Integrin-Dependent Adhesion to Fibronectin and Vcam-1 on Bone Marrow Hematopoietic Progenitor Cells. *Experimental Hematology,* 29, 3, 345-355.

Hidalgo, A., Weiss, L. & Frenette, P. 2002. Functional Selectin Ligands Mediating Human Cd34(+) Cell Interactions with Bone Marrow Endothelium Are Enhanced Postnatally. *The Journal of Clinical Investigation,* 110, 4, 559-569.

Ho, A. & Wagner, W. 2007. The Beauty of Asymmetry: Asymmetric Divisions and Self-Renewal in the Haematopoietic System. *Current Opinion in Hematology,* 14, 4, 330-336.

Hofmeister, C., Zhang, J., Knight, K., Le, P. & Stiff, P. 2007. Ex Vivo Expansion of Umbilical Cord Blood Stem Cells for Transplantation: Growing Knowledge from the Hematopoietic Niche. *Bone Marrow Transplantation,* 39, 1, 11-23.

Hooper, A. T., Butler, J. M., Nolan, D. J., Kranz, A., Iida, K., Kobayashi, M., Kopp, H. G., Shido, K., Petit, I., Yanger, K., James, D., Witte, L., Zhu, Z., Wu, Y., Pytowski, B., Rosenwaks, Z., Mittal, V., Sato, T. N. & Rafii, S. 2009. Engraftment and Reconstitution of Hematopoiesis Is Dependent on

Vegfr2-Mediated Regeneration of Sinusoidal Endothelial Cells. *Cell Stem Cell,* 4, 3, 263-274.

Huang, A., Chen, M., Huang, S. & Kao…, C. 2013. Cd164 Regulates the Tumorigenesis of Ovarian Surface Epithelial Cells through the Sdf-1α/Cxcr4 Axis. *Molecular Cancer,* 12, 115, 1-13.

Hung, S.-P., Yang, M.-H., Tseng, K.-F. & Lee, O. K. 2013. Hypoxia-Induced Secretion of Tgf-β1 in Mesenchymal Stem Cell Promotes Breast Cancer Cell Progression. *Cell Transplantation,* 22, 10, 1869-1882.

Iriuchishima, H., Takubo, K., Matsuoka, S., Onoyama, I., Nakayama, K. I., Nojima, Y. & Suda, T. 2011. Ex Vivo Maintenance of Hematopoietic Stem Cells by Quiescence Induction through Fbxw7 Overexpression. *Blood,* 117, 8, 2373-2377.

Ivanovic, Z. 2010. Hematopoietic Stem Cells in Research and Clinical Applications: The "Cd34 Issue". *World Journal of Stem Cells,* 2, 2, 18-23.

Ivanovic, Z., Dello Sbarba, P., Trimoreau, F., Faucher, J. L. & Praloran, V. 2000. Primitive Human Hpcs Are Better Maintained and Expanded in Vitro at 1 Percent Oxygen Than at 20 Percent. *Transfusion,* 40, 12, 1482-1488.

Ivanovic, Z., Hermitte, F., Brunet De La Grange, P., Dazey, B., Belloc, F., Lacombe, F., Vezon, G. & Praloran, V. 2004. Simultaneous Maintenance of Human Cord Blood Scid-Repopulating Cells and Expansion of Committed Progenitors at Low O2 Concentration (3%). *Stem Cells (Dayton, Ohio),* 22, 5, 716-724.

Izumchenko, E., Singh, M. K., Plotnikova, O. V., Tikhmyanova, N., Little, J. L., Serebriiskii, I. G., Seo, S., Kurokawa, M., Egleston, B. L., Klein-Szanto, A., Pugacheva, E. N., Hardy, R. R., Wolfson, M., Connolly, D. C. & Golemis, E. A. 2009. Nedd9 Promotes Oncogenic Signaling in Mammary Tumor Development. *Cancer Research,* 69, 18, 7198-7206.

Jinek, M. & Doudna, J. 2009. A Three-Dimensional View of the Molecular Machinery of Rna Interference. *Nature,* 457, 7228, 405-412.

Jing, D., Wobus, M., Poitz, D. M., Bornhauser, M., Ehninger, G. & Ordemann, R. 2011. Oxygen Tension Plays a Critical Role in the Hematopoietic Microenvironment in Vitro. *Haematologica,* 96, 1-29.

Jo, D. Y., Hwang, J. H., Kim, J. M., Yun, H. J. & Kim, S. 2003. Human Bone Marrow Endothelial Cells Elaborate Non-Stromal-Cell-Derived Factor-1 (Sdf-1)-Dependent Chemoattraction and Sdf-1-Dependent Transmigration of Haematopoietic Progenitors. *British Journal of Haematology,* 121, 4, 649-652.

Jung, Y., Wang, J., Havens, A., Sun, Y., Jin, T. & Taichman, R. S. 2005. Cell-to-Cell Contact Is Critical for the Survival of Hematopoietic Progenitor Cells on Osteoblasts. *Cytokine,* 32, 3-4, 155-162.

Jung, Y., Wang, J., Schneider, A., Sun, Y. X., Koh-Paige, A. J., Osman, N. I., Mccauley, L. K. & Taichman, R. S. 2006. Regulation of Sdf-1 (Cxcl12) Production by Osteoblasts; a Possible Mechanism for Stem Cell Homing. *Bone,* 38, 4, 497-508.

Katayama, Y., Battista, M., Kao, W. M., Hidalgo, A., Peired, A. J., Thomas, S. A. & Frenette, P. S. 2006. Signals from the Sympathetic Nervous System Regulate Hematopoietic Stem Cell Egress from Bone Marrow. *Cell,* 124, 2, 407-421.

Kiel, M. J. & Morrison, S. J. 2006. Maintaining Hematopoietic Stem Cells in the Vascular Niche. *Immunity,* 25, 6, 862-864.

Kiel, M. J. & Morrison, S. J. 2008. Uncertainty in the Niches That Maintain Haematopoietic Stem Cells. *Nature Reviews Immunology,* 8, 4, 290-301.

Kiel, M. J., Yilmaz, O. H., Iwashita, T., Yilmaz, O. H., Terhorst, C. & Morrison, S. J. 2005. Slam Family Receptors Distinguish Hematopoietic Stem and

Progenitor Cells and Reveal Endothelial Niches for Stem Cells. *Cell,* 121, 7, 1109-1121.

Kim, E.-J., Kim, N. & Cho, S.-G. 2013. The Potential Use of Mesenchymal Stem Cells in Hematopoietic Stem Cell Transplantation. *Experimental and Molecular Medicine,* 45, 1-10.

Kim, M., Gans, J. D., Nogueira, C., Wang, A., Paik, J. H., Feng, B., Brennan, C., Hahn, W. C., Cordon-Cardo, C., Wagner, S. N., Flotte, T. J., Duncan, L. M., Granter, S. R. & Chin, L. 2006. Comparative Oncogenomics Identifies Nedd9 as a Melanoma Metastasis Gene. *Cell,* 125, 7, 1269-1281.

Kim, S.-H., Xia, D., Kim, S.-W., Holla, V., Menter, D. & Dubois, R. 2010a. Human Enhancer of Filamentation 1 Is a Mediator of Hypoxia-Inducible Factor-1alpha-Mediated Migration in Colorectal Carcinoma Cells. *Cancer Research,* 70, 10, 4054-4063.

Kim, Y.-S., Wielgosz, M., Hargrove, P., Kepes, S., Gray, J., Persons, D. & Nienhuis, A. 2010b. Transduction of Human Primitive Repopulating Hematopoietic Cells with Lentiviral Vectors Pseudotyped with Various Envelope Proteins. *Molecular Therapy: The Journal of the American Society of Gene Therapy,* 18, 004cdbed-c9fa-a9f4-56b6-7cfd820daa89, 1310-1317.

Kinashi, T. 2005. Intracellular Signalling Controlling Integrin Activation in Lymphocytes. *Nature Reviews Immunology,* 5, 7, 546-559.

Kirito, K., Fox, N., Komatsu, N. & Kaushansky, K. 2005. Thrombopoietin Enhances Expression of Vascular Endothelial Growth Factor (Vegf) in Primitive Hematopoietic Cells through Induction of Hif-1α. *Blood,* 105, 11, 4258-4263.

Kita, K., Lee, J. O., Finnerty, C. C. & Herndon, D. N. 2011. Cord Blood-Derived Hematopoietic Stem/Progenitor Cells: Current Challenges in Engraftment,

Infection, and Ex Vivo Expansion. *Stem Cells International,* 2011, 276193.

Klein, C., Strobel, J., Zingsem, J., Richter, R., Goecke, T., Beckmann, M., Eckstein, R. & Weisbach, V. 2013. Ex Vivo Expansion of Hematopoietic Stem- and Progenitor Cells from Cord Blood in Coculture with Mesenchymal Stroma Cells from Amnion, Chorion, Wharton's Jelly, Amniotic Fluid, Cord Blood, and Bone Marrow. *Tissue Engineering. Part A,* 19, 23-24, 2577-2585.

Konopka, K., Stamatatos, L., Larsen, C. E., Davis, B. R. & Düzgüneş, N. 1991. Enhancement of Human Immunodeficiency Virus Type 1 Infection by Cationic Liposomes: The Role of Cd4, Serum and Liposome-Cell Interactions. *Journal of General Virology,* 72, 11, 2685-2696.

Kortesidis, A., Zannettino, A., Isenmann, S., Shi, S., Lapidot, T. & Gronthos, S. 2005. Stromal-Derived Factor-1 Promotes the Growth, Survival, and Development of Human Bone Marrow Stromal Stem Cells. *Blood,* 105, 10, 3793-3801.

Kranc, K., Schepers, H., Rodrigues, N., Bamforth, S., Villadsen, E., Ferry, H., Bouriez-Jones, T., Sigvardsson, M., Bhattacharya, S., Jacobsen, S. & Enver, T. 2009. Cited2 Is an Essential Regulator of Adult Hematopoietic Stem Cells. *Cell Stem Cell,* 5, 6, 659-665.

Kreiss, P., Mailhe, P., Scherman, D., Pitard, B., Cameron, B., Rangara, R., Aguerre-Charriol, O., Airiau, M. & Crouzet, J. 1999. Plasmid DNA Size Does Not Affect the Physicochemical Properties of Lipoplexes but Modulates Gene Transfer Efficiency. *Nucleic Acids Research,* 27, 19, 3792-3798.

Kubota, Y., Takubo, K. & Suda, T. 2008. Bone Marrow Long Label-Retaining Cells Reside in the Sinusoidal Hypoxic Niche. *Biochemical and Biophysical Research Communications,* 366, 2, 335-339.

Kumar, S., Tomooka, Y. & Noda, M. 1992. Identification of a Set of Genes with Developmentally Down-Regulated Expression in the Mouse Brain. *Biochemical and Biophysical Research Communications,* 185, 3, 1155-1161.

Kunisaki, Y., Bruns, I., Scheiermann, C., Ahmed, J., Pinho, S., Zhang, D., Mizoguchi, T., Wei, Q., Lucas, D., Ito, K., Mar, J., Bergman, A. & Frenette, P. 2013. Arteriolar Niches Maintain Haematopoietic Stem Cell Quiescence. *Nature,* 502, 7473, 637-643.

Kurtzberg, J. 2011. What's up with 2 Cord Transplantation? *Blood,* 117, 12, 3248-3249.

Laje, P., Zoltick, P. & Flake, A. 2010. Slam-Enriched Hematopoietic Stem Cells Maintain Long-Term Repopulating Capacity after Lentiviral Transduction Using an Abbreviated Protocol. *Gene Therapy,* 17, 3, 412-418.

Lam, B., Cunningham, C. & Adams, G. 2011. Pharmacologic Modulation of the Calcium-Sensing Receptor Enhances Hematopoietic Stem Cell Lodgment in the Adult Bone Marrow. *Blood,* 117, 4, 1167-1175.

Lane, S. W., De Vita, S., Alexander, K. A., Karaman, R., Milsom, M. D., Dorrance, A. M., Purdon, A., Louis, L., Bouxsein, M. L. & Williams, D. A. 2011. Rac Signaling in Osteoblastic Cells Is Required for Normal Bone Development but Is Dispensable for Hematopoietic Development. *Blood*.

Lansdorp, P., Sutherland, H. & Eaves, C. 1990. Selective Expression of Cd45 Isoforms on Functional Subpopulations of Cd34+ Hemopoietic Cells from Human Bone Marrow. *The Journal of Experimental Medicine,* 172, 1, 363-366.

Lapidot, T., Dar, A. & Kollet, O. 2005. How Do Stem Cells Find Their Way Home? *Blood,* 106, 6, 1901-1910.

Lapidot, T., Pflumio, F., Doedens, M., Murdoch, B., Williams, D. & Dick, J. 1992. Cytokine Stimulation of Multilineage Hematopoiesis from Immature Human Cells Engrafted in Scid Mice. *Science (New York, N.Y.),* 255, 5048, 1137-1141.

Larochelle, A., Gillette, J. M., Desmond, R., Ichwan, B., Cantilena, A., Cerf, A., Barrett, A. J., Wayne, A. S., Lippincott-Schwartz, J. & Dunbar, C. E. 2012. Bone Marrow Homing and Engraftment of Human Hematopoietic Stem and Progenitor Cells Is Mediated by a Polarized Membrane Domain. *Blood,* 119, 8, 1848-1855.

Laurenti, E., Doulatov, S., Zandi, S., Plumb, I., Chen, J., April, C., Fan, J.-B. & Dick, J. 2013. The Transcriptional Architecture of Early Human Hematopoiesis Identifies Multilevel Control of Lymphoid Commitment. *Nature Immunology,* 14, 7, 756-763.

Law, S. F., Estojak, J., Wang, B., Mysliwiec, T., Kruh, G. & Golemis, E. A. 1996. Human Enhancer of Filamentation 1, a Novel P130cas-Like Docking Protein, Associates with Focal Adhesion Kinase and Induces Pseudohyphal Growth in Saccharomyces Cerevisiae. *Molecular Cell Biology,* 16, 7, 3327-3337.

Law, S. F., O'neill, G. M., Fashena, S. J., Einarson, M. B. & Golemis, E. A. 2000. The Docking Protein Hef1 Is an Apoptotic Mediator at Focal Adhesion Sites. *Molecular Cell Biology,* 20, 14, 5184-5195.

Law, S. F., Zhang, Y. Z., Klein-Szanto, A. J. & Golemis, E. A. 1998. Cell Cycle-Regulated Processing of Hef1 to Multiple Protein Forms Differentially Targeted to Multiple Subcellular Compartments. *Molecular Cell Biology,* 18, 6, 3540-3551.

Leuci, V., Mesiano, G., Gammaitoni, L., Cammarata, C., Capellero, S., Todorovic, M., Jordaney, N., Circosta, P., Elia, A., Lesnikova, M., Georges, G. E., Piacibello, W., Fagioli, F., Cignetti, A., Aglietta, M. &

Sangiolo, D. 2011. Transient Proteasome Inhibition as a Strategy to Enhance Lentiviral Transduction of Hematopoietic Cd34+ Cells and T Lymphocytes: Implications for the Use of Low Viral Doses and Large-Size Vectors. *Journal of Biotechnology,* 156, 3, 218-226.

Leung, K., Chan, K. Y., Ng, P., Lau, T., Chiu, W., Tsang, K., Li, C., Kong, C. & Li, K. 2011. The Tetraspanin Cd9 Regulates Migration, Adhesion, and Homing of Human Cord Blood Cd34+ Hematopoietic Stem and Progenitor Cells. *Blood,* 117, 6, 1840-1850.

Levesque, J. P., Helwani, F. M. & Winkler, I. G. 2010. The Endosteal /`Osteoblastic/' Niche and Its Role in Hematopoietic Stem Cell Homing and Mobilization. *Leukemia,* 24, 12, 1979-1992.

Levesque, J. P., Leavesley, D. I., Niutta, S., Vadas, M. & Simmons, P. J. 1995. Cytokines Increase Human Hemopoietic Cell Adhesiveness by Activation of Very Late Antigen (Vla)-4 and Vla-5 Integrins. *The Journal of Experimental Medicine,* 181, 5, 1805-1815.

Levesque, J. P., Winkler, I. G., Hendy, J., Williams, B., Helwani, F., Barbier, V., Nowlan, B. & Nilsson, S. K. 2007. Hematopoietic Progenitor Cell Mobilization Results in Hypoxia with Increased Hypoxia-Inducible Transcription Factor-1 Alpha and Vascular Endothelial Growth Factor a in Bone Marrow. *Stem Cells,* 25, 8, 1954-1965.

Li, C., Issa, R., Kumar, P., Hampson, I., Lopez-Novoa, J., Bernabeu, C. & Kumar, S. 2003. Cd105 Prevents Apoptosis in Hypoxic Endothelial Cells. *Journal of Cell Science,* 116, Pt 13, 2677-2685.

Li, Y., Bavarva, J. H., Wang, Z., Guo, J., Qian, C., Thibodeau, S. N., Golemis, E. A. & Liu, W. 2011. Hef1, a Novel Target of Wnt Signaling, Promotes Colonic Cell Migration and Cancer Progression. *Oncogene,* 30, 23, 2633-2643.

Lin, W., Rui, B., Bixel, M. G., Dagmar, Z., Martin, S., Lars, S., Jody, J. H., Hugo, S., Hans, C., Georg, B., Friedemann, K. & Ralf, H. A. 2012. Identification of a Clonally Expanding Haematopoietic Compartment in Bone Marrow. *The EMBO Journal,* 32, 219-230.

Liu, H., Hung, Y., Wissink, S. & Verfaillie, C. 2000a. Improved Retroviral Transduction of Hematopoietic Progenitors by Combining Methods to Enhance Virus-Cell Interaction. *Leukemia,* 14, 2, 307-311.

Liu, X., Elia, A. E., Law, S. F., Golemis, E. A., Farley, J. & Wang, T. 2000b. A Novel Ability of Smad3 to Regulate Proteasomal Degradation of a Cas Family Member Hef1. *The EMBO Journal,* 19, 24, 6759-6769.

Lo Celso, C., Fleming, H. E., Wu, J. W., Zhao, C. X., Miake-Lye, S., Fujisaki, J., Cote, D., Rowe, D. W., Lin, C. P. & Scadden, D. T. 2009. Live-Animal Tracking of Individual Haematopoietic Stem/Progenitor Cells in Their Niche. *Nature,* 457, 7225, 92-96.

Loenarz, C., Coleman, M., Boleininger, A., Schierwater, B., Holland, P., Ratcliffe, P. & Schofield, C. 2011. The Hypoxia-Inducible Transcription Factor Pathway Regulates Oxygen Sensing in the Simplest Animal, Trichoplax Adhaerens. *EMBO Reports,* 12, 1, 63-70.

Logan, A., Lutzko, C. & Kohn, D. 2002. Advances in Lentiviral Vector Design for Gene-Modification of Hematopoietic Stem Cells. *Current Opinion in Biotechnology,* 13, 5, 429-436.

Lord, A., North, T. & Zon, L. 2007. Prostaglandin E2: Making More of Your Marrow. *Cell Cycle (Georgetown, Tex.),* 6, 24, 3054-3057.

Lundell, B., Mccarthy, J., Kovach, N. & Verfaillie, C. 1996. Activation-Dependent Alpha5beta1 Integrin-Mediated Adhesion to Fibronectin Decreases Proliferation of Chronic Myelogenous Leukemia Progenitors and K562 Cells. *Blood,* 87, 6, 2450-2458.

Lundell, B., Mccarthy, J., Kovach, N. & Verfaillie, C. 1997. Activation of Beta1 Integrins on Cml Progenitors Reveals Cooperation between Beta1 Integrins and Cd44 in the Regulation of Adhesion and Proliferation. *Leukemia,* 11, 6, 822-829.

Luni, C., Zagallo, M., Albania, L., Piccoli, M., Pozzobon, M., De Coppi, P. & Elvassore, N. 2011. Design of a Stirred Multiwell Bioreactor for Expansion of Cd34(+) Umbilical Cord Blood Cells in Hypoxic Conditions. *Biotechnology Progress,* 27, 4, 1154-1162.

Magnusson, M., Sierra, M., Sasidharan, R., Prashad, S., Romero, M., Saarikoski, P., Van Handel, B., Huang, A., Li, X. & Mikkola, H. 2013. Expansion on Stromal Cells Preserves the Undifferentiated State of Human Hematopoietic Stem Cells Despite Compromised Reconstitution Ability. *PLoS ONE,* 8, 1, 1-16.

Man, S., Tucky, B., Cotleur, A., Drazba, J., Takeshita, Y. & Ransohoff, R. 2012. Cxcl12-Induced Monocyte-Endothelial Interactions Promote Lymphocyte Transmigration across an in Vitro Blood-Brain Barrier. *Science Translational Medicine,* 4, 119, 1-10.

Mani, S. & Juliano, C. 2013. Untangling the Web: The Diverse Functions of the Piwi/Pirna Pathway. *Molecular Reproduction and Development,* 80, 8, 632-664.

Manié, S., Beck, A., Astier, A., Law, S., Canty, T., Hirai, H., Druker, B., Avraham, H., Haghayeghi, N., Sattler, M., Salgia, R., Griffin, J., Golemis, E. & Freedman, A. 1997. Involvement of P130(Cas) and P105(Hef1), a Novel Cas-Like Docking Protein, in a Cytoskeleton-Dependent Signaling Pathway Initiated by Ligation of Integrin or Antigen Receptor on Human B Cells. *The Journal of Biological Chemistry,* 272, 7, 4230-4236.

Manjunath, N., Wu, H., Subramanya, S. & Shankar, P. 2009. Lentiviral Delivery of Short Hairpin Rnas. *Advanced Drug Delivery Reviews,* 61, 9, 732-745.

Marquez-Curtis, L. A., Turner, A. R., Sridharan, S., Ratajczak, M. Z. & Janowska-Wieczorek, A. 2011. The Ins and Outs of Hematopoietic Stem Cells: Studies to Improve Transplantation Outcomes. *Stem Cell Rev,* 7, 3, 590-607.

Martin-Rendon, E., Hale, S. J., Ryan, D., Baban, D., Forde, S. P., Roubelakis, M., Sweeney, D., Moukayed, M., Harris, A. L., Davies, K. & Watt, S. M. 2007. Transcriptional Profiling of Human Cord Blood Cd133+ and Cultured Bone Marrow Mesenchymal Stem Cells in Response to Hypoxia. *Stem Cells,* 25, 4, 1003-1012.

Mazo, I., Massberg, S. & Von Andrian, U. 2011. Hematopoietic Stem and Progenitor Cell Trafficking. *Trends in Immunology,* 32, 10, 493-503.

Medvinsky, A., Rybtsov, S. & Taoudi, S. 2011. Embryonic Origin of the Adult Hematopoietic System: Advances and Questions. *Development,* 138, 6, 1017-1031.

Mellott, A., Forrest, M. & Detamore, M. 2013. Physical Non-Viral Gene Delivery Methods for Tissue Engineering. *Annals of Biomedical Engineering,* 41, 3, 446-468.

Méndez-Ferrer, S., Lucas, D., Battista, M. & Frenette, P. 2008. Haematopoietic Stem Cell Release Is Regulated by Circadian Oscillations. *Nature,* 452, 7186, 442-447.

Méndez-Ferrer, S., Michurina, T., Ferraro, F., Mazloom, A., Macarthur, B., Lira, S., Scadden, D., Ma'ayan, A., Enikolopov, G. & Frenette, P. 2010. Mesenchymal and Haematopoietic Stem Cells Form a Unique Bone Marrow Niche. *Nature,* 466, 7308, 829-834.

Miharada, K., Karlsson, G., Rehn, M., Rörby, E., Siva, K., Cammenga, J. & Karlsson, S. 2011. Cripto Regulates Hematopoietic Stem Cells as a Hypoxic-Niche-Related Factor through Cell Surface Receptor Grp78. *Cell Stem Cell,* 9, 4, 330-344.

Miharada, K., Karlsson, G., Rehn, M., Rörby, E., Siva, K., Cammenga, J. & Karlsson, S. 2012. Hematopoietic Stem Cells Are Regulated by Cripto, as an Intermediary of Hif-1α in the Hypoxic Bone Marrow Niche. *Annals of the New York Academy of Sciences,* 1266, 1, 55-62.

Minegishi, M., Tachibana, K., Sato, T., Iwata, S., Nojima, Y. & Morimoto, C. 1996. Structure and Function of Cas-L, a 105-Kd Crk-Associated Substrate-Related Protein That Is Involved in Beta 1 Integrin-Mediated Signaling in Lymphocytes. *The Journal of Experimental Medicine,* 184, 4, 1365-1375.

Mittal, V. 2004. Improving the Efficiency of Rna Interference in Mammals. *Nature Reviews Genetics,* 5, 5, 355-365.

Miyamoto, T. 2013. Role of Osteoclasts in Regulating Hematopoietic Stem and Progenitor Cells. *World Journal of Orthopedics,* 4, 4, 198-206.

Mohle, R., Bautz, F., Rafii, S., Moore, M. A., Brugger, W. & Kanz, L. 1998. The Chemokine Receptor Cxcr-4 Is Expressed on Cd34+ Hematopoietic Progenitors and Leukemic Cells and Mediates Transendothelial Migration Induced by Stromal Cell-Derived Factor-1. *Blood,* 91, 12, 4523-4530.

Mohyeldin, A., Garzón-Muvdi, T. & Quiñones-Hinojosa, A. 2010. Oxygen in Stem Cell Biology: A Critical Component of the Stem Cell Niche. *Cell Stem Cell,* 7, 2, 150-161.

Moore, M. & Hoskins, I. 1994. Ex Vivo Expansion of Cord Blood-Derived Stem Cells and Progenitors. *Blood Cells,* 20, 2-3, 468.

Moritz, T., Dutt, P., Xiao, X., Carstanjen, D., Vik, T., Hanenberg, H. & Williams, D. 1996. Fibronectin Improves Transduction of Reconstituting Hematopoietic Stem Cells by Retroviral Vectors: Evidence of Direct Viral Binding to Chymotryptic Carboxy-Terminal Fragments. *Blood,* 88, 3, 855-862.

Morrison, S. & Scadden, D. 2014. The Bone Marrow Niche for Haematopoietic Stem Cells. *Nature,* 505, 7483, 327-334.

Mortimer, D., Dayan, P., Burrage, K. & Goodhill, G. 2010. Optimizing Chemotaxis by Measuring Unbound–Bound Transitions. *Physica D: Nonlinear Phenomena,* 239, 9, 8.

Murray, L., Chen, B., Galy, A., Chen, S., Tushinski, R., Uchida, N., Negrin, R., Tricot, G., Jagannath, S. & Vesole, D. 1995. Enrichment of Human Hematopoietic Stem Cell Activity in the Cd34+Thy-1+Lin- Subpopulation from Mobilized Peripheral Blood. *Blood,* 85, 2, 368-378.

Myllyharju, J. 2013. Prolyl 4-Hydroxylases, Master Regulators of the Hypoxia Response. *Acta Physiologica (Oxford, England),* 208, 2, 148-165.

Myllyharju, J. & Koivunen, P. 2013. Hypoxia-Inducible Factor Prolyl 4-Hydroxylases: Common and Specific Roles. *Biological Chemistry,* 394, 4, 435-448.

Nagasawa, T., Hirota, S., Tachibana, K., Takakura, N., Nishikawa, S., Kitamura, Y., Yoshida, N., Kikutani, H. & Kishimoto, T. 1996. Defects of B-Cell Lymphopoiesis and Bone-Marrow Myelopoiesis in Mice Lacking the Cxc Chemokine Pbsf/Sdf-1. *Nature,* 382, 6592, 635-638.

Nagele, P. 2003. Misuse of Standard Error of the Mean (Sem) When Reporting Variability of a Sample. A Critical Evaluation of Four Anaesthesia Journals. *British Journal of Anaesthesia,* 90, 4, 514-516.

Naldini, L., Blömer, U., Gallay, P., Ory, D., Mulligan, R., Gage, F., Verma, I. & Trono, D. 1996. In Vivo Gene Delivery and Stable Transduction of Nondividing Cells by a Lentiviral Vector. *Science (New York, N.Y.),* 272, 5259, 263-267.

Natarajan, M., Stewart, J. E., Golemis, E. A., Pugacheva, E. N., Alexandropoulos, K., Cox, B. D., Wang, W., Grammer, J. R. & Gladson,

C. L. 2006. Hef1 Is a Necessary and Specific Downstream Effector of Fak That Promotes the Migration of Glioblastoma Cells. *Oncogene,* 25, 12, 1721-1732.

Nielsen, J. & Mcnagny, K. 2008. Novel Functions of the Cd34 Family. *Journal of Cell Science,* 121, Pt 22, 3683-3692.

Nilsson, S. K., Johnston, H. M., Whitty, G. A., Williams, B., Webb, R. J., Denhardt, D. T., Bertoncello, I., Bendall, L. J., Simmons, P. J. & Haylock, D. N. 2005. Osteopontin, a Key Component of the Hematopoietic Stem Cell Niche and Regulator of Primitive Hematopoietic Progenitor Cells. *Blood,* 106, 4, 1232-1239.

Nombela-Arrieta, C., Pivarnik, G., Winkel, B., Canty, K., Harley, B., Mahoney, J., Park, S.-Y., Lu, J., Protopopov, A. & Silberstein, L. 2013. Quantitative Imaging of Haematopoietic Stem and Progenitor Cell Localization and Hypoxic Status in the Bone Marrow Microenvironment. *Nature Cell Biology,* 15, 5, 533-543.

North, T., Goessling, W., Walkley, C., Lengerke, C., Kopani, K., Lord, A., Weber, G., Bowman, T., Jang, I.-H., Grosser, T., Fitzgerald, G., Daley, G., Orkin, S. & Zon, L. 2007. Prostaglandin E2 Regulates Vertebrate Haematopoietic Stem Cell Homeostasis. *Nature,* 447, 7147, 1007-1011.

Notta, F., Doulatov, S., Laurenti, E., Poeppl, A., Jurisica, I. & Dick, J. 2011. Isolation of Single Human Hematopoietic Stem Cells Capable of Long-Term Multilineage Engraftment. *Science (New York, N.Y.),* 333, 6039, 218-221.

O'neill, G. & Golemis, E. 2001. Proteolysis of the Docking Protein Hef1 and Implications for Focal Adhesion Dynamics. *Molecular and Cellular Biology,* 21, 15, 5094-5108.

Oguro, H., Ding, L. & Morrison, S. 2013. Slam Family Markers Resolve Functionally Distinct Subpopulations of Hematopoietic Stem Cells and Multipotent Progenitors. *Cell Stem Cell,* 13, 1, 102-116.

Ohashi, Y., Tachibana, K., Kamiguchi, K., Fujita, H. & Morimoto, C. 1998. T Cell Receptor-Mediated Tyrosine Phosphorylation of Cas-L, a 105-Kda Crk-Associated Substrate-Related Protein, and Its Association of Crk and C3g. *The Journal of Biological Chemistry,* 273, 11, 6446-6451.

Ong, L.-L., Li, W., Oldigs, J., Kaminski, A., Gerstmayer, B., Piechaczek, C., Wagner, W., Li, R.-K., Ma, N. & Steinhoff, G. 2010. Hypoxic/Normoxic Preconditioning Increases Endothelial Differentiation Potential of Human Bone Marrow Cd133+ Cells. *Tissue engineering. Part C, Methods,* 16, 5, 1069-1081.

Osawa, M., Hanada, K., Hamada, H. & Nakauchi, H. 1996. Long-Term Lymphohematopoietic Reconstitution by a Single Cd34-Low/Negative Hematopoietic Stem Cell. *Science (New York, N.Y.),* 273, 5272, 242-245.

Pan, Q., Van Der Laan, L., Janssen, H. & Peppelenbosch, M. 2012. A Dynamic Perspective of Rnai Library Development. *Trends in Biotechnology,* 30, 4, 206-215.

Papayannopoulou, T., Craddock, C., Nakamoto, B., Priestley, G. V. & Wolf, N. S. 1995. The Vla4/Vcam-1 Adhesion Pathway Defines Contrasting Mechanisms of Lodgement of Transplanted Murine Hemopoietic Progenitors between Bone Marrow and Spleen. *Proceedings of the National Academy of Sciences,* 92, 21, 9647-9651.

Papayannopoulou, T. & Nakamoto, B. 1993. Peripheralization of Hemopoietic Progenitors in Primates Treated with Anti-Vla4 Integrin. *Proceedings of the National Academy of Sciences,* 90, 20, 9374-9378.

Parmar, K., Mauch, P., Vergilio, J. A., Sackstein, R. & Down, J. D. 2007. Distribution of Hematopoietic Stem Cells in the Bone Marrow According

to Regional Hypoxia. *Proceedings of the National Academy Sciences of the USA,* 104, 13, 5431-5436.

Pasino, M., Lanza, T., Marotta, F., Scarso, L., De Biasio, P., Amato, S., Corcione, A., Pistoia, V. & Mori, P. 2000. Flow Cytometric and Functional Characterization of Ac133+ Cells from Human Umbilical Cord Blood. *British Journal of Haematology,* 108, 4, 793-800.

Pedersen, M., Löfstedt, T., Sun, J., Holmquist-Mengelbier, L., Påhlman, S. & Rönnstrand, L. 2008. Stem Cell Factor Induces Hif-1α at Normoxia in Hematopoietic Cells. *Biochemical and Biophysical Research Communications,* 377, 1, 98-103.

Peled, A., Grabovsky, V., Habler, L., Sandbank, J., Arenzana-Seisdedos, F., Petit, I., Ben-Hur, H., Lapidot, T. & Alon, R. 1999a. The Chemokine Sdf-1 Stimulates Integrin-Mediated Arrest of Cd34(+) Cells on Vascular Endothelium under Shear Flow. *The Journal of Clinical Investigation,* 104, 9, 1199-1211.

Peled, A., Kollet, O., Ponomaryov, T., Petit, I., Franitza, S., Grabovsky, V., Slav, M. M., Nagler, A., Lider, O., Alon, R., Zipori, D. & Lapidot, T. 2000. The Chemokine Sdf-1 Activates the Integrins Lfa-1, Vla-4, and Vla-5 on Immature Human Cd34+ Cells: Role in Transendothelial/Stromal Migration and Engraftment of Nod/Scid Mice. *Blood,* 95, 11, 3289-3296.

Peled, A., Petit, I., Kollet, O., Magid, M., Ponomaryov, T., Byk, T., Nagler, A., Ben-Hur, H., Many, A., Shultz, L., Lider, O., Alon, R., Zipori, D. & Lapidot, T. 1999b. Dependence of Human Stem Cell Engraftment and Repopulation of Nod/Scid Mice on Cxcr4. *Science,* 283, 5403, 845-848.

Pollard, P. J. & Kranc, K. R. 2010. Hypoxia Signaling in Hematopoietic Stem Cells: A Double-Edged Sword. *Cell Stem Cell,* 7, 3, 276-278.

Ponomaryov, T., Peled, A., Petit, I., Taichman, R. S., Habler, L., Sandbank, J., Arenzana-Seisdedos, F., Magerus, A., Caruz, A., Fujii, N., Nagler, A.,

Lahav, M., Szyper-Kravitz, M., Zipori, D. & Lapidot, T. 2000. Induction of the Chemokine Stromal-Derived Factor-1 Following DNA Damage Improves Human Stem Cell Function. *The Journal of Clinical Investigation,* 106, 11, 1331-1339.

Porter, R. & Calvi, L. 2009. Key Endothelial Signals Required for Hematopoietic Recovery. *Cell Stem Cell,* 4, 3, 187-188.

Pugacheva, E. N. & Golemis, E. A. 2005. The Focal Adhesion Scaffolding Protein Hef1 Regulates Activation of the Aurora-a and Nek2 Kinases at the Centrosome. *Nature Cell Biology,* 7, 10, 937-946.

Rafii, S., Mohle, R., Shapiro, F., Frey, B. M. & Moore, M. A. 1997. Regulation of Hematopoiesis by Microvascular Endothelium. *Leukemia and Lymphoma,* 27, 5-6, 375-386.

Rahman, M., Lane, A., Swindell, A. & Bartram, S. (eds.) 2006. *Introduction to Flow Cytometry,* Oxford: Serotec Ltd. Endeavour House,2006.

Ramalho-Santos, M. & Willenbring, H. 2007. On the Origin of the Term "Stem Cell". *Cell Stem Cell,* 1, 1, 35-38.

Rappold, I., Watt, S. M., Kusadasi, N., Rose-John, S., Hatzfeld, J. & Ploemacher, R. E. 1999. Gp130-Signaling Synergizes with Fl and Tpo for the Long-Term Expansion of Cord Blood Progenitors. *Leukemia,* 13, 12, 2036-2048.

Ratcliffe, P. 2013. Oxygen Sensing and Hypoxia Signalling Pathways in Animals: The Implications of Physiology for Cancer. *The Journal of Physiology,* 591, 8, 2027-2042.

Raya, A., Rodríguez-Pizà, I., Guenechea, G., Vassena, R., Navarro, S., Barrero, M., Consiglio, A., Castellà, M., Río, P., Sleep, E., González, F., Tiscornia, G., Garreta, E., Aasen, T., Veiga, A., Verma, I., Surrallés, J., Bueren, J. & Izpisúa Belmonte, J. 2009. Disease-Corrected Haematopoietic

Progenitors from Fanconi Anaemia Induced Pluripotent Stem Cells. *Nature,* 460, 7251, 53-59.

Regelmann, A., Danzl, N., Wanjalla, C. & Alexandropoulos, K. 2006. The Hematopoietic Isoform of Cas-Hef1-Associated Signal Transducer Regulates Chemokine-Induced inside-out Signaling and T Cell Trafficking. *Immunity,* 25, 6, 907-918.

Rehn, M., Olsson, A., Reckzeh, K., Diffner, E., Carmeliet, P., Landberg, G. & Cammenga, J. 2011. Hypoxic Induction of Vascular Endothelial Growth Factor Regulates Murine Hematopoietic Stem Cell Function in the Low-Oxygenic Niche. *Blood,* 118, 6, 1534-1543.

Reiser, J., Harmison, G., Kluepfel-Stahl, S., Brady, R. O., Karlsson, S. & Schubert, M. 1996. Transduction of Nondividing Cells Using Pseudotyped Defective High-Titer Hiv Type 1 Particles. *Proceedings of the National Academy of Sciences,* 93, 26, 15266-15271.

Robbins, M., Li, M., Leung, I., Li, H., Boyer, D., Song, Y., Behlke, M. & Rossi, J. 2006. Stable Expression of Shrnas in Human Cd34+ Progenitor Cells Can Avoid Induction of Interferon Responses to Sirnas in Vitro. *Nature Biotechnology,* 24, 5, 566-571.

Rocha, V. & Broxmeyer, H. E. 2010. New Approaches for Improving Engraftment after Cord Blood Transplantation. *Biology of Blood and Marrow Transplantation,* 16, 1, Supplement, S126-S132.

Rocha, V., Gluckman, E., Eurocord-Netcord, R., European, B. & Marrow Transplant, G. 2009. Improving Outcomes of Cord Blood Transplantation: Hla Matching, Cell Dose and Other Graft- and Transplantation-Related Factors. *British Journal of Haematology,* 147, 2, 262-274.

Roelz, R., Pilz, I., Mutschler, M. & Pahl, H. 2010. Of Mice and Men: Human Rna Polymerase Iii Promoter U6 Is More Efficient Than Its Murine Homologue

for Shrna Expression from a Lentiviral Vector in Both Human and Murine Progenitor Cells. *Experimental Hematology,* 38, 9, 792-797.

Rohll, J., Mitrophanous, K., Martin-Rendon, E., Ellard, F., Radcliffe, P., Mazarakis, N. & Kingsman, S. 2002. Design, Production, Safety, Evaluation, and Clinical Applications of Nonprimate Lentiviral Vectors. *Methods in Enzymology,* 346, 466-500.

Rood, P. M., Calafat, J., Von Dem Borne, A. E., Gerritsen, W. R. & Van Der Schoot, C. E. 2000a. Immortalisation of Human Bone Marrow Endothelial Cells: Characterisation of New Cell Lines. *European Journal of Clinical Investigation,* 30, 7, 618-629.

Rood, P. M., Dercksen, M. W., Cazemier, H., Kerst, J. M., Von Dem Borne, A. E., Gerritsen, W. R. & Van Der Schoot, C. E. 2000b. E-Selectin and Very Late Activation Antigen-4 Mediate Adhesion of Hematopoietic Progenitor Cells to Bone Marrow Endothelium. *Annals Hematology,* 79, 9, 477-484.

Rouault-Pierre, K., Lopez-Onieva, L., Foster, K., Anjos-Afonso, F., Lamrissi-Garcia, I., Serrano-Sanchez, M., Mitter, R., Ivanovic, Z., De Verneuil, H., Gribben, J., Taussig, D., Rezvani, H., Mazurier, F. & Bonnet, D. 2013. Hif-2α Protects Human Hematopoietic Stem/Progenitors and Acute Myeloid Leukemic Cells from Apoptosis Induced by Endoplasmic Reticulum Stress. *Cell Stem Cell,* 13, 5, 549-563.

Roy, S., Javed, S., Jain, S. K., Majumdar, S. S. & Mukhopadhyay, A. 2012. Donor Hematopoietic Stem Cells Confer Long-Term Marrow Reconstitution by Self-Renewal Divisions Exceeding to That of Host Cells. *PLoS ONE,* 7, 12, 1-11.

Rubinson, D., Dillon, C., Kwiatkowski, A., Sievers, C., Yang, L., Kopinja, J., Rooney, D., Zhang, M., Ihrig, M., Mcmanus, M., Gertler, F., Scott, M. & Van Parijs, L. 2003. A Lentivirus-Based System to Functionally Silence

Genes in Primary Mammalian Cells, Stem Cells and Transgenic Mice by Rna Interference. *Nature Genetics,* 33, 3, 401-406.

Sanjuan-Pla, A., Macaulay, I., Jensen, C., Woll, P., Luis, T., Mead, A., Moore, S., Carella, C., Matsuoka, S., Bouriez Jones, T., Chowdhury, O., Stenson, L., Lutteropp, M., Green, J., Facchini, R., Boukarabila, H., Grover, A., Gambardella, A., Thongjuea, S., Carrelha, J., Tarrant, P., Atkinson, D., Clark, S.-A., Nerlov, C. & Jacobsen, S. 2013. Platelet-Biased Stem Cells Reside at the Apex of the Haematopoietic Stem-Cell Hierarchy. *Nature,* 502, 7470, 232-236.

Scaradavou, A., Brunstein, C., Eapen, M., Le-Rademacher, J., Barker, J., Chao, N., Cutler, C., Delaney, C., Kan, F., Isola, L., Karanes, C., Laughlin, M., Wagner, J. & Shpall, E. 2013. Double Unit Grafts Successfully Extend the Application of Umbilical Cord Blood Transplantation in Adults with Acute Leukemia. *Blood,* 121, 5, 752-758.

Schajnovitz, A., Itkin, T., D'uva, G., Kalinkovich, A., Golan, K., Ludin, A., Cohen, D., Shulman, Z., Avigdor, A., Nagler, A., Kollet, O., Seger, R. & Lapidot, T. 2011. Cxcl12 Secretion by Bone Marrow Stromal Cells Is Dependent on Cell Contact and Mediated by Connexin-43 and Connexin-45 Gap Junctions. *Nature Immunology,* 12, 5, 391-398.

Scherr, M., Venturini, L. & Eder, M. 2009. Knock-Down of Gene Expression in Hematopoietic Cells. *Methods in Molecular Biology (Clifton, N.J.),* 506, 207-219.

Schioppa, T., Uranchimeg, B., Saccani, A., Biswas, S., Doni, A., Rapisarda, A., Bernasconi, S., Saccani, S., Nebuloni, M., Vago, L., Mantovani, A., Melillo, G. & Sica, A. 2003. Regulation of the Chemokine Receptor Cxcr4 by Hypoxia. *The Journal of Experimental Medicine,* 198, 9, 1391-1402.

Schomber, T., Kalberer, C., Wodnar-Filipowicz, A. & Skoda, R. 2004. Gene Silencing by Lentivirus-Mediated Delivery of Sirna in Human Cd34+ Cells. *Blood,* 103, 12, 4511-4513.

Sebrango, A., Vicuña, I., De Laiglesia, A., Millán, I., Bautista, G., Martín-Donaire, T., Regidor, C., Cabrera, R. & Fernandez, M. 2010. Haematopoietic Transplants Combining a Single Unrelated Cord Blood Unit and Mobilized Haematopoietic Stem Cells from an Adult Hla-Mismatched Third Party Donor. Comparable Results to Transplants from Hla-Identical Related Donors in Adults with Acute Leukaemia and Myelodysplastic Syndromes. *Best Practice and Research. Clinical Haematology,* 23, 2, 259-274.

Segura, M., Mangion, M., Gaillet, B. & Garnier, A. 2013. New Developments in Lentiviral Vector Design, Production and Purification. *Expert Opinion on Biological Therapy,* 13, 7, 987-1011.

Shamri, R., Grabovsky, V., Gauguet, J.-M., Feigelson, S., Manevich, E., Kolanus, W., Robinson, M., Staunton, D., Von Andrian, U. & Alon, R. 2005. Lymphocyte Arrest Requires Instantaneous Induction of an Extended Lfa-1 Conformation Mediated by Endothelium-Bound Chemokines. *Nature Immunology,* 6, 5, 497-506.

Shima, H., Takubo, K., Iwasaki, H., Yoshihara, H., Gomei, Y., Hosokawa, K., Arai, F., Takahashi, T. & Suda, T. 2009. Reconstitution Activity of Hypoxic Cultured Human Cord Blood Cd34-Positive Cells in Nog Mice. *Biochemical and Biophysical Research Communications,* 378, 3, 467-472.

Shweiki, D., Itin, A., Soffer, D. & Keshet, E. 1992. Vascular Endothelial Growth Factor Induced by Hypoxia May Mediate Hypoxia-Initiated Angiogenesis. *Nature,* 359, 6398, 843-845.

Silberstein, L. & Lin, C. 2013. A New Image of the Hematopoietic Stem Cell Vascular Niche. *Cell Stem Cell,* 13, 5, 514-516.

Silva, J., Li, M., Chang, K., Ge, W., Golding, M., Rickles, R., Siolas, D., Hu, G., Paddison, P., Schlabach, M., Sheth, N., Bradshaw, J., Burchard, J., Kulkarni, A., Cavet, G., Sachidanandam, R., Mccombie, W., Cleary, M., Elledge, S. & Hannon, G. 2005. Second-Generation Shrna Libraries Covering the Mouse and Human Genomes. *Nature Genetics,* 37, 11, 1281-1288.

Simsek, T., Kocabas, F., Zheng, J., Deberardinis, R., Mahmoud, A., Olson, E., Schneider, J., Zhang, C. & Sadek, H. 2010. The Distinct Metabolic Profile of Hematopoietic Stem Cells Reflects Their Location in a Hypoxic Niche. *Cell Stem Cell,* 7, 3, 380-390.

Singh, M., Cowell, L., Seo, S., O'neill, G. & Golemis, E. 2007. Molecular Basis for Hef1/Nedd9/Cas-L Action as a Multifunctional Co-Ordinator of Invasion, Apoptosis and Cell Cycle. *Cell Biochemistry Biophysics,* 48, 1, 54-72.

Singh, R., Franke, K., Kalucka, J., Mamlouk, S., Muschter, A., Gembarska, A., Grinenko, T., Willam, C., Naumann, R., Anastassiadis, K., Stewart, A., Bornstein, S., Chavakis, T., Breier, G., Waskow, C. & Wielockx, B. 2013. Hif Prolyl Hydroxylase 2 (Phd2) Is a Critical Regulator of Hematopoietic Stem Cell Maintenance During Steady-State and Stress. *Blood,* 121, 26, 5158-5166.

Sirinoglu Demiriz, I., Tekgunduz, E. & Altuntas, F. 2012. What Is the Most Appropriate Source for Hematopoietic Stem Cell Transplantation? Peripheral Stem Cell/Bone Marrow/Cord Blood. *Bone Marrow Research,* 2012, 834040.

Smith-Berdan, S., Nguyen, A., Hassanein, D., Zimmer, M., Ugarte, F., Ciriza, J., Li, D., García-Ojeda, M., Hinck, L. & Forsberg, E. 2011. Robo4

Cooperates with Cxcr4 to Specify Hematopoietic Stem Cell Localization to Bone Marrow Niches. *Cell Stem Cell,* 8, 1, 72-83.

Smith-Berdan, S., Schepers, K., Ly, A., Passegué, E. & Forsberg, E. 2012. Dynamic Expression of the Robo Ligand Slit2 in Bone Marrow Cell Populations. *Cell Cycle (Georgetown, Tex.),* 11, 4, 675-682.

Smith, L., Weissman, I. & Heimfeld, S. 1991. Clonal Analysis of Hematopoietic Stem-Cell Differentiation in Vivo. *Proceedings of the National Academy of Sciences of the USA,* 88, 7, 2788-2792.

Solanilla, A., Grosset, C., Duchez, P., Legembre, P., Pitard, V., Dupouy, M., Belloc, F., Viallard, J. F., Reiffers, J., Boiron, J. M., Coulombel, L. & Ripoche, J. 2003. Flt3-Ligand Induces Adhesion of Haematopoietic Progenitor Cells Via a Very Late Antigen (Vla)-4- and Vla-5-Dependent Mechanism. *British Journal of Haematology,* 120, 5, 782-786.

Spencer, J. A., Ferraro, F., Roussakis, E., Klein, A., Wu, J., Runnels, J. M., Zaher, W., Mortensen, L. J., Alt, C., Turcotte, R., Yusuf, R., Cote, D., Vinogradov, S. A., Scadden, D. T. & Lin, C. P. 2014. Direct Measurement of Local Oxygen Concentration in the Bone Marrow of Live Animals. *Nature,* 000, 00, 1-16.

Speth, J., Hoggatt, J., Singh, P. & Pelus, L. 2014. Pharmacologic Increase in Hif1α Enhances Hematopoietic Stem and Progenitor Homing and Engraftment. *Blood,* 123, 2, 203-207.

Stanevsky, A., Shimoni, A., Yerushalmi, R. & Nagler, A. 2010. Double Umbilical Cord Blood Transplant: More Than a Cell Dose? *Leukemia and Lymphoma,* 51, 6, 975-982.

Stefan, T. A., Maria, K. H. & Martin, E. M. N. 2002. The Structural Basis of Localization and Signaling by the Focal Adhesion Targeting Domain. *Structure,* 10, 3, 319-327.

Stegmeier, F., Hu, G., Rickles, R., Hannon, G. & Elledge, S. 2005. A Lentiviral Microrna-Based System for Single-Copy Polymerase Ii-Regulated Rna Interference in Mammalian Cells. *Proceedings of the National Academy of Sciences of the USA,* 102, 37, 13212-13217.

Stellos, K., Langer, H., Gnerlich, S., Panagiota, V., Paul, A., Schönberger, T., Ninci, E., Menzel, D., Mueller, I., Bigalke, B., Geisler, T., Bültmann, A., Lindemann, S. & Gawaz, M. 2010. Junctional Adhesion Molecule a Expressed on Human Cd34+ Cells Promotes Adhesion on Vascular Wall and Differentiation into Endothelial Progenitor Cells. *Arteriosclerosis, Thrombosis, and Vascular Biology,* 30, 6, 1127-1136.

Stiehl, T., Ho, A. & Marciniak-Czochra, A. 2014. The Impact of Cd34+ Cell Dose on Engraftment after Scts: Personalized Estimates Based on Mathematical Modeling. *Bone Marrow Transplantation,* 49, 1, 30-37.

Suda, T., Takubo, K. & Semenza, Gregg l. 2011. Metabolic Regulation of Hematopoietic Stem Cells in the Hypoxic Niche. *Cell Stem Cell,* 9, 4, 298-310.

Sugiyama, T., Kohara, H., Noda, M. & Nagasawa, T. 2006. Maintenance of the Hematopoietic Stem Cell Pool by Cxcl12-Cxcr4 Chemokine Signaling in Bone Marrow Stromal Cell Niches. *Immunity,* 25, 6, 977-988.

Summers, Y., Heyworth, C., De Wynter, E., Hart, C., Chang, J. & Testa, N. 2004. Ac133+ G0 Cells from Cord Blood Show a High Incidence of Long-Term Culture-Initiating Cells and a Capacity for More Than 100 Million-Fold Amplification of Colony-Forming Cells in Vitro. *Stem Cells (Dayton, Ohio),* 22, 5, 704-715.

Sun, J., Li, Y., Graziani, G., Filion, L. & Allan, D. 2013. E-Selectin Mediated Adhesion and Migration of Endothelial Colony Forming Cells Is Enhanced by Sdf-1α/Cxcr4. *PLoS ONE,* 8, 4, 1-11.

Sutherland, H., Lansdorp, P., Henkelman, D., Eaves, A. & Eaves, C. 1990. Functional Characterization of Individual Human Hematopoietic Stem Cells Cultured at Limiting Dilution on Supportive Marrow Stromal Layers. *Proceedings of the National Academy of Sciences of the USA,* 87, 9, 3584-3588.

Szyda, A., Paprocka, M., Krawczenko, A., Lenart, K., Heimrath, J., Grabarczyk, P., Mackiewicz, A. & Duś, D. 2006. Optimization of a Retroviral Vector for Transduction of Human Cd34 Positive Cells. *Acta Biochimica Polonica,* 53, 4, 815-823.

Tachibana, K., Urano, T., Fujita, H., Ohashi, Y., Kamiguchi, K., Iwata, S., Hirai, H. & Morimoto, C. 1997. Tyrosine Phosphorylation of Crk-Associated Substrates by Focal Adhesion Kinase. *Journal of Biological Chemistry,* 272, 46, 29083-29090.

Taichman, R. S. & Emerson, S. G. 1994. Human Osteoblasts Support Hematopoiesis through the Production of Granulocyte Colony-Stimulating Factor. *The Journal of Experimental Medicine,* 179, 5, 1677-1682.

Taichman, R. S., Reilly, M. J. & Emerson, S. G. 1996. Human Osteoblasts Support Human Hematopoietic Progenitor Cells in Vitro Bone Marrow Cultures. *Blood,* 87, 2, 518-524.

Takahashi, K. & Yamanaka, S. 2006. Induction of Pluripotent Stem Cells from Mouse Embryonic and Adult Fibroblast Cultures by Defined Factors. *Cell,* 126, 4, 663-676.

Takahashi, M., Matsuoka, Y., Sumide, K., Nakatsuka, R., Fujioka, T., Kohno, H., Sasaki, Y., Matsui, K., Asano, H., Kaneko, K. & Sonoda, Y. 2013. Cd133 Is a Positive Marker for a Distinct Class of Primitive Human Cord Blood-Derived Cd34-Negative Hematopoietic Stem Cells. *Leukemia*, 1-8.

Takubo, K., Goda, N., Yamada, W., Iriuchishima, H., Ikeda, E., Kubota, Y., Shima, H., Johnson, R. S., Hirao, A., Suematsu, M. & Suda, T. 2010. Regulation of the Hif-1alpha Level Is Essential for Hematopoietic Stem Cells. *Cell Stem Cell,* 7, 3, 391-402.

Takubo, K., Nagamatsu, G., Kobayashi, C., Nakamura-Ishizu, A., Kobayashi, H., Ikeda, E., Goda, N., Rahimi, Y., Johnson, R., Soga, T., Hirao, A., Suematsu, M. & Suda, T. 2013. Regulation of Glycolysis by Pdk Functions as a Metabolic Checkpoint for Cell Cycle Quiescence in Hematopoietic Stem Cells. *Cell Stem Cell,* 12, 1, 49-61.

Takubo, K. & Suda, T. 2012. Roles of the Hypoxia Response System in Hematopoietic and Leukemic Stem Cells. *International Journal of Hematology,* 95, 478-483.

Tarnowski, M., Liu, R., Wysoczynski, M., Ratajczak, J., Kucia, M. & Ratajczak, M. Z. 2010. Cxcr7: A New Sdf-1-Binding Receptor in Contrast to Normal Cd34+ Progenitors Is Functional and Is Expressed at Higher Level in Human Malignant Hematopoietic Cells. *European Journal of Haematology,* 85, 6, 472-483.

Teixido, J., Hemler, M. E., Greenberger, J. S. & Anklesaria, P. 1992. Role of Beta 1 and Beta 2 Integrins in the Adhesion of Human Cd34hi Stem Cells to Bone Marrow Stroma. *Journal of Clinical Investigation,* 90, 2, 358-367.

Tikhmyanova, N. & Golemis, E. 2011. Nedd9 and Bcar1 Negatively Regulate E-Cadherin Membrane Localization, and Promote E-Cadherin Degradation. *PLoS ONE,* 6, 7, 1-10.

Tikhmyanova, N., Little, J. & Golemis, E. 2010. Cas Proteins in Normal and Pathological Cell Growth Control. *Cellular and Molecular Life Sciences,* 67, 7, 1025-1048.

Till, J., Mcculloch, E. & Siminovitch, L. 1964. A Stochastic Model of Stem Cell Proliferation, Based on the Growth of Spleen Colony-Forming Cells. *Proceedings of the National Academy of Sciences of the USA,* 51, 29-36.

Trumpp, A., Essers, M. & Wilson, A. 2010. Awakening Dormant Haematopoietic Stem Cells. *Nature Reviews. Immunology,* 10, 3, 201-209.

Uchida, N., Combs, J., Chen, S., Zanjani, E., Hoffman, R. & Tsukamoto, A. 1996. Primitive Human Hematopoietic Cells Displaying Differential Efflux of the Rhodamine 123 Dye Have Distinct Biological Activities. *Blood,* 88, 4, 1297-1305.

Ulrich, M. 2005. Lentiviral Vector. *The Patent Cooperation Treaty (PCT), World Intellectual Property Organization*, International Publication Number WO 2005/123930 A1.

Valencia, S. & Hutt-Fletcher, L. 2012. Important but Differential Roles for Actin in Trafficking of Epstein-Barr Virus in B Cells and Epithelial Cells. *Journal of Virology,* 86, 1, 2-10.

Van Besien, K. 2013. Advances in Umbilical Cord Blood Transplantation- a Summary of the 11(Th) International Cord Blood Symposium San Francisco June 6(Th)-8(Th) 2013. *Leukemia and Lymphoma*, 1-8.

Van Buul, J. D., Voermans, C., Van Gelderen, J., Anthony, E. C., Van Der Schoot, C. E. & Hordijk, P. L. 2003. Leukocyte-Endothelium Interaction Promotes Sdf-1-Dependent Polarization of Cxcr4. *The Journal of Biological Chemistry,* 278, 32, 30302-30310.

Van Seventer, G. A., Salmen, H. J., Law, S. F., O'neill, G. M., Mullen, M. M., Franz, A. M., Kanner, S. B., Golemis, E. A. & Van Seventer, J. M. 2001. Focal Adhesion Kinase Regulates Beta1 Integrin-Dependent T Cell Migration through an Hef1 Effector Pathway. *European Journal of Immunology,* 31, 5, 1417-1427.

Varma, N., Janic, B., Ali, M., Iskander, A. & Arbab, A. 2011. Lentiviral Based Gene Transduction and Promoter Studies in Human Hematopoietic Stem Cells (Hhscs). *Journal of Stem Cells & Regenerative Medicine,* 7, 1, 41-53.

Vengellur, A. & Lapres, J. J. 2004. The Role of Hypoxia Inducible Factor 1alpha in Cobalt Chloride Induced Cell Death in Mouse Embryonic Fibroblasts. *Toxicological Sciences,* 82, 2, 638-646.

Vengellur, A., Phillips, J., Hogenesch, J. & Lapres, J. 2005. Gene Expression Profiling of Hypoxia Signaling in Human Hepatocellular Carcinoma Cells. *Physiological Genomics,* 22, 3, 308-318.

Voermans, C., Gerritsen, W., Von Dem Borne, A. & Van Der Schoot, C. 1999. Increased Migration of Cord Blood-Derived Cd34+ Cells, as Compared to Bone Marrow and Mobilized Peripheral Blood Cd34+ Cells across Uncoated or Fibronectin-Coated Filters. *Experimental Hematology,* 27, 12, 1806-1814.

Voermans, C., Rood, P. M. L., Hordijk, P. L., Gerritsen, W. R. & Van Der Schoot, C. E. 2000. Adhesion Molecules Involved in Transendothelial Migration of Human Hematopoietic Progenitor Cells. *Stem Cells,* 18, 6, 435-443.

Wagner, J. E., Rosenthal, J., Sweetman, R., Shu, X. O., Davies, S. M., Ramsay, N. K., Mcglave, P. B., Sender, L. & Cairo, M. S. 1996. Successful Transplantation of Hla-Matched and Hla-Mismatched Umbilical Cord Blood from Unrelated Donors: Analysis of Engraftment and Acute Graft-Versus-Host Disease. *Blood,* 88, 3, 795-802.

Wagner, W., Wein, F., Roderburg, C., Saffrich, R., Diehlmann, A., Eckstein, V. & Ho, A. 2008. Adhesion of Human Hematopoietic Progenitor Cells to Mesenchymal Stromal Cells Involves Cd44. *Cells, Tissues, Organs,* 188, 1-2, 160-169.

Wagner, W., Wein, F., Roderburg, C., Saffrich, R., Faber, A., Krause, U., Schubert, M., Benes, V., Eckstein, V., Maul, H. & Ho, A. 2007. Adhesion of Hematopoietic Progenitor Cells to Human Mesenchymal Stem Cells as a Model for Cell-Cell Interaction. *Experimental Hematology,* 35, 2, 314-325.

Watt, S., Butler, L., Tavian, M., Bühring, H., Rappold, I., Simmons, P., Zannettino, A., Buck, D., Fuchs, A., Doyonnas, R., Chan, J., Levesque, J., Peault, B. & Roxanis, I. 2000. Functionally Defined Cd164 Epitopes Are Expressed on Cd34(+) Cells Throughout Ontogeny but Display Distinct Distribution Patterns in Adult Hematopoietic and Nonhematopoietic Tissues. *Blood,* 95, 10, 3113-3124.

Watt, S. M. & Forde, S. P. 2008. The Central Role of the Chemokine Receptor, Cxcr4, in Haemopoietic Stem Cell Transplantation: Will Cxcr4 Antagonists Contribute to the Treatment of Blood Disorders? *Vox Sanguinis,* 94, 1, 18-32.

Weber, J. M. & Calvi, L. M. 2010. Notch Signaling and the Bone Marrow Hematopoietic Stem Cell Niche. *Bone,* 46, 2, 281-285.

Weissman, I. 2002. The Road Ended up at Stem Cells. *Immunological Reviews,* 185, 159-174.

Weissman, I., Heimfeld, S. & Spangrude, G. 1989. Haemopoietic Stem Cell Purification. *Immunology Today,* 10, 6, 184-185.

Winkler, I. G., Barbier, V., Wadley, R., Zannettino, A. C., Williams, S. & Levesque, J. P. 2010. Positioning of Bone Marrow Hematopoietic and Stromal Cells Relative to Blood Flow in Vivo: Serially Reconstituting Hematopoietic Stem Cells Reside in Distinct Nonperfused Niches. *Blood,* 116, 3, 375-385.

Woods, N., Mikkola, H., Nilsson, E., Olsson, K., Trono, D. & Karlsson, S. 2001. Lentiviral-Mediated Gene Transfer into Haematopoietic Stem Cells. *Journal of Internal Medicine,* 249, 4, 339-343.

Wuchter, P., Leinweber, C., Saffrich, R., Hanke, M., Eckstein, V., Ho, A., Grunze, M. & Rosenhahn, A. 2014. Plerixafor Induces the Rapid and Transient Release of Stromal Cell-Derived Factor-1 Alpha from Human Mesenchymal Stromal Cells and Influences the Migration Behavior of Human Hematopoietic Progenitor Cells. *Cell and Tissue Research,* 355, 2, 315-326.

Xie, Y., Yin, T., Wiegraebe, W., He, X. C., Miller, D., Stark, D., Perko, K., Alexander, R., Schwartz, J., Grindley, J. C., Park, J., Haug, J. S., Wunderlich, J. P., Li, H., Zhang, S., Johnson, T., Feldman, R. A. & Li, L. 2009. Detection of Functional Haematopoietic Stem Cell Niche Using Real-Time Imaging. *Nature,* 457, 7225, 97-101.

Yamazaki, S., Iwama, A., Takayanagi, S., Eto, K., Ema, H. & Nakauchi, H. 2009. Tgf-Beta as a Candidate Bone Marrow Niche Signal to Induce Hematopoietic Stem Cell Hibernation. *Blood,* 113, 6, 1250-1256.

Yao, S. Y., Soutto, M. & Sriram, S. 2008. Preconditioning with Cobalt Chloride or Desferrioxamine Protects Oligodendrocyte Cell Line (Mo3.13) from Tumor Necrosis Factor-Alpha-Mediated Cell Death. *Journal of Neuroscience Research,* 86, 11, 2403-2413.

Yin, A., Miraglia, S., Zanjani, E., Almeida-Porada, G., Ogawa, M., Leary, A., Olweus, J., Kearney, J. & Buck, D. 1997. Ac133, a Novel Marker for Human Hematopoietic Stem and Progenitor Cells. *Blood,* 90, 12, 5002-5012.

Yong, K., Fahey, A., Pizzey, A. & Linch, D. 2002. Influence of Cell Cycling and Cell Division on Transendothelial Migration of Cd34+ Cells. *British Journal of Haematology,* 119, 2, 500-509.

Yuan, J., Chan, S., Mortimer, D., Nguyen, H. & Goodhill, G. 2013. Optimality and Saturation in Axonal Chemotaxis. *Neural Computation,* 25, 4, 833-853.

Yun, H. J. & Jo, D. Y. 2003. Production of Stromal Cell-Derived Factor-1 (Sdf-1)and Expression of Cxcr4 in Human Bone Marrow Endothelial Cells. *Journal of Korean Medical Science,* 18, 5, 679-685.

Zhang, H., Akman, H., Smith, E., Zhao, J., Murphy-Ullrich, J. & Batuman, O. 2003a. Cellular Response to Hypoxia Involves Signaling Via Smad Proteins. *Blood,* 101, 6, 2253-2260.

Zhang, J., Niu, C., Ye, L., Huang, H., He, X., Tong, W.-G., Ross, J., Haug, J., Johnson, T., Feng, J., Harris, S., Wiedemann, L., Mishina, Y. & Li, L. 2003b. Identification of the Haematopoietic Stem Cell Niche and Control of the Niche Size. *Nature,* 425, 6960, 836-841.

Zheng, M. & Mckeown-Longo, P. 2006. Cell Adhesion Regulates Ser/Thr Phosphorylation and Proteasomal Degradation of Hef1. *Journal of Cell Science,* 119, Pt 1, 96-103.

Zheng, M. & Mckeown-Longo, P. J. 2002. Regulation of Hef1 Expression and Phosphorylation by Tgf-B1 and Cell Adhesion. *Journal of Biological Chemistry,* 277, 42, 39599-39608.

Zielske, S. & Gerson, S. 2002. Lentiviral Transduction of P140k Mgmt into Human Cd34(+) Hematopoietic Progenitors at Low Multiplicity of Infection Confers Significant Resistance to Bg/Bcnu and Allows Selection in Vitro. *Molecular Therapy: The Journal of the American Society of Gene Therapy,* 5, 4, 381-387.

Zou, Y. R., Kottmann, A. H., Kuroda, M., Taniuchi, I. & Littman, D. R. 1998. Function of the Chemokine Receptor Cxcr4 in Haematopoiesis and in Cerebellar Development. *Nature,* 393, 6685, 595-599.